THE IMMUNOLOGY OF ADENO-ASSOCIATED VIRUS SEROTYPE 2

DECLAN PAUL MADSEN, B.SC. (HONS)

NUI MAYNOOTH

Ollscoil na hÉireann Má Nuad

Thesis submitted to the National university of Ireland, Maynooth for the degree of Doctor of Philosophy

October 2009

Supervisor: Dr. Bernard Mahon

Head of Department: Prof. Kay Ohlendieck

Department of Biology,

National University of Ireland Maynooth,

Co. Kildare, Ireland.

TABLE OF CONTENTS

DECLARATION OF AUTHORSHIP

I certify that the work presented here is, to the best of my knowledge, original and the result of my own investigations, except where acknowledged otherwise. This work has not been submitted, either in whole or in part, for a degree at this or any other university.

_____ _____

Declan Paul Madsen, B.Sc. (Hons) Date

ACKNOWLEDGEMENTS

I would firstly like to thank my colleagues at the Institute of Immunology for all their help and support over the years. In particular Dr. Paul Corcoran who was the postdoc on the AAV project, Dr. Jenny Ryan and Dr. Karen English who worked on MSC projects parallel to mine and Laura Tobin who provided further support on the MSC project. Special mentions must go to Heather Kavanagh, who helped me out on several experiments (without getting any payback), to my very helpful undergraduate students Emma Cantwell and Rob Lumsden and to Karen Scanlon and Ciaran Skerry who, as well as helping me with work and providing many great ideas, also helped to keep me sane and motivated. I am also grateful for the support of Dr. Mary O'Gorman, Dr. David O'Connor and Emer Cahill at the Cellular Immunology Lab as well as Ellen Lewis and Dr. Cariosa Noone who trained me during my first months at the Viral Immunology Lab. I must also mention the PI at the Viral Immunology laboratory, Dr. Patricia Johnson, who first recruited me as an RA and later accepted me as a PhD student. Her guidance during the first year of my research was much appreciated. Throughout the course of my PhD my supervisor, Dr. Bernard Mahon, has been an invaluable guide and mentor, pushing me to be a better student and a better scientist. I would like to express my sincerest gratitude to him for everything he has done for me these last few years. I would also like to acknowledge the support provided by my colleagues in the Department of Biology at NUI Maynooth as well as our collaborators at REMEDI in NUI Galway and elsewhere. At Maynooth, Prof. Sean Doyle and Dr. Luke O'Shaughnessy for their help with the B19V ELISA, Dr. Stephen Carberry for his very patient support on the HPLC and Dr. Lisa Tang for her help with the plasmid work. At Galway, my thanks go to Prof. Timothy O'Brien, Dr. Siobhan Conroy and Aoife Duffy for their collaboration on the AAV project. A big thank-you must go to Dr. Anne-Marie McGauran for her collaboration on the BDNF project, my very first author credit. I would like to give particular thanks to Prof. Phil Hodgkin of WEHI in Melbourne for his enthusiasm, collaboration and invaluable guidance.

I would finally like to acknowledge the support of my friends and family, particularly my parents, Lorcan and Marie, whose constant encouragement has given me the confidence to succeed at every step of my education. I would also like to thank my brother Eoin, who never hesitated to point out when I was procrastinating, and my sister Saragh who has encouraged me over many cups of coffee throughout the last four years.

And last of all, I would like to thank my girlfriend Jenny. She has supported me throughout my PhD, has lived with me through most of it, and has shared with me the highs and lows of each and every one of those days. I simply could not have done this without her. I will always be grateful to her, and in awe of her strength and her boundless kindness. This thesis, my PhD, and these last four years are dedicated to her.

LIST OF ABBREVIATIONS

Abbreviation	Description
αVβ5	Alpha V beta 5 integrin
AAV	Adeno-associated virus
Ad	Adenovirus
APC	Antigen presenting cell
BSA	Bovine serum albumin
cαMEM	Complete modified Eagle's medium alpha
Cap	AAV capsid open reading frame
CD	Cluster of differentiation
cDMEM	Complete Dulbecco's modified Eagle's medium
cDNA	Complementary DNA
CFSE	Carboxyfluorescein diacetate, succinimidyl ester
CFU-F	Colony forming unit-fibroblastic
CTL	Cytotoxic T lymphocyte
CPM	Counts per minute
cRPMI	Complete Roswell Park Memorial Institute medium
DC	Dendritic cell
EB/AO	Ethidium bromide / acridine orange
EDTA	ethylenediaminetetraacetic acid

ELISA	Enzyme-linked immunosorbent assay
EtBr	Ethydium bromide
FCS	Fetal calf serum
FITC	Fluorescein Isothiocyanate
GAPDH	Glyceraldehyde 3-phosphate dehydrogenase
HEK-293	Human embryonic kidney cell line
HGF	Hepatocyte growth factor
HLA	Human leukocyte antigen
HPLC	High pressure liquid chromatography
HSPG	heparin sulphate proteoglycan
IBMX	3-isobutyl-methyl-xanthine
IDO	indoleamine-pyrrole 2,3-dioxygenase
IgG	Immunoglobulin G
IgM	Immunoglobulin M
IFN-γ	Interferon gamma
IL-10	Interleukin 10
IL-13	Interleukin 13
ITR	AAV inverted terminal repeat
MHC	Major histocompatibility complex
mRNA	Messenger RNA
MSC	Mesenchymal stem cell
ORF	Open reading frame

PBMC	Peripheral blood mononuclear cell
PBS	Phosphate buffered saline
PE	Phycoerythrin
PGE2	Prostaglandin E2
RT-PCR	Reverse transcriptase polymerase chain reaction
Rep	AAV replication open reading frame
TGF-β	Transforming growth factor beta 1
Th	T helper
TNF-α	Tumor necrosis factor alpha
Treg	T regulatory
VP1	AAV capsid protein

PEER-REVIEWED PUBLICATIONS

D. Madsen, E. R. Cantwell, P. A. Johnson, T. O'Brien, B.P. Mahon (2009) AAV-2 induces cell-mediated immune responses directed against multiple epitopes of the capsid protein VP1. Journal of General Virology 90(11):2622-2633.

ABSTRACT

Adeno-associated virus serotype 2 (AAV-2) has been developed as a gene therapy vector. Antibody and cell-mediated immune responses to AAV-2 or AAV-2 transfected cells may confound the therapeutic use of such vectors in the clinic. In this study, cell-mediated and humoral immune responses to AAV-2 were characterised from a panel of healthy blood donors. The extent of AAV-2-specific antibody in humans was determined by examination of circulating AAV-2-specific total IgG levels in plasma from 45 normal donors. 41 donors were seropositive and responses were dominated by IgG1 and IgG2 subclasses. Conversely, AAV-2-specific IgG3 levels were consistently low in all donors. Cell-mediated immune recall responses were detectable in nearly half the population studied. *In vitro* re-stimulation with AAV-2 of peripheral blood mononuclear cell (PBMC) cultures from 16 donors elicited interferon-gamma (IFN-γ) (10 donors), interleukin-10 (IL-10) (8 donors) and interleukin-13 (IL-13) (4 donors). Using a series of overlapping peptides derived from the sequence of the VP1 viral capsid protein, a total of 59 candidate T-cell epitopes were identified. HLA characterisation of donors revealed that the population studied included diverse haplotypes, but that at least 17 epitopes were recognised by multiple donors and could be regarded as immunodominant. These data indicate that robust immunological memory is established to AAV-2. The diversity of sequences recognised suggests that attempts to modify the AAV-2 capsid, as a strategy to avoid confounding immunity, will not be feasible.

It was hoped that murine mesenchymal stem cells (MSC) might be amenable to transformation using an AAV-2-based vector, rendering the MSC as a potential platform to deliver transgene products whilst avoiding the immune memory for AAV-2 characterised herein. However, murine MSC appeared resistant to transduction using an AAV-2 GFP vector. To assess the impact of transfection of MSC with a plasmid vector, a lipofection protocol, utilising a plasmid encoding indoleamine 2,3-dioxygenase (IDO), was instead adopted. Transfection was successful, MSC morphology was not altered and osteogenic and adipogenic functions remained. However, MSC cell numbers in culture declined sharply in the 24 hours following transfection and growth rates were poor for up to 7 days. Cell surface markers were also altered, with increased MHC class I observed in transfected cultures. Perhaps most significantly, transfected MSC displayed a reduced capacity to suppress mitogen-driven lymphocyte proliferation. Further optimisation of the lipofection protocol might reduce MSC death and restore proliferation, but the observed changes in murine MSC immunomodulatory function as a result of IDO transfection coupled with the cell death and loss of proliferation indicates that lipofection is a suboptimal method for the transfection of murine MSC.

CHAPTER 1

INTRODUCTION

1.1 GENE THERAPY

Gene therapy is the treatment of genetic disorders by insertion of functional replacement genes or gene silencing sequences into a recipient's cells. At the time of writing, well over 1,300 clinical trials utilising some form of gene therapy had been completed, approved or were in progress (Edelstein *et al.*, 2007). Gene therapy may be mediated by a wide range of gene delivery systems including naked DNA (Nishikage *et al.*, 2004; Pevsner-Fischer *et al.*, 2007), silencing oligonucleotides (Uprichard, 2005), liposomal complexes (Felgner *et al.*, 1987) and recombinant viruses (McTaggart & Al-Rubeai, 2002; Robbins & Ghivizzani, 1998). Viral vectors have to date been the most popular gene delivery systems used in trials, being central to two thirds of all gene therapy trials as of 2007, with vectors based on the adenoviruses or retroviruses used in nearly 48% of clinical trials overall (Edelstein *et al.*, 2007). Of the studies reviewed by Edelstein *et al*., lipofection and naked DNA transfection comprised the bulk of non-viral delivery systems. The dominance of viral vectors may be a reflection of their key advantages. These vectors have well defined tissue tropisms, and their envelopes and capsids can be modified to alter tissue specificity (Grimm *et al.*, 2003). Viruses also possess natural means to efficiently transduce host cells, whilst naked DNA may be inefficient even *in vitro*, often requiring administration by gene gun or the target cells to be made chemically competent or to undergo electroporation (Nishizaki *et al.*, 2000; Roos *et al.*, 2009). Mammalian viruses, having co-evolved with humans and related species, are also more likely to have adapted means to avoid or subvert human immune responses, which in a therapeutic setting might help to minimise recipient immune recognition of vectors or transduced cells.

Despite these features, clinical trials utilising adenoviral and retroviral vectors have met with mixed results, including a number of high-profile serious adverse events. In 1999, an 18 year old male patient enrolled in a phase I trial to assess the safety of vectors based on adenovirus serotype 5 (Ad5) for the treatment of partial ornithine transcarbamylase, experienced massive systemic inflammation and multi-organ failure, dying 96 hours following administration of the vector into his right hepatic artery (Raper *et al.*, 2003). Three years later, a phase I trial investigating the use of retroviral vectors for the treatment of X-linked severe combined immunodeficiency (SCID-X1) (Cavazzana-Calvo *et al.*, 2000) was halted when two of the ten children enrolled developed a leukaemia-like condition confirmed to be a direct result of insertional mutagenesis into a proto-oncogene (Hacein-Bey-Abina *et al.*, 2003). After the trial was re-started, a third child developed a similar condition, though triggered by a different insertional mutation. Although two of the children responded to chemotherapy and went into remission, one did not respond and died in 2004 (Hacein-Bey-Abina *et al.*, 2008). The safety profile of vectors based on adenoviruses and retroviruses has since improved, with no further fatalities reported. However, these early failures, especially in such small patient cohorts, undermined confidence in these systems, prompting research into alternative viral systems which might reduce the risks of severe immune responses and oncogenesis. Amongst these were vectors based on the adeno-associated viruses (AAV) which have seen increasing use in clinical trials in recent years (Coura & Nardi, 2007; Edelstein *et al.*, 2007; Edelstein *et al.*, 2004).

1.2 ADENO-ASSOCIATED VIRUSES

1.2.1 Wild type AAV

AAV was first discovered as a contaminant of adenovirus (Ad) viral stocks in 1965 (Atchison *et al.*, 1965; Blacklow *et al.*, 1967). Due to the lack of an obvious pathology resulting from AAV infection, the virus received little attention until the advent of gene therapy. AAV belongs to the Parvoviridae family of single-stranded non-enveloped viruses. The virus particle is 20-25 nm in diameter and consists of a single-stranded DNA (ssDNA) genome of 4.6 kilobase length for AAV-2 (Srivastava *et al.*, 1983), (varying between 4.5- 5.0 kilobases depending on serotype) (Figure 1.1 A) enclosed within a capsid composed of 60 monomer subunits arranged into a structure with icosahedral symmetry, with three subunits comprising each face of the icosahedron (Figure 1.1 B) (Xie *et al.*, 2002). There are two open reading frames, Rep and Cap, flanked by two identical inverted terminal repeats (ITR), each 145 base pairs (bp) in length (Figure 1.1 A) (Janik *et al.*, 1984; Mendelson *et al.*, 1986). The Rep open reading frame encodes four non-structural proteins, Rep78, Rep68, Rep52 and Rep40 which are involved in the viral replication cycle (Figure 1.2). These have molecular masses of 78, 68, 52 and 40 kDa respectively (Mendelson *et al.*, 1986). The Cap open reading frame codes for three structural proteins VP1, VP2 and VP3 (87, 73 and 62 kDa respectively; Figure 1.2) (Janik *et al.*, 1984) each of which comprises one capsid subunit, with 60 subunit monomers forming a capsid in the stoichiometric ratio of 1:1:10 (Buller & Rose, 1978). The VP2 and VP3 products are produced by alternative

mRNA splicing of VP1 and by alternative start codon usage (Becerra *et al.*, 1988; Cassinotti *et al.*, 1988).

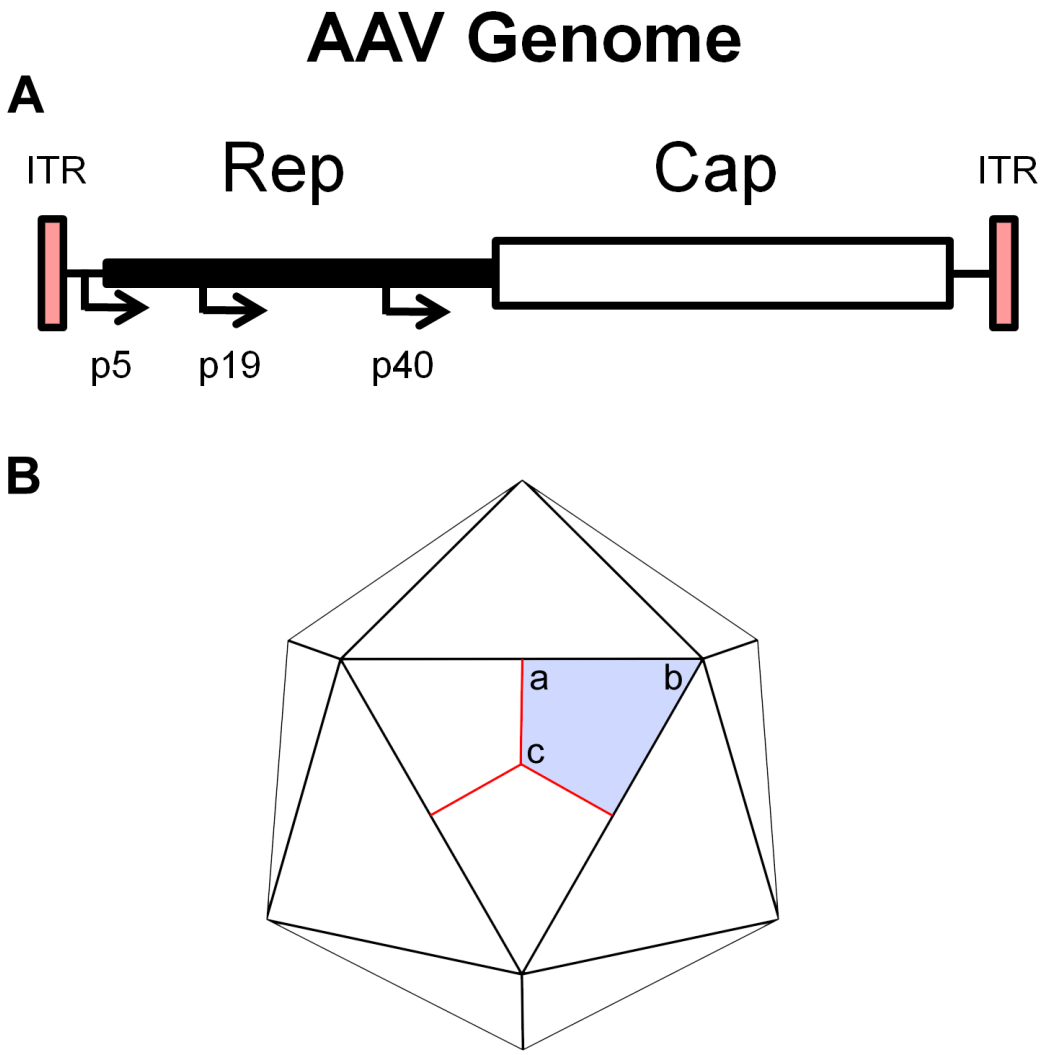

Figure 1.1 A schematic representation of the wild-type AAV genome (A) and the viral capsid (B). A) The ssDNA AAV genome is flanked by two ITR sequences and contains two open reading frames (Rep and Cap). There are three promoter regions (p5, p19 and p40). B) The viral capsid has T=1 icosahedral symmetry. Each of the 20 triangular faces is composed of three diamond-shaped subunits (example shaded blue) which are coded for by the Cap ORF. Thus the capsid is composed of 60 subunits. Each subunit meets its neighbours at three axes of icosahedral symmetry; the two-fold axis (a), the five-fold axis (b) and the three-fold axis (c). Figure 1.1 A was adapted by the author from Russell and Kay, 1999. Figure 1.1 B was rendered by the author, based on the structure determined by Xie *et al.*, 2002.

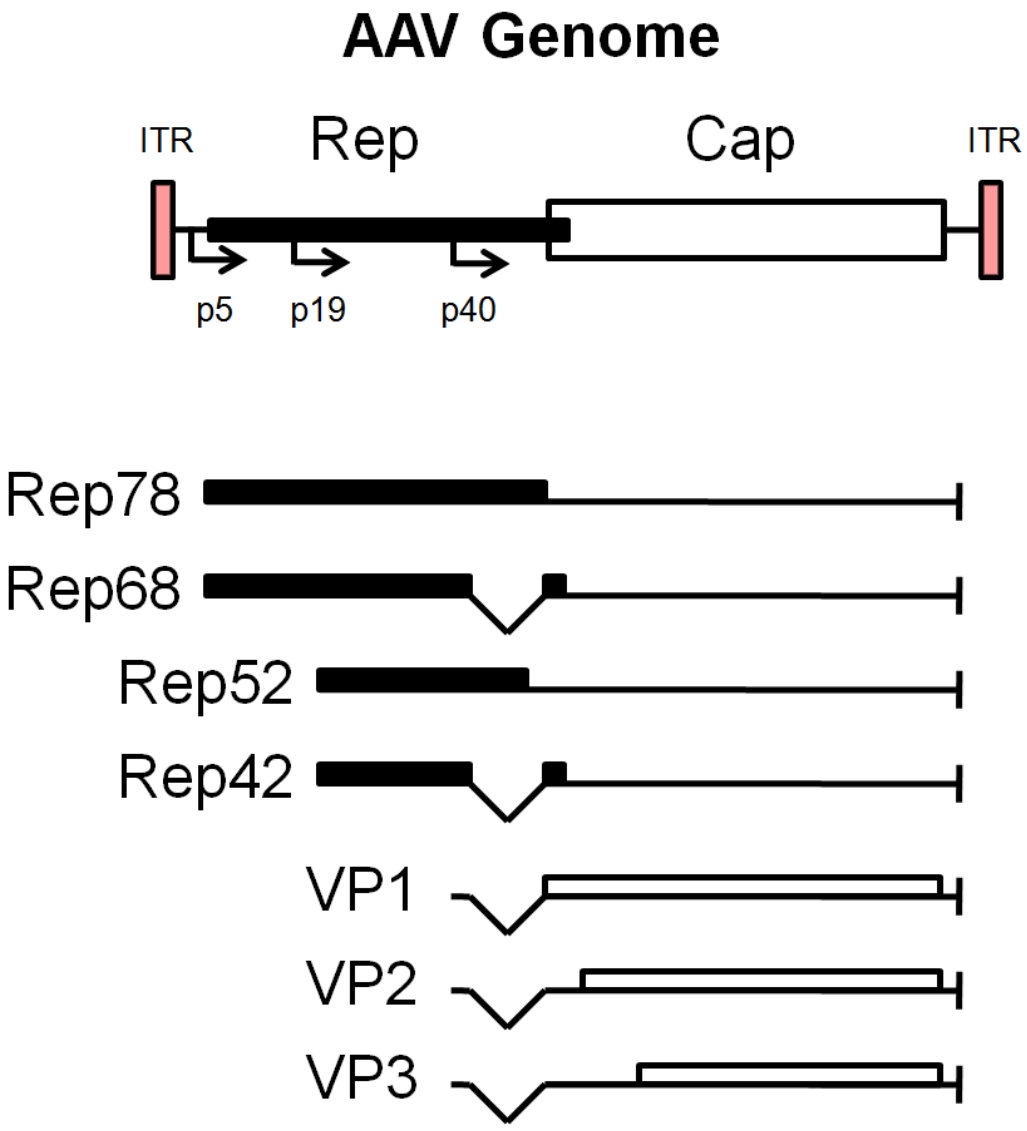

Figure 1.2 A schematic representation of the AAV-2 ssDNA genome and the gene products coded for by the Rep and Cap open reading frames. The Rep open reading frame codes for four non-structural products; Rep 78, Rep 68, Rep 52 and Rep 42. The Cap open reading frame codes for three capsid subunit monomers; VP1, VP2 and VP3. Each monomer acts as one of the 60 subunits of the viral capsid shown in Figure 1.1 B. Figure 1.2 adapted by the author from Russell and Kay, 1999.

At least eleven AAV serotypes, primarily differentiated by their immunoglobulin binding affinities, have been characterised to date (Atchison *et al.*, 1965; Blacklow *et al.*, 1967; Chiorini *et al.*, 1999; Mori *et al.*, 2004; Muramatsu *et al.*, 1996). AAV-2, 3, and 5 were isolated from human clinical specimens (Chiorini *et al.*, 1999). AAV-1 and 4 are of simian origin, although serotype 1 can infect humans (Atchison *et al.*, 1965). AAV-6 is considered to have arisen from a recombination of AAV-2 and AAV-1 due to co-infection, based on its similarity to AAV-1 and analysis of its genome (Rutledge *et al.*, 1998). AAV-7 and AAV-8 were isolated from rhesus monkey (Gao *et al.*, 2002), whilst serotypes 10 and 11 were identified in cynomolgus monkeys (Mori *et al.*, 2004).

The replication cycle of AAV has not been fully characterised (Douar *et al.*, 2001; Straus *et al.*, 1976; Xiao *et al.*, 2002). AAV is a replication defective and helper-dependent virus and requires co-infection with a helper virus such as Herpes virus, Vaccinia virus or Adenovirus (Ad) in order to complete its replication cycle (Atchison, 1970; Atchison *et al.*, 1965; Buller *et al.*, 1981; Schlehofer *et al.*, 1986). The exact mechanism of cell entry of many non-enveloped viruses is not known, and this is the case for many AAV serotypes. The primary receptor for cell surface binding of AAV-1 has not been identified. Serotypes 7 and 8 also have no known receptor, but they share close structural homology with AAV-1 and therefore may share a common receptor (Gao *et al.*, 2002). The primary receptor for AAV-2 is heparin sulphate proteoglycan (HSPG) (Summerford & Samulski, 1998). It appears that HSPG may, at least in part, determine the ability and efficiency of AAV serotypes to infect cells. Thus, the low levels of HSPG present on the lung epithelium may account for the difficulties facing

AAV-2 transduction of lung epithelial cells *in vivo* (Duan *et al.*, 1998; Halbert *et al.*, 1997).

The alpha V beta 5 (αVβ5) integrin and fibroblast growth factor-1 (FGF-1) are also involved as co-receptors in AAV-2 internalisation (Qing *et al.*, 1999; Summerford *et al.*, 1999). AAV-4 and 5 require the presence of membrane associated 2,3-linked sialic acid in order to have a tropism for lung epithelial cells (Walters *et al.*, 2001). Binding of these serotypes is not identical however, with AAV-5 binding sialic acid on *N*-linked carbohydrates, whereas AAV-4 interacts with sialic acid on *O*-linked carbohydrates (Walters *et al.*, 2002). Although it has been shown that AAV-3 interacts with HSPG in a similar manner to AAV-2 (Opie *et al.*, 2003), it is unclear whether this interaction is relevant to internalisation. Attempts to block transduction of lung epithelium by AAV-6 using soluble heparin sulfate (HS) do not demonstrate any significant neutralising effect (Halbert *et al.*, 2001), suggesting that this serotype does not require HS binding.

Following HSPG binding, AAV-2 is internalised via clathrin coated pits, possibly with the help of the αVβ5 receptor integrin (Summerford *et al.*, 1999). Mutagenesis of the capsid domain that interacts with αVβ5 reduces AAV-2 transduction of HEK-293 cells by one order of magnitude (Asokan *et al.*, 2006). Once internalised into the early endosome the acidic pH allows the virus to be released into the cytosol by a poorly understood process (Douar *et al.*, 2001). In the cytosol the virus migrates to the perinuclear compartment and translocates to the nucleus to unload the virus genetic material. Unpacking of the viral genome may occur shortly prior to or during nuclear

entry via the nuclear pore complex in the absence of a helper virus but when co-infected with Adenovirus helper, translocation appears more rapid and disassembly of the capsid occurs after nuclear entry (Xiao *et al.*, 2002). Following the release of genetic material, single-stranded AAV genomes convert to double-stranded forms and concatemers (Straus *et al.*, 1976; Vincent-Lacaze *et al.*, 1999). Replication is facilitated by the ITR which each form a T-shaped hairpin loop structure which allows self-priming activity at the free 3' hydroxyl group (Figure 1.4) (Hauswirth & Berns, 1979). In the absence of helper viruses AAV may preferentially integrate into a locus of chromosome 19 (19q13-qter, henceforth referred to as AAVS1) at a low frequency (Cheung *et al.*, 1980). AAV appears to package the ssDNA genome into preformed capsid particles, possibly via pores located at the five-fold axes of symmetry, mutation of which reduces packaging efficiency (Bleker *et al.*, 2006). The newly assembled virus particles are released from the host cell following helper virus-mediated cell lysis (Goncalves, 2005).

1.2.2 AAV as a gene therapy vector

Several serotypes of AAV have been investigated for use as gene therapy vectors or recombinant vaccine vehicles (Arruda *et al.*, 2005; High *et al.*, 2004; Kaplitt *et al.*, 2007; Moss *et al.*, 2007; Moss *et al.*, 2004; Wagner *et al.*, 2002; Zhang *et al.*, 2003). A selection of trials approved, completed and ongoing is summarised in Table 1.1. A number of features of AAV make it an attractive vector for gene therapy. AAV has the ability to transduce a wide range of dividing and non-dividing cell types and thus could target a great number of chronic genetic disorders such as haemophilia B, cystic fibrosis

and alpha-1-antitrypsin deficiency (Mueller & Flotte, 2008). Although the small genome of AAV limits its cloning capacity to about 4.4 kb (Dong *et al.*, 1996), this is still large enough to contain reporter genes, such as *GFP* and *Lac-Z* as well as therapeutic genes such as the cystic fibrosis transmembrane regulator (*CFTR*) gene for the treatment of cystic fibrosis (Wagner *et al.*, 1999) and the factor IX (*F.IX*) gene for the treatment of haemophilia B (Monahan *et al.*, 1998). Even with the full coding sequence of these genes included, tissue-specific regulatory sequences have also been successfully incorporated into AAV vectors. It is notable however, that even insertion of these relatively short sequences requires the removal of the entire viral genome, except for the ITR sequences (Figure 1.3), which are required for DNA packing into the capsid during vector preparation (Tratschin *et al.*, 1984). By far the most popular and best characterised AAV serotype used in clinical studies is AAV-2 (Mueller & Flotte, 2008), which will be the main focus for the remainder of this chapter.

Table 1.1 Selection of clinical trials currently approved by the US FDA as of February 2008[a]

Indication/transgene	Serotype	Route	Clinical phase	Status
alpha-1-Anitrypsin Deficiency/AAT	AAV-1	intramuscular	Phase I	Active
alpha-1-Anitrypsin Deficiency/AAT	AAV-2	intramuscular	Phase I	Completed
Alzheimer's/Nerve Growth Factor (B-NGF)	AAV-2	intracranial	Phase I/II	Inactive
Amaurotic Familial Idiocy (Batten's)/CLN2	AAV-2	intracranial	Phase I	Active
Arthritis/TNFR:Fc (tgAAC94)	AAV-2	intra-articular	Phase I	Completed
Arthritis/TNFR:Fc (tgAAC94)	AAV-2	intra-articular	Phase I/II	Active
Canavan's disease/aspartoacylase	AAV-2	intracranial	Phase I	Active
Cardiac failure/SERCA2a	AAV-6	intracardiac	Phase I	N/A
Cardiac failure/SERCA2a	AAV-1	intracardiac	Phase I	N/A
Cystic fibrosis/CFTR	AAV-2	intranasal	Phase I	Completed
Cystic fibrosis/CFTR	AAV-2	aerosol	Phase I	Completed
Cystic fibrosis/CFTR (tgAAVCF)	AAV-2	aerosol	Phase I	Inactive
Cystic fibrosis/CFTR (tgAAVCF)	AAV-2	intrasinusal	Phase I/II	Inactive
Duchenne muscular dystrophy/mini-dystrophin	AAV-5		Phase I	N/A
Epilepsy/neuropeptide Y (NPY)	AAV-1, 2	intracranial	Phase I	N/A
Factor IX deficiency/Factor IX minigene	AAV-2	intramuscular	Phase I	Completed
Factor IX deficiency/Factor IX minigene	AAV-2	intra-arterial	Phase I	Completed
Leber congenital amaurosis (Retinal degeneration)/RPE65	AAV-2	intraocular	Phase I	Active
Leber congenital amaurosis (Retinal degeneration)/RPE66	AAV-2	intraocular	Phase I	N/A
Limb girdle dystrophy/Gamma sarcoglycan	AAV-2		Phase I	N/A
Limb girdle dystrophy/Gamma sarcoglycan	AAV-1		Phase I	N/A
Parkinson's disease/GAD65	AAV-2	intracerebral	Phase I	Completed
Parkinson's disease/hAADC	AAV-2	intracerebral	Phase I	Active
Parkinson's disease/Secreted neurturin (Cere-120)	AAV-2	intracranial	Phase I	Completed
Parkinson's disease/Secreted neurturin (Cere-120)	AAV-2	intracranial	Phase II	Active
Parkinson's disease/GAD65	AAV-2	intracerebral	Phase II	N/A

[a] Data derived from multiple sources as reviewed in Mueller *et al*. (Mueller & Flotte, 2008)

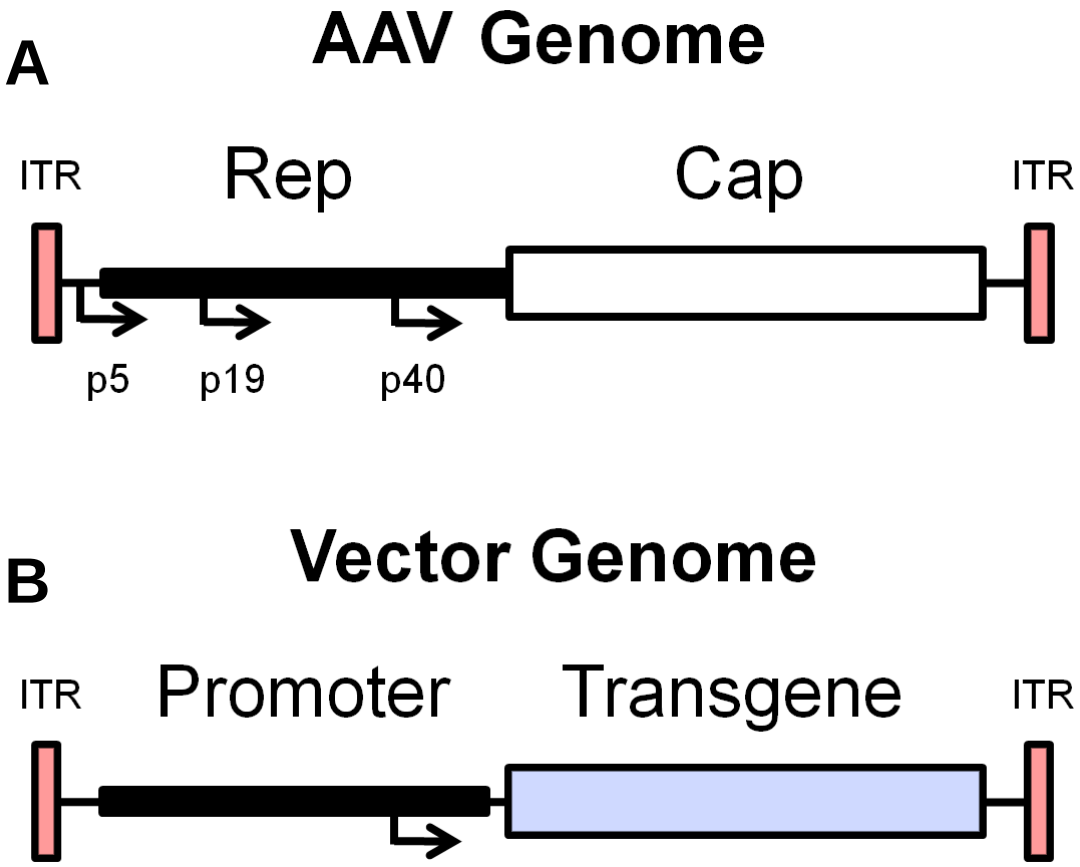

Figure 1.3 A schematic representation of the AAV-2 genome compared to a generalised recombinant AAV vector genome comprising a promoter and a transgene. In the vector, both the Rep ORF and Cap ORF are excised entirely, leaving the ITR sequences as the only remaining endogenous viral DNA in the vector. Figure 1.3 adapted by the author from Russell and Kay, 1999.

As mentioned in Section 1.2, AAV may integrate site-specifically into the host genome (Cheung *et al.*, 1980; Kotin *et al.*, 1990). This further enhances the appeal of AAV as a gene therapy vector, as integration of a transgene might allow for stable expression, thereby eliminating the need for re-administration. The ITR sequences, which each consist of a single strand of DNA in a T hairpin loop, contain a terminal resolution site (TRS), a Rep product binding site (RBS) as well as an exposed 3' hydroxyl terminus (Figure 1.4), have a priming activity during viral replication and are involved in integration but do not control the specificity of integration (Russell & Kay, 1999). The specificity of integration instead appears to be controlled by products of the Rep ORF, which is generally removed in vector preps (Weitzman *et al.*, 1994). It is unclear whether this specificity can be retained in a vector whilst still maintaining a useful cloning capacity. A loss of site-specificity raises the risk of a detrimental integration, potentially resulting in a loss of function mutation or perhaps oncogenesis, however it remains to be seen whether integration can be induced to occur with useful frequency, site-directed or otherwise.

AAV serotypes have widely varying tissue tropisms (Table 1.2). AAV-1, for example, preferentially infects muscle tissue (Chao *et al.*, 2000), whereas AAV-2 can infect a number of tissues such as muscle and the central nervous system but preferentially infects liver and kidney cells. AAV-3 infects hematopoietic stem cells, and AAV-5 has a tissue tropism for the retina (Rabinowitz *et al.*, 2004). As new applications of the vectors based upon these serotypes are investigated, further tissue tropisms are being revealed (Wu *et al.*, 2006).

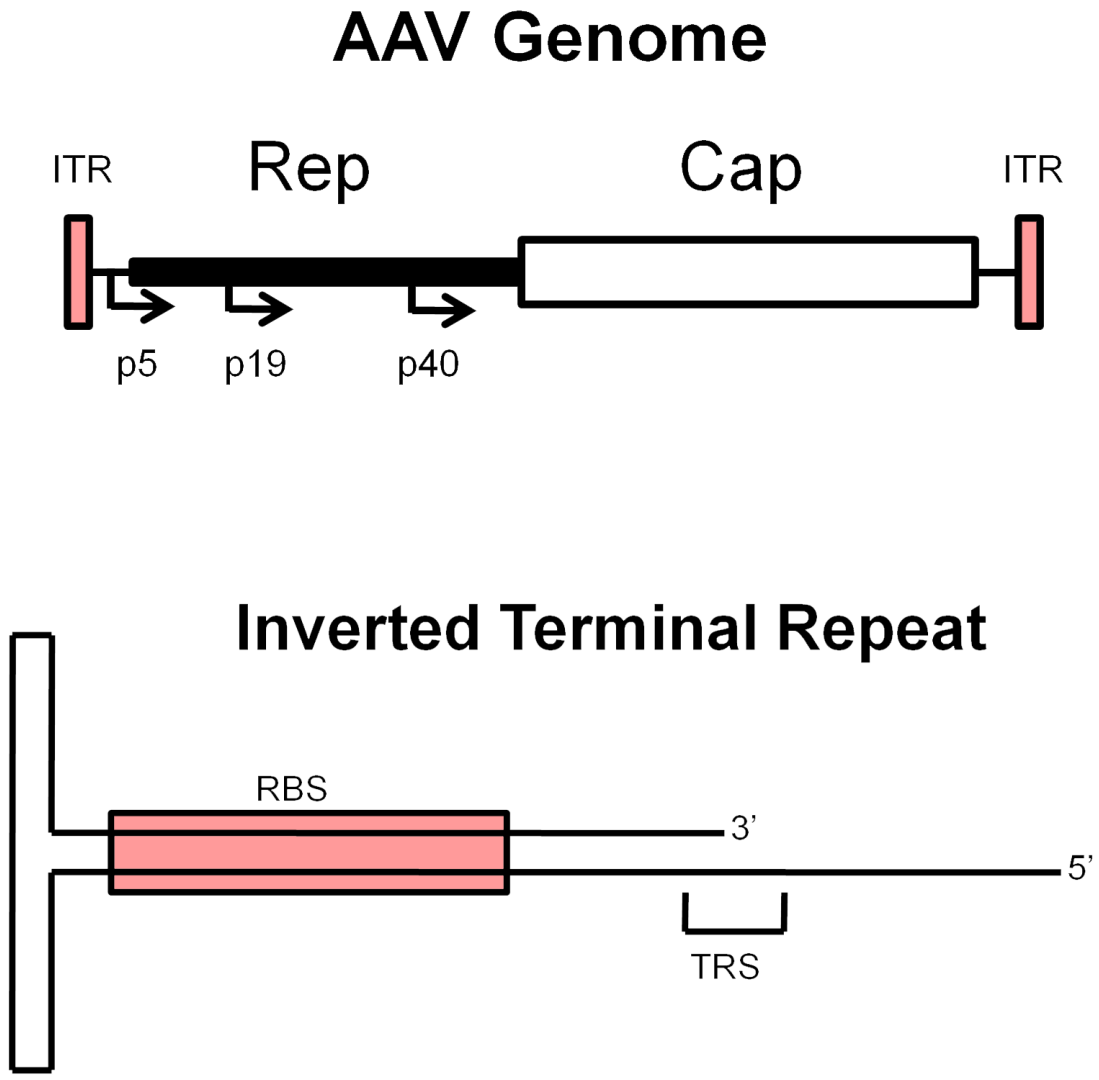

Figure 1.4 Expanded schematic view of the secondary structure of one of the ITR flanking regions of the wild type and vector AAV-2 genomes. The ITR consists of a single strand of DNA in a T hairpin loop. The ITR also contains a terminal resolution site (TRS), a Rep product binding site (RBS) as well as an exposed 3' hydroxyl terminus. Figure 1.4 adapted by the author from Russell and Kay, 1999.

Table 1.2 AAV tissue tropisms[a]

Tissue	Known infecting serotypes
Liver	2, 8, 9
Skeletal muscle	1, 2, 6, 7, 8, 9
CNS	1, 2, 4, 5
Retina	4, 5
Photoreceptor cells	5
Lung	9
Heart	8
Pancreas	8
Kidney	2

[a] Data derived from multiple sources as reviewed by Wu *et al*., 2006.

By far the most attractive feature of AAV as a vector is the apparent lack of a significant inflammatory response, which has been examined in recombinant infection studies in animal models (Zaiss *et al.*, 2002). Nevertheless, there is clearly some form of immune memory to AAV in humans, as evidenced by extensive evidence of AAV specific antibodies in approximately 80% of sampled populations (Chirmule *et al.*, 1999; Erles *et al.*, 1999). Numerous studies have demonstrated that humoral memory for AAV-2 may impact negatively on transduction (Halbert *et al.*, 1997; Xiao *et al.*, 1999; Xiao *et al.*, 2000). Although there was little evidence of cell-mediated recognition of AAV in humans at the commencement of this study (Chirmule *et al.*, 1999), more recent work has suggested that AAV may induce some cytotoxic responses (Chen *et al.*, 2006; Manno *et al.*, 2006; Sabatino *et al.*, 2005). It is possible that, given the poor inflammatory responses, the initiation of this memory may be heavily influenced by inflammation in response to the presence of pathogenic helper viruses during natural infection (Atchison, 1970; Buller *et al.*, 1981; Schlehofer *et al.*, 1986). Because adaptive immunity to AAV-2 is induced, it is clear that understanding of the immune response to the virus must be improved if AAV vectors are to be used effectively in a clinical setting.

1.3 IMMUNE RESPONSES TO AAV AND AAV VECTORS

1.3.1 Innate immunity to AAV-2

The modesty of AAV-specific immune responses reported to date have suggested a reduced risk of vector or transduced cell destruction following administration (Zaiss *et al.*, 2002; Zaiss & Muruve, 2005). The innate immune response to AAV-2 appears to be weak and transient in animal models and *in vitro* (Ohshima *et al.*, 2008; Stilwell & Samulski, 2004; Zaiss *et al.*, 2002). In mice, transient type 1 interferon and TNF-α mRNA production was shown to be induced following AAV-2 transduction of the liver (Zaiss *et al.*, 2002). Despite this, there was no detection of IFN-γ, IL-6 or IL-1β in that study. Similarly, transient expression of the chemokines RANTES, MIP-1β and MIP-2 has been observed in mouse models but only at exceptionally high AAV-2 doses (1×10^{11} total particles) (Zaiss *et al.*, 2002).

The response in the murine liver appears to be entirely dependent on the presence of liver dendritic cells (DC) (Zaiss & Muruve, 2005) as depletion of these cells appears to abrogate the innate response. Macrophage inhibitory cytokine (MIC-1) and interferon-induced staf50 are increased in fibroblasts cell cultures exposed to AAV capsid proteins (Stilwell & Samulski, 2004) and some infiltration of neutrophils, monocytes and NK cells is observed in livers of mice inoculated with AAV-2 (Zaiss *et al.*, 2002). In another animal model, canine bone marrow-derived DC could be activated by AAV-2 transfection and led to elevated CD80, CD86 and IFN-β mRNA (Ohshima, Shin *et al*. 2008). Despite these data, little is known about the course of the innate response to primary AAV-2 infection in humans, beyond the prevalence of

infection (Blacklow *et al.*, 1968b; Gao *et al.*, 2004). AAV-2 sequences have been detected in the total cellular DNA of greater than 6% of adult humans, with most frequent detection in the liver and bone marrow (Gao *et al.*, 2004). AAV-2 was also isolated from 23% of children examined in an US nursery population (Blacklow *et al.*, 1968a).

The classical complement pathway is only induced weakly by high titres of AAV-2 and the virus does not activate the alternative complement pathway (Zaiss *et al.*, 2008). The AAV-2 capsid binds complement protein iC3b and Factor H, both of which regulate the complement cascade by blocking the cleavage of C3 into C3a and C3b (Zaiss *et al.*, 2008). The prevalence of active AAV-2 infection and the viral tropism for the liver, raise the possibility that innate responses in humans might resemble those seen in mice; however no immunological data are available on the response to AAV-2 in human tissues.

1.3.2 Adaptive immunity to AAV-2

The introduction of an AAV vector into an organism presents the adaptive immune system with two potential targets. Firstly there is the transgene product, which could be presented in the context of MHC class I on the target cell. However, an immune response to a transgene product is not an issue specific to AAV-based vectors, unless it is found that the vector itself in some way modulates that response. The second potential target is the vector itself, processed elements of which might be presented to

$CD8^+$ cytotoxic T-cells via MHC class I molecules on target cells or MHC II on professional antigen presenting cells (APC), if APC are transduced or have engulfed vector particles. It is also possible that both phagocytic cells and the vector target cells might process the exogenous protein of the viral vector via an alternative antigen processing pathway (cross-presentation) and present the resulting peptides in the context of MHC class I (Peter *et al.*, 2005). The vector capsid may also be recognised by the humoral response, being either directly recognised by naive B cells or via T-cell-dependent or independent activation. AAV does not carry any matrix proteins within the capsid at the time of infection, a factor which limits the number of potential exogenous antigens to the VP capsid proteins only.

Despite the modest innate responses to AAV-2 (Ohshima *et al.*, 2008; Zaiss *et al.*, 2002), observation of the adaptive humoral response in animal models has demonstrated that AAV-2 infection consistently generates robust primary responses including neutralising antibody (Chirmule *et al.*, 2000; Halbert *et al.*, 1997; Halbert *et al.*, 1998; Xiao *et al.*, 1999; Xiao *et al.*, 2000). The humoral immune response to AAV-2 has been characterised in humans, but with varied reports of seroprevalence between 30-96% depending on the population sampled (Chirmule *et al.*, 1999; Erles *et al.*, 1999; Halbert *et al.*, 2006). This broad range might reflect the lack of standardised methods for assessing AAV-2 serology. AAV-2 infection is thought to have occurred in at least 20% of humans before the age of 10 years (Erles *et al.*, 1999). The detection of AAV DNA in amniotic fluid also suggests that virus may be present at birth in many humans,

possibly due to reactivated latent infection in the mother during pregnancy (Tobiasch *et al.*, 1994).

The cell-mediated adaptive immune response to AAV has received little attention and there has been some assumption that AAV does not provoke a significant response (Büning *et al.*, 2003; Hernandez *et al.*, 1999). The detection of AAV-2-specific IgM (Erles *et al.*, 1999) might indicate that AAV-2 behaves like a T-cell independent antigen. However there is evidence of notable cell-mediated responses to AAV-2 from a recent gene therapy trial which reported declining transgene expression and indications of tissue damage, with a concurrent $CD8^+$ cytotoxic T-cell response (Manno *et al.*, 2006). Mouse models have since been used to characterise some $CD8^+$ T-cell responses to AAV-2 in greater detail, demonstrating that exogenously-derived AAV-2 capsid epitopes are cross-presented to $CD8^+$ cytotoxic T-cells and that cytotoxic responses can be directed against transduced cells (Chen *et al.*, 2006; Li *et al.*, 2009; Li *et al.*, 2007; Wang *et al.*, 2007). However inbred mouse strains display limited MHC diversity in comparison to the highly polymorphic human HLA genes, and cell-mediated immunity in mice may not reflect immunity in human populations.

The detection of $CD8^+$ recognition of AAV-2 implies the presence of $CD4^+$ T helper cell responses, as these are typically a pre-requisite for cytotoxic responses. There is some evidence of $CD4^+$ helper T-cell responses to AAV-2 capsids in humans (Chirmule *et al.*, 1999) and mice (Chen *et al.*, 2006). Chirmule's group observed PBMC proliferation along with some IFN-γ production in cultures from a small subset of human donors, a finding suggestive of a Th1 response. Chen's group identified MHC

class II restricted epitopes on the AAV-2 capsid which stimulated IFN-γ production in mouse T-cells, again indicating $CD4^+$ recognition. The modest $CD4^+$ responses observed to date contrast with the robust CD4+ recall responses to the related Parvovirus B19 (B19V) previously found in PBMC cultures from late convalescent adults (Corcoran *et al.*, 2000). Based on the emerging data on cellular responses to AAV-2 in humans and animal models, it is clear that the cell-mediated response to AAV-2 needs further characterisation in the natural host if the virus is to be used confidently in a clinical setting.

1.4 STEM CELLS

In 1908 Alexander Maksimov suggested the use of the term "stem cell" to describe cells of a highly potent nature which he had earlier postulated to exist in the bone marrow (Maximow, 1906). However, the stem cell hypothesis remained unsupported until 1963 when McCulloch and Till demonstrated the colony-forming capacity of a subpopulation of spleen cells (Siminovitch *et al.*, 1963). They also showed that the colony forming cells were clonal in nature (Becker *et al.*, 1963). This work demonstrated one of the key traits now associated with stem cells; extended self-renewal in an undifferentiating state. Embryonic stem cells were first isolated from the blastocyst stage of murine embryo development in 1981 (Martin, 1981) but it was not until 1998 that embryonic stem cells could be reliably isolated from human blastocysts and cultured (Thomson *et al.*, 1998). Ethical issues surrounding embryonic stem cell research, in particular issues pertaining to the storage and usage of human embryos in

research, have hampered the development of the field considerably (Wert & Mummery, 2003). However, research into various forms of adult-derived stem cells has continued apace since their initial characterisation in cord blood samples in 1978 (Prindull *et al.*, 1978).

Stem cells are a highly diverse group of cells sharing a number of key features which make them of interest in therapeutic research. The cells are typically defined in functional terms as being unspecialised, self-renewing cells which may differentiate *in vivo* to generate cells of a specific tissue type or of multiple different types (Moore & Lemischka, 2006). Thus the two key features used to classify stem cells are typically the capacity for self-renewal and the capacity to produce specialised cells. Differentiation should arise from asymmetric cell division, whereby two daughter cells are generated; one remaining of the stem cell type and the other differentiating into a specialised cell type. On the basis of the extent of this development potential, potency, plasticity or differentiation capacity, stem cells may broadly classified as totipotent, pluripotent or multipotent (Martinez-Agosto *et al.*, 2007; Temple, 2001).

Totipotent stem cells are capable of producing cells of all types either directly or via further differentiation into less potent stem cells (Mountford, 2008). This potency extends to the production of extraembryonic cells such as the cells of the amniotic membrane and placenta. The pluripotent cells of the blastocyst, by contrast cannot produce extraembryonic cells but can differentiate into less potent stem cells of all three germ layers; the endoderm, mesoderm and ectoderm which give rise to all of the tissues and organs of triploblastic animals (Martinez-Agosto *et al.*, 2007). The stem cells of

these layers are typically referred to as multipotent and are typically capable of differentiation into cells of only their specific germ layer or tissue origin.

Multipotent stem cells are not confined to the tissues of developing embryos or foetuses but can be found in many tissues of adult animals (Mountford, 2008). Typically these multipotent cell types function to replace dead or damaged cells in their respective tissues. The perception that adult stem cells were typically unipotent and thus less flexible in differentiation function than ES cells resulted in a much greater focus on ES cells in therapeutic research. However, the observation that adult stem cells may display multipotency (Jackson *et al.*, 1999) and possibly pluripotency (Verfaillie, 2002) has generated renewed interest in adult stem cell lineages as therapeutic agents.

First identified and studied amongst the adult stem cells initially were the hematopoietic stem cells (HSC) found in the bone marrow (Shizuru *et al.*, 2005), peripheral blood and cord blood (Prindull *et al.*, 1978). These cells were shown firstly to restore cell populations of the hematopoietic lineage (Hellman *et al.*, 1970) and later cells of non hematopoietic lineage such as muscle, liver and lung (Jackson *et al.*, 1999; Krause *et al.*, 2001; Lagasse *et al.*, 2000). The cells are relatively well characterised in terms of cell surface markers, with CD34 generally considered to be a marker for hematopoietic potential, although this appears to vary over the developmental lifetime of the cell (Matsuoka *et al.*, 2001).

Another population of stem-like cells is found in the bone marrow, termed mesenchymal stem or marrow stromal cells (MSC), a cell type first identified by Friedenstein in 1966. The cells were fibroblast-like, adherent cells growing in bone

marrow cell culture (Friedenstein & Petrokova, 1966). MSC form part of the stromal trabecular scaffold, a structure closely associated with the endosteum and which interacts with hematopoietic stem cells (HSC) (Sakaguchi *et al.*, 2004). Human MSC were first isolated from postnatal bone marrow (Friedenstein *et al.*, 1974). They have been identified in diverse tissues such as skeletal muscle (Jankowski *et al.*, 2002), adipose tissue (De Ugarte *et al.*, 2003; Gronthos *et al.*, 2001), periosteum, trabecular bone and deciduous dental pulp (Miura *et al.*, 2003). In their undifferentiated state, MSC are spindle-shaped adherent cells (Friedenstein & Petrokova, 1966). Irrespective of origin, these cells have the capacity for extended self-renewal in an unspecialised state in culture. They also have the potential to differentiate into cartilage, bone, adipose tissue, skeletal and cardiac muscle, tendon, ligament, neural precursors, endothelial cells and pancreatic islet cells (Chen *et al.*, 2004; Crigler *et al.*, 2006; Ogura *et al.*, 2004; Oswald *et al.*, 2004; Pittenger *et al.*, 1999; Wakitani *et al.*, 1994).

Although MSC have been isolated from diverse tissues, the bone marrow remains the best characterised source, with an estimated prevalence of between 0.001% and 0.01% of the total bone marrow cell population (Pittenger *et al.*, 1999). Despite being relatively rare in the marrow, MSC are readily isolated and expanded *in vitro* by isolation of mononuclear cells and culture of adherent cells in medium containing FCS (Bruder *et al.*, 1997).

1.5 MESENCHYMAL STEM CELLS

A definitive characterisation of MSC remains a challenge, with many sources in the literature providing vague or conflicting definitions (Bianco *et al.*, 2008). Cell populations that might also be defined as MSC are also often identified as marrow stromal cells or marrow progenitor cells. Differences in phenotypic and functional characteristics are likely to be due to the lack of agreed methods for MSC isolation. There are significant differences between research groups regarding tissue origin, isolation methods and culture conditions (D'Ippolito *et al.*, 2004; Kucia *et al.*, 2006; Pittenger *et al.*, 1999).

Another source of ambiguity is the lack of any unique cell surface marker for human MSC. Despite these conflicts, some consensus can be found amongst the research groups as to how MSC are defined. Cell surface receptors such as Stro1, CD29, CD44, CD73, CD90, CD105 and CD166 are typically expressed on MSC regardless of tissue of origin (Barry *et al.*, 2005; Ryan *et al.*, 2005). By contrast, it is agreed that hematopoietic lineage markers such as CD11b, CD14 and CD45 should not be expressed (Barry *et al.*, 2005; Ryan *et al.*, 2005). A similarly conflicting set of data defines MSC functional characteristics. It is generally agreed that MSC adhere to tissue culture grade plastic within the first 5 days of culture isolation, that they should form fibroblast-like colonies and display a fibroblast-like, stellate or spindle-like morphology (Pittenger *et al.*, 1999). Also, MSC are multipotent and can differentiate into fibroblasts, osteocytes, chondrocytes and adipocytes (Chen *et al.*, 2004; Crigler *et al.*, 2006; Ogura *et al.*, 2004; Oswald *et al.*, 2004; Pittenger *et al.*, 1999; Wakitani *et al.*,

1994). Murine MSC share similar phenotypic and functional traits, some MHC class I surface expression along with Sca-1, CD44, CD90, CD105, CD106, but no MHC class II, CD11b, CD11c, CD14 or CD45 (English *et al.*, 2007).

The bone marrow can also give rise to a number of cell populations with stem cell-like properties, but which differ from MSC. One population, termed multipotent adult progenitor cells (MAPC), are indirectly isolated from marrow tissue, from long-term culture (Jiang *et al.*, 2002b). Isolation was initially from culture of greater than 6 months in media supplemented with epidermal growth factor (EGF), platelet-derived growth factor (PDGF-BB), and leukaemia inhibitory factor (LIF). These cells have been isolated from human, mouse and rat long-term culture. They are characterised phenotypically as expressing SSEA-1, Oct-3, Oct-4 and Rex-1 but being negative for cKit, MHC I, MHC II, CD31, CD34, CD44 and CD45 (Reyes & Verfaillie, 2001). Functionally, the cells display a capacity to differentiate *in vitro* beyond mesenchymal cell types to give astrocytes, endothelial cells and hepatocytes (Jiang *et al.*, 2002a). It has also been shown that these cells can be isolated from diverse mouse tissues such as the brain and skeletal muscle (Jiang *et al.*, 2002b).

Marrow-isolated adult multilineage-inducible (MIAMI) cells are another multipotent bone marrow population (D'Ippolito *et al.*, 2004). The cells are isolated by adhesion to fibronectin coated dishes. They express the Oct-4 and Rex-1 transcription factors under hypoxic culture conditions and have been shown to differentiate into the mesenchymal stem cell lineages as well as neural and pancreatic lineages (D'Ippolito *et al.*, 2004). In 2006, a population of very small embryonic-like (VSEL) cells was

isolated from murine bone marrow. VSEL cells are phenotypically positive for Sca-1, CD45, SSEA-1 and positive for the transcription factors Oct-4, Nanog, Rex-1 and Rif-1 (Kucia *et al.*, 2006). When cultured using a sarcoma feeder cell layer, VSEL cells form embryoid bodies (Kucia *et al.*, 2006). Another population with similarities to MSC were isolated from human cord blood. The cells, dubbed unrestricted somatic stem cells (USSC), display a capacity to differentiate into hepatic cells and cardiomyocytes (Kogler *et al.*, 2004). At least one study has suggested that MSC-like cord blood cells cannot form fibroblastic colony forming units (CFU-F), a trait that stands in marked contrast to bone marrow MSC (Wexler *et al.*, 2003). MAPC, VSEL and MIAMI cells have only been derived from culture and it is unclear whether these represent populations which exist normally *in vivo* (D'Ippolito *et al.*, 2004; Jiang *et al.*, 2002b; Reyes & Verfaillie, 2001).

1.5.1 Heterogeneity and ageing of MSC

The cells typically isolated using most MSC isolation protocols are functionally heterogeneous and may contain a mixture of undifferentiated progenitors and lineage-restricted precursors with varying differentiation capacities (Muraglia *et al.*, 2000). This heterogeneity within isolated populations is further compounded by differences between the populations isolated by different groups. The results of efforts to culture and differentiate MSC have shown highly variable results (Jiang *et al.*, 2002a; Pittenger *et al.*, 1999) and thus the molecular mechanisms that control MSC self renewal and differentiation are difficult to study. As MSC are increasingly studied for characteristics

such as immunomodulation, the heterogeneity introduced during isolation as well as the lack of standardised isolation protocols are likely to further impact on the comparability of data sets between groups as well as the objective reproducibility of results.

One of the defining characteristics of stem cell is their potential for self-renewal over extended culture times. This self renewal is based on clonal expansion, a form of mitosis resulting in two identical daughter cells (Bruder *et al.*, 1997). The molecular mechanisms which govern this capacity for self renewal are not well understood and much research is ongoing into the factors which control MSC decisions to clonally expand or differentiate, functions which need to be controllable if MSC are to be clinically useful. Self-renewal has been broadly associated with telomerase activity (Greenwood & Lansdorp; Parsch *et al.*, 2004). Telomeres are regions of repetitive DNA found at the ends of chromosomes which protect the chromosome from damage during chromosomal replication. Telomeres are replenished and extended by telomerase and without the activity of this enzyme, cell proliferation ceases and the cell undergoes senescence.

It has been observed that the decline in stem cell self-renewal correlates with a decline in telomere length and telomerase activity. In contrast to ES cells, MSC have a reduced capacity for self-renewal due to reduced telomerase activity (Verfaillie, 2002). MSC can become senescent following repeated passaging *in vitro* culture (Bonab *et al.*, 2006; DiGirolamo *et al.*, 1999) and a decrease in plasticity can also be observed in late passages (DiGirolamo *et al.*, 1999). Other studies have shown that donor age affects the rate of *in vitro* senescence in MSC (Stenderup *et al.*, 2003). Cell age, be it due to long

term passage or donor aging, increases the probability of transformation due to the accumulation of chromosomal abnormalities. This tendency highlights the risk of possible tumour development in a therapeutic setting and indeed some studies have demonstrated spontaneous transformation in both human and murine MSC (Miura *et al.*, 2006; Rubio *et al.*, 2005). These findings suggest that early passages of MSC should be used in therapy to avoid the risk of transformation and should thus be the main focus of research to that end.

1.5.2 MSC potency

It has generally been assumed that the differentiation of pluripotent stem cells into germ layer stem cells during embryogenesis is an irreversible event and that all of the subsequently differentiating stem cells, progenitor cells and mature cells of each lineage maintain that specification throughout adulthood. It has however been found that adult stem cells can differentiate into tissues of an alternate germ origin (Rossant, 2006; Wagers & Weissman, 2004). This capacity to differentiate is termed adult stem cell potency, and several mechanisms have been proposed to account for this effect. Some studies have suggested that stem cells will undergo de-differentiation to a more potent cell type before undergoing differentiation into a cell of the trans-tissue origin, a process referred to as trans-differentiation. It has also been proposed that trans-differentiation may be mediated by signals in the new local microenvironment (Okada, 1980). Alternatively, it has been suggested that potency in therapeutic settings is acquired as a result of cell-cell fusion between donor stem cells and host tissue cells

(Wang *et al.*, 2003). Gender mismatched bone marrow derived cells were shown to undergo fusion with recipient hepatocytes. Cytogenic analysis of the repopulated hepatocytes showed that the cells were found to be heterozygous for donor-specific alleles indicating incidences of diploid to diploid fusion and diploid to tetraploid fusion (Wang *et al.*, 2003). Contradicting this, Tran *et al.* showed that trans-differentiation and not cell-cell fusion was responsible for differentiation of bone marrow-derived cells into epithelial cells (Tran *et al.*, 2003). The group demonstrated that male bone marrow transplant into female recipients resulted in the detection of diploid Y-chromosomal buccal cells, ruling out the involvement of cell-cell fusion.

It is clear that the means by which multipotent cells exhibit greater plasticity is not well understood and it is likely that a combination of the mechanisms investigated are at work in the *in vivo* setting. Although the level of potency exhibited in these studies support the hypothesis that cells with potency close to pluripotency exist within the adult, it is not yet clear whether such cells are common or truly present *in vivo* rather than being an artefact of cell culture techniques.

Differentiation is tightly regulated and controlled by various transcription factors, cytokines, growth factors and extracellular matrix molecules. The regulation of adult stem cell differentiation involves transcriptional modification. Several genes have been identified whose expression is increased during MSC differentiation into osteocytes, adipocytes and chondrocytes, which may represent master control genes (Baksh *et al.*, 2004; Song *et al.*, 2006). Song *et al.* identified eight genes covering a broad range of cellular functions, suggesting the complexity of differentiation

commitment. The genes included period homolog1 (PER1), nebulette (NEBL), neuronal cell adhesion molecule (NRCAM), FK506 binding protein 5 (FKBP5), interleukin 1 type II receptor (IL1R2), zinc finger protein 145 (ZNF145), tissue inhibitor of metallo-proteinase 4 (TIMP4), and serum amyloid (Song *et al.*, 2006). It appears that adipogenesis is regulated by the nuclear receptor and transcription factor peroxisome proliferators-activated receptor gamma (PPAR-γ) as well as fatty acid synthase. Adipogenesis can be suppressed by IL-1 and TNF-α through the NF-κB pathway (Suzawa *et al.*, 2003). Some cell signalling pathways that have been implicated in stem cell differentiation include the Stat3, Notch, TGF-β and Wnt pathways. Notch activity has been shown to affect a diverse range of developmental processes controlling cell differentiation, proliferation, morphogenesis and organ formation (Artavanis-Tsakonas *et al.*, 1995). It has also been shown that components of this signalling pathway showed altered transcriptional regulation during human EC and ES cell differentiation (Walsh & Andrews, 2003). Bone morphogenic protein (BMP) plays an important role in a number of diverse embryonic events including the induction of mesoderm, hematopoeisis and epidermis formation and signals via the TGF-β pathway (Johansson & Wiles, 1995; Wiles & Johansson, 1999). It has been recently suggested that the self-renewal of murine HSC (Reya *et al.*, 2003) and osteogenesis in murine MSC are regulated by the Wnt/β-catenin signalling pathway (Chang *et al.*, 2007).

1.5.3 MSC biology *in vivo*

MSC contribute to the repair of tissue damage *in vivo* (Amado *et al.*, 2005), but evidence of significant engraftment or *in vivo* differentiation is less convincing (Iso *et al.*, 2007). Despite initial encouraging results from *in vivo* studies, it has not been conclusively demonstrated that adult stem cells engraft and differentiate into the required specialised tissues to repair damaged or diseased tissue (Jones & McGonagle, 2007). It is now believed that factors secreted by MSC, such as hepatocyte growth factor (HGF), are responsible for promoting the survival repair and proliferation of injured cells or through promotion or resident local progenitors (Crigler *et al.*, 2006; Zwezdaryk *et al.*, 2007). This hypothesis is supported by observations that MSC express the interleukin 1 receptor antagonist (Ortiz *et al.*, 2007) which alters the tissue microenvironment.

1.6 MSC IMMUNOMODULATION

The non-embryonic source of MSC and their reduced likelihood of neoplasia due to a more limited differentiation potential, have made these cells attractive candidates for application in regenerative medicine (Barry & Murphy, 2004). However, whilst self-derived MSC should pose few immunological problems, in practice regenerative medicine is likely to rely on banked, HLA-mismatched (allogeneic) cells to repair or replace damaged tissue. Normally, allogeneic cells are deleted by the host immune response (Cerottini & Brunner, 1974). Surprisingly however, there have been many

findings which demonstrate that MSC do not obey the normal rules of allogeneic rejection (Aggarwal & Pittenger, 2005; Spaggiari *et al.*, 2006; Tse *et al.*, 2003).

MSC possess a wide variety of immunomodulatory capabilities (Figure 1.5), constitutively producing Th suppressive cytokines such as prostaglandin E2 (PGE2) and transforming growth factor beta 1 (TGF-β1). When stimulated with IFN-γ MSC will also produce indoleamine 2,3-dioxygenase (IDO) which is known to inhibit T-cell proliferation and NK function (Frumento *et al.*, 2002; Meisel *et al.*, 2004). Numerous studies have demonstrated that both murine and human MSC suppress both alloantigen- and mitogen-driven T-cell proliferation *in vitro* (Di Nicola *et al.*, 2002; Glennie *et al.*, 2005; Krampera *et al.*, 2003; Ryan *et al.*, 2005). It has similarly been shown that MSC physically hindered B cell proliferation (Augello *et al.*, 2005), and inhibited NK cell proliferation and cytotoxicity (Spaggiari *et al.*, 2006).

Murine MSC responded to stimulation with Pam3Cys, a ligand for TLR2, by producing increased IL-6, as well as reducing their basal motility, increasing clonal expansion and reducing differentiation along the osteogenic, adipogenic and chondrogenic pathways (Pevsner-Fischer *et al.*, 2007) (Figure 1.5). Stimulation of TLR 3 and 4 in human MSC results in increased IDO activity. Given than MSC have been demonstrated to express mRNA for TLR 1-8, it is likely that they are sensitive to other innate immune signals (Opitz *et al.*, 2009; Pevsner-Fischer *et al.*, 2007). MSC also possess receptors for a range of soluble factors associated with adaptive immune responses including receptors for IFN-γ, IL-13, IL-10, IL-17 and IL-4 suggesting a capacity to respond differentially to local Th1, Th2, T-reg and Th17 responses (da Silva

Meirelles *et al.*, 2008; Silva *et al.*, 2003). MSC also express receptors for a range of chemokines including CCR1, CCR4, CCR7, CCR10 and CXCR5 (Von Lüttichau *et al.*, 2005). The broad palette of immune receptors and homing receptors expressed by MSC suggests a highly responsive, versatile and complex relationship with both the innate and adaptive arms of the immune response and it is likely that further investigations will continue to yield a diversity of interactions between MSC and the immune system.

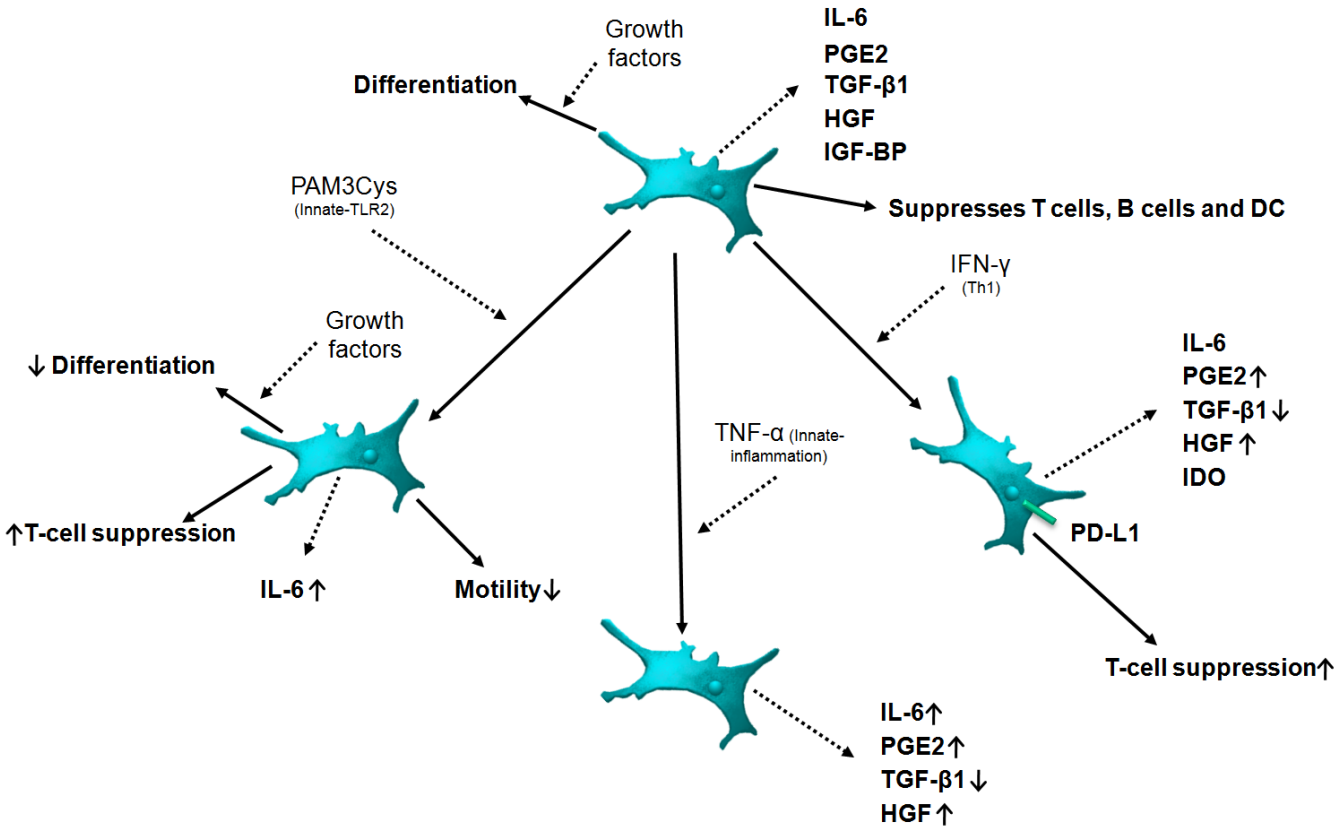

Figure 1.5 MSC mediate a wide range of immunomodulatory functions. These functions may themselves be modulated in response to stimulation with signals from the innate (TLR2 ligands and TNF-α) and adaptive (IFN-γ) arms of the immune response. Stimulation of MSC with a TLR2 ligand induces a phenotype with increased IL-6 production, reduced motility and differentiation potential. TNF-α stimulation modulates the cytokine milieu produced by MSC. IFN-γ stimulation also modulates this cytokine milieu as well as inducing IDO and PD-L1, and enhancing T cell suppressive activity. Figure uses data from multiple sources (English *et al.*, 2007; English *et al.*, 2008; Pevsner-Fischer *et al.*, 2007).

MSC appear to maintain their immunomodulatory functions even in models of inflammation (English *et al.,* 2007). Incubation of murine MSC with the pro-inflammatory cytokines IFN-γ and TNF-α did not negatively impact upon MSC-mediated immunosuppression of splenocyte proliferation. Furthermore, expression of PGE2, programmed death ligand 1 (PD-L1) and IDO was differentially regulated by the two cytokines. Cyclooxegenase 2 (COX-2) and PGE2 expression was upregulated by both IFN-γ and TNF-α whilst the surface expression of PD-L1 was induced by IFN-γ but not TNF-α. Using blocking studies, English *et al*. demonstrated that PD-L1 induction was non-essential in the suppressive role of MSC, whilst IDO appeared to be a pre-requisite (English *et al.,* 2007). Similar studies in humans have shown that IFN-γ stimulation enhances MSC-mediated suppression of T-cell proliferation, and that TNF-α and IFN-γ stimulation of human MSC produces differential phenotypes similar to those seen in murine studies (Ryan *et al.,* 2007).

MSC also appear to modulate dendritic cell (DC) function. In a study by English *et al.* in 2008, DC co-cultured with murine MSC and stimulated with TNF-α failed to upregulate maturation markers (English *et al.*, 2008). MSC were also shown to reduce the capacity of ovalbumin-pulsed DC to support antigen specific CD4+ T-cell proliferation. Co-culture of MSC with DC resulted in reduced expression of CCR7 by DC following stimulation and significantly less DC migration in response to CCL19. MSC also prevented loss of E-cadherin by DC, a protein which functions to anchor DC to tissues (English *et al.*, 2008).

The capacity for MSC to escape immune recognition and to suppress T-cell activation, both *in vivo* and *in vitro*, is counterintuitive and it is difficult to suggest an evolutionary benefit for such a function given that allotransplanation is a procedure with no obvious natural analogue. The only comparable natural occurrence in mammals is the induction of maternal tolerance of the fetal allograft, raising the possibility that MSC immune evasion in allogeneic conditions is an exapted function that may share many features with the fetal immune evasion. A number of *in vivo* studies have suggested a role for MSC in the acquisition of alloantigen tolerance. Koc *et al.* showed no evidence of alloreactive T-cells and no incidence of GVHD when allogeneic MSC were transplanted into patients with Hurler's syndrome or metachromatic leukodystrophy (Koc *et al.*, 2002).

1.7 TRANSFECTION AND TRANSDUCTION OF MSC

The recognition of viral-based gene therapy vectors by the recipient immune system may be a significant obstacle to meeting safety and efficacy requirements (Hacein-Bey-Abina *et al.*, 2008; Manno *et al.*, 2006; Raper *et al.*, 2003). Although vector modification and recipient immunosuppression represent possible solutions to this problem (Halbert *et al.*, 1998; Manning *et al.*, 1998), an alternative strategy would be to conduct transductions on human cells *ex vivo* and then infuse those cells, now expressing the therapeutic gene product, into the recipient (Gadi *et al.*, 2001). Typically such a strategy would demand that the transduced cells be autologous to the recipient, which is not practical for all applications. However, as MSC have been shown to evade

allorecognition (Barry *et al.*, 2005; Ryan *et al.*, 2005) and to have significant immunomodulatory capabilities (English *et al.*, 2007; English *et al.*, 2008; Ryan *et al.*, 2007), they may represent attractive candidate cells for such *ex vivo* transduction. For certain applications such as tissue engineering, it may also be desirable to modify MSC to constitutively express cis-acting growth factors (Partridge & Oreffo, 2004). Virally transduced MSC and transfected MSC have been investigated for use in tissue engineering (Partridge & Oreffo, 2004) and the delivery of therapeutics to tumours, into which MSC readily engraft (Mohr *et al.*, 2008; Studeny *et al.*, 2002). Requirements of such applications are efficient transduction, stable transgene expression over an extended time and minimal cytotoxic effects. It is also preferable to retain the other potential therapeutic characteristics of MSC, such as immunomodulatory capacity and potency.

A comparative study of several viral and non-viral gene delivery systems was carried out by McMahon *et al*. using bone-marrow derived rat MSC (McMahon *et al.*, 2006). Lentiviral vectors gave transduction efficiencies of up to 95%, and resulted in only low levels of MSC toxicity. MSC potency was also not affected by the transduction protocol. Adenovirus-based vectors also proved relatively effective, but a significant dose-dependent increase in cell death was observed. Rat MSCs were refractory to transduction by AAV serotypes 1, 2, 4, 5, and 6. Transfection using plasmid DNA with Lipofectamine resulted in moderate transfection levels at the cost of some cytotoxicity. Electroporation was both highly cytotoxic and failed to produced adequate transfection (McMahon *et al.*, 2006).

Human MSC transduced with an adenovirus-based vector carrying the apoptosis-inducing TNF-related apoptosis-inducing factor (TRAIL) gene were shown to give efficient induction of TRAIL production and to inhibit the growth of A549 xenografts in mice (Mohr *et al.*, 2008). Ad-transduced MSC did not induce PBMC proliferation *in vitro*, allaying concerns that Ad transduction might render the MSC more immunogenic. The majority of gene therapy treatments for bone repair investigated to date have also used vectors based on adenovirus (Chang *et al.*, 2003; Kofron & Laurencin, 2006; Lieberman *et al.*, 1998). Typically the transgenes delivered are members of the bone morphogenetic protein (BMP) family. BMP2-producing murine MSC induced heterotrophic bone formation when administered to severe combined immune deficient mice (Lieberman *et al.*, 1998).

Viral-based vector systems are generally held to be preferable for MSC applications, particularly those based on lentivirus and adenovirus (Chang *et al.*, 2003; McMahon *et al.*, 2006; Mohr *et al.*, 2008) due to their well-established safety profile in conventional gene therapy combined with optimal transduction efficiency and low cytotoxicity (Djeha *et al.*, 2001; Kremer & Perricaudet, 1995; Levine *et al.*, 2006).

1.8 AIMS

It was hypothesised that immune memory for AAV-2 in the Irish population may confound the use of AAV-2 vectors. Although a thorough test of this hypothesis would require extensive clinical work beyond the scope of the present study, an examination of adaptive immune memory for AAV-2 in an Irish blood donor group (Chapters 3 and 4) would none-the-less provide evidence to support or reject this hypothesis. Secondary to this hypothesis, it was suggested that confounding effects, if present, might be mitigated by identification and modification of common immunogenic elements of the AAV-2 virus. This hypothesis might be adequately tested by examination of *in vitro* responses to specific elements of the AAV-2 capsid (Chapter 5) in the Irish blood donor group previously examined. Finally, it was hypothesised that AAV-2 might be a useful vector for the transduction of MSC. This would be tested by performing *in vitro* transduction of murine MSC and examining the cultures for transgene product upregulation as well as verifying that the other therapeutic characteristics of MSC remain intact.

Thus, the aims of this study were:

a) To characterise the humoral immunological memory for AAV-2 in a human population (Chapter 3)

b) To characterise the human cell-mediated recall response to AAV-2 in the same population (Chapter 4)

c) To identify the AAV-2 capsid sequences recognised (epitopes) by the cell-mediated human immune response (Chapter 5)

d) To assess the impact of AAV-2 transduction on murine MSC (Chapter 6).

In this way, a greater understanding of AAV-2 interaction with the human immune system would be achieved and clinical/therapeutic practise could be refined.

CHAPTER 2

MATERIALS AND METHODS

2.1 MATERIALS

2.1.1 Materials for cell isolation and cell culture

2.1.1.1 Low endotoxin fetal calf serum (LE FCS)

LE FCS (BioSera, East Sussex, UK) was heat-inactivated (LE HI FCS) at 60˚C for 20 minutes prior to being aliquoted for storage at -20˚C. All new batches of LE FCS were batch tested for their capacity to stimulate lymphocyte proliferation (Section 2.2.5.1) prior to use in culture media.

2.1.1.2 Complete Roswell Park Memorial Institute medium 1640 (cRPMI)

cRPMI was constituted as RPMI 1640 (Invitrogen, Carlsbad, CA) with 1 unit/ml penicillin (Invitrogen), 1 µg/ml streptomycin (Invitrogen), 2mM L-glutamine (Invitrogen), 25 µM β-mercaptoethanol (Invitrogen) and 10% (v/v) LE HI FCS. cRPMI was stored at 4˚C and warmed to 37˚C prior to use with cells. cRPMI was used for all extended incubations involving human peripheral blood mononuclear cells (PBMC) or murine lymphocytes.

2.1.1.3 Complete Hank's balanced salt solution (cHBSS)

cHBSS was constituted as HBSS (Invitrogen) with 10 mM 4-(2-hydroxyethyl)-1-piperazineethanesulfonic acid buffer (HEPES; Sigma-Aldrich) and 1% (v/v) LE HI FCS. cHBSS was stored at 4˚C and warmed to 37˚C prior to use with cells. cHBSS was used for the dilution of human whole blood and mouse spleen homogenates.

2.1.1.4 Complete Dulbecco's modified Eagle's medium (cDMEM)

cDMEM contained low glucose DMEM (Invitrogen) with 1 unit/ml penicillin, 1 µg/ml streptomycin and 10% (v/v) LE HI FCS. cDMEM was stored at 4˚C and warmed to 37˚C prior to use with cells. cDMEM was used for thawing and long term culture of cryopreserved human embryonic kidney cells (HEK-293).

2.1.1.5 Complete modified Eagle's medium alpha (cαMEM)

cαMEM was constituted as MEM-α medium (Invitrogen) with 1 unit/ml penicillin, 1 µg/ml streptomycin, 2mM L-glutamine, 10% (v/v) LE HI FCS and 10% (v/v) HI horse serum (HS). cαMEM was stored at 4˚C and warmed to 37˚C prior to use with cells. cαMEM was used for thawing of cryopreserved murine mesenchymal stem cells (MSC) and for long term culture of MSC.

2.1.1.6 OptiMEM (transfection studies)

OptiMEM (Invitrogen) was stored at 4˚C and warmed to 37˚C prior to use with cells. OptiMEM was used serum-free for the dilution of transfection reagents.

2.1.1.7 Media for cryopreservation

Human PBMC were suspended in RPMI 1640 (Invitrogen) supplemented with 20% (v/v) heat inactivated LE FCS and 10% (v/v) dimethylsulphoxide (DMSO; Sigma-Aldrich, Arklow, Ireland). Murine MSC were suspended in MEM-α supplemented with 20% (v/v) LE FCS and 10% (v/v) DMSO (Sigma-Aldrich). HEK293 cells were suspended in DMEM supplemented with 20% (v/v) LE FCS and 10% (v/v) DMSO.

2.1.1.8 Trypsin-ethylenediaminetetraacetic acid (EDTA)

0.25 mM Trypsin-EDTA (Invitrogen) was used to detach adherent MSC and HEK293 cells from culture vessels. Trypsin-EDTA was stored at -20˚C and warmed to 37˚C before use with cell cultures.

2.1.1.9 Phosphate buffered saline (PBS)

PBS was used at a working concentration of 137 mM NaCl, 10 mM sodium phosphate dibasic, 2.7 mM KCl, 2 mM potassium phosphate monobasic. Buffer was prepared in dH_2O and the pH was adjusted to 7.4. The working dilution was made up from a 10x stock solution and was sterilised by autoclaving for all cell culture applications.

2.1.1.10 Ethidium bromide / acridine orange (EB/AO)

EB/AO for viable cell counting (Sigma-Aldrich) was dissolved at a stock concentration of 1 µg/ml EB and 1 µg/ml AO in PBS. Due to its carcinogenic properties, EB/AO-contaminated consumables and sharps were segregated and disposed of as chemically hazardous waste.

2.1.2 Materials for molecular methods

2.1.2.1 General materials for molecular methods

Water: Nuclease-free distilled H_2O (Promega, Dublin, Ireland) was used for dilutions of nucleic acid solutions. *TAE buffer:* Tris-acetate EDTA buffer was prepared

as a 10x stock solution containing 48.4 g of Tris base, 11.42 ml of glacial acetic acid, 100 ml of 500 mM Na_2 EDTA (pH 8.0) made up to 1000 ml with dH_2O.

2.1.2.2 Materials for RNA isolation

Trizol: Trizol (Invitrogen) was stored at 4˚C and was used for lysis of all cell types. *Poly-acryl carrier:* Poly-acryl carrier (Molecular Research Inc., Cincinnati, OH) was stored at 4˚C. *DNAse*: Genomic DNA was removed from RNA isolates by addition of DNAse I (118068-015; Invitrogen) as detailed in Section 2.2.4.1.

2.1.2.3 Materials for cDNA synthesis

cDNA master mix: Master mix for cDNA synthesis contained Superscript II reverse transcriptase (200 U/ml; Invitrogen), 5x first strand buffer (Y02353; Invitrogen), $MgCl_2$ (25 mM; Promega), dNTP mixture (100 mM; Promega), Oligo dT primer (0.5 mg/ml; Promega); dithiothreitol (0.1 M DTT; Invitrogen) RNAse inhibitor (10 U/ml; Invitrogen) prepared as described in method 2.2.4.2.

2.1.2.4 Materials for polymerase chain reaction (PCR)

Primers: Primers for detection of specific products are listed and detailed in full (Table 2.1). All primers were designed using Primer3 (Whitehead Institute, Cambridge, MA), validated using NetPrimer (Premier Biosoft, Palo Alto, CA) and synthesised by MWG Operon, (Ebersberg, Germany). *PCR master mix:* Primers and cDNA were mixed with 10x thermophilic DNA polymerase buffer (M190A; Promega), $MgCl_2$, dNTP mixture and Taq polymerase (GoTaq; Promega) as described in Sections 2.2.4.3 and 2.2.4.4.

Table 2.1 Primers for RT-PCR

Product	Product length (bp)	Direction	Primer sequence (5'-3')	Tm (?C)	GC content (%)
IDO	218	F	GGCTAGAAATCTGCCTGTGC	59.98	55.00
		R	AGAGCTCGCAGTAGGGAACA	60.16	55.00
GAPDH	487	F	CTGCACCACCAACTGCTTAG	59.51	55.00
		R	CCAGGAAATGAGCTTGACAAA	60.23	42.86

Primers were designed using Primer 3 based on the coding IDO or GAPDH coding sequences. Primers were synthesised by MWG Operon.

DNA was isolated from PBMC using a Generation Capture Column kit (Qiagen, California, USA) following the manufacturer's protocol. Briefly, cell suspensions were passed through a solid matrix column which lysed cells on contact whilst retaining DNA. The column was then washed using a provided purification buffer before the DNA was eluted from the column at high temperature (95˚C) using the provided elution buffer.

2.1.3 Materials for immunoassays

2.1.3.1 General ELISA reagents

Flat bottomed, 96-well polystyrene microtitre plates (MaxiSorp; Nunc, Langenselbold, Germany) were used as the reactive surface for all ELISA experiments. PBS was prepared as in Section 2.1.1.9 without sterilisation. 0.05% (v/v) Tween 20 (Sigma-Aldrich) in PBS was used as the normal washing buffer. For the coating buffer, a 100 mM solution of $NaHCO_3$ in dH_2O and a 100 mM solution Na_2CO_3 in dH_2O were

mixed in a ratio 7:3. This solution was then diluted 1:3 in dH_2O. Coating buffer was stored at 4˚C and used within 1 week. Streptavidin-horseradish peroxidise (Strep-HRP; RPN1231V; GE Healthcare) was used for colorimetric detection of biotinylated detection antibodies in all ELISA experiments. 3,3',5,5'-Tetramethylbenzidine (TMB; Sigma-Aldrich) was used as a substrate for strep-HRP in all ELISA experiments.

2.1.3.2 Materials for total IgG ELISA

0.5% (v/v) Tween 20 (Sigma-Aldrich) in PBS was used as a highly concentrated washing buffer during some steps. AAV-2 antigen was as described in Section 2.1.5.1. Antigen was diluted in using carbonate coating buffer and adsorbed onto to polystyrene plates. The reactive surface was blocked using PBS containing 5% (w/v) Sucrose (Sigma-Aldrich), 1% (w/v) BSA and 0.05% (v/v) Tween 20. 1% (w/v) skimmed milk powder (Marvel) in PBS was used for the dilution of analyte samples and detection antibody. Anti-human IgG conjugated to biotin (Sigma-Aldrich) diluted in reagent diluent, was used for analyte detection.

2.1.3.3 Materials for IgG subclass ELISA

Anti-human IgG1, 2, 3 and 4 antibodies conjugated to biotin (Merck, Nottingham, England) and diluted in reagent diluent, were used for IgG1, 2, 3 and 4 analyte detection, respectively. A pooled control serum containing standardized concentrations of human IgG subclasses 1, 2, 3 and 4 (Nordic Labs, Tilburg, Holland) was used as a reference serum and was directly coated to the assay plate.

2.1.3.4 Materials for cytokine ELISA

5% (w/v) BSA was dissolved in PBS and mixed overnight at 4^{o}C and used as a blocking buffer for IL-10 and IFN-γ ELISA experiments. Buffer was stored at 4^{o}C and used within 1 week. The reagent diluent was 1% (w/v) Marvel milk powder dissolved in PBS and mixed overnight at 4^{o}C. Diluent was stored at 4^{o}C and used within 2 days. RPMI 1640 (Invitrogen) was used as a diluent for the recombinant IFN-γ and IL-10 standards as supernatant samples were dissolved in cRPMI. Anti-human IL-10 (Immunotools, Friesoythe, Germany), diluted in carbonate coating buffer served as a capture antibody for IL-10. Anti-human IFN-γ (Immunotools), diluted in carbonate coating buffer was used as a capture antibody for IFN-γ. Anti-human IL-10 biotin (Immunotools) was diluted in reagent diluent and was used as a detection antibody for IL-10. Anti-human IFN-γ biotin (Immunotools) was diluted in reagent diluent and served as a detection antibody for IFN-γ. Recombinant human IL-10 (rhIL-10) standards (Immunotools) were serially diluted in standard diluent. Recombinant human IFN-γ (rhIFN-γ) standards (Immunotools) were also serially diluted in standard diluent.

5% (w/v) sucrose and 1% (w/v) bovine serum albumin (BSA; Sigma-Aldrich) were dissolved in PBS and mixed overnight at 4˚C. This buffer served as a blocking reagent for the IL-13 ELISA. Blocking buffer was stored at 4˚C and used within 1 week. 0.1% (w/v) BSA and 0.05% Tween 20 (Sigma-Aldrich), dissolved in PBS and mixed overnight at 4˚C, was used as a reagent diluent for the IL-13 ELISA. Diluent was stored at 4˚C and used within 1 week. RPMI 1640 (Invitrogen) was used as a diluent for the recombinant IL-13 standard as supernatant samples were dissolved in cRPMI. Anti-

human IL-13 (R&D Systems, Minneapolis, MN) was diluted in carbonate coating buffer and used as a capture antibody for IL-13. Anti-human IL-13 biotin (R&D Systems) was diluted in reagent diluent and used as a detection antibody for IL-13. Recombinant human IL-13 (rhIL-13) standards (R&D Systems) were serially diluted in standard diluent.

2.1.3.5 Materials for Bradford method protein quantification

Bovine serum albumin (BSA) was used as a protein standard: A 1 mg/ml BSA (Sigma-Aldrich) stock solution was prepared in dH_2O and stored at -20^oC. Bio-Rad Protein Assay Dye Reagent (Bio-Rad, Hertfordshire, UK) was used to determine protein sample concentrations colourimetrically according to a well established method (Bradford, 1976).

2.1.3.6 Materials for western blot

The following materials and reagents were employed: A resolving gel consisting of 2.5 ml H_2O, 5 ml 30% acrylamide bis (Bio-Rad), 2.5 ml 1.5 M Tris (Sigma-Aldrich), 0.1 ml 10% (w/v) SDS (Sigma-Aldrich), 0.1 ml 10% (w/v) APS (Sigma-Aldrich), 4 µl TEMED (Sigma-Aldrich). A stacking gel comprising 3.4 ml H_2O, 830 µl acrylamide bis, 630 µl Tris, 50 µl 10% (w/v) SDS, 50 µl 10% (w/v) APS, 4 µl TEMED. A loading buffer containing 70 mM Tris-HCl, 26.3% (v/v) glycerol, 10% (w/v) SDS, 0.5% (w/v) bromophenol blue in dH_2O. 5% (v/v) β-mercaptoethanol was added to loading buffer immediately prior to use. The running buffer was 240 mM Tris, 1.9 M glycine (Merck KGaA, Darmstadt, Germany), 35 mM SDS in 1000 ml of dH_2O.

Nitrocellulose membranes (Sartorius Stedim Biotech S.A., Aubagne, France) were used as the blotting surface. Mouse- and human-reactive anti-IDO IgG (Millipore, Billerica, MA), raised in mouse were used as detecting antibodies and for secondary antibody goat anti-mouse IgG was used (Millipore). Transfer buffer was 25 mM Tris, 190 mM glycine, 20% (v/v) methanol in 1000 ml dH_2O. Transfer buffer was used only if pH on formulation was between 8.0 and 8.3. If pH was outside of this range, the buffer was discarded. Strep-HRP was as described in Section 2.1.3.1. The colourimetric reagent used was BM Chemiluminescence Western Blotting Substrate (Roche Diagnostics GmbH, Mannheim, Germany).

2.1.4 Materials for cell function assays

2.1.4.1 Materials for *in vitro* human lymphoproliferative responses

Lymphoprep (Axis-Shield, Oslo, Norway) was used undiluted for isolation of human PBMC by density centrifugation. *AAV-2:* AAV-2 vectors used for PBMC stimulations were as described in Section 2.1.5.1 *5*% ethylenediaminetetraacetic acid (EDTA; Sigma-Aldrich) was diluted to 5% (w/v) in dH_2O before being autoclaved for use with human PBMC. Tritiated thymidine (^{3}H-thymidine; GE Healthcare) was provided labelled at carbon 6 with a single tritium [6-^{3}H]. Radioactivity of stock at purchase was 37 MBq/ml. Material was stored at 4˚C.

Peptides synthesised from the AAV-2 VP1 capsid sequence were provided by Mimotopes Pty Ltd (Clayton, Victoria). The peptides were provided as a set of 91 20-

mer sequences each having a 12-mer overlap with the adjacent sequence (Table 2.2). The full VP1 sequence incorporates the VP2 and VP3 peptides of the AAV-2 capsid (Xie *et al.*, 2002), thus the overlapping VP1 peptides allow for full coverage of the AAV-2 capsid. Peptides were reconstituted in 0.1% (v/v) acetic acid at a concentration of 25 mg/ml, aliquoted and stored at -80^{o}C. Before use, peptides were diluted in PBS to a working concentration of 1 mg/ml. All peptides supplied had an average purity of >70%.

Table 2.2 Sequences of the 20-mer peptides derived from the AAV-2 VP1 capsid protein[a]

1	MAADGYLPDWLEDTLSEGIR	**21**	KAGQQPARKRLNFGQTGDAD	**41**	KEVTQNDGTTTIANNLTSTV	**61**	PCYRQQRVSKTSADNNNSEY	**81**	HPPPQILIKNTPVPANPSTT
2	DWLEDTLSEGIRQWWKLKPG	**22**	KRLNFGQTGDADSVPDPQPL	**42**	TTTIANNLTSTVQVFTDSEY	**62**	SKTSADNNNSEYSWTGATKY	**82**	KNTPVPANPSTTFSAAKFAS
3	EGIRQWWKLKPGPPPPKPAE	**23**	GDADSVPDPQPLGQPPAAPS	**43**	TSTVQVFTDSEYQLPYVLGS	**63**	NSEYSWTGATKYHLNGRDSL	**83**	PSTTFSAAKFASFITQYSTG
4	LKPGPPPPKPAERHKDDSRG	**24**	PQPLGQPPAAPSGLGTNTMA	**44**	DSEYQLPYVLGSAHQGCLPP	**64**	ATKYHLNGRDSLVNPGPAMA	**84**	KFASFITQYSTGQVSVEIEW
5	KPAERHKDDSRGLVLPGYKY	**25**	AAPSGLGTNTMATGSGAPMA	**45**	VLGSAHQGCLPPFPADVFMV	**65**	RDSLVNPGPAMASHKDDEEK	**85**	YSTGQVSVEIEWELQKENSK
6	DSRGLVLPGYKYLGPFNGLD	**26**	NTMATGSGAPMADNNEGADG	**46**	CLPPFPADVFMVPQYGYLTL	**66**	PAMASHKDDEEKFFPQSGVL	**86**	EIEWELQKENSKRWNPEIQY
7	GYKYLGPFNGLDKGEPVNEA	**27**	APMADNNEGADGVGNSSGNW	**47**	VFMVPQYGYLTLNNGSQAVG	**67**	DEEKFFPQSGVLIFGKQGSE	**87**	ENSKRWNPEIQYTSNYNKSV
8	NGLDKGEPVNEADAAALEHD	**28**	GADGVGNSSGNWHCDSTWMG	**48**	YLTLNNGSQAVGRSSFYCLE	**68**	SGVLIFGKQGSEKTNVDIEK	**88**	EIQYTSNYNKSVNVDFTVDT
9	VNEADAAALEHDKAYDRQLD	**29**	SGNWHCDSTWMGDRVITTST	**49**	QAVGRSSFYCLEYFPSQMLR	**69**	QGSEKTNVDIEKVMITDEEE	**89**	NKSVNVDFTVDTNGVYSEPR
10	LEHDKAYDRQLDSGDNPYLK	**30**	TWMGDRVITTSTRTWALPTY	**50**	YCLEYFPSQMLRTGNNFTFS	**70**	DIEKVMITDEEEIRTTNPVA	**90**	TVDTNGVYSEPRPIGTRYLT
11	RQLDSGDNPYLKYNHADAEF	**31**	TTSTRTWALPTYNNHLYKQI	**51**	QMLRTGNNFTFSYTFEDVPF	**71**	DEEEIRTTNPVATEQYGSVS	**91**	TNGVYSEPRPIGTRYLTRNL
12	PYLKYNHADAEFQERLKEDT	**32**	LPTYNNHLYKQISSQSGASN	**52**	FTFSYTFEDVPFHSSYAHSQ	**72**	NPVATEQYGSVSTNLQRGNR		
13	DAEFQERLKEDTSFGGNLGR	**33**	YKQISSQSGASNDNHYFGYS	**53**	DVPFHSSYAHSQSLDRLMNP	**73**	GSVSTNLQRGNRQAATADVN		
14	KEDTSFGGNLGRAVFQAKKR	**34**	GASNDNHYFGYSTPWGYFDF	**54**	AHSQSLDRLMNPLIDQYLYY	**74**	RGNRQAATADVNTQGVLPGM		
15	NLGRAVFQAKKRVLEPLGLV	**35**	FGYSTPWGYFDFNRFHCHFS	**55**	LMNPLIDQYLYYLSRTNTPS	**75**	ADVNTQGVLPGMVWQDRDVY		
16	AKKRVLEPLGLVEEPVKTAP	**36**	YFDFNRFHCHFSPRDWQRLI	**56**	YLYYLSRTNTPSGTTTQSRL	**76**	LPGMVWQDRDVYLQGPIWAK		
17	LGLVEEPVKTAPGKKRPVEH	**37**	CHFSPRDWQRLINNNWGFRP	**57**	NTPSGTTTQSRLQFSQAGAS	**77**	RDVYLQGPIWAKIPHTDGHF		
18	KTAPGKKRPVEHSPVEPDSS	**38**	QRLINNNWGFRPKRLNFKLF	**58**	QSRLQFSQAGASDIRDQSRN	**78**	IWAKIPHTDGHFHPSPLMGG		
19	PVEHSPVEPDSSSGTGKAGQ	**39**	GFRPKRLNFKLFNIQVKEVT	**59**	AGASDIRDQSRNWLPGPCYR	**79**	DGHFHPSPLMGGFGLKHPPP		
20	PDSSSGTGKAGQQPARKRLN	**40**	FKLFNIQVKEVTQNDGTTTI	**60**	QSRNWLPGPCYRQQRVSKTS	**80**	LMGGFGLKHPPPQILIKNTP		

[a] Each VP1 peptide was designed to have a 12-mer overlap with adjacent peptides. Peptides 90 and 91 had a 17-mer overlap.

2.1.4.2 Materials for *in vitro* murine MSC immunomodulatory activity

Ficoll (Histopaque 1083; Sigma-Aldrich) was used undiluted for isolation of murine blood mononuclear cells from spleen homogenates by density centrifugation. Carboxyfluorescein diacetate, succinimidyl ester (CFSE; Sigma-Aldrich) was used for detection of murine lymphocyte proliferation by flow cytometry.

2.1.4.3 Materials for differentiation of MSC into osteoclasts (bone cells)

A 10 mM stock solution of Dexamethasone (Sigma-Aldrich) was made by dissolving 0.039 g dexamethasone in 10 ml dH_2O. Dexamethasone was diluted 1:1000 prior to use. 5 mM β-glycerophosphate (Sigma-Aldrich) was made by dissolving 0.864 g of β-glycerophosphate into 8 ml of αMEM. A 50 mM solution of L-ascorbic acid (Sigma-Aldrich) was made by dissolving 0.014 g L-ascorbic acid in 1 ml αMEM. 0.1 mg/ml L-thyroxine was made up by dissolving 0.01 g of L-thyroxine in 100 ml αMEM. To make osteogenesis differentiation medium, cαMEM was supplemented with 1 nM dexamethasone, 2 mM β-glycerophosphate, 50 nM L-ascorbic acid and 50 ng/ml L-thyroxine. Medium was stored at 4˚C for up to one month. Medium was filter sterilised and warmed to 37˚C before use. Staining of differentiated cultures was performed using Alizarin Red S: The working solution was prepared with 0.5 g of Alizarin red S (Sigma-Aldrich) dissolved in 50 ml dH2O. pH was adjusted to between 4.1 and 4.3 using 0.1% (v/v) ammonium hydroxide.

2.1.4.4 Materials for differentiation of MSC into adipocytes (fat cells)

A 10 mM stock solution of Dexamethasone (Sigma-Aldrich) was made by dissolving 0.039 g dexamethasone in 10 ml dH_2O. Dexamethasone was filter sterilised and diluted 1:1000 prior to use. Insulin (Sigma-Aldrich) was prepared at a stock concentration of 20 mg/ml in 100 mM acetic acid. Stocks were stored at -20˚C. Insulin was diluted 1:10 and filter sterilised before addition to adipogenesis medium. 500 mM 3-isobutyl-methyl-xanthine (IBMX; Sigma-Aldrich) was prepared by dissolving 250 mg of IBMX in 2.25 ml DMSO. Stocks were stored at 4˚C and were filter sterilised before use. 10 mg/ml indomethacin 500 mM was prepared by dissolving 10 mg of indomethacin in 1 ml ethanol. Stocks were stored at 4˚C and were filter sterilised before use. Adipogenic differentiation medium was composed of cαMEM supplemented with 10 nM dexamethasone, 5 ng/ml of insulin, 16.65 ng/ml indomethacin and 0.11 ng/ml IBMX. Medium was stored at 4˚C for up to one month. Medium was filter-sterilised and warmed to 37˚C before use. Differentiated cultures were stained with Oil Red O. A stock solution was prepared by adding 0.3 g of Oil Red O (Sigma-Aldrich) to 100 ml isopropanol. The working solution was made by adding 6 parts of stock solution to 4 parts of dH_2O. The solution was mixed and then allowed to stand for 10 minutes at room temperature before being filter sterilised. Working solution was made fresh for each assay run.

2.1.4.5 Materials for HPLC detection of kynurenine concentrations

The mobile phase was an isocratic buffer made up as a mixture of 5 mM aqueous zinc acetate solution, dissolved in high-performance liquid chromatography (HPLC)-grade water, and HPLC-grade acetonitrile (Sigma-Aldrich) at a ratio of 92:8 and a pH of 4.9 (Vignau *et al*., 2004). Quantification was facilitated by use of a purified L-kynurenine reference standard (K8625; Sigma-Aldrich).

2.1.5 Materials for transfection and transduction

2.1.5.1 AAV-2*GFP*

AAV-2 vectors were kindly provided by REMEDI at NUI Galway and consisted of an unmodified AAV-2 capsid encasing a modified AAV-2 genome encoding an *eGFP* reporter gene regulated by a CMV promoter (Figure 2.1). Virus preparations were purified using an iodixanol density gradient followed by elution through a heparin column. Titres were determined by real time PCR following DNase 1 and proteinase K degradation steps. Concentrations were expressed as DNase resistant particles per microlitre (drp/µl). Virus preparations were resuspended in sterile PBS-MK buffer (PBS, 1 mM $MgCl_2$, 2.5 mM KCl) and stored at -80^{o}C until use. All reagents for vector preparation were filter sterilized or autoclaved prior to use.

2.1.5.2 Materials for transfection with human IDO gene

The pCMV-Sport6 IDO plasmid (Figure 2.2) was kindly provided by REMEDI at NUI Galway and consisted of a pCMV-Sport6 plasmid (Invitrogen) with a human IDO gene ligated into the multiple cloning site between the NotI and SalI restriction sites. The transgene was regulated by a constitutive CMV promoter. The plasmid also contained an ampicillin resistance gene (*AmpR*). Lipofectamine 2000: Lipofectamine liposomal vectors were acquired from Invitrogen.

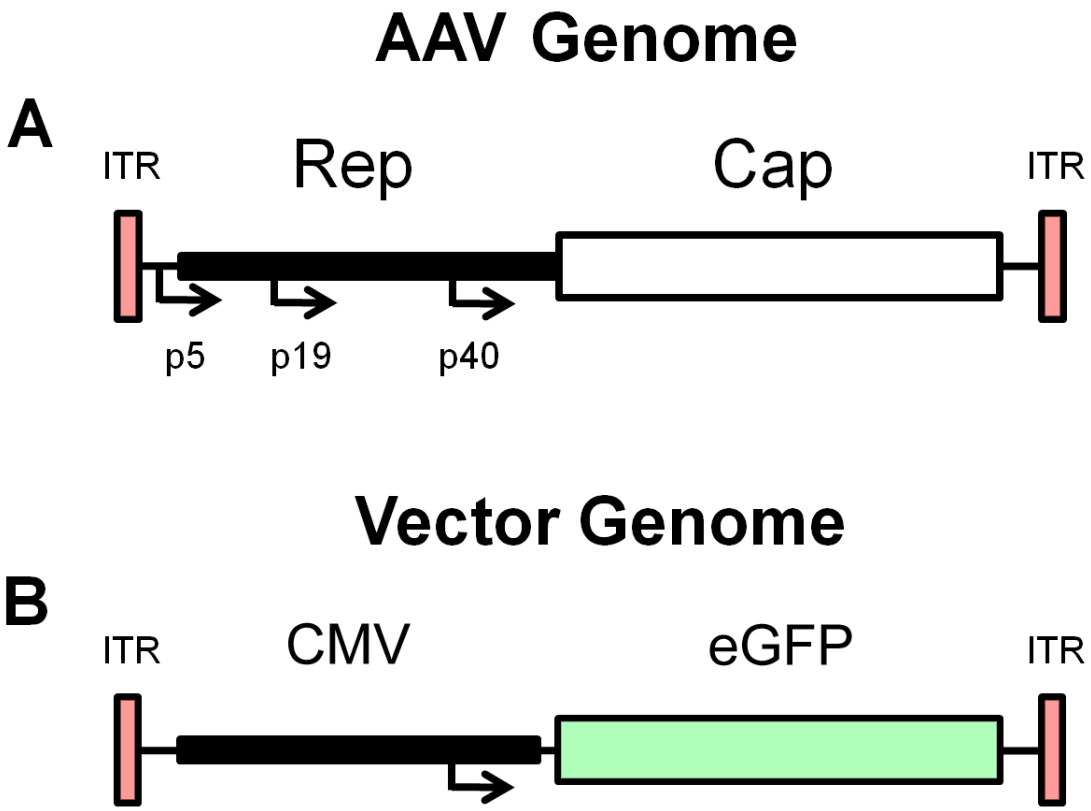

Figure 2.1 A schematic representation of the wild type AAV-2 genome (A) and the recombinant vector genome as kindly provided by REMEDI, NUI Galway (B). In the vector, both the Rep and Cap open reading frames are excised entirely. An *eGFP* reporter gene regulated by a constitutive cytomegalovirus (CMV) promoter replaces these open reading frames, leaving the non-coding inverted terminal repeats (ITR) as the only remaining parts of the endogenous AAV-2 genome.

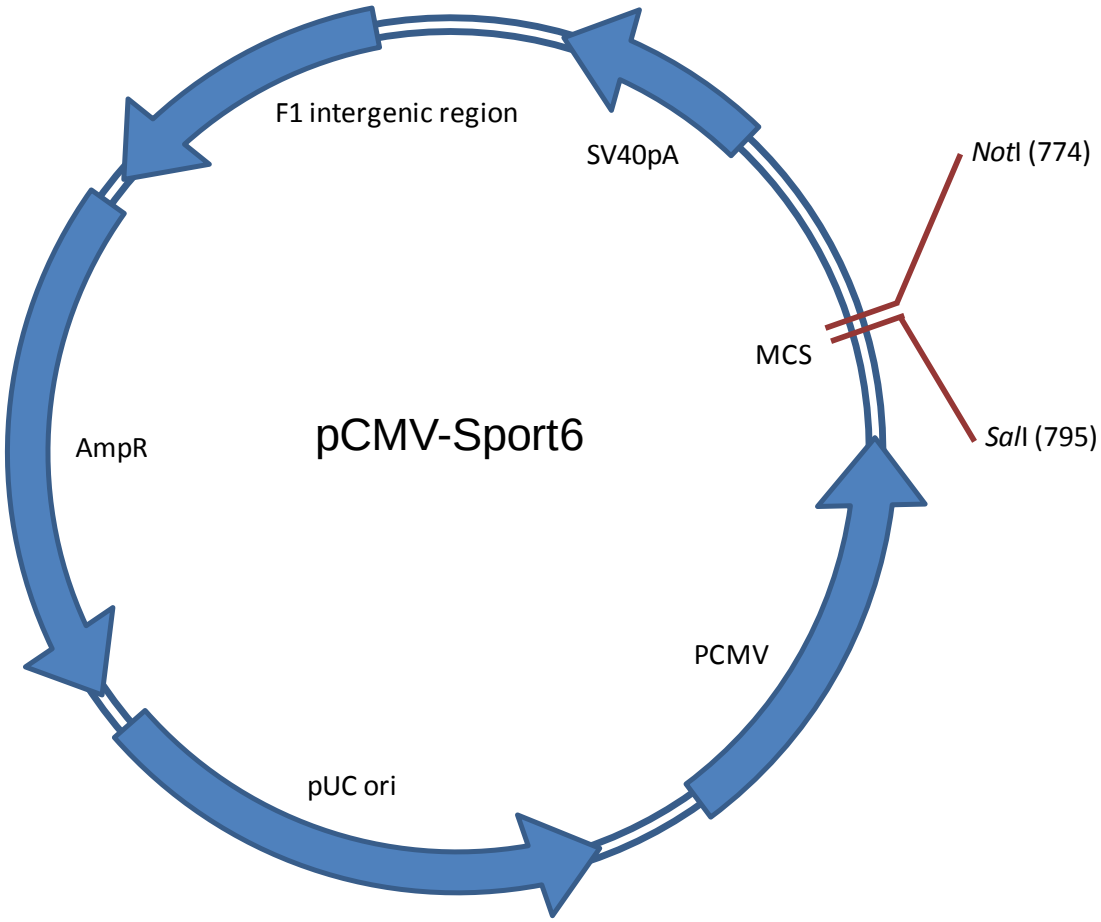

Figure 2.2 A schematic of the pCMV-Sport6 plasmid (Invitrogen) used in conjunction with Lipofectamine 2000 to transfect the murine *IDO* gene into murine MSC under the control of the CMV constitutive promoter. The plasmid contained an AmpR ampicillin resistance gene usable as a selection marker in bacterial culture. The transgene, a murine *IDO* gene was ligated between the NotI and SalI restriction sites.

2.2 METHODS

2.2.1 Cell isolation methods

2.2.1.1 Human peripheral blood mononuclear cell (PBMC) isolation by density gradient centrifugation

Human whole blood from healthy donors was provided by the Irish Blood Collections office at Blood Transfusion Service (St. James's Hospital, Dublin 2). PBMC were isolated by density centrifugation using Lymphoprep density centrifugation solution (Bøyum, 1968). Whole blood was prepared in sterile T-75 tissue culture flask containing 5 ml of filter-sterilised 5% EDTA and then diluted approximately 1:4 with cHBSS. Sterile 50 ml tubes were prepared, each containing 10 ml of Lymphoprep. Diluted blood was then layered on to the Lymphoprep using transfer pipettes to a total volume of 40 ml. Tubes were centrifuged at 400 × g for 25 minutes with acceleration settings at minimum and the rotor break switched off. Following centrifugation, the mononuclear cell layers were removed into fresh 50 ml tubes. Cells were diluted at least 1:2 with cHBSS. Tubes were centrifuged at 800 × g for 5 minutes with normal break and acceleration settings. Supernatants were discarded and the pellets were resuspended in 10 ml of cHBSS. Tubes were again centrifuged for 5 minutes at 800 × g. Supernatants were once again discarded and the pellets were resuspended in 2 ml cRPMI. Suspensions were pooled by donor and each was filtered through a 40 μm mesh filter to remove any remaining clots, debris or cell clumps. Cell counts were then performed using a 1:50 dilution of PBMC suspension in a solution of EB/AO.

2.2.1.2 Mouse splenocyte isolation by density centrifugation

Splenocytes were isolated by density centrifugation using Ficoll density centrifugation solution. Spleens were isolated from female BALB/c mice and homogenised through a 40 µm mesh filter into cHBSS. Splenocytes cells were isolated by density centrifugation rather than by red blood cell lysis in order to maximise mononuclear cell yield for downstream naive T-cell isolation. Cell suspensions were layered onto Ficoll and centrifuged at 600 × g for 25 minutes with centrifuge acceleration on the lowest setting and rotor brake disabled. Mononuclear cell layers were removed and pooled in cRPMI. Splenocytes were pelleted by centrifugation at 600 × g and resuspended in fresh cRPMI.

2.2.1.3 Mouse naive T-cell isolation by magnetic depletion

Splenocytes were processed using a naive T-cell isolation kit (MAGM205; R and D Systems) according to manufacturer's protocol. The kit included a biotinylated antibody cocktail and streptavidin-conjugated ferrofluid designed to deplete a splenocyte suspension of monocytes and mature lymphocytes, leaving a $CD3^+$ $CD4^+$ $CD62L^+$ enriched population. Cells were suspended in kit selection buffer at a concentration of 2×10^8 cells/ml in sterile polystyrene FACS tubes. 10 µl of antibody cocktail solution was added per 1×10^7 cells to be processed and the cells were mixed gently. Cells were incubated at 4˚C for 15 minutes. 12.5 µl of ferrofluid solution was added per 1×10^7 cells to be processed and the cells were again mixed gently. Cells were incubated at 4˚C for 15 minutes and then tubes were placed in a magnetic block and incubated for 6 minutes at room temperature. After this incubation step, cells still in

suspension were removed from tubes whilst still in the magnetic block. Cells were placed in fresh tubes and incubated in the magnetic block for a further 6 minutes. Unbound cell suspensions, containing the depleted naive CD4+ cell population were removed from tubes, centrifuged at 600 × g for 5 minutes and resuspended in cRPMI.

Table 2.3 Conjugated anti-mouse antibodies used for flow cytometry

Target	Fluorochrome	Isotype	Manufacturer
CD3e	FITC	Ham IgG	Immunotools
CD62L	PE	Rat IgG2a	Immunotools
MHC I	FITC	Mu IgG2a	eBioscience
MHC II	PE	Rat IgG2b	eBioscience
CD90	FITC	Mu IgG1	Immunotools
Sca-1	PE	Rat IgG2a	eBioscience

Hamster antibody (Ham). Mouse antibody (Mu).

2.2.2 Cell culture methods

2.2.2.1 Culture of murine MSC

Murine mesenchymal stem cells (MSC) were kindly provided by Dr. Karen English and Laura Tobin at the Mahon laboratory, isolated as previously described (English *et al.*, 2007). MSC for use in this study were obtained from cryopreserved stocks stored at a concentration of 1×10^6 cells/ml between passages 3 and 9. On recovery, cells were resuspended in 33 ml of cαMEM and seeded into a T-175 vented-cap tissue culture flask (Sarstedt, Nümbrecht, Germany). Cultures were incubated at 37˚C and 5% CO_2. Growth medium was replaced every 3-4 days and cultures were split once they reached 70% confluence. MSC were used up to a maximum of passage 12. Cultures were split by removal of growth medium, washing with sterile PBS and incubation with Trypsin-EDTA for up to 15 minutes. Once cells were observed to detach from the culture flask, Trypsin-EDTA activity was neutralised with an equal volume of cαMEM. Cells were pelleted by centrifugation at 600 × g for 5 minutes and then resuspended in cαMEM for counting with EB/AO and seeding into fresh culture flasks. Seeding density was 2×10^3 cells per cm^2.

MSC were validated by examination of morphology, potency, immunomodulatory capacity as described in Chapter 6. Surface expression of MHC class I, MHC class II, CD90 and Sca-1 was also assessed by flow cytometry as described in Chapter 6. Fluorescently-labelled antibodies used are listed in Table 2.3.

2.2.2.2 Culture of human HEK-293 cells

Human embryonic kidney cells (HEK-293) were obtained from cryopreserved stocks stored at a concentration of 1×10^6 cells/ml. Cells were resuspended in 33 ml of cDMEM per recovered cryotube and seeded into a T-175 vented-cap tissue culture flask (Sarstedt). Cultures were incubated at 37˚C and 5% CO_2. Growth medium was replaced every 3-4 days and cultures were split once they reached 70% confluence. Passage was performed as for murine MSC (Section 2.2.2.1) with cαMEM substituted with cDMEM.

2.2.2.3 Cell cryopreservation in liquid nitrogen

Cells required for storage were removed from long term culture and spun down at 600 × g for 5 minutes. A 50% recovery rate was assumed when calculating cells needed for storage. The pellet was resuspended in a small volume of freezing medium (Section 2.1.1.7) to give a final concentration of 2×10^7 cells/ml. Suspensions were distributed into cryotubes (Nunc) at 2 ml per tube. Cryotubes were transferred to N_2 vapour phase for 24 hours after which the tubes were moved to N_2 liquid storage.

2.2.3 Molecular techniques

2.2.3.1 RNA isolation

Cells were lysed in trizol at a concentration of 1×10^6 cells per ml. 5µl of Polyacryl Carrier was immediately added to the lysate and mixed. If RNA isolation was

to take place at a later time, lysates were frozen at –80°C for up to one week. 200 µl of chloroform was added per ml of lysate and samples were shaken for 15 seconds. Samples were allowed to stand at room temperature for 15 minutes before being centrifuged at 12,000 × g for 15 minutes in a temperature controlled centrifuge set to 4°C. The upper, clear, aqueous phase (200-300 µl) was transferred to new tubes and 250 µl of 2-isopropanol was added to each and carefully mixed with a pipette. Samples were then centrifuged at 12,000 × g and 4°C for 10 minutes. The resulting supernatants were removed and discarded. At least 500 µl of 75% ethanol was then added to wash pellets. A final centrifugation step was performed on the samples at 12,000 × g and 4°C for 5 minutes. Supernatants were decanted and the samples were inverted on tissue paper and then air dried to remove any remaining liquid. RNAse-free sterile H_2O at room temperature was added and mixed with a pipette. Samples were left standing at 65°C in a water bath for 15 minutes before being frozen at –80°C.

Prior to cDNA synthesis, RNA samples were treated to remove genomic DNA contamination. A mixture of 1 µl DNAse 1 and 1 µl DNAse buffer (200 mM Tris-HCl (pH 8.4), 20 mM MgCl2, and 500 mM KCl; Invitrogen) diluted in 3 µl RNAse-free H_2O was added to each sample in a 1:1 volume ratio and incubated at room temperature for 15 minutes. 1 µl of 25 mM EDTA (Invitrogen) was added per 10 µl sample and samples were incubated on a thermocycler at 65˚C for 10 minutes. For each RNA sample, two DNAse treatments were performed; one to be used for cDNA synthesis and one to be an RNA control.

2.2.3.2 cDNA synthesis

DNAse treated RNA samples were reverse-transcribed into complementary DNA (cDNA). A master mix was prepared containing 2.5 mM 10x buffer, 1.25 mM MgCl2, 1 mM dNTP mix, 1 µg Oligo dT primer, 500 units of superscript II RT and10 units of RNA inhibitor dissolved in nuclease-free dH_2O. Master mix was made up at a volume of 40 µl per RNA sample. 40 µl of master mix was added to 10 µl RNA sample. Samples were then incubated on a thermocycler for 10 minutes at 25˚C followed by 1 hour at 42˚C and 5 minutes at 95˚C. The resulting cDNA products were quantified using a UV spectrophotometer by reading the optical density at a wavelength of 260 nm. Once quantified, cDNA samples were used immediately for PCR or stored at -20˚C and used within one month.

2.2.3.3 Validation of cDNA samples

In order to validate the synthesis of functional cDNA, reverse transcription polymerase chain reaction (RT-PCR) was used to amplify cDNA for the detection of transcription of the housekeeping gene glyceraldehyde 3-phosphate dehydrogenase (GAPDH). The cDNA samples used for all PCR experiments were equilibrated to a concentration of 1 µg in a 25 µl reaction volume. Each reaction contained cDNA along with 2.5 mM $MgCl_2$, 1 mM dNTP mixture, 0.6 units of Taq polymerase, a 1:10 dilution of 10x reaction buffer and 0.4 pmol of GAPDH primers (Table 2.1).

To control for genomic DNA contamination, cDNA was substituted with an equal volume of the corresponding RNA sample. To control for contamination of

master mix reagents, cDNA was substituted with an equal volume of nuclease-free H_2O. Samples were then incubated on a thermocycler following the PCR programme detailed in Table 2.4.

Table 2.4 Standard RT-PCR program

Step	Temp (°C)	Time (min)	Repeats
Denaturation	95	10 min	0
Annealing	75	45 sec	
	A[a]	45 sec	
	72	45 sec	35[b]
Extension	72	10 min	0
Hold	4	Infinite	

[a] Annealing temperatures were 60˚C for the GAPDH and IDO primers.

[b] Annealing cycle was repeated 30 times for GAPDH.

2.2.3.4 PCR for detection of IDO

The cDNA samples used for all PCR experiments were equilibrated to a concentration of 1 µg in a 25 µl reaction volume. This equilibration of starting cDNA concentration allowed semi-quantitative determination of the relative levels of target RNA. Each reaction contained cDNA along with a Taq polymerase reaction mixture (AmpliTaq; Applied Biosystems, Foster City, CA) and 0.4 pmol of the relevant primers (Table 2.1). Controls for genomic DNA contamination and nuclease free water controls were prepared as for the GAPDH PCR (Section 2.2.4.3). Samples were then amplified using a thermocycler following the PCR programme described in Table 2.4.

2.2.3.5 Analysis of PCR products by gel electrophoresis

PCR products were visualised by agarose gel electorphoresis. Gels containing 1.3% (w/v) agarose (Sigma-Aldrich) and 0.2 µg/ml ethidium bromide (EB; Sigma-Aldrich) in TAE were used for GAPDH and IDO PCR products. Samples were mixed 1:1 with blue-orange tracking dye (Promega) and 10 µl was added to each gel lane. A 100 bp DNA ladder (Promega) was also added to each gel to facilitate product band molecular weight determination. 100 volts was passed through the gel for 50 minutes or until the tracking dye had migrated to the end of the gel. The presence of EB in the gel allowed DNA bands to be visualised and imaged using a UV light.

2.2.3.6 Genomic DNA isolation

Genomic DNA was isolated using a Generation Capture Column Kit (Qiagen). Human PBMC suspensions were passed through a solid matrix column which lysed

cells on contact whilst retaining DNA. The column was then washed using a provided purification buffer before the DNA was eluted from the column at high temperature (95˚C) using the provided elution buffer. Kits contained capture columns designed to fit into 1.5 ml tubes, 1.5 ml waste and sample collection tubes, DNA purification solution and DNA elution solution. A capture column was placed into a 1.5 ml waste tube. 200 µl of cell suspension containing a maximum of 1×10^7 cells was pipetted onto the column and incubated for 30 minutes at room temperature. 400 µl on DNA purification solution was added and the column was incubated at room temperature for 1 minute. The waste tube containing the column was then centrifuged at 6,000 × g for 10 seconds. The column was removed from the waste tube and inserted into a fresh waste tube. 400 µl of DNA purification solution was added to the column and incubated at room temperature for 1 minute. Waste tube and column were once again centrifuged at 6,000 × g for 10 seconds. 200 µl of DNA elution solution was added to the column followed by a 10 second centrifugation at 6,000 × g. The waste tube was discarded and the column was inserted into a 1.5 ml sample collection tube. 100 µl of DNA elution solution was added to the column which was incubated at 99˚C for 10 minutes. The sample collection tube and column were centrifuged at 6,000 × g for 10 seconds, the column was discarded and the eluted DNA sample was immediately analysed.

2.2.3.7 Characterisation of HLA haplotypes

HLA haplotypes were determined for 16 PBMC donors producing *in vitro* proliferative responses to AAV-2 stimulation. Sequence-specific primer (SSP) PCR for HLA A, B, C, DR and DQ were performed. DNA was isolated from PBMC using a

Generation Capture Column kit (Qiagen, California, USA) according to the manufacturer's protocol. HLA A, B, C, DR and DQ PCR was performed using an SSP-based PCR kit (Texas BioGene, Texas, USA) featuring a split 96-well tray format. Each tray could be used to determine the haplotype of the HLA A, B C, DR and DQ loci. Each well contained lyophilised primers for sequences specific for a variety of alleles of these loci. The resulting PCR samples were resolved on a 2% agarose gel with ethidium bromide to allow UV imaging of DNA bands. The allele for a given locus could be determined by the combination of bands present and their molecular weights. Analysis of the gels was performed using SSPal HLA analysis software (Texas BioGene) following the manufacturer's protocol.

2.2.3.8 Lysis of cells for SDS-PAGE

Cells were resuspended in radioimmunoprecipitation assay (RIPA) buffer (Sigma) and protease inhibitor (Sigma) in a 7:1 ratio. Cells were resuspended at a concentration of 2×10^7 cells/ml and mixed by pipetting. Lysates were stored at -80˚C.

2.2.4 Immunoassays

2.2.4.1 Enzyme-Linked Immunosorbant Assays: Design and Optimisation

An enzyme-linked immunosorbant assay (ELISA) is an assay used to detect antibodies or antigens in a sample using an antigen-specific antibody linked to an enzyme (Engvall & Perlmann, 1971; Van Weemen & Schuurs, 1971). Enzyme linkage allows detection of the analyte component of a sample using a colorimetric or

fluorometric substrate. The three main ELISA formats are the sandwich, indirect and competitive assays. In a sandwich assay, an antibody specific for the analyte is coated onto a surface. The antibody, termed the capture antibody, is immobilised on the surface by adsorption. The surface is then blocked with a solution containing adsorbing molecules, such as proteins or carbohydrates unlikely to be recognised non-specifically by the assay reagents. Blocking covers up any unused binding sites on the reactive surface. The surface is then exposed to the sample and, if the analyte is present, it will be bound by the immobilised capture antibody. A second analyte-specific antibody is added to the plate, preferably one with specificity for an epitope that will not be blocked or sterically hindered by the binding of the capture antibody. This second antibody, termed the detection antibody, will often either be directly labelled with an enzyme, or will be conjugated to biotin, allowing a wide range of biotin ligand-conjugated enzymes to be applied. A colorimetric or fluorometric substrate for the enzyme is added and the absorbance or emission is measured. The resulting values can then be converted to an analyte concentration by comparison to a standard curve.

At each stage, reagents are incubated on the reactive surface for various time periods, typically from 30 minutes up to 24 hours, and at various controlled temperatures, typically between 4˚C and 37˚C. At the start of each step, unbound reagents from the previous step are aspirated from the reactive surface. The surface is then typically washed using a pH controlled buffer containing a detergent. Washing is primarily conducted to remove non-specifically bound reagents which may increase the assay background reading or compete with specifically-bound reagents at the current step. Indirect assays are used to detect the presence of antibodies specific for a given

antigen in a sample, usually a bodily fluid such as blood serum. Indirect assays follow a very similar protocol to the sandwich assay; however there is no capture antibody. Instead, the antigen of interest is immobilised on the reactive surface and antibody-containing samples are used as the analyte. In a competitive ELISA, a sandwich or indirect ELISA is conducted as normal, however the analyte is pre-incubated with an unlabelled specific antibody (in the case of a sandwich ELISA) or with the antigen (in the case of an indirect ELISA, where the analyte is an antibody). Thus, when the analyte is incubated on the reactive surface, specific binding to the capture antibody or surface bound antigen will be reduced by the pre-incubation. This allows indirect quantification of the analyte, and can also be used to validate the specificity of the assay.

When a new ELISA is developed, each step of the assay must be optimised to ensure specificity, sensitivity and dynamic range in the final read-out. Specificity is a measure of the proportion of samples negative for a given property that are successfully identified as negative (Altman and Bland 1994). In ELISA, specificity is heavily dependent on the extent to which reagents at various steps engage in non-specific binding. A related concept is sensitivity, a measure of the proportion of samples positive for a given property which are successfully identified as positive (Altman & Bland, 1994). In ELISA, the sensitivity of the assay will depend on how likely it is that reagents will bind specifically and how strong that binding will be. In particular, frequent binding in the presence of a scare ligand and resistance to loss of binding during subsequent steps will enhance sensitivity. Thus, sensitivity and specificity are concepts closely related to type I and type II errors in statistics. Often, because of the aforementioned processes which underlie specificity and sensitivity in ELISA

experiments, it may not be possible to achieve both 100% specificity and 100% sensitivity, demanding a compromise. The dynamic range of the assay is the ratio between the ideal highest readout and ideal lowest readout, also referred to as the signal-to-background ratio. The dynamic range of the assay will impact on how accurately differences between analyte levels will be detected, particularly when levels near the negative background level of the assay, thus impacting on assay specificity and sensitivity. The range obtained is itself heavily influenced by both the sensitivity and specificity of the assay as well as the choice of readout reagents and equipment. Dynamic range is also of importance when constructing standard curves for the quantification of the assay readout. The greater the range in the readout for the standards, the higher the precision in the quantitation of the assay read-out will be. Indirect assays are of greatest use when studying the humoral immune responses to a virus such as AAV (Chapter 3).

2.2.4.2 Detection of AAV-2-specific total IgG: Method 1

AAV-2-specific total IgG in human plasma samples was detected using an indirect ELISA. 96-well flat bottomed, high-binding MaxiSorp immuno-plates (Nunc) were used as a reactive surface for all iterations of the ELISA. Sodium hydrogen phosphate (1M Na_2HPO_4; Sigma-Aldrich) was used as an antigen coating buffer with AAV-2 antigen at a concentration of 2×10^{11} drp/ml. 50 µl of each sample dilution was added to the plate in triplicate. A negative control consisting of 50 µl PBS was also added in triplicate. Samples were incubated on the plate for 2 hours at 37^{o}C. This incubation step was not modified at any point during optimisation. The plate was

washed using low detergent washing buffer (Section 2.1.3.1) and a solution of HRP-labelled goat anti-human IgG (Perkin-Elmer, Waltham, MA) was prepared at a concentration of 2 μg/ml. 50 μl of antibody was added to each well and the plate was incubated for two hours at room temperature. The plate was incubated at room temperature for 20 minutes and then washed. 50 μl of TMB substrate was added to each well and the reaction was allowed to proceed for 20 minutes at room temperature. The reaction was then stopped by addition of 50 μl of 1M H_2SO_4 to each well. The plate was then read on a microplate spectrophotometer at a wavelength of 450 nm. All washing steps were performed using 0.05% Tween 20 in PBS and blocking was performed using a solution of milk protein.

2.2.4.3 Detection of AAV-2-specific total IgG: Optimised method

Plates were coated with AAV-2 at a concentration of 1×10^9 drp/ml in carbonate coating buffer (150 mM Na_2CO_3, 350 mM $NaHCO_3$, pH9.6) for 12h at 4°C. Plates were blocked using 5% (w/v) Sucrose, 1% (w/v) BSA, 0.05% (v/v) Tween 20 in PBS. Human blood plasma was diluted 1:2000 in 1% (w/v) skimmed milk powder in PBS and incubated on the plates at 37°C for 2h. Plates were probed for human IgG using an anti-human IgG-biotin (Sigma-Aldrich). Detection was performed using a strep-HRP conjugate and TMB substrate. Five washes were performed between each step using 0.05% (v/v) Tween 20 in PBS. In the absence of AAV-2-specific IgG international standards, two known donors (#22 and #41) were selected as representative seropositive and seronegative samples. These were included in all assays. AAV-2-specific IgG data for the negative reference sample was assigned an AAV-2 antibody titre of 1 unit, whilst

the reference seropositive donor was assigned an AAV-2 antibody titre of 10 units. This allowed quality control to be performed to control for intra-assay variation, to normalize results and to allow a meaningful comparison of data between assays. Samples were considered seropositive if they scored above the seronegative cut off plus two standard deviations.

2.2.4.4 Verification of total IgG ELISA antigen coating

Antigen was directly probed using a mouse anti-AAV VP IgG (Source) diluted 1:1000 in PBS. 50 µl of this antibody was added to each well following a normal washing step. Detection antibody was incubated on the plate at room temperature for 2 hours. A secondary antibody, a goat anti-mouse IgG labelled with alkaline phosphatase (AKP) was diluted to 1:5000 in PBS. Following another normal washing step, 50ul was added to each well and incubated at room temperature for 2 hours. The plate was washed and the assay was visualised using a p-nitrophenol (pnp) substrate. The assay was read at a wavelength of 405 nm.

2.2.4.5 Determination of AAV-2-specific IgG ELISA specificity

96-well flat bottomed, high-binding MaxiSorp immuno-plates (Nunc) were coated with 100 µl AAV-2 (1×10^9 drp/ml) in carbonate coating buffer or carbonate coating buffer alone (negative control) and incubated overnight at 4^oC. Plates were placed under UV light for 15 minutes to inactivate the virus. Plates were washed and aspirated five times, blocked and incubated overnight at 4^oC as per Section 3.3. In 1.5ml tubes, test samples were incubated with AAV-2 or AAV-5 at concentrations of

2×10^{10} drp/ml serial diluted (1:4) to 1.25×10^{9} drp/ml and incubated for 2 hours at 37°C with agitation. A sample from each donor was also incubated at 37°C with no AAV vector added. A negative control containing no serum was also incubated with AAV-2 or AAV-5. Blocked plates were washed as before and 50µl of pre-incubated test samples, AAV-2 or AAV-5 samples were added to wells in triplicate and incubated for 2 hours at 37°C with 5% CO_2. Plates were UV inactivated for 15 minutes, washed and aspirated five times in high detergent wash buffer and incubated with 50 µl anti-human IgG-biotin (700 ng/ml) for 2 hours at room temperature. Plates were washed and aspirated five times in low detergent wash buffer and incubated with streptavidin-HRP conjugate (1:200) for 20 minutes at room temperature. Plates were washed as above and TMB substrate was added. When a strong signal was apparent, development was stopped with 1M H_2SO_4. Absorbance values were read at 450 nm and were analysed for significance against the non-AAV incubated sample using the Student's paired t-test as before.

2.2.4.6 Determination of AAV-2-specific IgG neutralising activity

Plasma samples were co-incubated with AAV-2*GFP* at a concentration of for 24 hours. The vectors and plasma mixtures were then incubated with HEK-293 cells following the AAV-2*GFP* transduction protocol (Section 2.2.6.1). Neutralising activity was demonstrated by reductions in the levels of GFP expression in the HEK-293 target cells, as assessed by flow cytometry and detected on FL1.

2.2.4.7 Detection of AAV-2-specific total IgG subclasses

Assays were performed in an adaptation of the protocol for total IgG detection (Section 2.2.4.2). In addition, control serum containing pooled, standardized concentrations of human IgG subclasses 1, 2, 3 and 4 (Nordic Labs, Tilburg, Holland) was used as a reference serum. Reference serum was diluted to 1:3000 in coating buffer and underwent a 7-point, 2-fold serial dilution in triplicate before being coated directly to the assay plate. The resulting bound concentrations of IgG subclasses are detailed in Table 2.5. Plates were probed for human IgG using anti-human IgG subclass-biotin antibodies for subclasses IgG1-IgG4 (Merck, Nottingham, England). Detection and washing were performed as for the total IgG ELISA.

2.2.4.8 Detection of human cytokines

Cytokine levels for IFN-γ, IL-13 and IL-10 in supernatants from PBMC cultures producing proliferation in response to AAV-2 stimulation were determined by sandwich ELISA. Commercial human IFN-γ and human IL-10 ELISA kits (Immunotools, Friesoythe, Germany) or matched antibodies for human IL-13 (R&D Systems, Minneapolis, USA) were used for cytokine detection. For IFN-γ and IL-10 assays, capture antibody (Section 2.1.3.4) was diluted 1:100 in carbonate coating buffer. For IL-13, antibody was diluted in carbonate coating buffer to a working concentration of 4 μg/ml. In excess of 4.8 ml of coat solution was prepared for each 96-well plate to be coated. Plates were coated with 50 μl of coat solution per well and incubated overnight at 4^{o}C.

Table 2.5 IgG subclass standard concentrations

IgG1 (pg/ml)	IgG2 (pg/ml)	IgG3 (pg/ml)	IgG4 (pg/ml)
1860000	1030000	130000	180000
930000	520000	65000	92000
460000	260000	32500	46000
230000	128000	16250	23000
120000	64000	8100	11500
58000	32000	4000	5700
29000	16000	2000	2900

Plates were washed with 300 µl per well of washing buffer such that each well was washed and aspirated 3 times. 250-300µl of blocking buffer was added to each well and the plates were incubated for two hours at room temperature or overnight at 4^{o}C. Plates were washed three times with washing buffer. A 7-point, 2-fold dilution of recombinant IFN-γ or IL-10 standard in standard diluent was performed, starting with a high standard at a concentration of 1000 pg/ml. For IL-13, seven recombinant human IL-13 (rhIL-13) standards were prepared from stock solution, starting with a high standard at a concentration of 8000 pg/ml and diluting 1:2 in standard diluent. 30µl per well of samples and standards were added to the coated and blocked wells. The plates were incubated overnight at 4^{o}C and then washed five times.

IFN-γ and IL-10 detection antibodies were diluted 1:100 in reagent diluent and 50µl of detection antibody solution was added to each well. IL-13 detection antibody

was diluted in reagent diluent to a working concentration of 400 ng/ml. The plates were then incubated for two hours at room temperature and washed five times with washing buffer. Strep-HRP conjugate was diluted 1:200 in reagent diluent and 50µl was added to each well. The plates were incubated at room temperature for 20 minutes. The plates were washed three times and developed with 50µl of TMB per well for 20 minutes. Development was performed out of direct light. The development reaction was stopped with 50µl per well of 1M H_2SO_4. Plates were read using a spectrophotometer at a wavelength of 450 nm.

2.2.4.9 Bradford protein quantification assay

The Bradford protein quantification assay (Bradford, 1976) was used to determine protein concentrations in samples for western blotting (Section 2.2.4.10). A 1 mg/ml BSA protein stock solution was prepared in dH_2O and stored at –20^oC. Five protein concentration standards (200, 100, 50, 25 and 0 µg/ml) were prepared using aliquots of this stock. Standards were prepared by adding 800 µl of dH_2O to each tube. A volume of dH_2O equal to the volume of BSA to be added was then removed. With the same pipette and pipette tip, the BSA was added to the tube. The samples were thawed to 4^oC and vortexed to break up frozen material. If the samples required clarification, they were centrifuged for 5 minutes at 13,000 × g to remove cellular material. Samples were diluted in dH_2O to 1:200, 1:2000 and 1:20,000. Dilutions of samples and standards were prepared simultaneously. The required total amount of Bio-Rad reagent (200 µl per sample or standard) was poured into a universal, covered with tinfoil and allowed to come to room temperature. The samples and standards were

vortexed for 10 seconds. All of the tubes were then opened and 200 µl of Bio-Rad reagent was added to each to each. The tubes were then closed and each was mixed by inversion 3 times and vortexed for 10 seconds. Once all tubes had been inverted and vortexed, 200 µl of each sample or standard was added to a 96-well plate in triplicate. Samples and standards were mixed an equal number of times with the pipette before removal from the tube. The absorbance was then read at a wavelength of 595 nm using a spectrophotometer.

2.2.4.10 Western blot for detection of IDO protein

Resolving and stacking gels were prepared as described in Section 2.1.3.7 and were used within 24 hours of setting. The protein concentration in samples for analysis (Section 2.2.3.8) were determined using the Bradford assay (Section 2.2.4.9) and then normalised to a concentration of 5 mg/ml. 10 µl samples were mixed 1:1 with loading buffer (Section 2.1.3.7) and heated to 95˚C for 5 minutes. Gels were placed in a vertical electrophoresis unit filled with a 1:10 dilution of running buffer (Section 2.1.3.6). Samples, along with a marker ladder, were then loaded into the stacking gel. The gel was subjected to 50 volts for 30 minutes to allow protein samples to migrate through the stacking gel and onto the resolving gel. The gel was then subjected to 120 volts and run until the marker dye and loading buffer had reached the bottom of the resolving gel.

Protein was then electroblotted to nitrocellulose membranes (Sartorius Stedim Biotech, Aubagne, France) following an adaptation of the method of Burnett (Burnette, 1981). The gel was placed onto a nitrocellulose membrane and sandwiched between two filter papers, two sponges and placed into an ice-cooled electrophoresis rig filled

with transfer buffer. A magnetic mixing bead was placed into the electrophoresis rig and the rig was placed onto a magnetic stirrer in order to ensure even cooling of the rig. Transfer of protein from the gel onto the nitrocellulose membrane was conducted by passing 100 volts through the gel for 1 hour. The presence of the stained molecular weight ladder on the nitrocellulose membrane verified the electro transfer.

Nitrocellulose membranes were blocked by submerging in 5% (w/v) skimmed milk powder and 0.05% (v/v) Tween 20 in PBS for 1 hour at room temperature and then washed with TBS-Tween 20 washing buffer for 20 minutes. Three 20 minute washes were performed between all remaining steps. Each membrane was incubated with mixing overnight at 4˚C with primary antibody (mouse anti-IDO IgG; Millipore, Billerica, MA) at a dilution of 1:500 in TBS buffer. Secondary antibody (goat anti-mouse IgG; Sigma) was incubated with the membrane for 1 hour at room temperature with mixing. Chemiluminescence reagent (Roche) was prepared as a 100:1 dilution of solution A and solution B which was incubated on the membrane at room temperature for with mixing for 1 minute.

Chemiluminescence reagent was drained from the membrane which was then wrapped in cling film, placed into an x-ray cassette (Hypercassette; GE Healthcare) and transferred to a dark room. Film was placed on top of the membrane and left to expose for 1 minute, 5 minutes, 30 minutes or 1 hour. Film was developed by washing in development fluid (Kodak GBX Developer; Sigma-Aldrich) and then rinsed in water. Film was then fixed in Kodak GBX Fixer solution (Sigma-Aldrich) and again rinsed in water.

2.2.5 Methods for the assessment of cell function

2.2.5.1 Detection of *in vitro* human lymphoproliferative responses to AAV-2 and AAV-2 capsid peptides

Human PBMC were suspended in cRPMI at a concentration of 2×10^6 cells per ml. Cells were plated in triplicates onto a 96-well tissue culture plate with 200 µl of PBMC suspension added to each well. A solution of AAV-2 vectors (Section 2.1.5.1) in cRPMI was prepared with a concentration of 5×10^8 drp/µl. 25 µl of AAV-2 solution was added to each test well, giving a final concentration of 1×10^8 drp/µl. Multiplicity of infection (MOI) was 5×10^4. For the capsid peptide stimulation, AAV-2 was replaced with peptides derived from the AAV-2 VP1 capsid protein (Section 2.1.4.1) at a concentration of 100 µg/ml. ConA at a stock concentration of 1 mg/ml was diluted 1:25 in cRPMI. 25 µl of ConA solution was added to each positive control well. Negative control wells were equilibrated to match positive control and test wells by addition of 25 µl per well of cRPMI. The plate was then incubated at 37°C with 5% CO_2 for 96 hours.

After 96 hours, 100 µl of supernatant was removed from each well and frozen at -20°C for further analysis by cytokine ELISA. The removed medium on all wells was replaced with cRPMI containing ^{3}H-thymidine. ^{3}H-thymidine was added to each well giving a final dilution of 1:400 from stock, equivalent to 92.5 µBq/ml. The plates were then incubated at 37°C with 5% CO_2 for 5 hours. After 5 hours the plates were either frozen at -20°C for analysis on another date or harvested immediately. Cultures were harvested using a 96-well plate harvester (Molecular Devices, Sunnyvale, CA). The well contents were filtered onto glass fibre 96-well size filter mats. The filter mats were

dried at 40°C before being sealed in plastic pockets containing 3.5 ml of scintillation fluid (GE Healthcare). The sealed mats were then analysed using a beta scintillation counter, producing a beta decay count per minute (CPM) reading for each well. Results obtained were expressed as stimulation indices (SI), calculated as the fold proliferation increase over the negative control (Corcoran *et al.*, 2000). For assays employing VP1 peptides, SI values were considered positive if they were greater than one standard deviation above the mean SI for all peptide stimulated wells.

2.2.5.2 Detection of *in vitro* murine MSC immunomodulatory activity by ^{3}H-thymidine incorporation assay

Normal, plasmid transfected, mock-transfected or IFN-γ stimulated murine MSC or growth media alone were incubated on the plates for 24 hours at 37˚C and 5% CO_2 to allow cell adhesion. Murine splenocytes were isolated as described in Section 2.2.1.2 and were suspended in cRPMI at a concentration of 2×10^6 cells per ml. Cells were plated in triplicates onto a 96-well tissue culture plate with 200 µl of splenocyte suspension added to each well. ConA at a stock concentration of 1 mg/ml was diluted 1:25 in cRPMI. 25 µl of ConA solution was added to each well to be mitogen stimulated. Negative control wells were equilibrated to match positive control and test wells by addition of 25 µl per well of cRPMI. The plate was then incubated at 37°C with 5% CO_2 for 96 hours.

^{3}H-thymidine was added to each well giving a final dilution of 1:400 from stock, equivalent to 92.5 µBq/ml. The plates were then incubated at 37°C with 5% CO_2 for 5 hours. After 5 hours the plates were either frozen at -20°C for analysis on another date

or harvested immediately. Cultures were harvested using a 96-well plate harvester as detailed in Section 2.2.5.1. Results obtained were expressed as stimulation indices (SI), calculated as the fold proliferation increase over the negative control.

2.2.5.3 Detection of *in vitro* murine MSC immunomodulatory activity by CFSE timecourse assay

96-well sterile culture plates were coated overnight at 4˚C with 20 µg/ml anti-CD3e mitogen diluted in sterile PBS or PBS alone. Plates were then washed with sterile PBS and normal MSC, transfected MSC or growth media alone were incubated on the plates for 24 hours at 37˚C and 5% CO_2 to allow cell adhesion.

Murine splenocytes were isolated as described in Section 2.2.1.2. These were then used for naive T-cell isolation as described in 2.2.1.3. Cells were suspended in sterile PBS with 0.1% BSA at a concentration of 1×10^7 cells/ml. CFSE (Sigma-Aldrich) was added to give a final concentration of 10 µM and cells were vortexed. Cells were incubated in a 37^{o}C water bath for 10 minutes and mixed frequently. The reaction was quenched by diluting cells 1:10 with cRPMI. Cells were then centrifuged at 800 × g for 5 minutes. Cells were resuspended in at least 1 ml of cRPMI and incubated at room temperature for 10 minutes to allow cells to excrete excess CFSE dye. Cells were centrifuged at 800 × g for 5 minutes and the cells were resuspended in required final volume of cRPMI. Stained T-cells were seeded into the culture plate at required density.

Culture plates were then incubated at 37˚C and 5% CO_2 for a period of 5 days. During this time, cells were harvested from the plate once every 24 hours. Directly prior to harvest, 3000 Calibrite-PE beads were added to each well, ensuring that the same pipette tip was used for all wells. Each well was mixed by pumping with a fresh pipette tip. 10 µl of propidium iodide (1ug/ml) was added to each well. Wells were mixed thoroughly and transfer to 5 ml polystyrene tubes for FACS analysis.

2.2.5.4 Differentiation of MSC into osteoclasts (bone cells)

Murine MSC were seeded into 6 well plates at a density of 50 cells per cm^2 in 2 ml cαMEM. Plates were incubated at 37^{o}C and 5% CO_2 for 10 days. During this time, growth medium was replaced every 3-4 days. On day 11, expansion medium was aspirated and replaced with either bone differentiation medium or fresh cαMEM. Plates were incubated at 37^{o}C and 5% CO_2 for 3 weeks. During this time, medium was replaced with every 3-4 days. After 3 weeks of incubation, differentiation medium was removed and cells were washed with PBS. Cells were fixed by addition of 10% formalin for 20 minutes at room temperature and then stained with 0.5 ml per well of Alizarin Red for 20 minutes at room temperature. Wells were then washed with dH_2O until wash became clear. Plates were then examined by light microscope for red mineral deposits.

2.2.5.5 Differentiation of MSC into adipocytes (fat cells)

Murine MSC were seeded into 6 well plates at a density of 50 cells per cm^2 in 2 ml cαMEM. Plates were incubated at 37^{o}C and 5% CO_2 for 10 days. During this time,

growth medium was replaced every 3-4 days. On day 11, medium was aspirated and replaced with either fat differentiation medium or fresh cαMEM. Plates were incubated at 37^{o}C and 5% CO_2 for 3 weeks. During this time, medium was replaced every 3-4 days. After 3 weeks of incubation, medium was removed and cells were washed with PBS. Cells were fixed by addition of 10% formalin for 20 minutes at room temperature and then stained with 0.5ml of freshly-diluted Oil Red-O working solution per well for 20 minutes at room temperature. Wells were then washed with dH_2O until wash became clear. Plates were then examined by light microscope for red fat globules.

2.2.5.6 Determination of kynurenine concentration

IDO activity was quantified by measuring the concentration of the tryptophan metabolite kynurenine in cell culture supernatants. Protein components of the supernatants such as FCS were precipitated by addition of 20% (w/v) trichloroacetic acid (10% final volume) and centrifugation at 13,000 rpm for 10 minutes at 4˚C. Kynurenine was measured by reversed-phase high performance liquid chromatography (HPLC), in an adaptation of a method published elsewhere (Vignau *et al.*, 2004), using a 1200 series HPLC with a diode array detector (Agilent Technologies, Santa Clara, CA). An Eclipse XD8-C18 column (Agilent Technologies) with an 8 nm pore was used for sample separation. The mobile phase was a mixture of 5 mM aqueous zinc acetate solution and acetonitrile (Sigma-Aldrich) prepared as described in Section 2.1.4.5. A sample injection volume of 20 µl was used. Absorbance was measured across the full range of wavelengths from 190 to 950 nm. The concentration of kynurenine was quantified by comparison with a kynurenine standard (Sigma-Aldrich) ranging from 0-

100 µM (Figure 2.4). Kynurenine was identified in the standards as a peak with a retention time of 3.0 to 3.1 minutes detectable at 345 nm. Control kynurenine was dissolved in the same growth medium as the supernatant samples and was subjected to the same precipitation process, thus any background kynurenine level, spontaneous L-tryptophan metabolism or any catalysed L-tryptophan metabolism endogenous to the complete growth medium was accounted for. This also compensated for the reported capacity of the TCA precipitation method to breakdown L-tryptophan into kynurenine (Miller *et al.*, 2006).

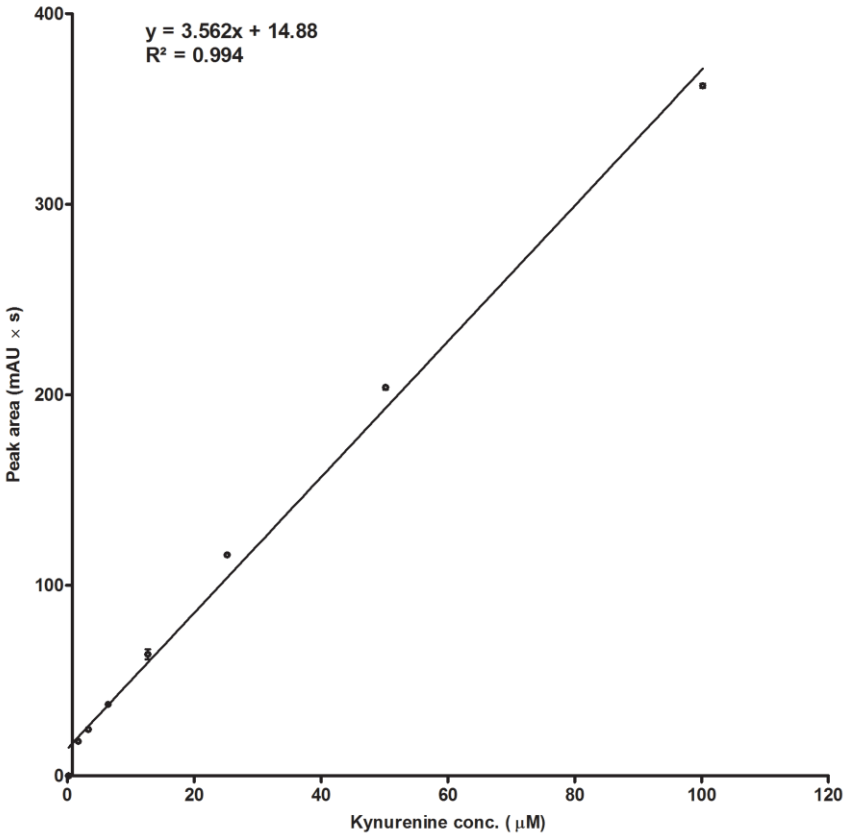

Figure 2.4 A representative standard curve for the quantification of kynurenine concentrations in culture supernatants by HPLC. The standard curve was determined in duplicate for each HPLC run and error, where present, is indicated with bars. Kynurenine had a retention time of between 3 and 3.1 minutes when eluted using an isocratic zinc acetate acetonitrile mobile phase. The concentration of the standards had a linear relationship with the area of the kynurenine peak. Given the peak area (y), kynurenine levels in samples could thus be calculated by solving the equation of the line for x.

2.2.6 Transformation of murine MSC

2.2.6.1 Transduction of mesenchymal stem cells with AAV-2*GFP*

Murine MSC were seeded on 24 well culture plates in cαMEM at a concentration of 1×10^4 cells/ml. Plates were incubated overnight at 37°C and 5% CO_2 to allow MSC to adhere to the plate surface. After 24 hours, medium was removed and replaced with AAV-2 in complete cαMEM at MOI of 1000, 10000 or with complete αMEM alone. Plates were incubated at 37°C and 5% CO_2 for 24 hours. Medium was removed and cells were washed twice with sterile PBS to remove free virus. Fresh cαMEM was added to all wells and plates were incubated at 37°C and 5% CO_2 for 24 hours.

2.2.6.2 Transfection of mesenchymal stem cells with pCMV-Sport6 IDO

Murine MSC were seeded into 24 well plates at a density of 5×10^5 cells per well in 500 µl of cαMEM. Cells were allowed to adhere and grow by incubation at 37°C and 5% CO_2 for 24 hours. For each well to be transfected, 0.8 µg of pSport6CMV-IDO (Figure 2.2) plasmid DNA was diluted in 50µl of OptiMEM I medium. 2.0 µl of Lipofectamine 2000 (Invitrogen) was diluted in 50 µl of OptiMEM I medium for each well to be transfected. DNA and lipofectamine were incubated at room temperature for 5 minutes before being gently mixed and incubated for a further 20 minutes at room temperature to allow DNA-Lipofectamine complex formation. 100 µl of complexes was added to each well to be transfected. Plates were gently mixed by rocking and incubated at 37°C and 5% CO_2 for 24 hours. Transfection was validated by PCR for the IDO transgene (Section 2.2.4.4).

2.2.7 Molecular modelling

The 3D structure of AAV-2 VP1 (structure 1lp3) was obtained from the Protein Data Bank (PDB) and was imaged using Christoph Gille's Structure based Sequences Alignment Program (STRAP; Institut für Biochemie, Charité, Berlin). STRAP was also used to highlight residues corresponding to the candidate T-cell epitopes identified using methods described in Section 2.2.5.1. Where required, Photoshop CS3 (Adobe Systems, San Jose, CA) was used for compositing of symmetry axes and labels.

2.2.8 Multiple sequence alignments

Alignment of AAV VP1 amino acid sequences was carried out using ClustalW (EMBL-European Bioinformatics Institute) on default settings.

2.3 STATISTICAL METHODS

2.3.1 General statistical analysis

For ELISA and proliferation assays, statistical significance values between test replicates and controls were calculated using a paired, two-tailed Student's t-test. Differences were considered statistically significant if $p \leq 0.05$. For proliferation assays employing the synthetic VP1 peptides, SI values were considered positive if they were greater than one standard deviation above the mean SI for all peptide stimulated wells. Correlations were assessed using the Pearson product-moment correlation coefficient.

All statistical analyses were conducted using Prism 5 (GraphPad Software Inc., La Jolla, CA) or Excel 2007 (Microsoft Corporation, Redmond, WA).

2.3.2 Precursor cohort analysis

CFSE timecourse data (Section 2.2.5.3) was analysed to establish progressor fraction, mean time to first division and mean subsequent division time. Calculations were based on precursor cohort numbers, a means of tracking the fate of the starting cell population or precursor cohort. Precursor cohort numbers were calculated using the method of Hawkins *et al.* (Hawkins *et al.*, 2007). Progressor fraction was calculated as the fraction of the total precursor cohort in any division above division 1. Mean time to first division was calculated as the weighted mean time at which cells enter division 2. Mean subsequent division time was calculated as the mean time taken for cells to enter divisions subsequent to division 2 (Hawkins *et al.*, 2007).

2.4 ETHICS

Human whole blood was provided by the Irish Blood Transfusion Service having been obtained by venipuncture with informed consent. Murine materials including bone marrow aspirates and splenocytes and human materials including whole blood were acquired and used in accordance with ethical approval from the local Research Ethics Committee (NUI Maynooth).

CHAPTER 3

THE HUMAN SEROLOGICAL RESPONSE TO AAV-2

3.1 INTRODUCTION

The reported seroprevalence of AAV-2-specific antibody in humans is highly variable. Many groups have examined AAV-2-specific IgG (Chirmule *et al.*, 1999; Erles *et al.*, 1999; Murphy *et al.*, 2009), IgM (Erles *et al.*, 1999; Murphy *et al.*, 2009) or total antibody (Moskalenko *et al.*, 2000) in humans but the reported extent of prevalence varied from 30% to 96% depending on geographical location, assay sensitivity and subject age. Studies of humoral immunity in animals following AAV administration have also demonstrated robust induction of antibody (Chirmule *et al.*, 2000). In order to assess the extent of immunity to AAV-2 pre-existing in an Irish population, samples of whole blood were taken from healthy Irish blood donors provided by the Irish Blood Transfusion Service (IBTS). A total of 45 donors were sampled and assessed for humoral immunity to AAV-2 and a subset of these was examined for cellular immunity to AAV-2 including specific epitope recognition (Chapters 4 and 5). This chapter will detail the optimisation of methods to detect AAV-2-specific antibodies in plasma samples derived from this donor group and will then report the results of the serological study.

Previously, the antibody response to AAV-2 has been quantified using a variety of methods (Chirmule *et al.*, 1999; Erles *et al.*, 1999; Moskalenko *et al.*, 2000), but no standardised method for assessing the levels of AAV-2-specific human IgG in serum or plasma existed at the beginning of this study. It was therefore necessary to define the parameters by which AAV-2 seroprevalence would be assessed here. The first two sections of this chapter will describe the development and optimisation of ELISA assays

designed to measure AAV-2-specific IgG and IgG subclass concentrations in blood plasma samples. The remainder of the chapter will characterise the IgG and IgG subclasses in humoral responses to AAV-2 in the Irish population.

3.2 Development and Optimisation of an Anti-AAV-2 IgG Antibody ELISA

3.2.1 Initial ELISA design

At the study outset (June 2005), no AAV-2 antibody specific immunoassays or standardised AAV-2 positive sera were commercially available. Methods in the literature for assessing titres of AAV-2-specific immunoglobulins in human amniotic fluid (Boyle *et al.*, 2003) or serum (Chirmule *et al.*, 1999) also varied considerably. It was therefore necessary to develop a new assay to meet our specific needs.

It was decided that the ELISA would take the form of an indirect binding assay (Chapter 1.9). AAV-2 virus particles were to be coated onto a polystyrene plate using a pH-adjusted coating buffer. A MaxiSorp polystyrene surface (Nunc, Langenselbold, Germany) was chosen as it would be versatile, having a high affinity for molecules with mixed hydrophilic and hydrophobic domains, allowing the easy adaptation of the assay for a range of antigens. The reactive surface would then be blocked to prevent non-specific binding of later reaction components. After appropriate washing steps the analyte, diluted human plasma, would then be added. The detection antibody would be an anti-human IgG conjugated to streptavidin-horseradish peroxidase. The level of

analyte would then be quantified colourimetrically by adding a TMB substrate, the colour change being proportionate to the antibody concentration over a limited range.

Several core elements of the ELISA were considered likely to require optimisation. Composition of the antigen coating buffer and concentration of AAV-2 capsid antigen as well as coating time and conditions would need to be assessed first. Washing buffer components and washing procedure at multiple steps would likely have a significant impact on assay sensitivity and specificity. Blocking buffer components, blocking time and conditions would be similarly important. A range of plasma sample and detection antibody dilution factors, reagent diluent components as well as incubation time and conditions for these reagents would need to be assessed. Finally, as standardised reference sera were not available, control samples would need to be selected to allow intra-batch normalisation.

Optimisation was carried out as a pilot study using a panel of six plasma samples isolated from healthy Irish blood donors (Section 3.2.2). Once the basic assay conditions were established, one strongly-binding plasma (Donor 4) and one non-binding plasma (Donor 1) were selected to act as positive and negative controls, respectively. These would allow both for an initial assessment of sensitivity and intra-batch normalisation during the remainder of the optimisation process. Once the optimisation was completed, a panel of plasma samples (n = 45, including some samples from the original pilot group) were assessed using the definitive method. New reference samples would be selected at that point as the optimisation process would deplete the available samples from the pilot group. The new samples would be obtained from

donors who would also be assessed for cell-mediated immune responses to AAV-2, described in Chapter 4.

3.2.2 Optimisation of a method to detect AAV-2-specific IgG

Initially, optimisation was focused on titrating analyte (IgG) binding. The ELISA was first carried out as described in Chapter 2.2.4.2. A positive reference plasma sample (Donor 2) was used as the analyte. The analyte samples were diluted 1:2 in PBS and serially diluted to 1:20, 1:200 and 1:2000. A PBS analyte control was also included. A Sodium hydrogen phosphate solution was used as the antigen coating buffer with AAV-2 antigen at a concentration of 2×10^{11} drp/ml as described in Chapter 2.2.4.2. All washing steps were performed using 0.05% Tween 20 in PBS and a solution of milk protein selected as the blocking agent.

The results (Figure 3.1 A) showed a significant difference between the absorbance readings at 450 nm (A_{450}) for the PBS control and the sample wells. Each sample replicate was compared to the PBS control using a paired t-test and all four sample replicates showed a significance of $p \leq 0.05$. The PBS control represented the background in this iteration of the experiment. While the absorbance of control was significantly lower than the samples, it still represented a significant reading above blank wells. This suggested that non-specific binding of reagents was occurring. Furthermore, no statistically significant titration of the analyte could be observed. This suggested that either a high degree of non-specific binding was also occurring during the

analyte binding stage of the assay or that the range of analyte dilutions used represented saturating concentrations.

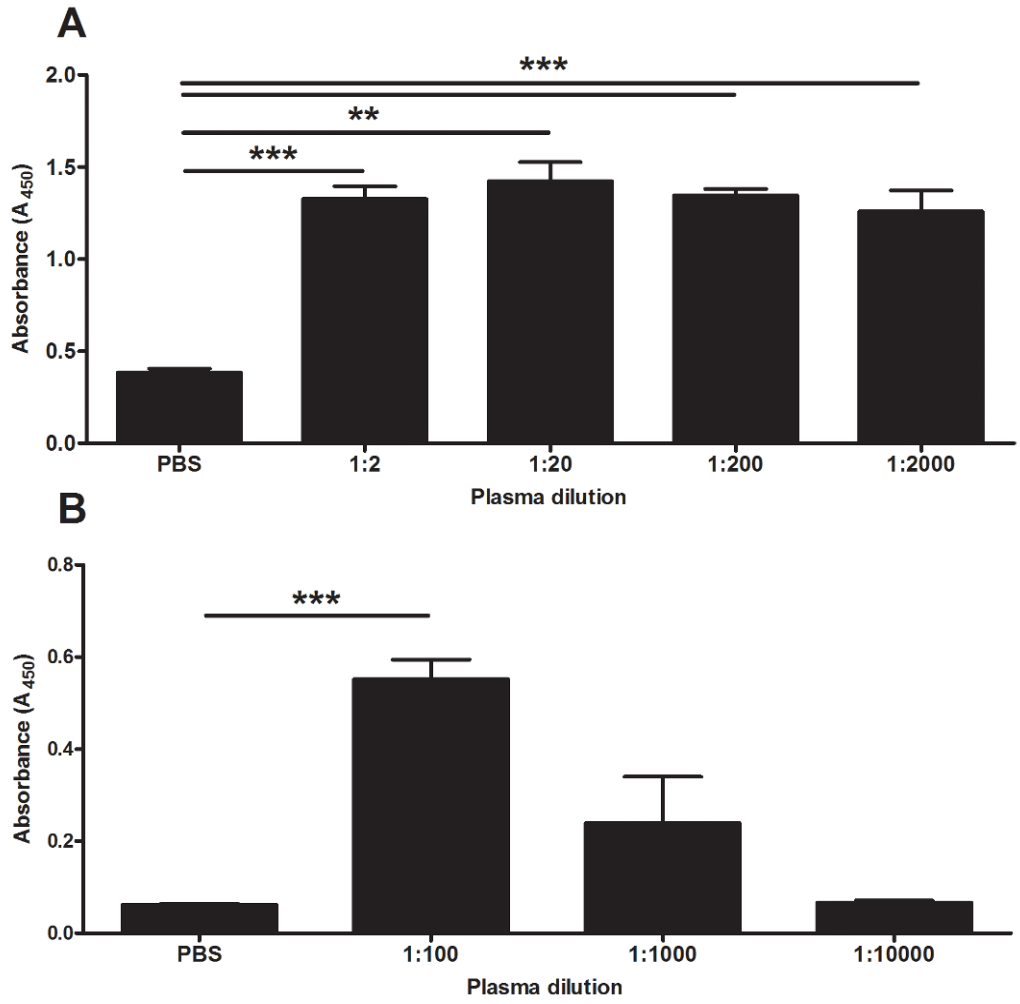

Figure 3.1 A) Optimisation of the AAV-2-specific human IgG ELISA. Plasma samples were diluted to the indicated factor in PBS and analysed for the presence of AAV-2-specific total IgG. B) A wider sample dilution range and a more specific IgG detection antibody produced a detectable analyte titration. Absorbance levels at 450 nm represent the mean of triplicate determinations. Error bars indicate the standard deviation in each case.

In order to address this possibility, the ELISA protocol was modified to cover a wider sample dilution range. Dilutions chosen in this case were 1:100, 1:1000 and 1:10000. Also, to enhance the specificity of the assay, a biotin-labelled anti-human IgG detection antibody (Sigma) replaced the HRP-labelled anti-human IgG and was used at a concentration of 70ng/ml. The detection step was otherwise carried out as before. Following the incubation with detection antibody, the plate was washed, then 50 µl of streptavidin-HRP conjugate (diluted 1:200 in PBS), was added to each well. The improved protocol allowed a titration of analyte (Figure 3.1 B). The 1:100 dilution was significantly above PBS background, whilst the 1:1000 and 1:10000 dilutions were not.

Despite this result, the volumes of antigen used for the assay were considered to be too high to allow this approach to be useful in the laboratory. The assay was therefore adapted to test two lower antigen coating concentrations; 1×10^{11} drp/ml and 5×10^{10} drp/ml. At an analyte dilution of 1:100, no significant difference in plasma binding was detected between the two antigen coating dilutions (Figure 3.2 A). At a sample dilution of 1:1000, a significant ($p = 0.03$) absorbance difference at 450nm was detectable between the two antigen coating dilutions, however the difference was small (0.016). It was clear from these results that a reduction in the antigen concentration was not impacting on the extent of plasma sample binding, suggesting that the analyte binding observed did not represent antigen-specific binding.

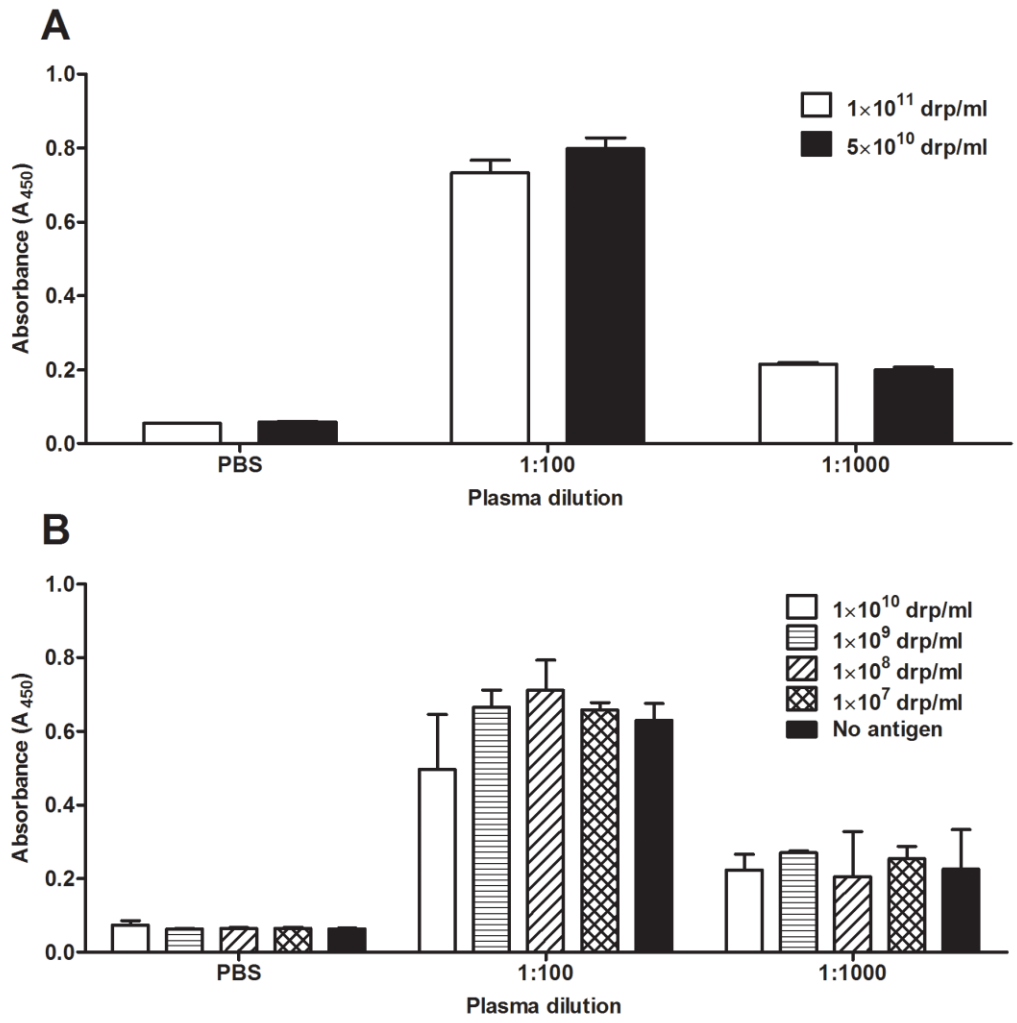

Figure 3.2 Optimisation of antigen coating concentrations for the AAV-2-specific IgG ELISA. A) Titration of AAV-2 antigen coating. Antigen was coated at 1×10^{11} drp/ml (open bars) and 5×10^{10} drp/ml (shaded bars) and probed with PBS or with plasma analyte at dilutions of 1:100 and 1:1000 B) The range of antigen coating concentrations was extended and antigen negative controls were incorporated into the assay. A four point, ten-fold titration of the antigen was tested (see key) using the indicated dilutions of detection antibody. Absorbance levels at 450 nm represent the mean of triplicate determinations. Error bars indicate the standard deviation in each case.

To fully examine this problem, a wider antigen binding range was examined and antigen negative controls were incorporated into the assay. A four point, ten-fold titration of the antigen was tested, once again using PBS controls and analyte diluted at 1:100 and 1:1000. Blocked, antigen-free wells were also probed with analyte in order to serve as antigen negative controls. The results (Figure 3.2 B) failed to demonstrate any statistically significant difference between any of the antigen concentrations at either analyte dilution. Most notably, no significant difference could be measured between the antigen coated wells and the blocked antigen negative wells at any sample dilution. The results of this assay indicated that either antigen was not coating the plate and/or that sample was binding non-specifically to the polystyrene surface, possibly indicating a failure in the blocking process or inadequate washing. The latter was a surprising possibility as other antigen ELISA in the laboratory used these or similar approaches without non-specific binding.

The efficacy of antigen coating to the assay plate was determined by direct probing with an AAV-2-specific mouse antibody. Coating was performed at a concentration of 1×10^8 drp/ml in triplicate using phosphate coating buffer. Additionally, a triplicate was coated in the same manner using a carbonate coating buffer (150 mM Na_2CO_3, 350 mM $NaHCO_3$, pH 9.6) to determine whether an alternative buffer might enhance antigen binding. An antigen-negative triplicate was also included on the plate. Coating and blocking were carried out as before. No analyte step was included in this experiment. Antigen was directly probed using a mouse anti-AAV VP IgG (ARP American Research Products Inc., Belmont, MA) conjugated to an alkaline phosphatise enzyme (AKP). VP1 antibody binding was colorimetrically detected using a para-

nitrophenylphosphate (pNPP) substrate and quantified at 405 nm. Both antigen coated triplicates showed a strong signal that was significantly ($p \leq 0.005$, indicated with **) above the antigen negative background (Figure 3.3 A). The triplicate wells coated using the carbonate coating buffer showed a slightly higher absorbance than the wells where antigen was formulated in a phosphate buffer. The data demonstrated that the antigen was successfully coating the plate and was detectable at a concentration lower than that used in previous iterations of the assay. Antigen coating issues could thus be ruled out as a confounding factor. Although the difference observed between the two coating buffers did not have statistical significance, the carbonate coating buffer was adopted for all subsequent iterations of the assay.

Since antigen coating was verified, it was likely that the lack of assay specificity was due to non-specific binding of the analyte or some reagent applied after that step. Non-specific binding in ELISA may be minimised by optimising blocking, detection antibody application and plate washing. The blocking conditions of the assay were thus modified in an attempt to reduce non-specific binding of the reagents to the plates and to each other. The reagent diluents for the sample, detection antibody and strep-HRP conjugate dilutions were changed from PBS to 1% (w/v) milk protein in PBS with 0.05% (v/v) Tween 20. The plate blocking time was extended to 24 hours at 4^{o}C. In addition, a checkerboard reagent titration of antigen coat concentration and plasma sample concentration was performed.

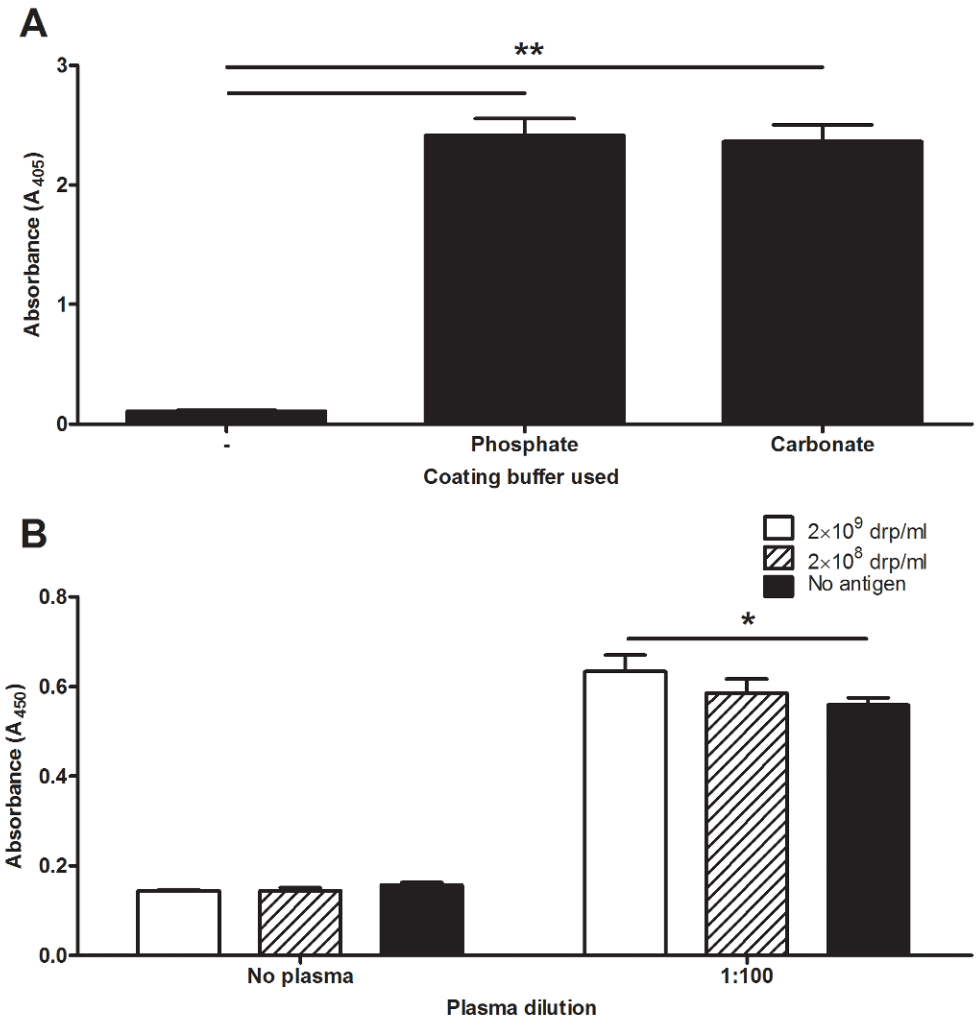

Figure 3.3 Optimisation of antigen coating buffers and antigen coat concentrations for the AAV-2-specific IgG ELISA. A) Optimisation of coating buffers. $NaHPO_4$ buffer (Phosphate) was compared to $NaHCO_3$ / Na_2CO_3 buffer (Carbonate). Both signals were significantly above background. B) Titration of antigen coating concentrations. Absorbance levels at 405 or 450 nm represent the mean of triplicate determinations. Error bars indicate the standard deviation in each case.

Antigen was coated at concentrations of 2×10^9 drp/ml and 2×10^8 drp/ml and blocked as normal using 10% (w/v) skimmed milk powder in PBS Tween. A set of antigen-free wells was also blocked. Plasma samples were added at a dilution of 1:100. Detection antibody was also used at a higher concentration of 700ng/ml. Absorbance could be titrated against antigen concentration (Figure 3.3 B) but the signal strength above background was poor ($p \leq 0.05$, indicated with *). The highest concentration of antigen coating produced an A_{450} only marginally above the blocked antigen free background wells. It could be concluded from these data that the major source of the non-specific binding derived from a component within donor plasma. Further optimisation of the assay therefore focused on efforts to reduce this background level by further modifying blocking and washing steps.

Two alternate blocking buffers, 5% (w/v) sucrose, 1% (w/v) BSA and 0.05% (v/v) Tween 20 in PBS or 5% (v/v) FCS with 0.05% Tween 20 in PBS, were tested for their capacity to reduce the non-specific background using analyte at 1:200 and 1:2000 dilution factors (Figure 3.4 A). Blocking with an FCS-based buffer (FCS) resulted in a significant ($p \leq 0.05$, indicated with *) signal (antigen positive; Ag+) above background (antigen negative; Ag-) when the analyte (Donor 4) was diluted to 1:2000. The sucrose blocking buffer performed optimally, giving a signal that was significantly above background for both analyte dilutions ($p \leq 0.005$, indicated with **). The sucrose buffer was thus adopted from that point onward. The introduction of a modified washing step after sample incubation reduced the antigen negative background significantly ($p \leq 0.0005$, indicated with ***). Washing at this step was performed with 5 washes and aspirates using a washing buffer with increased detergent concentration (0.5% (v/v)

PBS-T). It was this final optimisation step which rendered the ELISA usable and thus no further modifications were made to the protocol (Chapter 2.2.4.3).

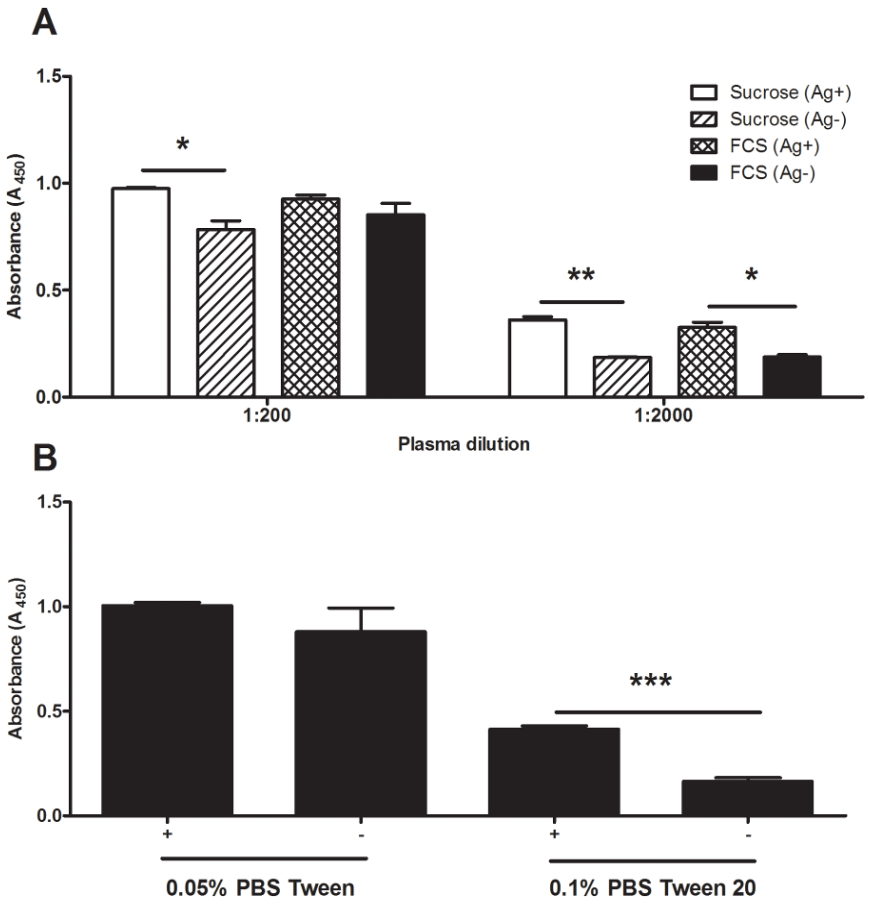

Figure 3.4 Optimisation of blocking buffer and post plasma binding wash step for the IgG ELISA. A) Comparison of FCS and Sucrose blocking buffers using antigen coated (Ag+) and antigen free (Ag-) wells. B) Comparison of washing steps using 0.05% Tween PBS and 0.1% Tween PBS. Antigen positive (+) and antigen negative (-) wells are indicated. Absorbance levels at 450 nm represent the mean of triplicate determinations. Error bars indicate the standard deviation in each case. Each optimisation step was conducted once.

3.2.3 Pilot study

Quantitative analysis of serological results was hampered by a lack of any established AAV-2-specific IgG standard sera at the study outset. As a consequence, the results obtained were assessed relative to in-house reference standards chosen from the study group. A pilot study was conducted to optimise this process. In the pilot study group one donor was identified with strong specific AAV-2-specific reactivity (Donor 4) and another with no significant detectable AAV-2-specific recognition (Donor 1). These plasma samples were chosen to be the positive and negative reference controls respectively for the duration of the pilot study. These controls were included on all plates read during the pilot study, allowing normalisation of results across multiple plates and accounting for intra-batch variation. Blocked antigen negative wells were also incubated with these control plasma samples. Assay results were discarded if the seropositive control plasma signal detected in antigen positive wells was not significantly above the corresponding antigen negative wells.

An arbitrary unit was assigned to positive and negative samples where the absorbance obtained from the positive reference sample was defined as 10 units and the negative reference sample defined as 1 unit. A linear trend line was constructed (Chapter 2.2.4.3). The equation of the line was determined and was used to calculate a unit value relative to the controls for each sample absorbance value. Standard curve construction and sample unit calculations were repeated for each plate. Thus the designated seropositive and seronegative control plasma samples served to normalise the

results obtained from each individual ELISA plate as well as to control for reagent functionality and quality assurance of non-specific backgrounds.

The score results (units of IgG) obtained for an initial panel of donors (donors 1, 2, 3, 4, 6 and 10) (Figure 3.5) did not show a clear delineation between AAV-2 seropositive and seronegative samples as has been previously seen for the related parvovirus B19 (B19V) (Corcoran *et al.*, 2004). In this pilot study, donors 3 and 6 were clearly seropositive for AAV-2-specific IgG. However, the sample size was too small to draw any definite conclusions regarding the definition of AAV-2 seronegative and seropositive samples or to comment on the extent of AAV-2 seroprevalence in the Irish blood donor population, issues that were more effectively addressed in the full serology study discussed later.

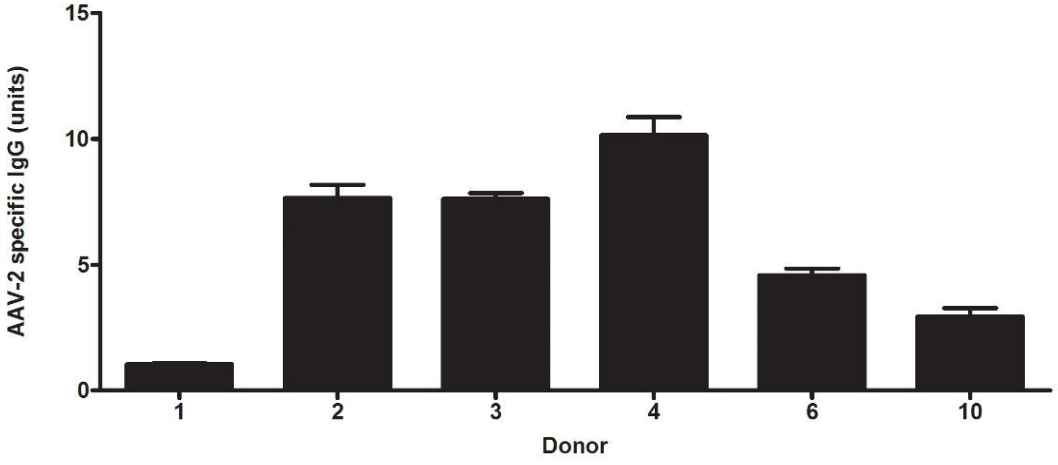

Figure 3.5 Optimisation of total IgG ELISA. Plasma samples from donors 1-4, 6 and 10 were analysed as per Chapter 2.2.4.2. AAV-2-specific IgG concentrations are presented as units, calculated as described in Chapter 2.2.4.2. Antigen specific IgG levels represent the mean of triplicate determinations and error bars indicate the standard deviation.

3.2.4 Determination of IgG ELISA antigen specificity

The specificity of the total IgG ELISA was examined using an antigen competition ELISA. Human plasma samples were pre-incubated alone, or with either high concentrations of AAV-2 or with AAV-5. The ELISA was then carried out as normal. If the assay was specific, the AAV-2 pre-incubation should reduce the amount of available specific IgG in the plasma sample through competition. As a result, the colorimetric signal should be reduced in a dose-dependent manner.

The competition assay was carried out on a seropositive control plasma sample (Donor 41). The assay was performed as described (Chapter 2.2.4.5). Plasma was diluted 1:200 and pre-incubated at 37^{o}C alone, with AAV-2 or with AAV-5. Pre-incubation with AAV-2 or AAV-5 was carried out over three virus concentrations between 1.25×10^{9} and 2.00×10^{10} drp/ml. Pre-incubation concentrations were limited by supplies of AAV-2. Incubation with 5.00×10^{9} drp/ml produced significant competition (Figure 3.6 A, $p \leq 0.05$, *) and 2.00×10^{10} drp/ml produced very significantly reduced antibody binding (Figure 3.6 A, $p \leq 0.0005$, ***). The lowest AAV-2 concentration of 1.25×10^{9} drp/ml used did not reduce the level of specific IgG. No reduction was observed in response to AAV-5 pre-incubation at any concentration (Figure 3.6 B). Taken together these data indicate that the ELISA protocol described in Chapter 2.2.4.3 was specific for AAV-2.

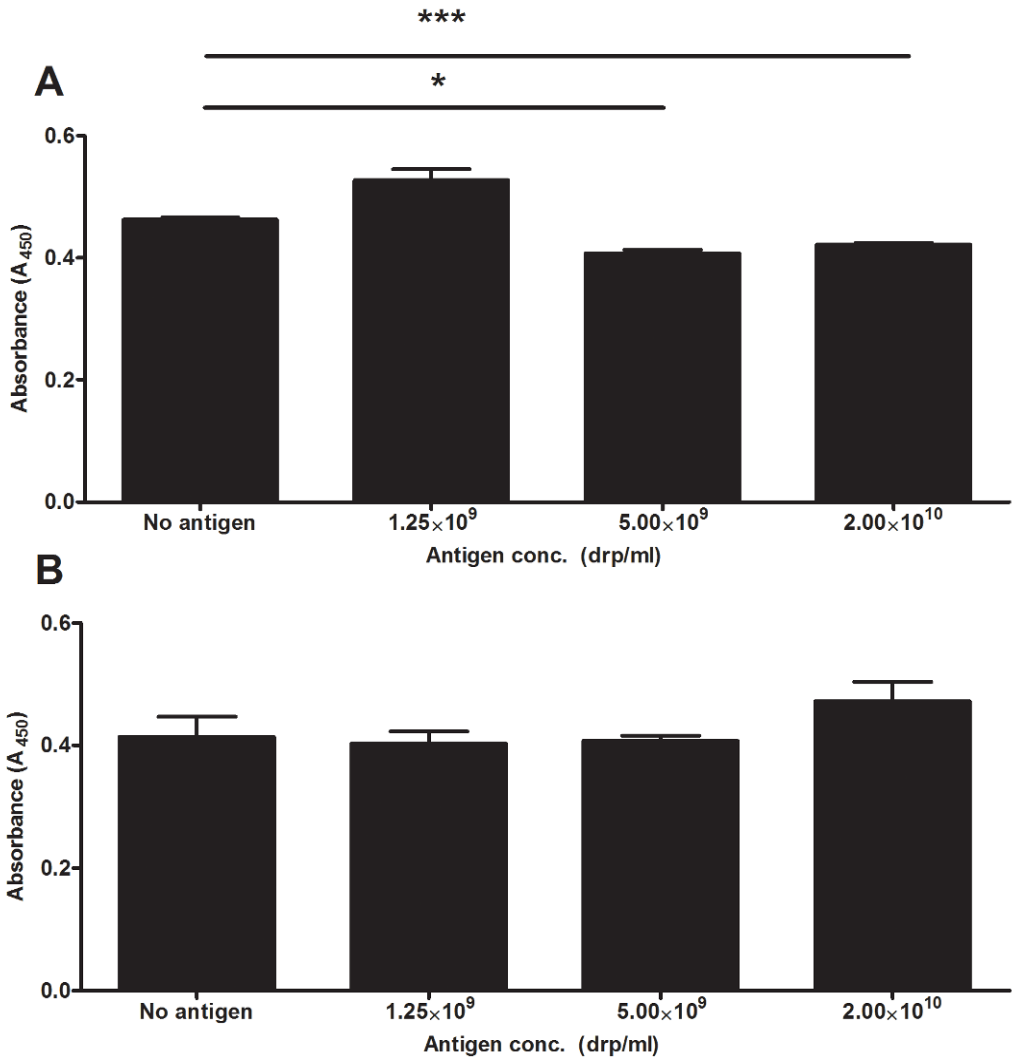

Figure 3.6 Pre-incubation of plasma analyte with AAV-2 confirms the specificity of the IgG ELISA by competitive blocking. A) Analyte was pre-incubated with AAV-2 at 1.25×10^9, 5.00×10^9 and 2.00×10^{10} drp/ml and then tested by ELISA for blocking of AAV-2-specific IgG. B) Pre-incubation with AAV-5 antigen did not produce significant blocking of AAV-2-specific IgG at any concentration.

3.3 DEVELOPMENT AND OPTIMISATION OF AAV-2-SPECIFIC IGG SUBCLASS ELISA

The IgG subclass ELISA assays were adapted from the finalised anti AAV-2 IgG ELISA protocol (Chapter 2.2.4.3) with minor modifications. The main change to the protocol was the replacement of the anti-human IgG detection antibodies with one of four anti-human IgG subclass antibodies (Calbiochem). As a very early run of the assay failed to show a positive signal for any of the 4 subclasses across a panel of plasma samples it was decided that a plate-bound IgG standard serum should be used both as a positive control during optimisation of the assay and as a means of quantifying the results in the finalised assay in terms of IgG subclass concentration. A commercial pooled human IgG solution (NOR-01; Nordic Labs, Tilburg, Holland) containing validated IgG subclass concentrations was chosen and used for all assays.

3.3.2 Optimisation of ELISA

The IgG subclass assay was designed to be similar to the pan-IgG assay, thus only the human standard serum and the four IgG subclass detection antibodies would require optimisation. Therefore, a checkerboard titration was carried out. Three dilutions within the recommended working ranges of each of the four detection antibodies were used; 1:500, 1:1000 and 1:2000. Each antibody dilution was used to probe a six-point, ten-fold serial dilution of human serum control, ranging from 1:100 to $1:10^7$.

Results from this (Figure 3.7) allowed for the selection of optimal detection antibody and human standard serum dilutions. Titration of the control serum revealed an upper dynamic detection limit for IgG1 and IgG2 near 10 µg/ml. Above this concentration, the detection curves plateaued, showing that increasing antibody did not increase signal. Similarly, the curves plateau below 10 ng/ml in both cases. The detection antibodies for IgG3 and IgG4 could not accurately detect their respective antigens above concentrations of 1×10^6 pg/ml. However these antibodies were more sensitive than the anti-IgG1 and anti-IgG2 antibodies, detecting concentrations down to 1×10^4 pg/ml. All four detection antibodies had a wide IgG detection range at a mean working plasma dilution of 1:1000. The detection antibodies would all be used at a dilution of 1:1000.

Although it was established that the assay could specifically detect IgG subclasses 1-4 in a plate bound control serum, it was not clear that the assay was capable of detecting antigen bound IgG subclasses in seropositive plasma samples. As it was not possible to pre-select plasma samples seropositive for AAV-2-specific IgG subclasses, it was decided that the ELISA would be modified to detect IgG subclasses specific for the related B19V VP2 antigen in serum samples from validated B19V seropositive donors (n = 8). B19V VP2 antigen and seropositive serum samples were kindly provided by Dr. Luke O'Shaughnessey and Prof. Sean Doyle of the NUIM Biotechnology laboratory. B19V antigen VP2 was coated onto polystyrene plates in place of the AAV-2 VP1 antigen. Confirmed B19V-seropositive serum samples were used at the analyte stage. The ELISA was otherwise carried out as normal.

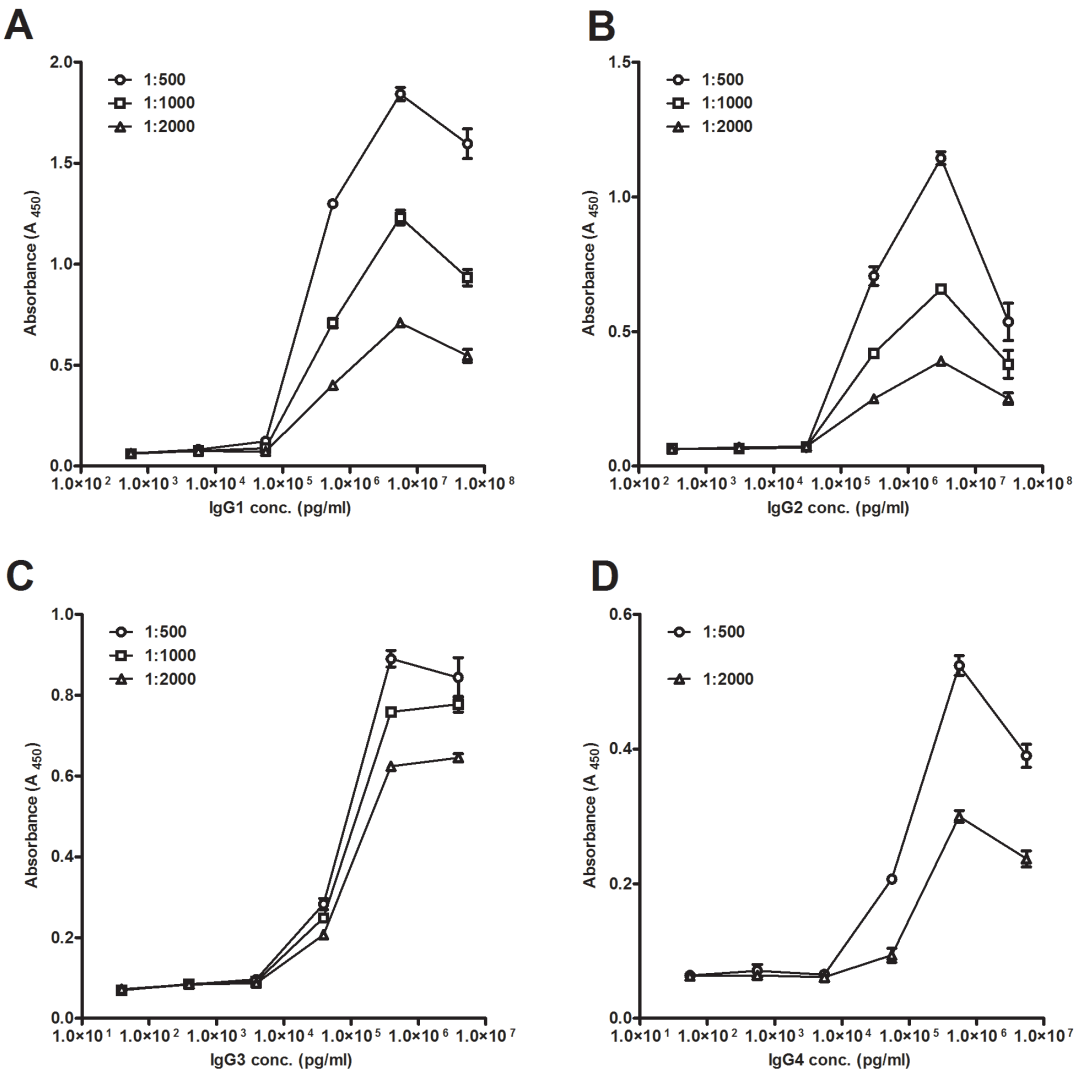

Figure 3.7 Optimisation of the IgG subclass ELISA. The detectable concentration range of pooled human standard serum was tested using various dilutions of the anti-human IgG subclass detection antibodies. Human standard serum containing validated concentrations of IgG subclasses 1-4 was titrated with a 6 point, 10-fold dilution. Control serum was coated onto assay plates and probed using detection antibodies against IgG1 (A), IgG2 (B), IgG3 (C) or IgG4 (D) at a range of dilutions as indicated. Points represent the mean of triplicate determinations and error bars represent the standard deviation.

All four IgG subclasses were detectable in the B19V seropositive serum samples (Figure 3.8). B19V-specific IgG1 was detectable in all 8 samples and was the highest of the four subclasses (1818 ±254 µg/ml). IgG2 was detectable in 2 samples (19.03 ±9.51 µg/ml), IgG3 in all 8 samples (1.79 ±1.36 µg/ml) and IgG4 in 2 samples (21.32 ±18.38 µg/ml). Based on studies of B19V IgG subclass levels in humans, it was expected that IgG1 would comprise the largest fraction of specific IgG overall, with levels of IgG2, IgG3 and IgG4 being lower (Franssila *et al.*, 1996). In particular, it was expected that IgG3 levels would be generally low unless donors were recently convalescent with some IgG 4 being present representing late convalescent donors. The results obtained here supported these assumptions. The subclass ELISA was demonstrated to detect both plate bound control IgG subclasses and to quantitatively detect antigen bound IgG subclasses in serum and was thus considered functional.

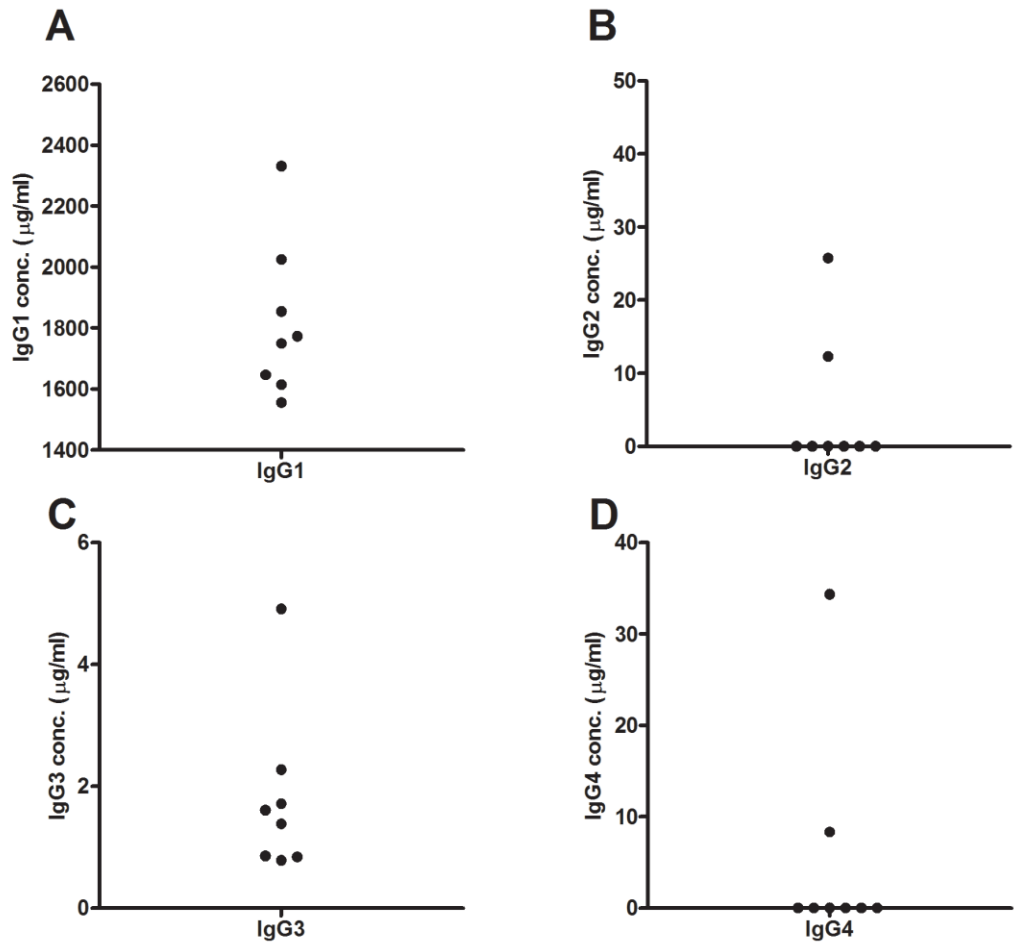

Figure 3.8 Validation of the IgG subclass ELISA using B19V VP2 antigen at the coating stage and B19V seropositive plasma samples at the analyte stage. Each of subclasses 1-4 was detectable in at least 2 samples. A) Detection of subclass IgG1. B) Detection of subclass IgG2. C) Detection of subclass IgG3. D) Detection of subclass IgG4. Points represent the mean of duplicate determinations.

3.4 AAV-2-specific Total IgG is Prevalent in the Irish Blood Donor Population

Following optimisation and the pilot study, blood plasma and peripheral blood mononuclear cells (PBMC) were isolated from a new blood donor cohort (n = 39) so that cellular responses to AAV-2 could be studied directly in parallel to serological responses. The cellular responses to AAV-2 in this donor group are detailed in Chapter 4. The plasma samples chosen as controls during the optimisation and pilot experiments had been significantly depleted during these processes and so new positive and negative control samples were chosen from amongst the first set of samples assayed from the new donor group. Plasma from donor 22 was chosen as a negative and plasma from donor 41 was chosen as a positive internal reference standard. Both plasma samples were included on all plates assayed thereafter. Reference curves derived from these new controls were similar to those generated during the pilot study (Chapter 2.2.4.3). As sufficient sample volumes remained from each of the pilot study samples for a single ELISA run, these were re-examined and normalised along with the new samples, giving a total panel of 45 samples.

Plasma isolated from whole blood was assayed for the presence of AAV-2-specific IgG by indirect ELISA using the in-house reference sera as controls. Samples were considered AAV-2 seropositive if they displayed a specific IgG signal two standard deviations greater than the standard seronegative reference sample. 41 of the donors assayed displayed AAV-2-specific IgG above this cut off and were therefore considered seropositive (Figure 3.9). This figure is close to that reported by Chirmule *et*

al. for a US population (Chirmule *et al.*, 1999). Using this approach the mean titre of AAV-2-specific IgG observed was 9.4 ±5.2 units, indicating a range of seropositivity in the study population (Figure 3.9).

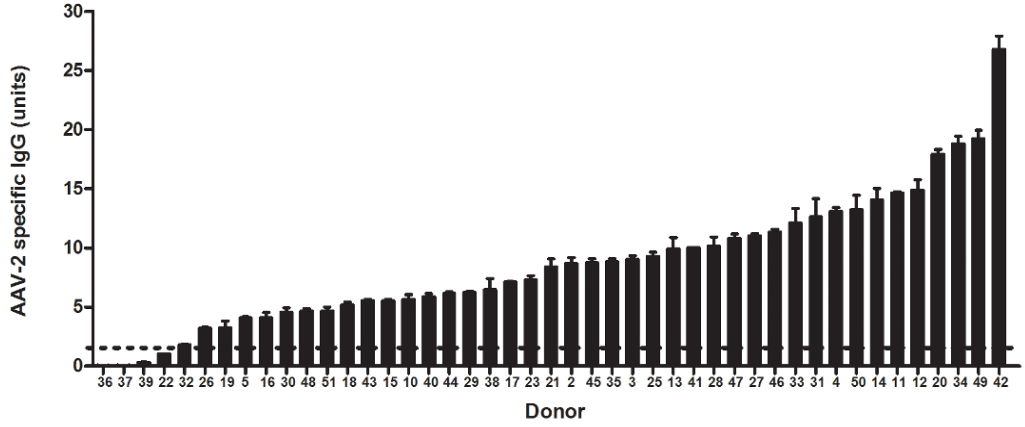

Figure 3.9 Detection of AAV-2-specific total IgG levels in donor plasma (n = 45). Negative cut-off (broken line) was defined at 2 standard deviations above the concentration of a known seronegative standard. Specific IgG levels were determined in triplicate by indirect AAV-2 antigen ELISA. Error bars represent the standard deviation. Total IgG levels were normalised by comparison to positive and negative reference samples.

3.5 AAV-2-SPECIFIC IGG1 AND IGG2 ARE COMMON IN SEROPOSITIVE DONORS

Whilst total IgG gives an indicator of virus exposure in a population, it does little to inform understanding of the immunological mechanisms in operation. Therefore plasma samples from IgG seropositive donors were further examined to determine the IgG subclasses involved in the specific recognition of AAV-2 (Figure 3.10, 3.11). IgG1 is commonly involved in antiviral responses (Franssila *et al.*, 1996; Gregoreka *et al.*, 2000; Toptygina *et al.*, 2005) and would be a likely component of responses to AAV-2 as that subclass is typically involved in humoral responses to the closely related parvovirus infections (Corcoran *et al.*, 2000; Franssila *et al.*, 1996). Significant levels of AAV-2-specific IgG1 were detected in all IgG positive samples assayed ($p \leq 0.05$), with a mean concentration of 11.9 ±6.7 µg/ml (Figure 3.10 A). A subset of the samples (n = 5) displayed very high IgG1 levels (>20.0 µg/ml). This elevation did not appear to correlate with total IgG levels or to have any relationship with levels of any other subclass. IgG1 is the most prevalent subclass seen in the circulation. IgG2 is the second most prevalent subclass and is also a major component of many antiviral responses. AAV-2-specific IgG2 was prevalent amongst the donors sampled in this study and was detected in 39 of 41 seropositive samples at a similar mean concentration to those observed for IgG1 (10.8 ±7.5 µg/ml) (Figures 3.10 A & B).

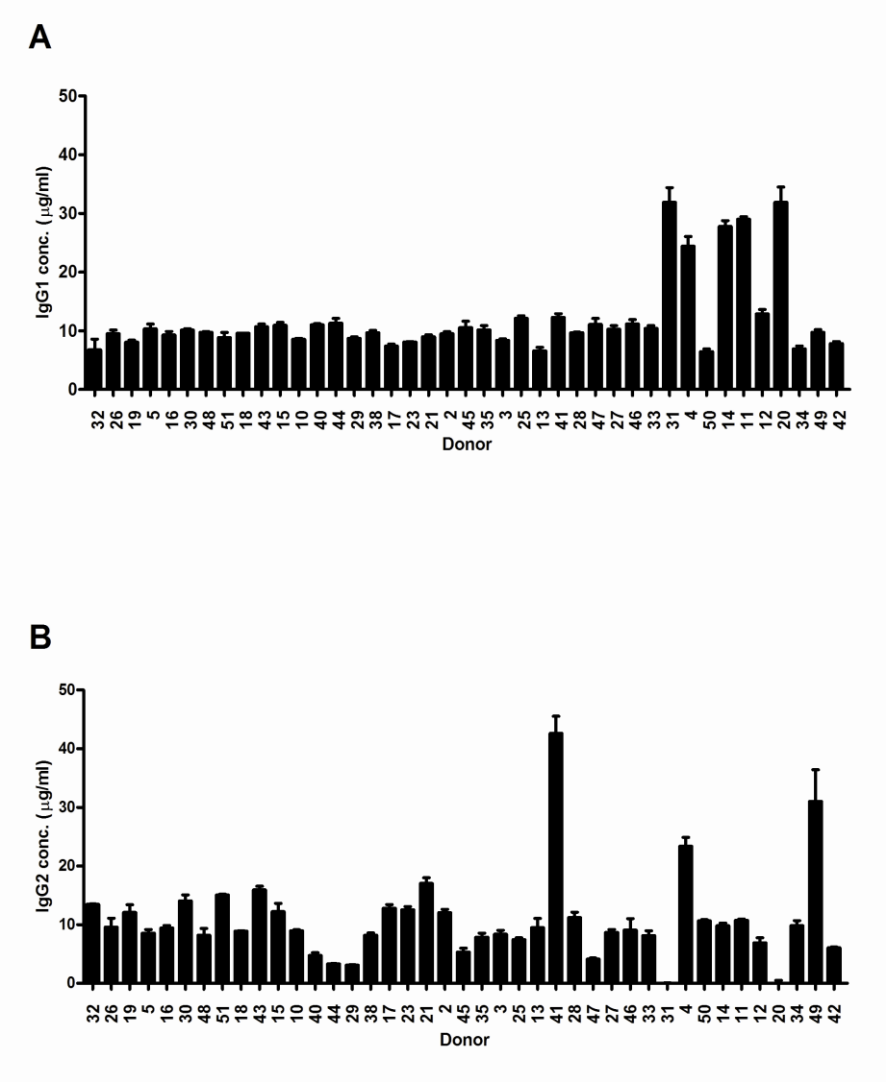

Figure 3.10 Detection of AAV-2-specific IgG subclasses levels in AAV-2 seropositive donor plasma samples (n = 41) by ELISA. (A) Detection of subclass IgG1. (B) Detection of subclass IgG2. IgG subclass levels were determined in triplicate and quantified by comparison to a pooled human IgG reference serum. Error bars represent the standard deviation.

3.6 AAV-2-SPECIFIC IGG3 IS MINIMAL AND IGG4 IS VARIABLE IN SEROPOSITIVE DONORS

IgG3 is a major mediator of humoral and cell-mediated responses against soluble antigen, having the strongest capacity to engage the complement cascade as well as having a high affinity for the FcγRI, FcγRII and FcγRIII receptors of phagocytes and B-cells (Jefferis & Lund, 2002). Despite having a role in immunity to parvovirus B19 (Franssila, Söderlund *et al*. 1996), little AAV-2-specific IgG3 was detected in the donor population (mean 0.7 ±0.2 µg/ml) (Figure 3.11 A). Depite this consistent low level of IgG3, AAV-2-specific antibody of this subclass was detected in plasma from all donors and the levels detected were consistent across all sero-positive donors.

IgG4 is typically the rarest of the four IgG subclasses in humans, comprising only 4% of circulating total IgG (Jefferis & Kumararatne, 1990). The subclass has a role in humoral responses to some viruses but has no complement activation function and a relatively low Fc affinity by comparison to IgG1 and IgG3 (Jefferis & Kumararatne, 1990). Concentrations of AAV-2-specific antibody of the IgG4 subclass were variable (mean 2.5 ±3.8 µg/ml) (Figure 3.11 B). Nine of the 41 seropositive donors showed no detectable AAV-2-specific IgG4 and only four of the samples (from donors 26, 30, 33 and 49) displayed IgG4 concentrations greater than one standard deviation above the mean.

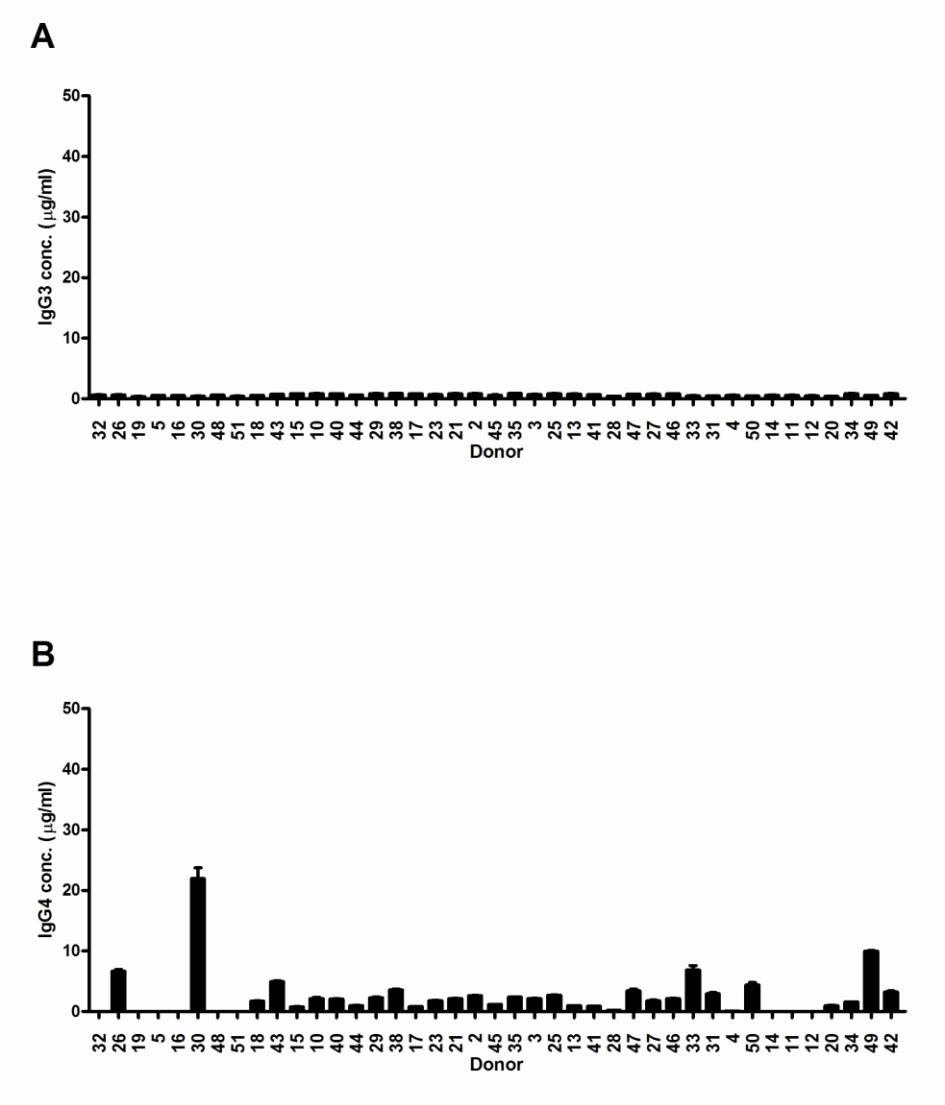

Figure 3.11 Detection of AAV-2-specific IgG subclasses levels in AAV-2 seropositive donor plasma samples (n = 41) by ELISA. (A) Detection of subclass IgG3. (B) Detection of subclass IgG4. IgG subclass levels were determined in triplicate and quantified by comparison to a pooled human IgG reference serum. Error bars represent the standard deviation.

3.7 AAV-2-SPECIFIC NEUTRALISING ANTIBODIES ARE DETECTABLE IN SEROPOSITIVE DONORS

Binding of AAV-2-specific antibody to AAV-2-based vectors may recruit complement and increase uptake of viral particles by phagocytes, thus reducing the therapeutic efficacy of the vectors. Another major influence on therapeutic efficacy is neutralisation, whereby antibody specific for critical sites on the virus capsid bind and block capsid binding to cell surface receptors. Animal studies have highlighted the significant impact of neutralization upon transduction with AAV-2 (Chirmule *et al.*, 2000; Moskalenko *et al.*, 2000; Peden *et al.*, 2004). In humans, humoral memory for AAV-2 has been shown to exhibit neutralising activity in some individuals in different populations (Chirmule *et al.*, 1999; Erles *et al.*, 1999).

Although AAV-2-specific IgG is prevalent in the human population, the capacity of the antibody to block virus binding sites for infection or transduction is typically more limited, and not readily assessable by ELISA (Moskalenko *et al.*, 2000). To assess the prevalence of neutralising antibody in this study group, a model system was devised to measure the reduction in transformation of a target cell line. A panel of six AAV-2-specific IgG-seropositive plasma samples (from donors 17, 19, 21, 34, 42, 51) was co-incubated with an AAV-2 vector encoding a *GFP* gene under the control of a CMV promoter. The vectors were then incubated with HEK-293 cells following the HEK-293 transduction protocol (Chapter 2.2.6.1). Neutralising activity was demonstrated by reduction in the levels of *GFP* expression in the HEK-293 target cells, as assessed by flow cytometry (Figure 3.12). The negative control (cells alone) exhibited a background

MFI of 5.7 and the positive control (cells incubated with AAV-2*GFP* alone) supported increased fluorescence (MFI=13.3). MFI was reduced by comparison to positive controls in all vector-transduced cultures pre-incubated with seropositive plasma samples. Plasma from donor 51 reduced the MFI to 11.1 and plasma from donor 42 reduced the MFI to near background (5.8).

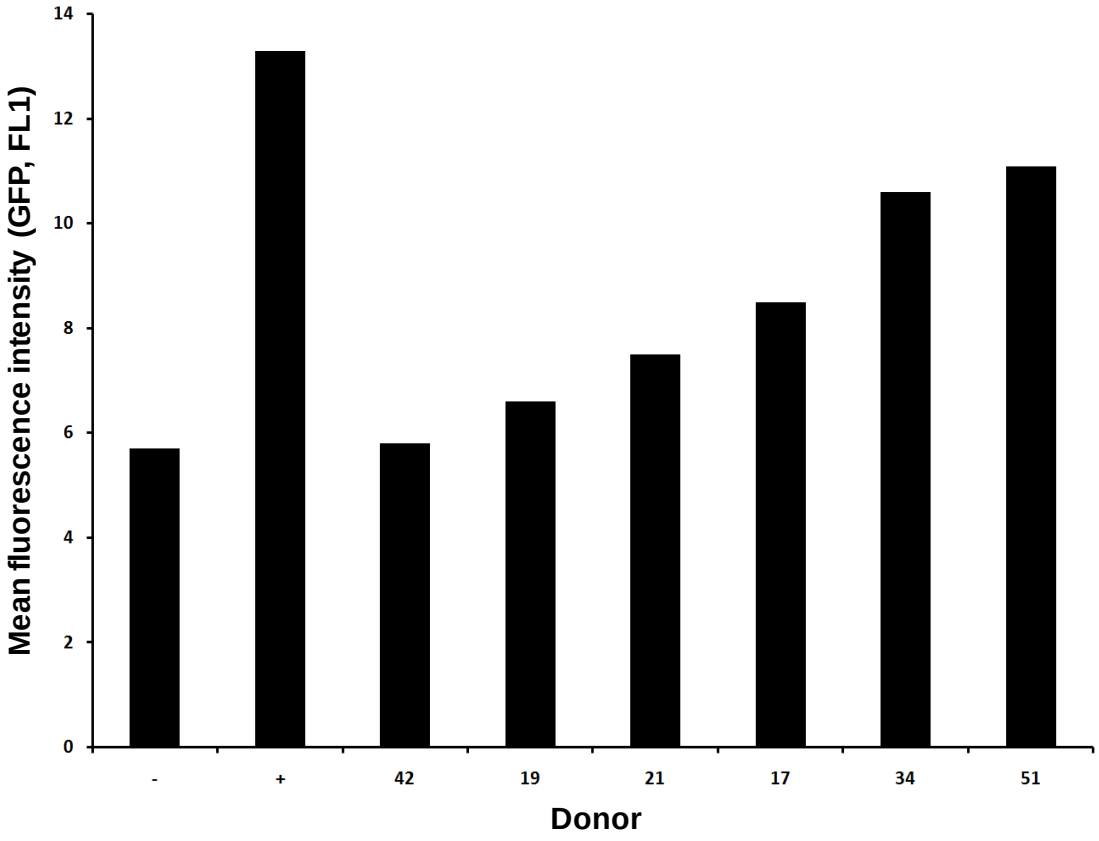

Figure 3.12 AAV-2 seropositive plasma was assessed for neutralising activity against an AAV-2*GFP* vector. Recombinant AAV-2 vectors encoding *GFP* were transduced into HEK-293 cells. HEK-293 were transduced with AAV-2*GFP* untreated (+) or following incubation with plasma samples from a selection of healthy AAV-2 seropositive donors (17, 19, 21, 34, 42, 51). *GFP* expression was reported as the mean fluorescence intensity as assessed by flow cytometry and compared to a non-transduced negative control (-).

3.8 SUMMARY

Given the known prevalence of AAV-2 infection in humans (Chirmule *et al.*, 1999; Erles *et al.*, 1999; Halbert *et al.*, 2006), it was conceivable that widespread humoral memory for the virus might negatively impact on the usefulness of the virus as a gene therapy vector. In this study, 41 of 45 donors tested displayed significant titres of AAV-2-specific IgG in blood plasma (Figure 3.9). This represents a high prevalence when compared to AAV-2 seroprevalence data obtained in other European studies but is similar to that seen in US populations (Chirmule *et al.*, 1999; Erles *et al.*, 1999; Halbert *et al.*, 2006). However, as no AAV-2-specific IgG standards existed and there was no standardised method for assaying AAV-2 antibody level, it is possible that the high variability observed between studies is a result of differing methodologies as it is of geographical differences and population demographics. Despite these differences, the available evidence suggests that humoral memory for AAV-2 is prevalent in the Irish population.

Plasma samples from a panel of six of the donors determined to be AAV-2 seropositive were also assessed for their capacity to neutralise the transduction of a cell line using an AAV-2-based gene therapy vector. All six samples demonstrated some capacity to neutralise AAV-2 transduction of HEK-293 cells. This suggested that neutralising antibodies for AAV-2 are also common in the Irish blood donor population; however the small size of the study group prevented a meaningful comparison with neutralisation results from other studies. AAV-2-specific IgG in this population consisted primarily of the IgG1 and IgG2 subclasses (Figure 3.10 and 3.11), with low

levels of IgG3 present in all donors (Figure 3.11 A) and some evidence of variable IgG4 in a smaller subset (Figure 3.11 B).

CHAPTER 4

THE HUMAN CELL-MEDIATED IMMUNE RESPONSE TO AAV-2

4.1 INTRODUCTION

Although the humoral response to AAV-2 has been characterised herein (Chapter 3) and elsewhere (Chirmule *et al.*, 1999; Halbert *et al.*, 2006), cell-mediated immune responses to AAV have received little attention. There have been some assumptions that AAV does not provoke such a response, or that the response is minimal (Büning *et al.*, 2003; Hernandez *et al.*, 1999; Samulski & Giles, 2005; Zaiss & Muruve, 2005). There has been some evidence of cell-mediated responses to AAV-2 in humans from a study of a North American population, in which responses were found o be modest and low in frequency (Chirmule *et al.*, 1999). More recently, a clinical trial for gene therapy to correct haemophilia B (High *et al.*, 2004) showed declining transgene expression and indications of tissue damage expression simultaneous to an apparent cytotoxic T-cell response (Manno *et al.*, 2006).

Findings in humans have been followed by studies in mouse models that have been used to characterise T-cell responses to AAV-2 in greater detail (Chen *et al.*, 2006; Li *et al.*, 2009; Li *et al.*, 2007; Wang *et al.*, 2007). However, inbred mouse strains used in research display limited MHC diversity by comparison to the highly polymorphic HLA genes in an outbred population. The obvious prevalence of the humoral response to AAV-2 in humans and emerging data on the cell-mediated response in mice (Li *et al.*, 2009; Li *et al.*, 2007) suggested that assumptions that AAV-2 immunity is T-cell independent might not be sound. Given these findings and their potential relevance to application of AAV-based vectors in the clinic, it was clear that the cell-mediated

response to AAV-2 needed further characterisation in the natural host if such vectors were to be reliably used in a clinical setting.

In order to characterise the cell-mediated response to AAV-2 in humans, the recall response to AAV-2 was characterised *ex vivo* from a panel of 41 human blood donors. This panel of donors represented a subset of the 45 donors examined for humoral responses in Chapter 3. IgG responses (Chapters 3.4, 3.5 and 3.6) were correlated with proliferative cell-mediated responses from the corresponding donors. Furthermore these were associated with an analysis of the profile of cytokine responses induced by AAV-2 stimulation.

4.2 AAV VECTORS STIMULATE *EX VIVO* HUMAN PBMC PROLIFERATION IN A DOSE-DEPENDENT MANNER

It has been speculated that AAV-2 does not elicit cell-mediated immune responses (Büning *et al.*, 2003; Hernandez *et al.*, 1999; Samulski & Giles, 2005; Zaiss & Muruve, 2005), however the diversity of class switched AAV-2-specific IgG responses detected in the human cohort examined herein (Chapters 3.4, 3.5 and 3.6) suggested that T-cell help had been evoked by AAV-2 exposure in the study cohort. Therefore the lymphoproliferative immune response to AAV-2 was examined. To determine whether AAV-2 could induce PBMC proliferation and to assess the dose range, human PBMC isolated from whole blood donation, were co-incubated with AAV-2 at a range of concentrations.

AAV-2 was observed to induce significant ($p \leq 0.05$ compared to control) PBMC proliferation at doses of 2×10^{10} and 2×10^{9} drp/ml (Figure 4.1). Below a dose of 2×10^{9} drp/ml, stimulation indices were not significantly greater than negative controls. It was thus decided that for future stimulations, a dose of 2×10^{10} drp/ml would be used.

4.3 AAV-2-STIMULATED CELL-MEDIATED RECALL IMMUNE RESPONSES IN HUMANS

To determine the prevalence and strength of cell-mediated responses to AAV-2 in a larger sample set, PBMC were isolated from the same panel of donors described previously (n = 41) (Chapter 3.5). These cultures were stimulated *ex vivo* with AAV-2 and assessed for their capacity to support AAV-2-specific proliferation. As before, the resulting proliferative responses were expressed as fold responses above negative controls to give stimulation indices (SI). The resulting proliferative responses displayed a distribution falling into three distinct populations (Figure 4.2), a non-proliferating group (n = 13) with SI values ≤ 1.5, an intermediate group (n = 16) with SI values > 1.5 and ≤ 3.0, and a strongly-proliferating group (n = 12) with SI values > 3.0. These results were analysed for statistical significance by comparison to negative controls using the Student's T test. AAV-2-specific positives were defined as producing both an SI > 1.5 (the upper cut-off for the non-proliferating group) with a significance of $p \leq 0.05$ compared to controls. By this stringent definition 19 of 41 Irish blood donors sampled displayed significant proliferation in response to stimulation (Figure 4.3).

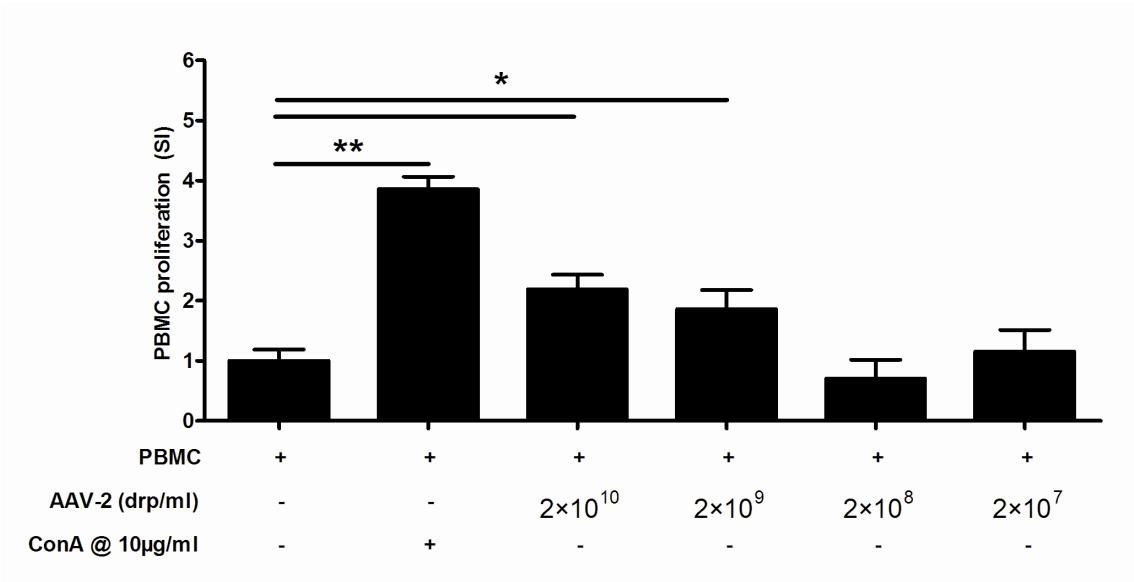

Figure 4.1 Dose-response of PBMC (donor 4) stimulated with AAV-2. Human PBMC were cultured for 96 hours in medium alone, stimulated with 10 µg/ml ConA mitogen or with AAV-2 at doses ranging from 2×10^{7} up to 2×10^{10} drp/ml. PBMC proliferation is expressed in stimulation indices (SI) which is defined as fold proliferation over unstimulated negative control. Results are representative of two independent experiments and SI values reported represent the mean of triplicate determinations. Error bars represent the standard deviation.

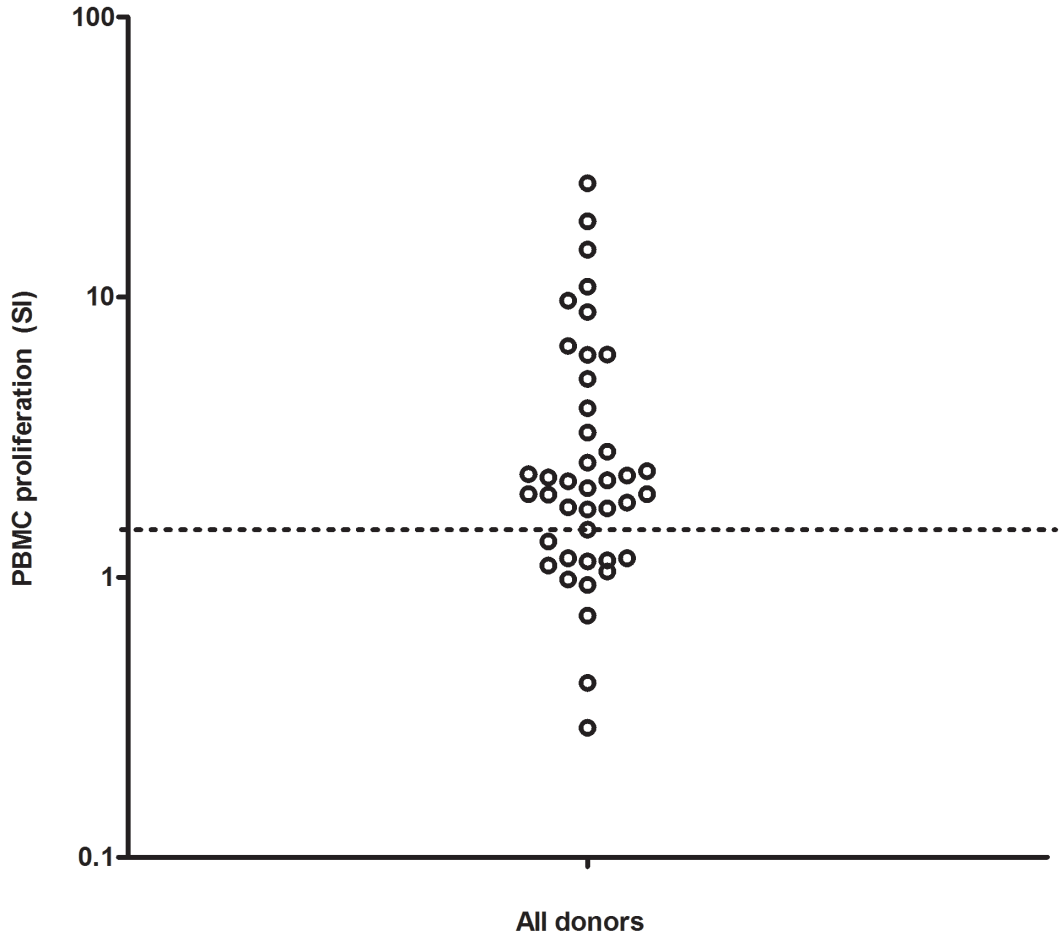

Figure 4.2 Distribution of PBMC proliferative responses to AAV-2 stimulation. Proliferation was determined *in vitro* by ^{3}H-thymidine incorporation assay (Chapter 2.2.5.1) using PBMC from a human cohort (n = 41). Each point represents a single independent experiment for one donor culture, determined in triplicate. Proliferation is expressed in stimulation indices (SI). Three distinct populations are discernable; a non-proliferating group (n = 13) with SI values ≤ 1.5 indicated by the broken horizontal line, an intermediate group (n = 16) with SI values > 1.5 and ≤ 3.0, and a strongly-proliferating group (n = 12) with SI values > 3.0.

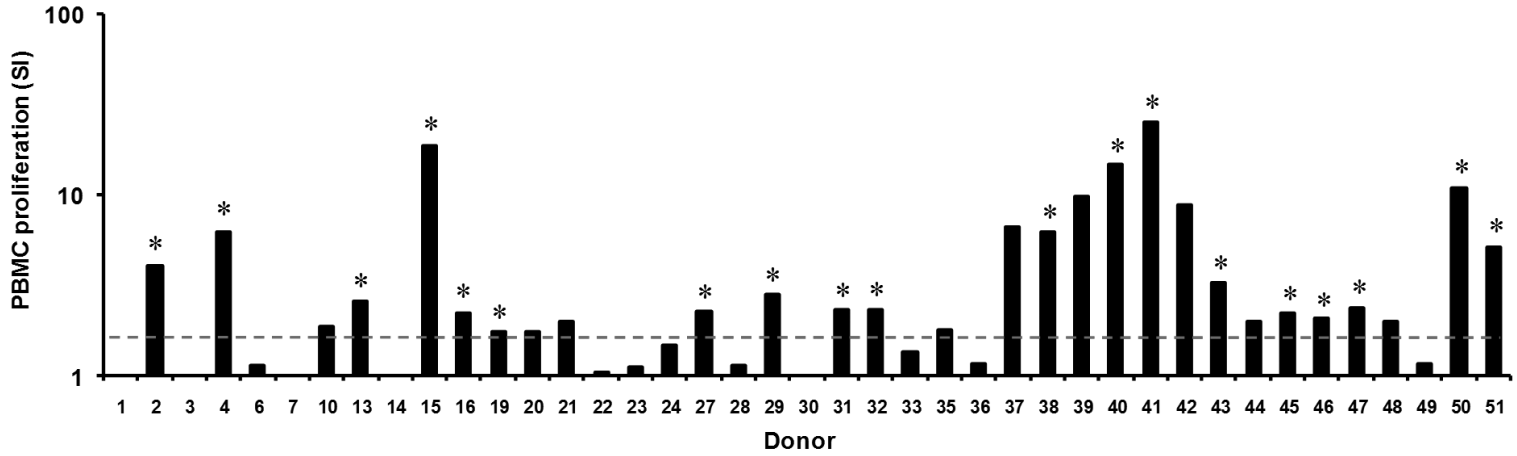

Figure 4.3 AAV-2 stimulation of PBMC isolated from 41 human donors. Each bar represents a single independent experiment for one donor culture. For each culture, proliferation for was determined in triplicate by ^{3}H-thymidine incorporation assay. Proliferation levels are reported as stimulation indices, defined as the fold proliferation level above unstimulated background. Responses are defined as positive if they produced an SI > 1.5 (broken line) with a statistical significance measured by paired t-test of $p \leq 0.05$ (*).

4.4 The Presence of AAV-2-specific Total IgG did not Predict T-cell Memory

A total 41 of the 45 human plasma samples previously examined (Chapter 3.5) contained AAV-2-specific IgG, an indicator of prior infection and humoral memory for the virus. In all cases where significant PBMC proliferation was detected in culture, the corresponding plasma samples were seropositive for AAV-2-specific IgG (Table 4.1). However, the presence of AAV-2-specific IgG did not predict the presence of a proliferative response indicating that serological assays will not be a reliable means of assessing whether candidate gene therapy recipients are likely to mount a proliferative response to AAV-2. This may be due to differences in the sensitivity of serological assays versus cell-based assays.

4.5 Neither the Strength of Total IgG, nor the Distribution of IgG Subclass Responses Predicted T-cell Responses to AAV-2

The prevalence of humoral memory for AAV-2 in humans raises the possibility that assaying for circulating antibody may provide a convenient indicator for general AAV-2 immunity in prospective gene therapy recipients. To determine if IgG ELISA results are a feasible surrogate measure of cell-mediated memory, a selection of AAV-2-specific total IgG results (Chapter 3.2.3) were correlated with PBMC proliferation results from cultures isolated from the corresponding donors.

TABLE 4.1 Serological, lymphoproliferative profiles of cultures proliferating in response to AAV-2

Donor #	AAV-2 specific total IgG (units)	AAV-2 specific IgG subclass (% total IgG)[a]				PBMC proliferation (SI)
		1	2	3	4	
19	3.23	39	59	2	0	1.75
46	11.33	48	39	3	9	2.08
45	8.73	60	30	3	7	2.20
16	4.10	48	49	3	0	2.22
27	11.01	48	41	3	8	2.27
31	12.63	90	0	1	8	2.31
32	1.78	32	64	3	0	2.33
47	10.80	57	21	4	18	2.39
13	9.90	37	53	4	5	2.57
43	5.54	33	49	2	15	3.29
51	4.66	37	62	2	0	5.10
38	6.46	43	37	4	16	6.25
50	13.20	29	48	2	20	10.91
40	5.88	59	25	4	11	14.77
15	5.55	44	49	3	3	18.65
41	10.00	22	75	1	2	25.50

[a] AAV-2-specific IgG subclass levels were determined by indirect ELISA (Chapter 3.5 and 3.6). Detectable specific subclass levels are expressed as a percentage of the total specific IgG.

T cell responses were only detected in patients who were seropositive (Figure 4.4 A, Table 4.1), however the high prevalence and the small number of seronegative donors in this study did not allow a meaningful comparison or correlation to be drawn on this relationship. There was no correlation between the level of AAV-2 IgG detected in donor plasma and the presence of a T-cell recall response or the amount of proliferation produced by PBMC cultures from those donors (Figure 4.4 A, Table 4.1). When AAV-2-specific IgG subclass levels were compared to PBMC proliferation, there appeared to be only a weak correlation (Figure 4.4 B) ($r = 0.25$) between the combined levels of the subclasses and the extent of proliferation. There were no obvious correlations between the PBMC proliferation levels and circulating IgG subclass levels for subclasses 1-3 for any donor. The highest levels of IgG4 tended to be detected in plasma from donors from whom PBMC cultures produced AAV-2 stimulated proliferation with an SI of greater than 3.0. However this association was extremely weak ($r = -0.13$) and the two most strongly proliferating cultures (from donors 15 and 41) corresponded with very low IgG4 levels. Overall these data suggest that diagnostic assessments of AAV cellular immunity are not likely to be reliably inferred from using serological responses as a surrogate.

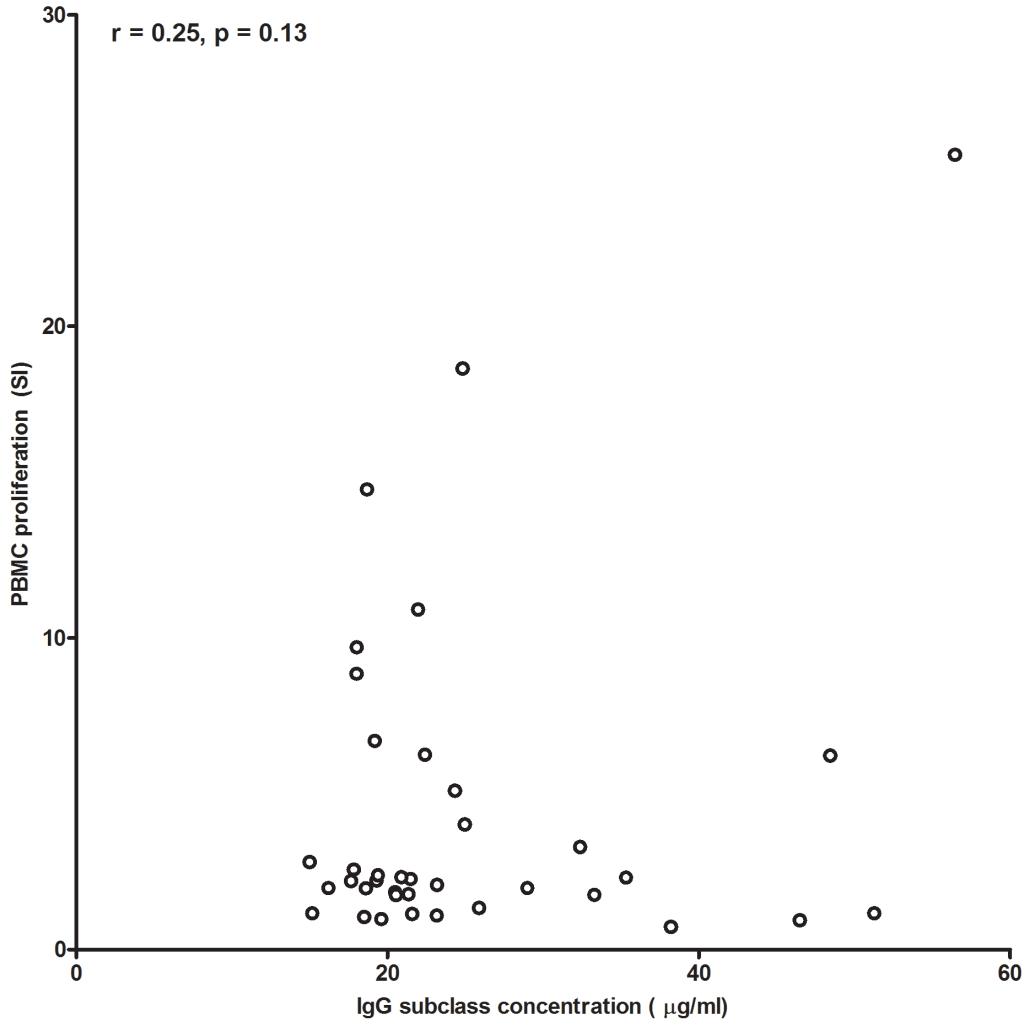

Figure 4.4 Comparison of combined AAV-2-specific IgG subclass 1-4 concentrations with corresponding antigen specific PBMC proliferation. Correlation was assessed by Pearson product-moment correlation coefficient. PBMC proliferation (SI) in response to AAV-2 stimulation does not correlate with the combined concentration of AAV-2-specific IgG subclasses ($r = 0.25$, $p = 0.14$). Results from each donor culture for IgG are representative of single independent experiments, each performed in triplicate.

4.6 AAV-2 Induced T Helper Responses with Different Cytokine Profiles

Polarisation of antigen specific T helper responses along the T helper 1 (Th1), T helper 2 (Th2), T helper 17 (Th17) and T regulatory (T-reg) arms of the adaptive response might have a significant impact on the outcome of putative cell-mediated responses to AAV-2. In particular, vigorous Th1 responses, detectable by T-cell secretion of IFN-γ, may mediate cytotoxic responses directed against host cells transiently presenting AAV-2 antigens. To assess the T helper polarisation of responses to AAV-2 *in vitro,* supernatants from cultures (donors, n=16) that proliferated in response to antigen were assessed for the production of IFN-γ, IL-10 and IL-13, cytokines characteristic of Th1, Th2 and T-reg polarised recall responses respectively. This subset was selected as it was considered unrealistic to screen samples from donors where no proliferation was observed. Ten cultures (donors #13, 15, 27, 31, 32, 38, 40, 41, 50 and 51) produced significantly ($p \leq 0.05$) increased IFN-γ (Figure 4.5). Cultures from four donors (#27, 31, 32 and 46) showed increased IL-13 (Figure 4.6). IL-10 levels were increased in eight cultures (from donors #31, 38, 40, 43, 45 47, 50 and 51; mean concentration 140 pg/ml) (Figure 4.7). Whilst the cytokine profiles produced in response to AAV-2 were diverse, these data support the induction of CD4+ T-cell responses against AAV-2 in a subset of the healthy human population.

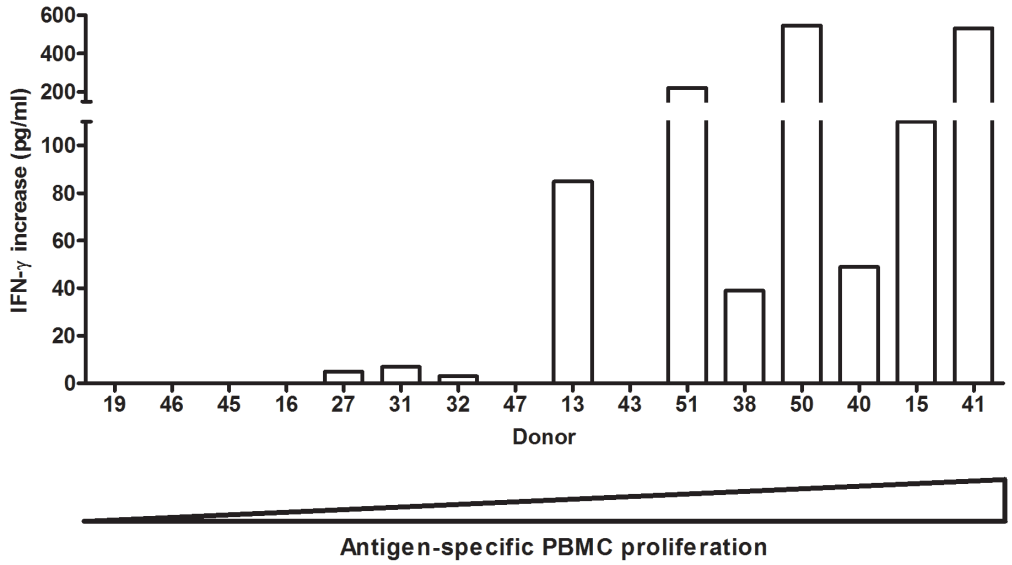

Figure 4.5 Determination of IFN-γ production in PBMC cultures stimulated with AAV-2. Supernatants from 10 PBMC cultures stimulated with AAV-2 displayed production of IFN-γ as detected by sandwich ELISA. Results from each donor culture are representative of single independent experiments; each performed in triplicate and reported as the increase in IFN-γ relative to negative controls. All IFN-γ increases reported were significantly ($p \leq 0.05$) above respective negative background levels as determined by Student's t-test. Results for each donor are arranged in order of increasing antigen specific PBMC proliferation.

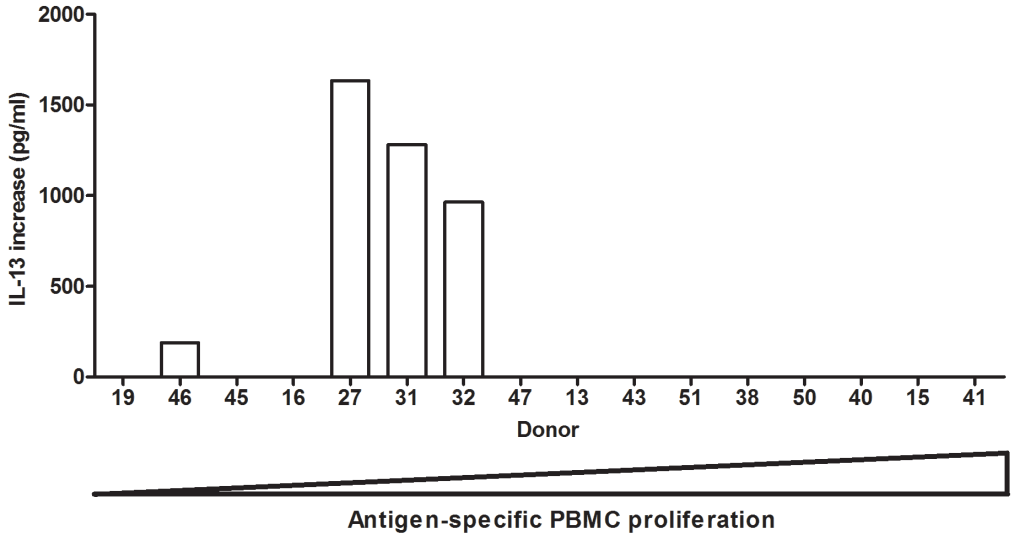

Figure 4.6 Determination of IL-13 production in PBMC cultures stimulated with AAV-2. Supernatants from 4 PBMC cultures stimulated with AAV-2 displayed production of IL-13 as detected by sandwich ELISA. Results from each donor culture are representative of single independent experiments; each performed in triplicate and reported as the increase in IL-13 relative to negative controls. All IL-13 increases reported were significantly ($p \leq 0.05$) above respective negative background levels as determined by Student's t-test. Results for each donor are arranged in order of increasing antigen specific PBMC proliferation.

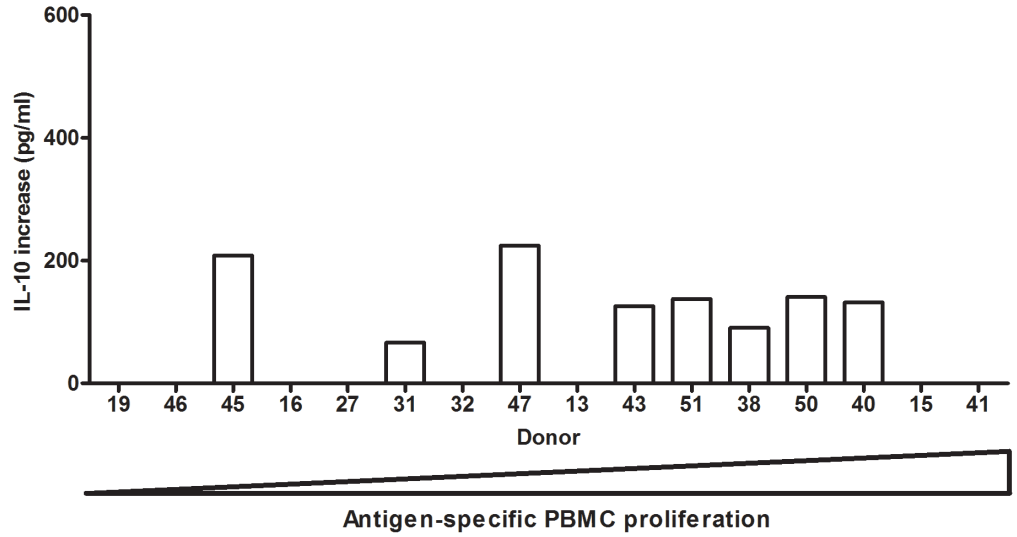

Figure 4.7 Determination of IL-10 production in PBMC cultures stimulated with AAV-2. Supernatants from 8 PBMC cultures stimulated with AAV-2 displayed production of IL-10 as detected by sandwich ELISA. Results from each donor culture are representative of single independent experiments; each performed in triplicate and reported as the increase in IL-10 relative to negative controls. All IL-10 increases reported were significantly ($p \leq 0.05$) above respective negative background levels as determined by Student's t-test. Results for each donor are arranged in order of increasing antigen specific PBMC proliferation.

4.7 Polarisation of Proliferative Responses to AAV-2 Varied Between Donors

Production of IFN-γ, IL-13 or IL-10 was detected in PBMC cultures from 14 of 16 donors examined. These cytokine responses were compared with the corresponding lymphoproliferative responses (Section 4.5) in ascending order of strength (Table 4.2). IL-10 responders were distributed between cultures of all proliferation levels, whereas IFN-γ and IL-13 levels showed a weak correlation with the extent of PBMC proliferation (Table 4.2). IFN-γ levels tended to be increased in cultures from donors whose PBMC proliferation levels were strong (SI > 3.0) (as determined by Pearson product-moment correlation coefficient ($r = 0.69$, $p = 0.0031$)), whereas IL-13 was only detected in cultures from donors whose PBMC proliferation levels had been weakly positive (SI < 2.5) (Table 4.2).

For individual donors, IFN-γ and IL-13 levels appeared to be inversely proportional to one another and in many cases were mutually exclusive (Figure 4.8, Table 4.2). It thus appears that AAV-2 induces polarised Th1 responses in some donors and Th2 responses in others.

TABLE 4.2 Cytokine profiles of cultures proliferating in response to AAV-2

PBMC proliferation (SI)	Cytokine increase (pg/ml)[a]		
	IFN-γ	IL-10	IL-13
1.75	-	-	-
2.08	-	-	189
2.20	-	209	-
2.22	-	-	-
2.27	5	-	1633
2.31	7	67	1281
2.33	3	-	962
2.39	-	225	-
2.57	85	-	-
3.29	-	126	-
5.10	221	138	-
6.25	39	91	-
10.91	546	141	-
14.77	49	132	-
18.65	110	-	-
25.50	532	-	-

[a] Cytokine levels in proliferation assay supernatants were determined by sandwich ELISA. Intermediate and negative cytokine production levels are indicated (-). Increases, where applicable, are measured in picograms per millilitre (pg/ml).

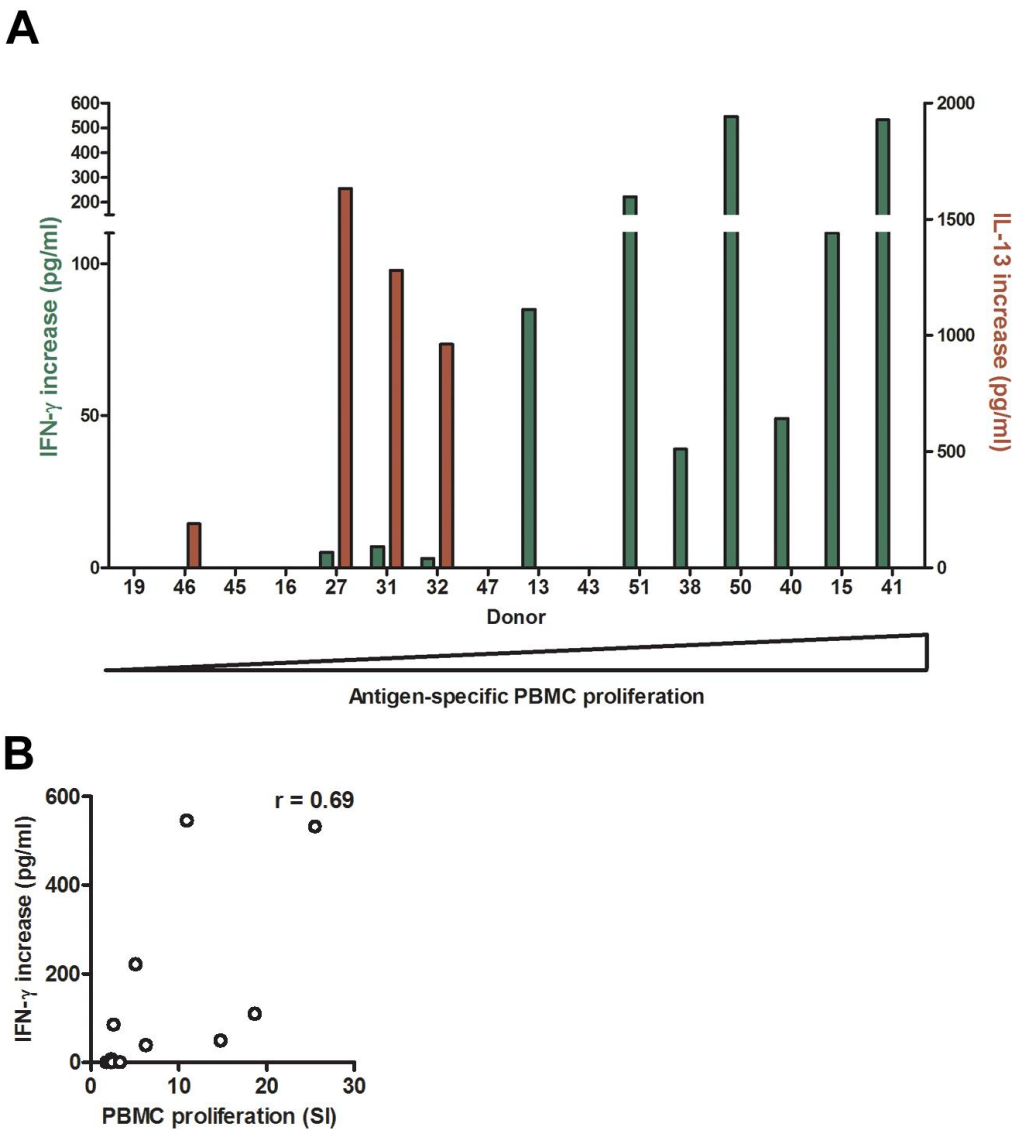

Figure 4.8 A) Comparison of IFN-γ (green bars) and IL-13 (red bars) increases in supernatants from PBMC cultures stimulated with AAV-2. Results are representative of single independent experiments; each performed in triplicate and reported as the cytokine increase relative to negative controls. All increases reported were significantly ($p \leq 0.05$) above respective negative background levels as determined by Student's t-test. Results for each donor are arranged in order of increasing antigen specific PBMC proliferation. B) Comparison of proliferative responses and IFN-γ production. A weak correlation ($r = 0.69$, $p = 0.0031$) was found between IFN-γ production and the strength of PBMC proliferation.

4.8 SUMMARY

At the study outset, there was an assumption that AAV-2 induced weak cell-mediated immune response or that the response is absent (Büning *et al.*, 2003; Hernandez *et al.*, 1999; Samulski & Giles, 2005; Zaiss & Muruve, 2005), and few studies had examined this question in humans (Chirmule *et al.*, 1999; Manno *et al.*, 2006). This study represented the first detailed examination of human cell-mediated responses to AAV-2 and demonstrated that AAV-2 evoked robust proliferative and cytokine recall responses detectable in PBMC. Of the 41 donors assayed for AAV-2 stimulated PBMC proliferation, 19 demonstrated a statistically significant proliferative response to the antigen (Figure 4.3). Of these, 9 donors supported stimulation indices of between 1.5 and 3.0; 10 donors produced higher stimulation indices, with 4 of these producing SI values above 10 (Figure 4.2 and 4.3). Chirmule *et al.* also examined human PBMC proliferation in response to AAV-2 but found that only 3 of their 57 subjects produced a stimulation index greater than 2.0 (Chirmule *et al.*, 1999). This discrepancy is most likely due to the relatively low concentration of AAV-2 used for the re-stimulation, a multiplicity of infection (MOI) of 100, compared to an MOI of 10,000 (2×10^{10} drp/ml) for this study, as well as an extended stimulation time of 168 hours in culture compared to 96 hours for this study. However, study population differences cannot be ruled out as an additional significant factor in this discrepancy.

Having demonstrated that the cell-mediated response to AAV-2 is more prevalent than previously thought, it was decided that a more detailed examination of the response in these positive cultures was warranted. Given that some of the

proliferative responses observed were relatively strong and polarised towards a Th1 response, there is clearly some risk that cytotoxic T-cell responses may be raised against AAV-2 and AAV-2-transduced cells in many recipients in a clinical setting. Thus, an examination of stimulating epitopes on the AAV-2 capsid protein was pursued in order to establish whether common targets might be identified with a view to modifying or blocking immunostimulatory sequences. Further, an analysis of any correlation between stimulating sequences and donor HLA expression might provide a means to predict the likely sequence specificity of candidate patients. These avenues of investigation are explored in Chapter 5.

CHAPTER 5

IDENTIFICATION OF AAV-2 EPITOPES RECOGNISED BY HUMAN T-CELLS

5.1 INTRODUCTION

Examination of *in vitro* cell-mediated responses to AAV-2 (Chapter 4) revealed evidence of T-cell responses in a population of healthy Irish blood donors (n = 41). These responses varied in strength and quality as determined by proliferation and cytokine production respectively. PBMC from 19 of the 41 sampled donors displayed proliferative responses accompanied by varying cytokine responses following *in vitro* AAV-2 re-stimulation. It was important to characterise the precise targets of human recognition of AAV-2 for three reasons. First, CD4+ responses against AAV-2 may confound use of AAV-2 as a vector for gene therapy, so knowledge of T-cell epitopes recognised by humans may allow engineering or modification of the virus to replace strong epitopes. Second, AAV-2 is an important human parvovirus; knowledge of epitopes may inform broader understanding of human immunology relating to these viruses and related viruses such as B19V (Corcoran *et al.*, 2004). Thirdly, AAV-2 could be used as a vaccine carrier and it would be important to design modifications of the capsid sequence that avoid destruction of T-cell epitopes (Liu *et al.*, 2000; Zhang *et al.*, 2003). The first goal of this chapter was to identify the T-cell epitopes of AAV-2 recognised by a human population. A strategy was adopted whereby cryopreserved PBMC from identified donors would be cultured and stimulated with a panel of short overlapping peptides derived from the AAV-2 VP1 capsid sequence to identify T-cell epitopes. Epitopes identified would be correlated with the expression of specific HLA alleles.

Mouse models have previously been used to characterize some T-cell responses to AAV-2 in some detail, including examinations of MHC expression and correlation with immunostimulatory epitopes within the AAV-2 capsid (Chen *et al.*, 2006; Li *et al.*, 2007; Wang *et al.*, 2007). However, inbred mouse strains display limited MHC diversity in comparison to the highly polymorphic human HLA. Furthermore mouse infection models may not represent the course of natural AAV-2 infection in humans, specifically failing to account for the influence of significant MHC polymorphism on antigen presentation and the influence of helper virus co-infection in shaping the effector and memory responses against AAV-2. Thus, the second goal of this chapter was to characterise the HLA haplotypes of the Irish blood donor population studied. Following this, a bioinformatics approach was used to predict putative AAV-2 T-cell epitopes predicted for the haplotypes described. Finally the results of both approaches were compared.

5.2 Identification of 59 Novel AAV-2 Epitopes Recognised by an Irish Population

There has been limited examination of the targets of cell-mediated immunity to AAV-2 in humans. Therefore the ability of synthetic peptides corresponding to the entire sequence of the AAV-2 VP1 capsid protein to support recall responses from human PBMC was examined. Frozen PBMC from the 16 donors characterised in Chapters 3 and 4 were reconstituted and stimulated with overlapping 20-mer peptides corresponding to the complete protein sequence of VP1 (Chapter 2, Table 2.2). This

group represented a subgroup of the 19 donors whose PBMC produced significant proliferation in response to stimulation with whole AAV-2 capsid, specifically those donors from whom sufficient cryopreserved PBMC were available.

The sequence for VP1 contains the full sequence of the alternative capsid proteins VP2 and VP3, thus a strategy which examines VP1 covers the full range of epitopes present on the virus capsid. Cultures were assessed for proliferation in response to the 20-mer peptides (Figure 5.1 - 5.8). A stringent definition of an epitope was chosen; only stimulating pairs of adjacent 20-mer sequences were considered to represent an antigenic sequence recognised by T-cells, with the 12-mer consensus sequence overlap assumed as containing the T-cell epitope. Peptides were considered to be stimulating when they elicited a stimulation index greater than one standard deviation above the mean proliferation level for all donors. Using this definition, a total of 59 epitopes were identified (Table 5.1) across the entire donor group, a finding which undermined the notion that the AAV-2 capsid may be easily modified to remove sequences which are recognised by T-cells.

Table 5.1 A) AAV-2 VP1 capsid sequences recognised by human PBMC

Peptide	Donor	Sequence	Peptide	Donor	Sequence
1	**16, 50**	DWLEDTLSEGIR	**21**		
2	**50**	EGIRQWWKLKPG	**22**	**16**	GDADSVPDPQPL
3	**50**	LKPGPPPPKPAE	**23**		
4	**50**	KPAERHKDDSRG	**24**		
5			**25**	**51**	NTMATGSGAPMA
6			**26**		
7	**16, 50**	NGLDKGEPVNEA	**27**		
8	**50**	VNEADAAALEHD	**28**		
9	**50**	LEHDKAYDRQLD	**29**	**50**	TWMGDRVITTST
10	**50**	RQLDSGDNPYLK	**30**	**16, 50, 51**	TTSTRTWALPTY
11			**31**	**16, 51**	LPTYNNHLYKQI
12			**32**	**16, 51**	YKQISSQSGASN
13	**50**	KEDTSFGGNLGR	**33**	**16, 51**	GASNDNHYFGYS
14	**50, 51**	NLGRAVFQAKKR	**34**		
15	**40, 50**	AKKRVLEPLGLV	**35**		
16	**50**	LGLVEEPVKTAP	**36**	**16**	CHFSPRDWQRLI
17	**50**	KTAPGKKRPVEH	**37**	**16**	QRLINNNWGFRP
18			**38**	**16**	GFRPKRLNFKLF
19			**39**	**16, 50**	FKLFNIQVKEVT
20			**40**	**16, 19, 50, 51**	KEVTQNDGTTTI

Table 5.1 B) AAV-2 VP1 capsid sequences recognised by human PBMC

Peptide	Donor	Sequence	Peptide	Donor	Sequence
41	**19, 50**	TTTIANNLTSTV	**61**	**50**	PCYRQQRVSKTS
42			**62**	**50**	SKTSADNNNSEY
43			**63**	**50**	NSEYSWTGATKY
44			**64**	**13, 50, 51**	ATKYHLNGRDSL
45			**65**	**13**	RDSLVNPGPAMA
46	**16**	CLPPFPADVFMV	**66**		
47	**16**	VFMVPQYGYLTL	**67**	**51**	DEEKFFPQSGVL
48	**50**	YLTLNNGSQAVG	**68**		
49	**50**	QAVGRSSFYCLE	**69**	**50**	QGSEKTNVDIEK
50	**16, 50**	YCLEYFPSQMLR	**70**	**13, 50**	DIEKVMITDEEE
51			**71**		
52			**72**		
53			**73**		
54	**16**	AHSQSLDRLMNP	**74**	**16**	RGNRQAATADVN
55	**16**	LMNPLIDQYLYY	**75**	**13**	ADVNTQGVLPGM
56	**13**	YLYYLSRTNTPS	**76**		
57	**13**	NTPSGTTTQSRL	**77**		
58	**13, 16**	QSRLQFSQAGAS	**78**	**13**	IWAKIPHTDGHF
59	**16**	AGASDIRDQSRN	**79**	**13**	DGHFHPSPLMGG
60	**50**	QSRNWLPGPCYR	**80**	**13**	LMGGFGLKHPPP

Table 5.1 C) AAV-2 VP1 capsid sequences recognised by human PBMC

Peptide	Donor	Sequence	Peptide	Donor	Sequence
81			**87**	**13**	ENSKRWNPEIQY
82			**88**	**13**	EIQYTSNYNKSV
83	**16**	PSTTFSAAKFAS	**89**		
84	**51**	KFASFITQYSTG	**90**	**51**	TVDTNGVYSEPR
85	**51**	YSTGQVSVEIEW	**91**	**16, 51**	NGVYSEPRPIGTRYLT
86	**13, 50, 51**	EIEWELQKENSK			

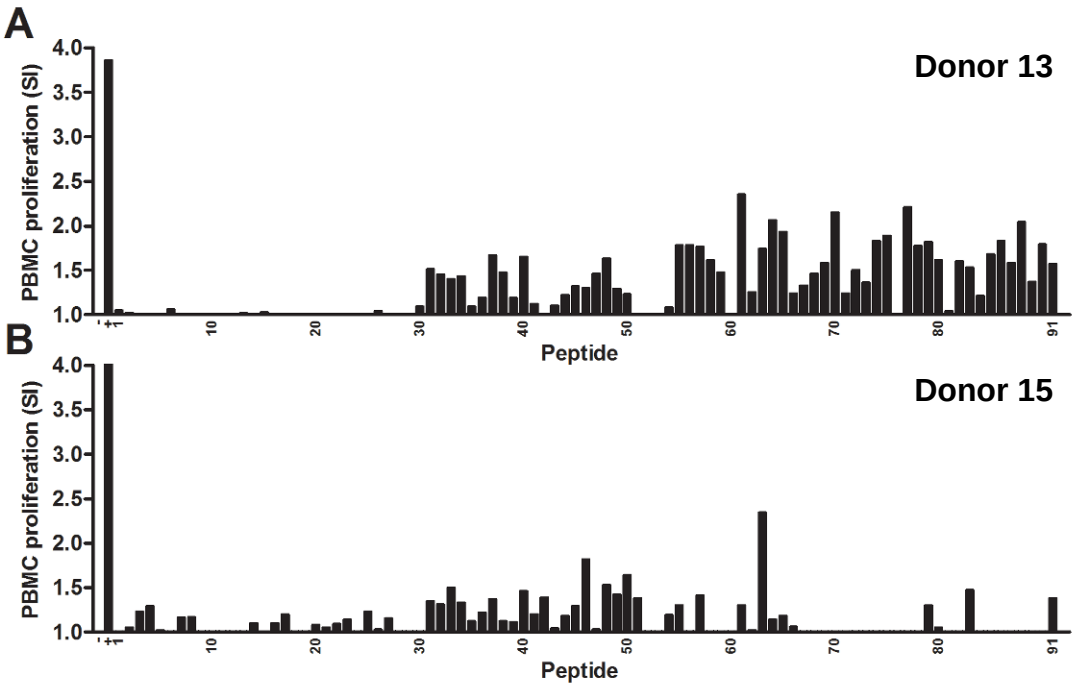

Figure 5.1 Identification of human T-cell epitopes on AAV-2 capsid protein VP1. PBMC from donors studied in Chapters 3 and 4 were stimulated *in vitro* as described in Chapter 2.2.5.1. Stimulation was performed using overlapping synthesised peptides (described in Chapter 2.1.4.1 and Table 2.2) corresponding to the VP1 capsid sequence of AAV-2. Peptide used (horizontal axis) is graphed against SI (as described in Chapter 2.2.5.1, horizontal axis) along with unstimulated negative controls (-) and ConA simulated positive controls (+). Experiment was performed for A) donor 13 and B) donor 15 and was performed once for each donor. Bars represent the mean of triplicate determinations.

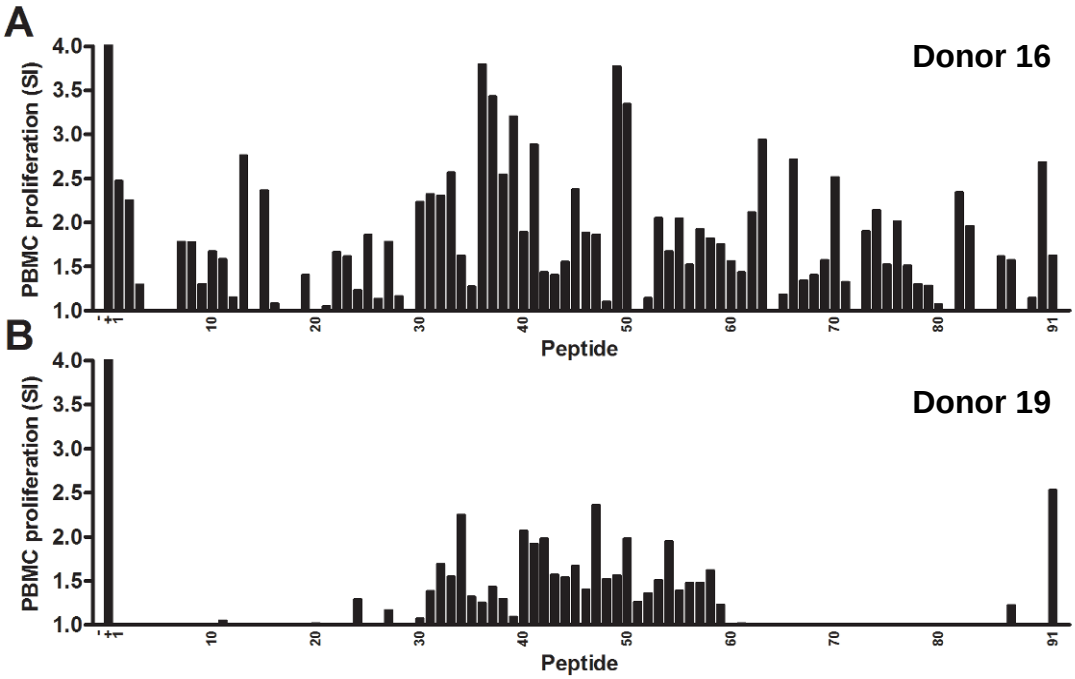

Figure 5.2 Identification of human T-cell epitopes on AAV-2 capsid protein VP1. PBMC from donors studied in Chapters 3 and 4 were stimulated *in vitro* as described in Chapter 2.2.5.1. Stimulation was performed using overlapping synthesised peptides (described in Chapter 2.1.4.1 and Table 2.2) corresponding to the VP1 capsid sequence of AAV-2. Peptide used (horizontal axis) is graphed against SI (as described in Chapter 2.2.5.1, horizontal axis) along with unstimulated negative controls (-) and ConA simulated positive controls (+). Experiment was performed for A) donor 16 and B) donor 19 and was performed once for each donor. Bars represent the mean of triplicate determinations.

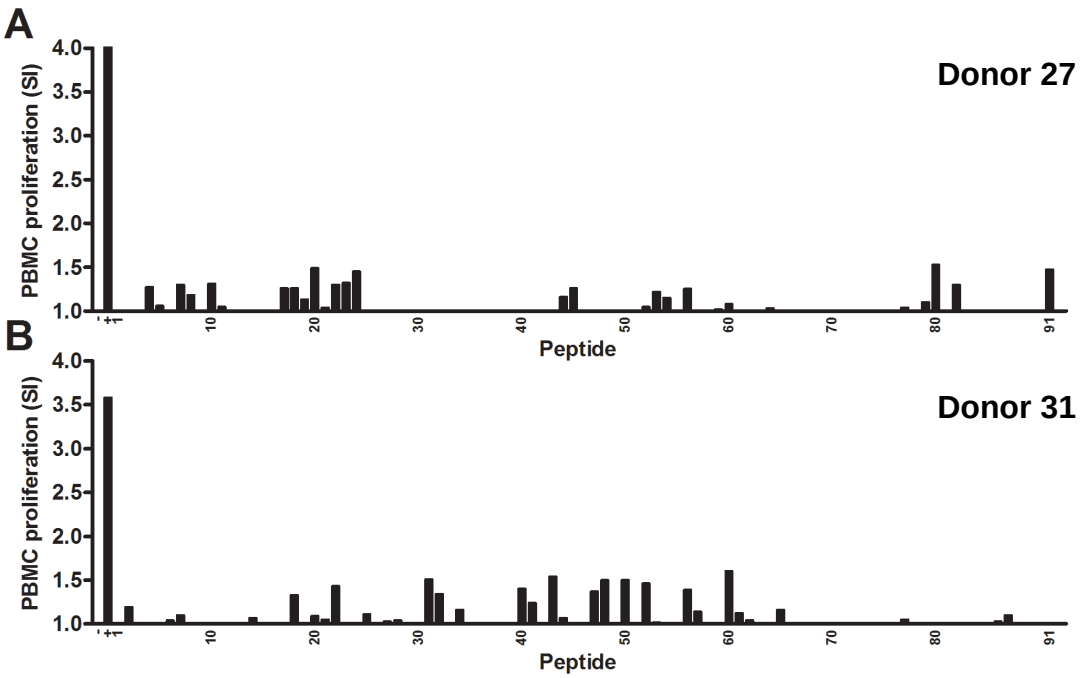

Figure 5.3 Identification of human T-cell epitopes on AAV-2 capsid protein VP1. PBMC from donors studied in Chapters 3 and 4 were stimulated *in vitro* as described in Chapter 2.2.5.1. Stimulation was performed using overlapping synthesised peptides (described in Chapter 2.1.4.1 and Table 2.2) corresponding to the VP1 capsid sequence of AAV-2. Peptide used (horizontal axis) is graphed against SI (as described in Chapter 2.2.5.1, horizontal axis) along with unstimulated negative controls (-) and ConA simulated positive controls (+). Experiment was performed for A) donor 27 and B) donor 31 and was performed once for each donor. Bars represent the mean of triplicate determinations.

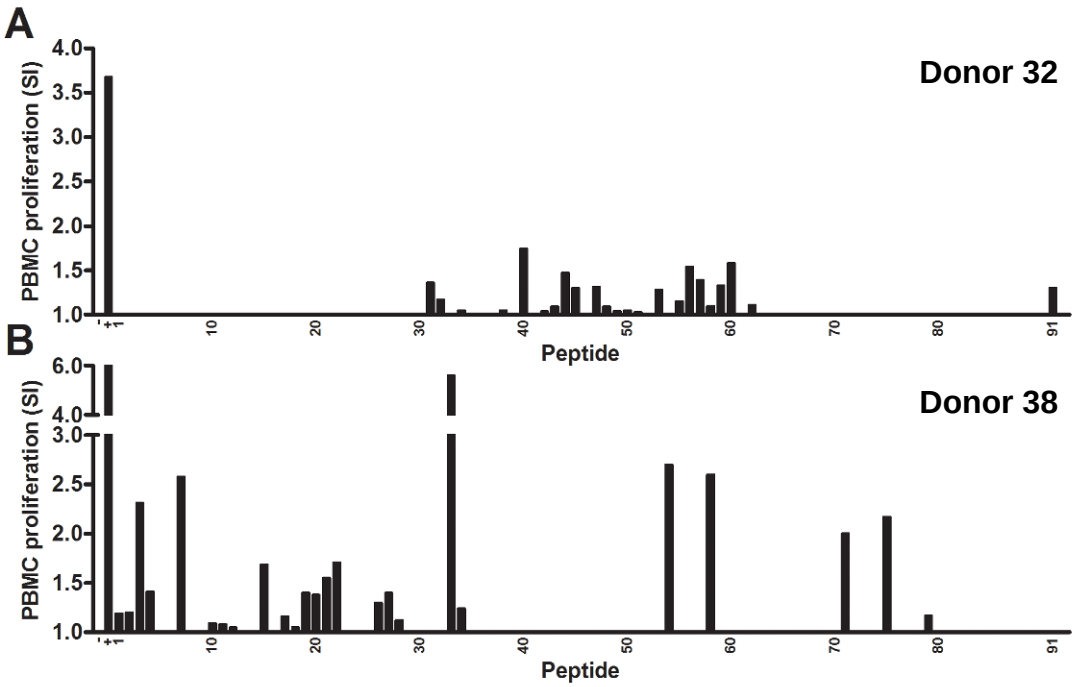

Figure 5.4 Identification of human T-cell epitopes on AAV-2 capsid protein VP1. PBMC from donors studied in Chapters 3 and 4 were stimulated *in vitro* as described in Chapter 2.2.5.1. Stimulation was performed using overlapping synthesised peptides (described in Chapter 2.1.4.1 and Table 2.2) corresponding to the VP1 capsid sequence of AAV-2. Peptide used (horizontal axis) is graphed against SI (as described in Chapter 2.2.5.1, horizontal axis) along with unstimulated negative controls (-) and ConA simulated positive controls (+). Experiment was performed for A) donor 32 and B) donor 38 and was performed once for each donor. Bars represent the mean of triplicate determinations.

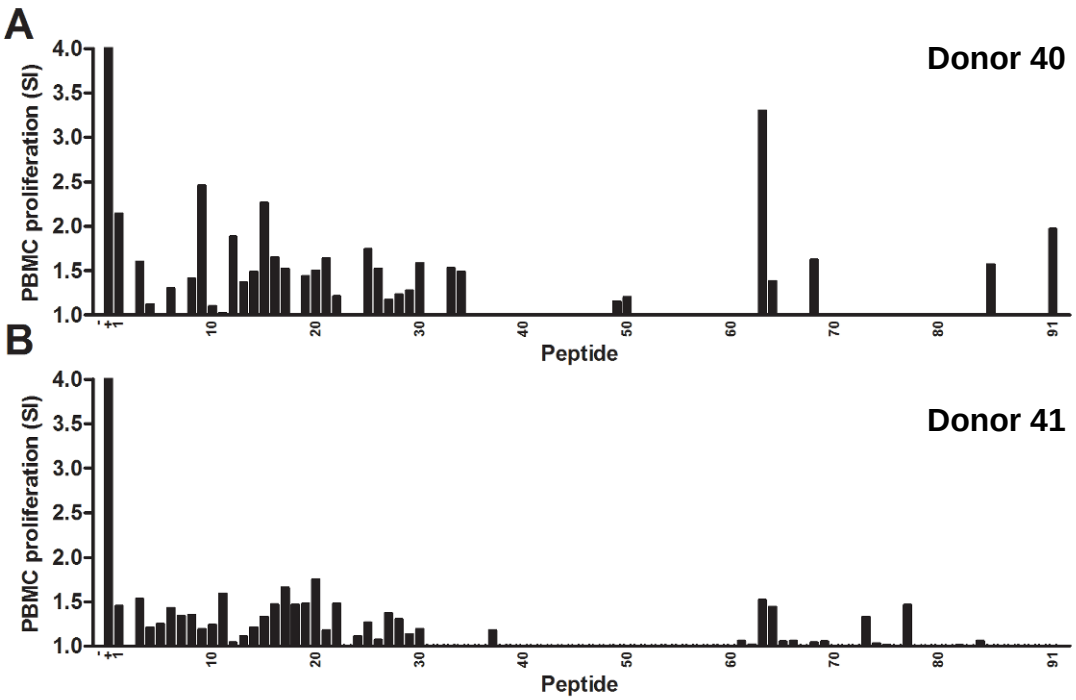

Figure 5.5 Identification of human T-cell epitopes on AAV-2 capsid protein VP1. PBMC from donors studied in Chapters 3 and 4 were stimulated *in vitro* as described in Chapter 2.2.5.1. Stimulation was performed using overlapping synthesised peptides (described in Chapter 2.1.4.1 and Table 2.2) corresponding to the VP1 capsid sequence of AAV-2. Peptide used (horizontal axis) is graphed against SI (as described in Chapter 2.2.5.1, horizontal axis) along with unstimulated negative controls (-) and ConA simulated positive controls (+). Experiment was performed for A) donor 40 and B) donor 41 and was performed once for each donor. Bars represent the mean of triplicate determinations.

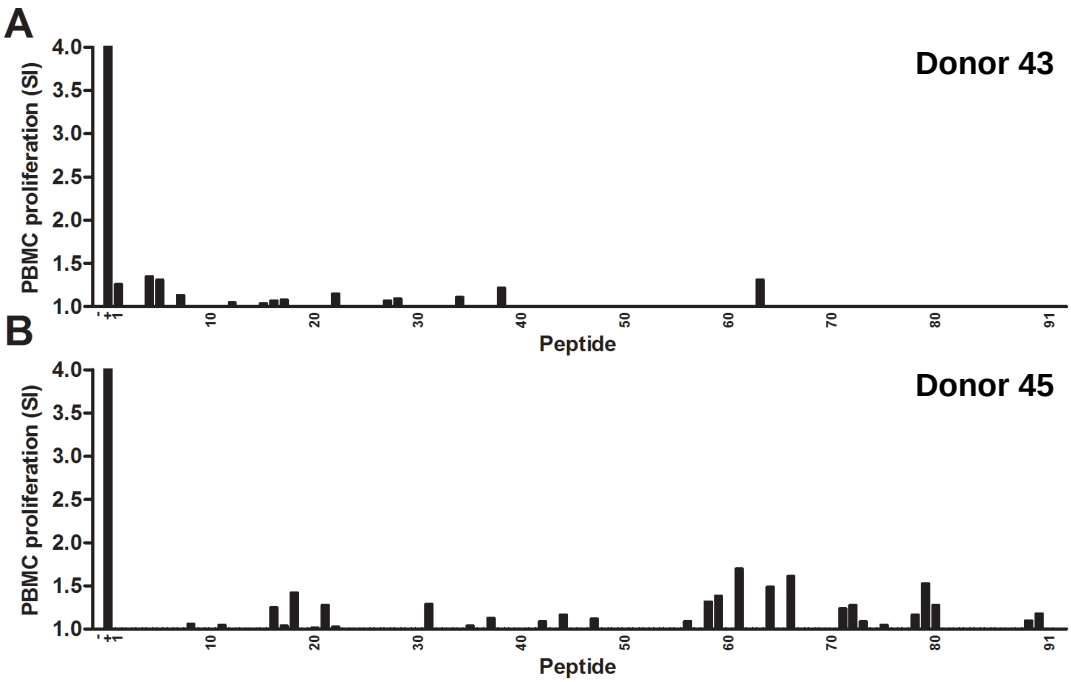

Figure 5.6 Identification of human T-cell epitopes on AAV-2 capsid protein VP1. PBMC from donors studied in Chapters 3 and 4 were stimulated *in vitro* as described in Chapter 2.2.5.1. Stimulation was performed using overlapping synthesised peptides (described in Chapter 2.1.4.1 and Table 2.2) corresponding to the VP1 capsid sequence of AAV-2. Peptide used (horizontal axis) is graphed against SI (as described in Chapter 2.2.5.1, horizontal axis) along with unstimulated negative controls (-) and ConA simulated positive controls (+). Experiment was performed for A) donor 43 and B) donor 45 and was performed once for each donor. Bars represent the mean of triplicate determinations.

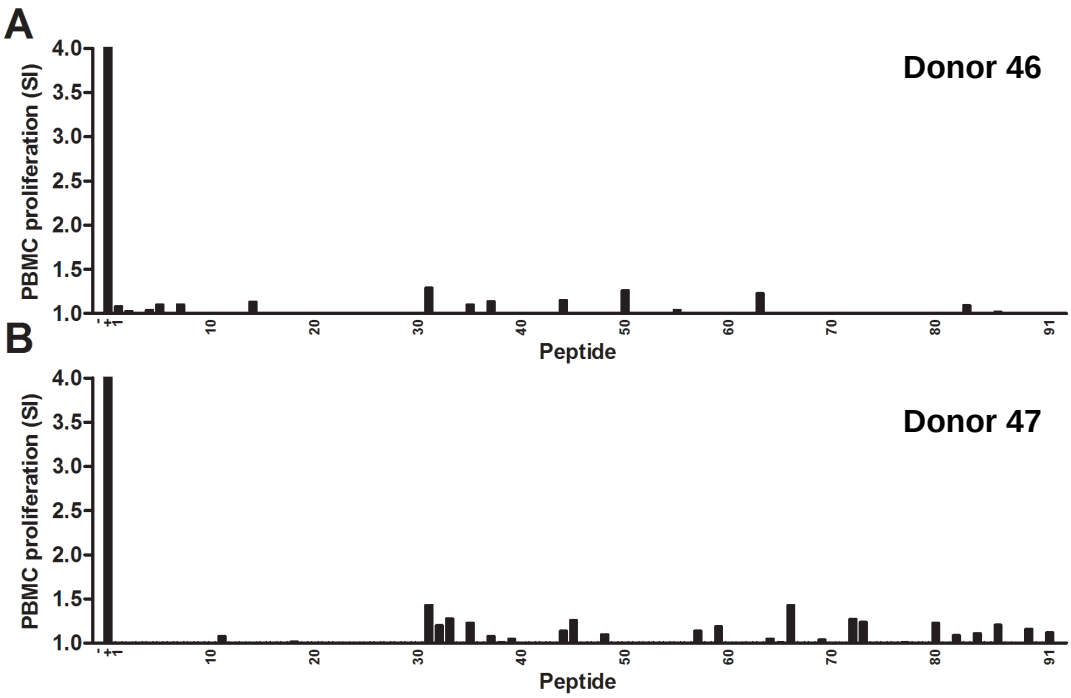

Figure 5.7 Identification of human T-cell epitopes on AAV-2 capsid protein VP1. PBMC from donors studied in Chapters 3 and 4 were stimulated *in vitro* as described in Chapter 2.2.5.1. Stimulation was performed using overlapping synthesised peptides (described in Chapter 2.1.4.1 and Table 2.2) corresponding to the VP1 capsid sequence of AAV-2. Peptide used (horizontal axis) is graphed against SI (as described in Chapter 2.2.5.1, horizontal axis) along with unstimulated negative controls (-) and ConA simulated positive controls (+). Experiment was performed for A) donor 46 and B) donor 47 and was performed once for each donor. Bars represent the mean of triplicate determinations.

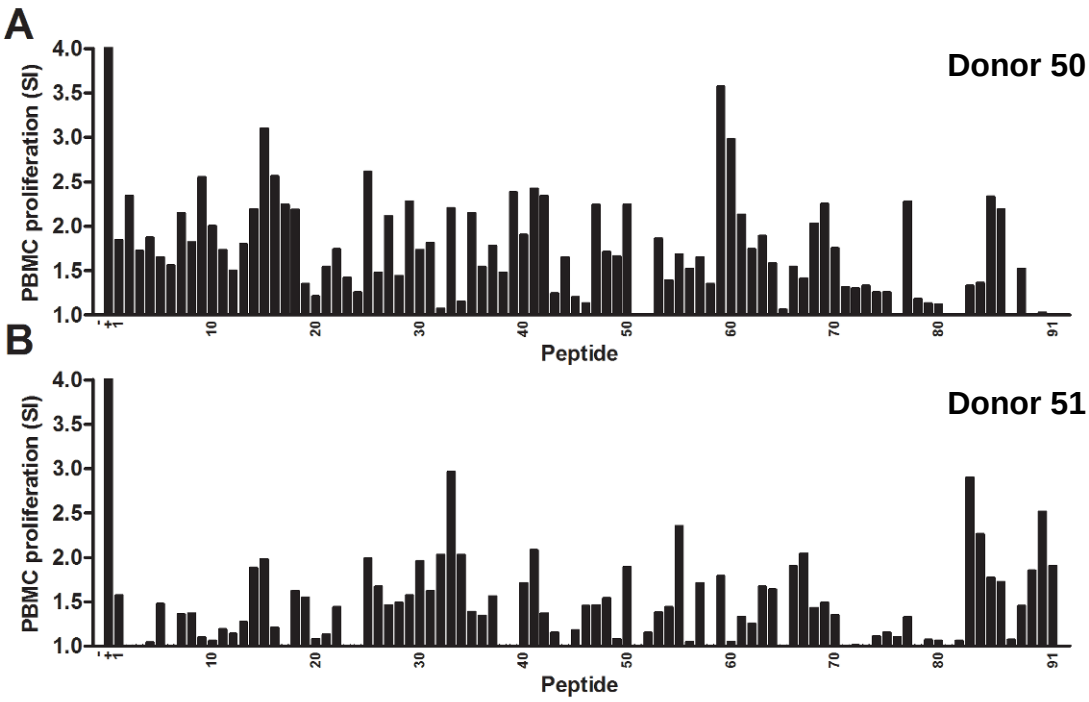

Figure 5.8 Identification of human T-cell epitopes on AAV-2 capsid protein VP1. PBMC from donors studied in Chapters 3 and 4 were stimulated *in vitro* as described in Chapter 2.2.5.1. Stimulation was performed using overlapping synthesised peptides (described in Chapter 2.1.4.1 and Table 2.2) corresponding to the VP1 capsid sequence of AAV-2. Peptide used (horizontal axis) is graphed against SI (as described in Chapter 2.2.5.1, horizontal axis) along with unstimulated negative controls (-) and ConA simulated positive controls (+). Experiment was performed for A) donor 50 and B) donor 51 and was performed once for each donor. Bars represent the mean of triplicate determinations.

5.3 IDENTIFICATION OF 17 AAV-2 EPITOPES RECOGNISED PROMISCUOUSLY BY HUMAN T-CELLS

Despite the wide range of epitopes identified across the donor group, 17 stimulating sequences were identified that were recognised by two or more donors (Table 5.1, labelled as sequences A-Q). These 17 common antigenic sequences were identified as commonly recognised across a total of six donors (Table 5.3), hereafter called consensus sequences.

Sequence A (KEVTQNDGTTTI) was the most commonly-recognised epitope, eliciting PBMC proliferation in cultures from 4 different donors (donors 16, 19, 50 and 51; Tables 5.2 and 5.3). Sequences B, C and D were each recognised in cultures from 3 different donors and sequences E – Q were each recognised by 2 different donors (Tables 5.2 and 5.3). The frequent recognition of these epitopes in the study group suggested that it might be reasonable to consider these sequences as representative of immunodominant epitopes. Although the wide diversity of epitopes recognised by single donors (Table 5.1) might render mass production of modified, non-immunogenic AAV capsids unfeasible, the presence of a selection of immunodominant epitopes suggested that these might be attractive candidates for capsid modification in individual recipient-specific cases where alternatives to capsid modification may be undesirable.

TABLE 5.2 Common VP1 consensus sequences[a] recognised by human PBMC

Peptide			VP1 consensus sequence	Respondant donors	SYFPEITHI		Seq.
					Class I score[b]	Class II score[c]	
321	**-**	**333**	KEVTQNDGTTTI	16, 19, 50, 51	24	20	**A**
505	**-**	**517**	ATKYHLNGRDSL	13, 50, 51			**B**
241	**-**	**253**	TTSTRTWALPTY	16, 50, 51	21	24	**C**
681	**-**	**693**	EIEWELQKENSK	13, 50, 51	21	26	**D**
9	**-**	**21**	DWLEDTLSEGIR	16, 50	21	32	**E**
57	**-**	**69**	NGLDKGEPVNEA	16, 50	20	27	**F**
113	**-**	**125**	NLGRAVFQAKKR	50, 51	28	20	**G**
121	**-**	**133**	AKKRVLEPLGLV	40, 50	29	20	**H**
249	**-**	**261**	LPTYNNHLYKQI	16, 51	24	24	**I**
257	**-**	**269**	YKQISSQSGASN	16, 51	-	23	**J**
265	**-**	**277**	GASNDNHYFGYS	16, 51	26	-	**K**
313	**-**	**325**	FKLFNIQVKEVT	16, 50	-	23	**L**
329	**-**	**341**	TTTIANNLTSTV	19, 50	22	24	**M**
393	**-**	**405**	YCLEYFPSQMLR	16, 50	21	28	**N**
457	**-**	**469**	QSRLQFSQAGAS	13, 16	-	25	**O**
553	**-**	**565**	DIEKVMITDEEE	13, 50	21	30	**P**
716	**-**	**728**	TNGVYSEPRPIGTRYLT	16, 51	24	21	**Q**

[a] Consensus sequences were derived from the 12-mer overlap between pairs of PBMC stimulating VP1 peptides with the exception of the overlap between peptides 90 and 91 which was 17-mer. Pairs of peptides were considered positive if both supported an SI value greater than one standard deviation above the mean SI for all donors.

[b] VP1 sequence was analysed using SYFPEITHI prediction for alleles of the HLA-A and HLA-B loci, output sequences were nonamers.

[c] VP1 sequence was analysed using SYFPEITHI prediction for alleles of the HLA-DRB locus, output sequences were 15-mers. For both class I and II, the best score obtained was reported. Scores below 20 were not reported.

5.4 Characterisation of the HLA Haplotypes of the Irish Donor Population Used in this Study

T cell recognition of antigen in mammals is MHC restricted. Humans are an outbred population with highly polymorphic HLA expression profiles. In order to establish if the AAV-2 epitopes identified were associated with particular haplotypes, the HLA haplotype for each AAV-2 respondent donor was determined. To achieve this, an sequence specific primer (SSP) PCR approach was adopted. The HLA-A, B, C, DRB and DQB loci were characterised using a commercial SSP PCR kit (Texas Biogene, Richardson, TX). The kit did not include primers for the HLA-DP, DRA or DQA loci. SSP PCR used a panel of lyophilised sequence-specific primers in a tray format. Wells contained multiple primers acting as templates for products of differing sizes. Genomic DNA was dissolved in a master mix and added to the primer tray, and PCR was performed (Chapter 2.2.4.7), resulting in multiple DNA products for each target locus. Genomic DNA was isolated from cryopreserved PBMC from the panel of 16 responding donors. The combination of products and their size as read on an agarose gel could be used to identify the allele at the locus of interest following the documentation provided by the manufacturer (example gel depicted in Figure 5.9).

As would be expected in an outbred population, the donors characterised displayed considerable haplotype diversity (Table 5.3). No obvious correlations between HLA expression and epitope recognition were detectable in a sample of this size. However, the key observation from this study was that the dominant 17 epitopes described in Table 5.2 were recognised by donors of different HLA haplotypes,

indicating that these epitopes of the AAV-2 capsid are recognised promiscuously. It is therefore reasonable to consider these epitopes immunodominant.

TABLE 5.3 HLA haplotypes of donors responding to AAV-2

Donor #	Class I HLA alleles[a]	Class II HLA alleles[a]
13	A2, B7, B13, Cw5, Cw7	DR4/DR53, DR7/DR53, DQ2, DQ8(3)
15	B7, B8, Cw7	DR17(3)/DR52, DR15(2)/DR51, DQ2, DQ6(1)
16	A1, Cw7, Cw7	DR17(3)/DR52, DR51, DQ2, DQ6(1)
19	A68, B8, Cw7, Cw8	DR3/DR52, DR17(3)/DR52, DQ2, DQ6(1)
27	A1, A2, B*4440, B*5615, Cw5, Cw7	DQ2, DQ7(3)
31	A1, B8, B51(5)	DR17(3)/DR52, DR8, DQ2, DQ4
32	A1, A29(19), Cw7, Cw7	DR17(3)/DR52, --/DR52, DQ2, DQ6(1)
38	A1, B63(15), B44(12), Cw5, Cw7	DR4/DR53, DR13(6)/DR52, DQ7(3), DQ6(1)
40	Cw1, Cw7	DR1, DR7/DR53, DQ2, DQ5(1)
41	A2, B44(12), B47, Cw4	DR4/DR53, DR7/DR53, DQ2, DQ7(3)
43	A31(19), B7, B71(70), Cw18||Cw6, Cw18	DR4/DR53, DR15(2)/DR51, DQ6(1), DQ6(1)
45	A2, A24(9), B7, B18, Cw5, Cw7	DR17(3)/DR52, DR15(2)/DR51, DQ2, DQ6(1)
46	B55(2), Cw1, Cw4	DR103, DR13(6)/DR52, DQ5(1), DQ6(1)
47	A1, B42	DR4/DR53, DR4/DR53, DQ8(3), DQ5(1)
50	A31(9), B*14, B*14, Cw*06, Cw*08	DR13(6)/DR52, DR15(2)/DR51, DQ9(3)
51	A66(10)/A26(10), B44(12), B57(17), Cw5, Cw6	DR4/DR53, DR15(2)/DR51, DQ6(1), DQ6(1)

[a] HLA type I and II alleles were determined by SSP PCR. Alleles omitted where not determined.

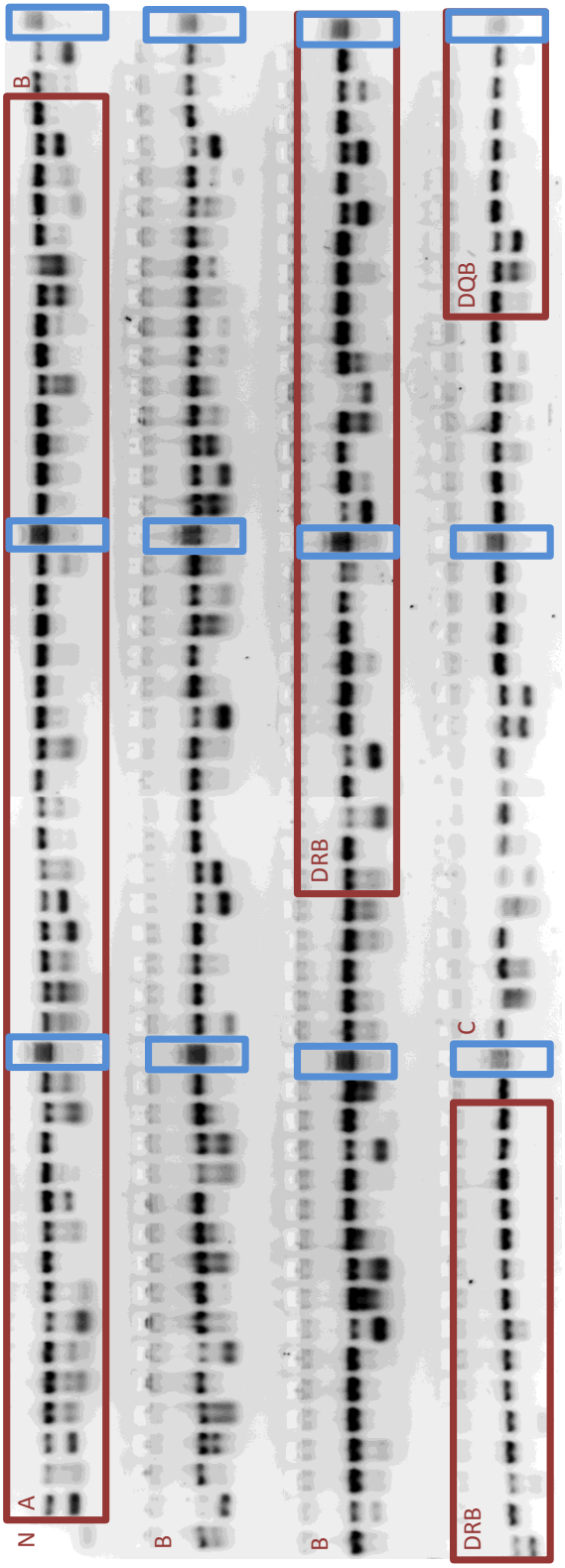

Figure 5.9 SSP PCR gel for Donor 19. Lanes for each HLA allele (A, B, C, DRB, DRQ) are labelled. Negative H_2O control (N). Ladder lanes are marked in blue. Band combinations were analysed using Texas BioGene SSPal software.

5.5 ANTIGENIC SEQUENCES IDENTIFIED CORRESPOND TO HLA-RESTRICTED EPITOPES PREDICTED *IN SILICO*

Probable HLA- and MHC-restricted epitopes may be predicted from an input protein sequence algorithmically and several such algorithms have been developed (Bhasin & Raghava, 2004; Rammensee *et al.*, 1999). The SYFPEITHI algorithm evaluates every amino acid within an input protein sequence and assigns a score to each. The SYFPEITHI database and epitope scoring algorithm was thus used to generate a panel of probable HLA-restricted epitopes derived from the AAV-2 VP1 capsid sequence. The scores assigned are based upon the frequency and binding effect of amino acids identified at each location within naturally-occurring HLA ligands, with the frequencies and binding effects being derived from a database of identified natural HLA ligands. Each amino acid in the input sequence is assigned a score ranging from 1 (indicating a slight benefit to HLA binding) to 15 (indicating an optimal anchor residue), or is assigned a negative score if the amino acid has a detrimental impact on HLA binding. These scores are also dependant on the input HLA type. At the time of testing, the algorithm only permitted assessment of a limited panel of class I and class II HLA types (Table 5.4) and the VP1 sequence was assessed for all available human class I and class II types. For the class I epitopes, the sequence window size was limited to nonamers, whilst the class II sequences were 15-mers. A panel of putative epitopes covering the full range of scores above 0 was generated for each HLA allele. In each case, the SYFPEITHI score of the highest-scoring sequence possessing greater than 85% homology with the epitopes previously identified (Tables 5.1 and 5.2) was reported. Only scores greater than 20 were reported.

TABLE 5.4 Donor PBMC with diverse HLA haplotypes recognise common consenus sequences

Donor	HLA class I[a]			HLA class II[a]		Consensus sequences recognised
	A	B	C	DR	DQ	
13	ND	ND	Cw1, Cw7	DR1, DR7/DR53	DQ2, DQ5(1)	C, N, O
16	A68	B8	Cw7, Cw8	DR3/DR52, DR17(3)/DR52	DQ2, DQ6(1)	A, B, D, E, H, I, J, K, M, N, P, Q
19	A2	B7, B13	Cw5, Cw7	DR4/DR53, DR7/DR53	DQ2, DQ8(3)	L
40	A1	B42	ND	DR4/DR53, DR4/DR53	DQ8(3), DQ5(1)	G
50	ND	B55(2)	Cw1, Cw4	DR103, DR13(6)/DR52	DQ5(1), DQ6(1)	A, B, C, D, E, F, G, K, L, M, O
51	A31(19)	B7, B71(70)	Cw18/Cw6, Cw18	DR4/DR53, DR15(2)/DR51	DQ6(1), DQ6(1)	A, B, C, F, H, I, J, P, Q

[a] HLA serotypes were determined by SSP PCR for HLA loci A, B, C DR and DQ.

The 17 immunodominant sequences described in table 5.1 each showed greater than 85% homology with high-scored class I or class II HLA-restricted VP1 epitopes predicted by the algorithm (Table 5.1). Combined with the frequency with which these epitopes elicited proliferation in PBMC cultures (Section 5.3) and the promiscuous recognition across multiple Class I and Class II HLA types (Section 5.4), the high SYFPEITHI scores gave further confidence that this panel of 17 sequences represented immunodominant epitopes in the study group.

5.6 HLA Haplotypes of Donors Displaying Memory for AAV-2 do not Differ from the General Population

The haplotypes of AAV-2-respondant donors displayed considerable diversity (Table 5.3). This was also the case for donors responding to the most common stimulating capsid sequences (Table 5.4). Although it is reported here that the DQ2, DQ3 (DQ7(3), DQ8(3), DQ9(3)) and DQ6(1) serotype alleles are present at a high frequency in our study group, these results broadly agree with recent detailed examinations of HLA allele frequencies in the Irish population, in which these serotypes represented the three most commonly identified (Dunne *et al.*, 2008). Thus, although the HLA data presented here is less exhaustive, the donors from which AAV-2-specific PBMC were isolated display HLA diversity comparable to the general Irish population.

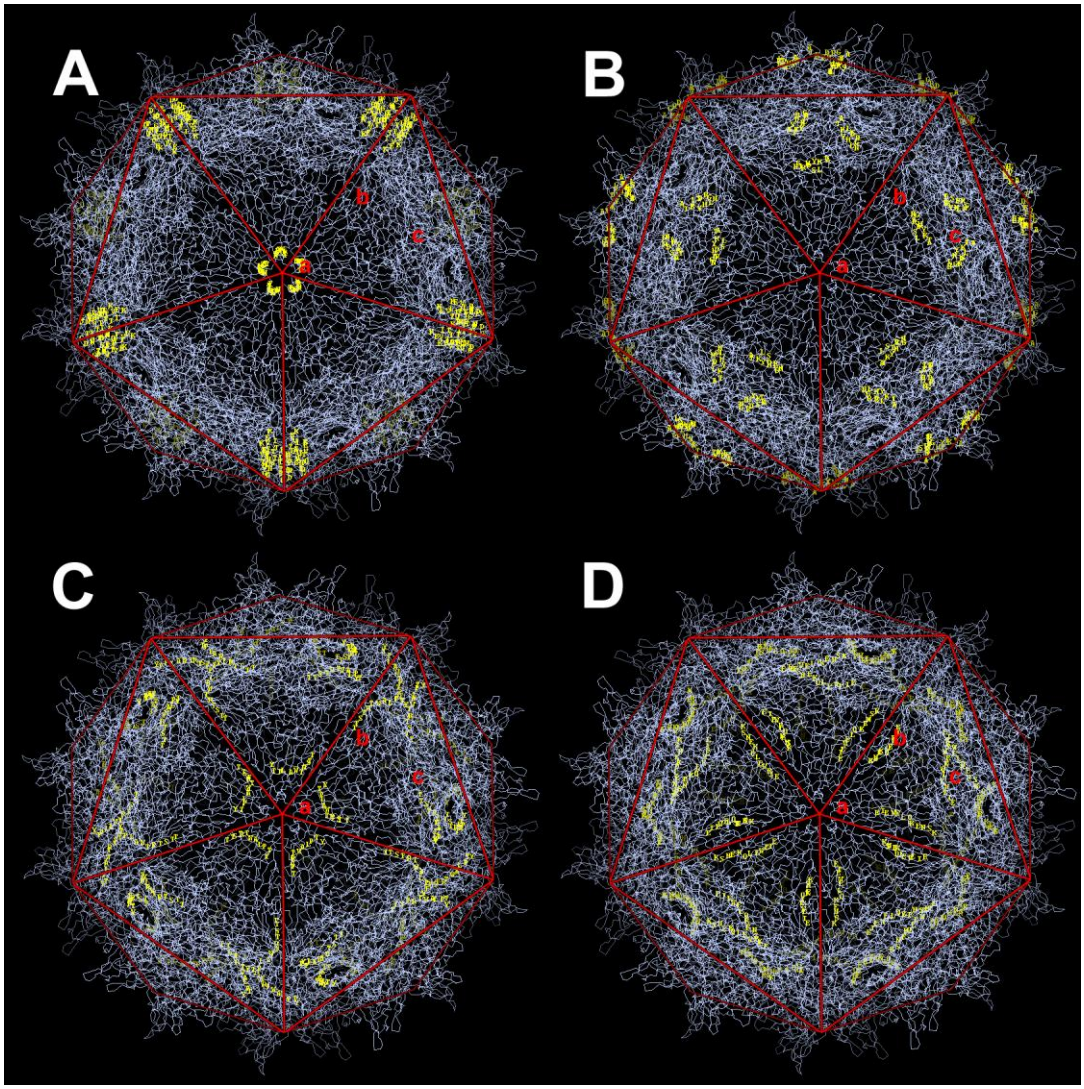

Figure 5.10 3D structural diagram of the AAV-2 capsid showing the location of the immunodominant epitopes A-D (yellow) in the context of the capsid structure (blue). The icosahedral symmetry of the capsid is indicated in each case (red lines) and the 5-fold, 2-fold and 3-fold axes of symmetry, which form the boundaries where VP subunits associate, are labelled (a, b and c, respectively). In each case, capsid structure is presented as a 60 subunit polymer consisting entirely of VP3 subunits. Structure is as determined by Xie *et al.*, 2002 and is rendered using STRAP.

5.7 IMMUNODOMINANT EPITOPES OF AAV-2 COMPRISE FUNCTIONALLY SIGNIFICANT REGIONS OF THE VP1 CAPSID 3D STRUCTURE

Various motifs within the 3D structure of the AAV-2 capsid are involved in receptor binding and replication functions (Tratschin *et al.*, 1984, Girod *et al.*, 2002, Asokan *et al.*, 2006, DiPrimio *et al.*, 2008). Since the immunodominant epitopes identified in Section 5.3 might be targets for modification in order to minimise adaptive recognition of the virus in a therapeutic setting, it was important to establish whether these epitopes lay within functionally important regions of the capsid. Thus, where possible, the immunodominant epitope sequences were mapped onto a 3D structure of the AAV-2 capsid.

The most commonly-recognised immunodominant epitope identified in this study was sequence A (KEVTQNDGTTTI; Chapter 5, Table 5.1), which shared 4-mer homology with two other immunodominant epitopes, sequences L (FKLFNIQVKEVT) and M (TTTIANNLTSTV). These sequences would thus be attractive targets for modification. When sequence A was mapped onto the 3d model of the AAV-2 capsid (Figure 5.10) it was found that the sequence lies within part of the loop formed between beta strands H and I (HI loop) of the VP subunit, though to be essential for viral capsid assembly and viral DNA packaging into the capsid (DiPrimio *et al.*, 2008). Sequence B (ATKYHLNGRDSL) was found to be located at the base of a cluster of protrusions on the AAV-2 capsid, which is composed of overlapping loops from three subunits associating at the 3-fold symmetry axis at the centre of each icosahedral face (Figure 5.10). This sequence has been shown to have an integrin-binding function (Asokan *et*

al., 2006). Sequence C is located in the region directly adjacent to the 5 fold capsid pore structure composed of sequences A, L and M (Figure 5.10 and Figure 5.11). Sequence D is located along the icosahedral vertex connecting 5-fold symmetry axes, close to the 2-fold subunit border region (Figure 5.10). Sequence N which is located close to the 5-fold axis may also serve a scaffolding function for the capsid pore (Figure 5.11). Sequence Q, like sequence D, is located close to the 2-fold subunit border (Figure 5.11). Epitope sequences E-H are located within the N-terminal VP1 unique region and thus could not be mapped onto the 3D structure as it was composed exclusively of VP3 subunits. The location and function of the unique region within the capsid 3D structure is not well-established (Kronenberg *et al.*, 2005).

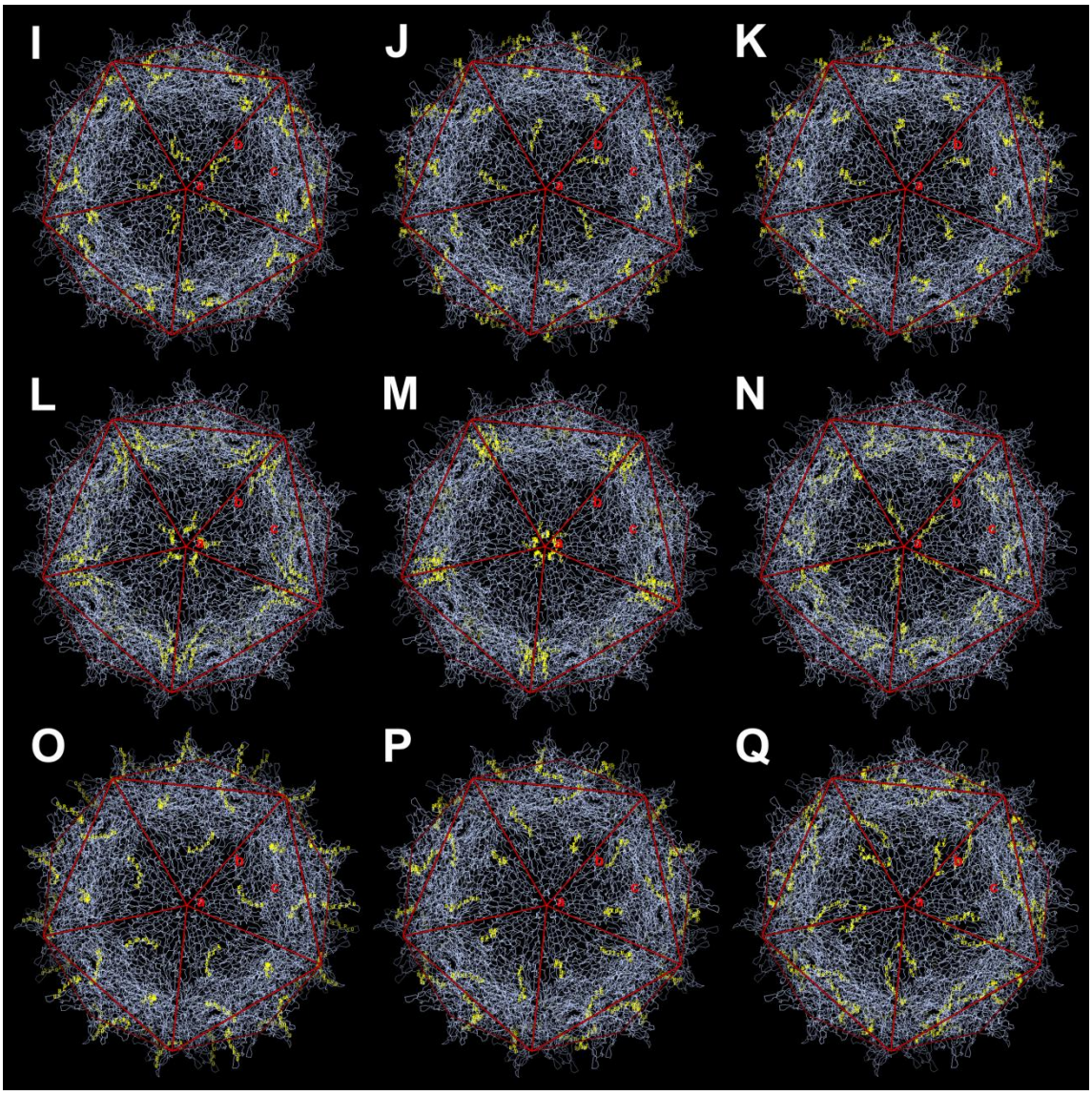

Figure 5.11 3D structural diagram of the AAV-2 capsid showing the location of the immunodominant epitopes I-Q (yellow) in the context of the capsid structure (blue). The icosahedral symmetry of the capsid is indicated in each case (red lines) and the 5-fold, 2-fold and 3-fold axes of symmetry, which form the boundaries where VP subunits associate, are indicated (a, b and c, respectively). In each case, capsid structure is presented as a 60 subunit polymer consisting entirely of VP3 subunits. Structure is as determined by Xie *et al*., 2002 and is rendered using STRAP.

5.8 Immunodominant Epitopes of AAV-2 are Highly Conserved in AAV Serotypes 1, 4, 6 and 8

An alternative to the modification of AAV-2 capsids is use of capsids from other AAV serotypes. The sequences of the VP1 capsid proteins vary between AAV serotypes and this may mean that immunodominant epitopes present on the AAV-2 capsid may not be conserved in other serotypes. When the VP1 sequences for AAV serotypes 1, 2, 4, 6 and 8 are compared for the conservation of the 4 most commonly-recognised immunodominant epitopes described here (Section 5.3) it is evident that sequences A and D are fully or highly conserved across all 5 serotypes (Figure 5.12). Sequence C was fully conserved across all 5 serotypes whilst sequence B was less well conserved across the top 4 immunodominant epitopes. The epitopes were least conserved in AAV-4; although sequence C was fully conserved, only 7 of 12 amino acids from epitope A were conserved, whilst sequences B and D were represented by 5 of 12 and 8 of 12 amino acids respectively (Figure 5.12).

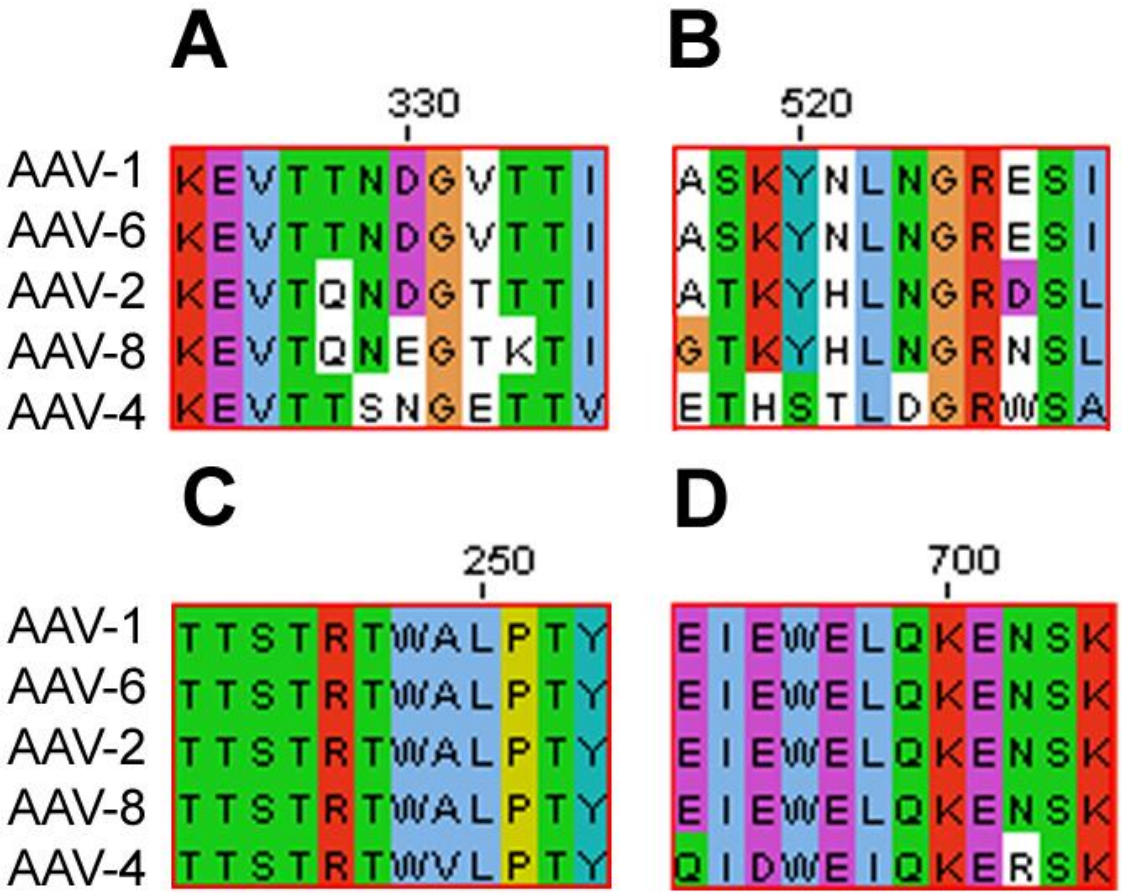

Figure 5.12 Multiple sequence alignment of immunodominant epitopes A-D. The VP1 capsid sequence of AAV-2 was aligned with the VP1 sequences of AAV-1, AAV-4, AAV-6 and AAV-8 using ClustalW. Residue numbers are indicated with digits above each alignment.

5.9 SUMMARY

Stimulation of PBMC from a subset of donors (n=16) with overlapping VP1 capsid peptides allowed the identification of 59 AAV-2-specific T-cell epitopes. The AAV-2 capsid is composed of three proteins; VP1, VP2 and VP3 in a ratio of 1:1:10 (Xie *et al.*, 2002). VP2 and VP3 are products of the splicing of Cap open reading frame mRNA, and both proteins represent subsequences of the VP1 protein. Thus, the entire capsid sequence may be represented by VP1. Using a restrictive definition, 17 candidate epitope sequences were identified as recognised by at least two donors (Table 5.2). A further 42 sequences were recognised by a single donor each (Table 5.1). The stringent epitope definition combined with limitations in assay sensitivity due to the modest level of PBMC proliferation induced by AAV-2 and its components mean that some of the more limited proliferative responses observed may have represented false negative results. Thus, it is likely that further single-case candidate epitopes or confirmations of existing single-case candidate epitopes were not detected. The panel of single-case and frequently recognised candidate epitopes includes sequences (Tables 5.1 and 5.2) previously identified in human and mouse studies (Chen *et al.*, 2006; Manno *et al.*, 2006; Sabatino *et al.*, 2005).

No significant correlation could be identified between donor HLA class I and class II haplotypes and the corresponding epitopes recognised. The haplotypes of AAV-2 respondent donors displayed considerable diversity (Table 5.4). This was also the case for donors responding to the most common stimulating capsid sequences (Table

5.3). Although it is reported here that the DQ2, DQ3 (DQ7(3), DQ8(3), DQ9(3)) and DQ6(1) serotype alleles are present at a high frequency in our study group, these results broadly agree with recent detailed examinations of HLA allele frequencies and haplotypes in the Irish population in which these three serotypes represented the three most commonly identified (Dunne *et al.*, 2008). Thus, although the HLA data presented here is less exhaustive, the donors from which AAV-2-specific PBMC were isolated display HLA diversity comparable to the general Irish population. The observation that a number of epitopes can be recognised by donors of different HLA haplotypes indicates that epitopes A, B, C and K are candidate immunodominant human epitopes.

The induction of humoral immune responses by AAV-2 characterised in Chapters 3 gave some cause for concern that AAV-2-based gene therapy vectors might face neutralisation and targeted complement degradation if administered to AAV-2 primed recipients in the Irish population. The cell-mediated responses characterised in Chapters 4 might result in targeted destruction of AAV-2 vector transduced cells. Although it has been suggested (Manno *et al.*, 2006) that vector modification strategies might be employed to circumvent both humoral and cell-mediated adaptive responses, the diverse panel of candidate immunostimulatory targets identified in this chapter undermines the practicality of such an approach. Although other means of preventing immune memory recognition of AAV-2 are discussed in Chapter 7, one alternative strategy considered for investigation here would be to conduct transductions on human cells *ex vivo* and then infuse those cells into the recipient. Typically such a strategy would demand that the transduced cells be autologous to the recipient, which is not practical for all applications. However some types of adult stem cells such as

mesenchymal stem cells (MSC) have been shown to evade allorecognition and would thus be attractive candidate cells for such *ex vivo* transduction. The transduction of murine MSC with gene delivery vectors including AAV-2 is investigated in Chapter 6.

CHAPTER 6

THE IMPACT OF GENE DELIVERY ON MESENCHYMAL STEM CELLS

6.1 INTRODUCTION

Mesenchymal stem cells (MSC) are candidate agents for a variety of regenerative therapies (Djouad *et al.*, 2009; Markert *et al.*, 2009). MSC possess a number of traits which make them attractive mediators of regenerative therapy. They can be repeatedly subcultured whilst maintaining an undifferentiated state (Bianco *et al.*, 2008). MSC are known to have a broad immunomodulatory functions (Aggarwal & Pittenger, 2005; Barry *et al.*, 2005; English *et al.*, 2007; English *et al.*, 2008; Ryan *et al.*, 2007) and thus may be attractive gene therapy vectors in their own right if engraftment can be ensured. They can undergo *in vitro* differentiation into cartilage, bone and fat tissue when cultured in media supplemented with appropriate growth factors (Mackay *et al.*, 1998; Pittenger *et al.*, 1999; Wakitani *et al.*, 1994). There is also evidence that MSC can contribute to tissue regeneration and repair *in vivo*, although it is unclear whether this is mediated by cell fusion, healing factor secretion, *in vitro* differentiation, or a combination of these mechanisms (Koc *et al.*, 2002; Tran *et al.*, 2003; Wang *et al.*, 2003). Also, the previously-mentioned immunomodulatory capacity appears to afford allogeneically transplanted MSC some protection from allorejection (Deng *et al.*, 2004).

This feature makes MSC of particular interest in transplant immunology. It is conceivable that even if MSC cannot fulfil their differentiation potential *in vivo*, that MSC may have a therapeutic function when used in conjunction with organ transplantation, perhaps modulating the effects of graft versus host disease (Bartholomew *et al.*, 2002; Le Blanc *et al.*, 2004). As differing factors mediate their immunomodulatory effects by different means, it was hypothesised that the overall

inhibition effect might be due to a combination of factors captured in the precursor cohort model of lymphocyte proliferation (Hawkins *et al.*, 2007). Carboxyfluorescein diacetate succinimidyl ester (CFSE) staining of naive T-cells co-incubated with MSC and examination of their proliferation by flow cytometry at multiple time points should highlight the relative importance of these factors. Thus, a combination of tritiated thymidine incorporation and CFSE staining in conjunction with precursor cohort analysis was used to assess the immunomodulatory capacity of MSC.

The therapeutic potential of MSC may also be enhanced by transgenic modification. If MSC can be genetically modified using viral vectors, this immunomodulatory function may serve to block potentially deleterious host immune responses to the vector. Viral vector modification of MSC might provide therapies for the treatment of bone lesions (Gadi *et al.*, 2001) and cancers (Mohr *et al.*, 2008; Studeny *et al.*, 2002). The approach here was to determine whether murine MSC could be efficiently transduced using an AAV vector carrying a reporter transgene. Initial studies would examine transduction using an *eGFP* reporter gene, and then progress to using a transgene with a therapeutic function. The inhibition of T-cell proliferation mediated by MSC is dependent on a number of cell contact-dependent and independent factors. One potential goal for genetic modification of MSC would be the enhancement the immunomodulatory function. As the immunomodulatory function of MSC is at least partially mediated by indoleamine-pyrrole 2,3-dioxygenase (IDO) in both mouse models and in humans (English *et al.*, 2007; Ryan *et al.*, 2007; Yang *et al.*, 2009), it was decided that the candidate transgene tested would be the IDO gene. For the transduced

MSC to maintain their therapeutic potential, it would thus be important to determine whether features such as immunomodulation and differentiation capacity were impacted by the transduction protocol.

6.2 CHARACTERISATION OF MURINE MSC

Murine mesenchymal stem cells (male BALB/c) were obtained from Dr. Karen English and Laura Tobin. These cells had previously been characterised and displayed fibroblastic morphology, self-renewal, potency and immunomodulatory behaviour. The cells were also positive for Sca-1, MHC class I and CD44 and negative for MHC class II, CD90, CD80, CD105, CD45, CD11b and CD34 (English, Barry *et al*. 2007). Following recovery of the cells from cryopreservation, these characteristics were reassessed to ensure that the results of this study would be comparable to previous work. The MSC used in this study displayed spindle-like fibroblastic morphology when examined by light microscopy (Figure 6.1 A), were MHC class I and Sca-1 positive and MHC class II and CD90 negative as assessed by flow cytometry (Figure 6.1 B). Potency was validated by differentiation assays for adipogenesis (Chapter 2.2.5.4) and osteogenesis (Chapter 2.2.5.5). The MSC used here did not spontaneously differentiate but on appropriate stimulation differentiated into both fat and bone cells within 21 days of culture (Figure 6.2). Thus the cells were characteristic of MSC.

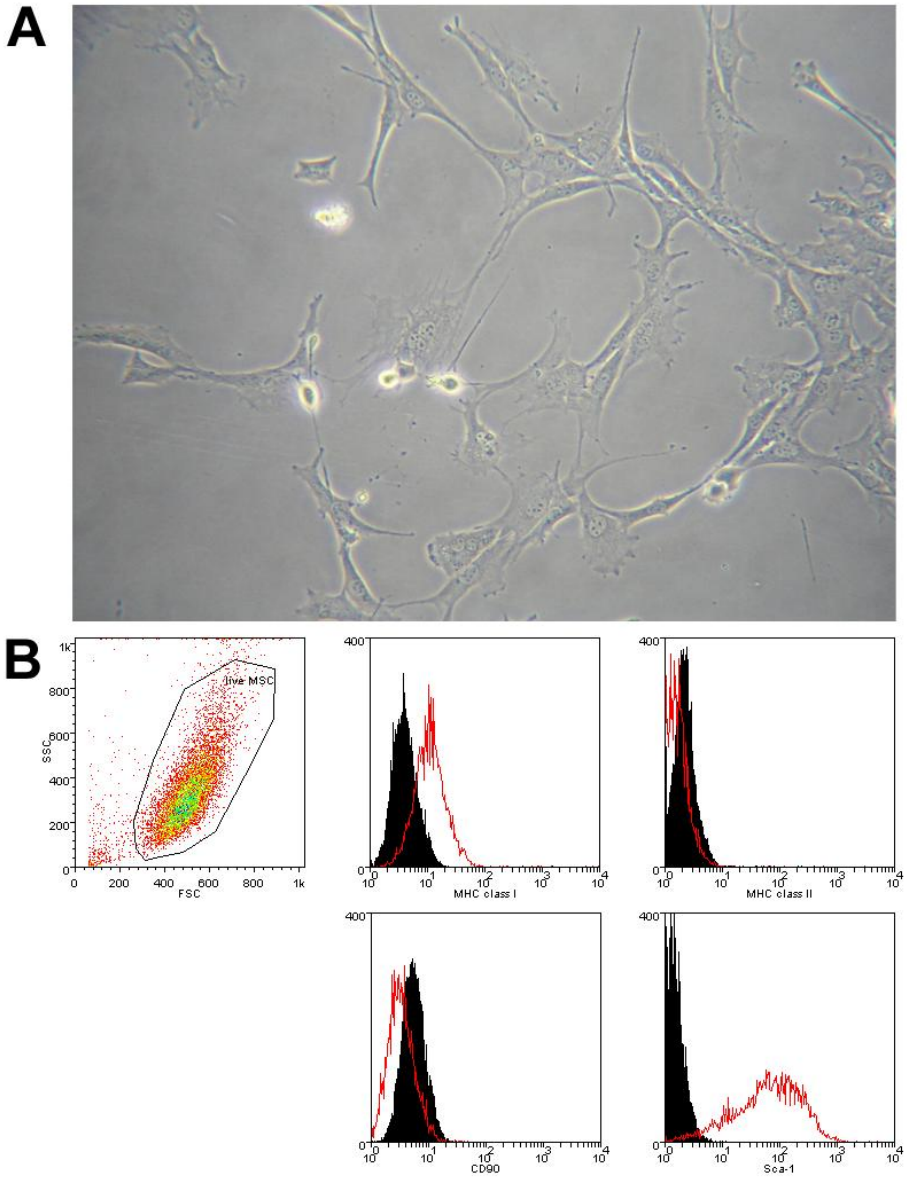

Figure 6.1 Characterisation of the morphology and surface marker expression profile of murine mesenchymal stem cells. A) Murine MSC as examined under light microscope. Light microscopy was performed at 200x magnification. B) Analysis by of murine MSC by flow cytometry, showing forward (FSC) and side scatter (SSC) as well as expression of MHC class I, Sca-1, MHC class II and CD90. Black peaks are isotype controls, whilst red peaks show receptor expression.

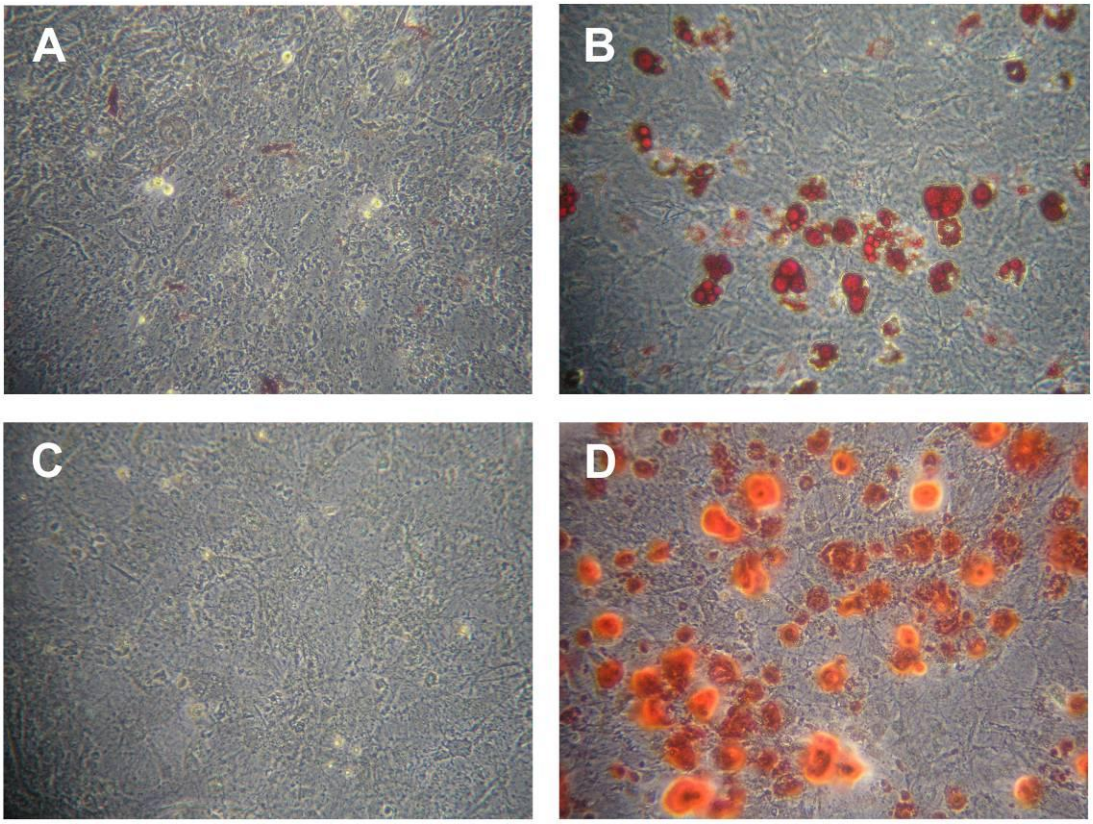

Figure 6.2 Characterisation of the potency of murine MSC *in vitro*. MSC were cultured in growth medium or in differentiation medium for 21 days. A) MSC cultured in growth medium show no evidence of adipogenesis when stained with Oil Red O, whilst B) MSC cultured in adipogenesis medium showed distinctive red-stained adipocytes. C) MSC cultured in growth medium showed no evidence of the presence of osteocytes when stained with Alizarin Red S, whilst D) MSC cultured in osteogenesis medium displayed many red cells and large plaques of red- and orange-stained calcified deposits. Light microscopy was performed at 200x magnification.

MSC immunomodulation was assessed by co-incubation of MSC with mitogen stimulated splenocytes. A dose of 1×10^5 MSC/ml significantly ($p \leq 0.05$) suppressed mitogen stimulated splenocyte proliferation (Figure 6.3 A). This immunomodulatory function extended to MHC mismatched lymphocytes. Mouse naive T-cells (female BALB/c) were stimulated with αCD3e and IL-2 and incubated in medium alone or with varying concentrations of allogeneic murine MSC (female C3H). At a concentration of 1×10^5 MSC/ml, T-cell proliferation was significantly ($p \leq 0.05$) inhibited compared with mitogen stimulated controls (Figure 6.3 B). This result is broadly in agreement with previous work demonstrating a dose-dependent suppression of murine splenocyte (English *et al.*, 2007) and human PBMC proliferation (Ryan *et al.*, 2007).

6.3 Low Concentrations of Allogeneic MSC Synergise with Mitogen to Promote T-cell proliferation

Concentrations of MHC-mismatched MSC of 1×10^5 or greater inhibited mitogen-stimulated naive T-cell proliferation (Figure 6.3). At 2×10^4 MSC/ml proliferation of stimulated naive T-cells was observed, however this increase did not reach statistical significance. However at 5×10^3 cells/ml, MSC significantly ($p \leq 0.05$) enhanced mitogen driven naive T-cell proliferation (Figure 6.3 B). Given that murine MSC do not express MHC class II and modest levels of MHC class I, it is unclear whether this enhanced proliferation is in response to allorecognition between the BALB/c strain T-cell receptor and the C3H strain MSC MHC I receptor, or is the result of MSC derived soluble factors.

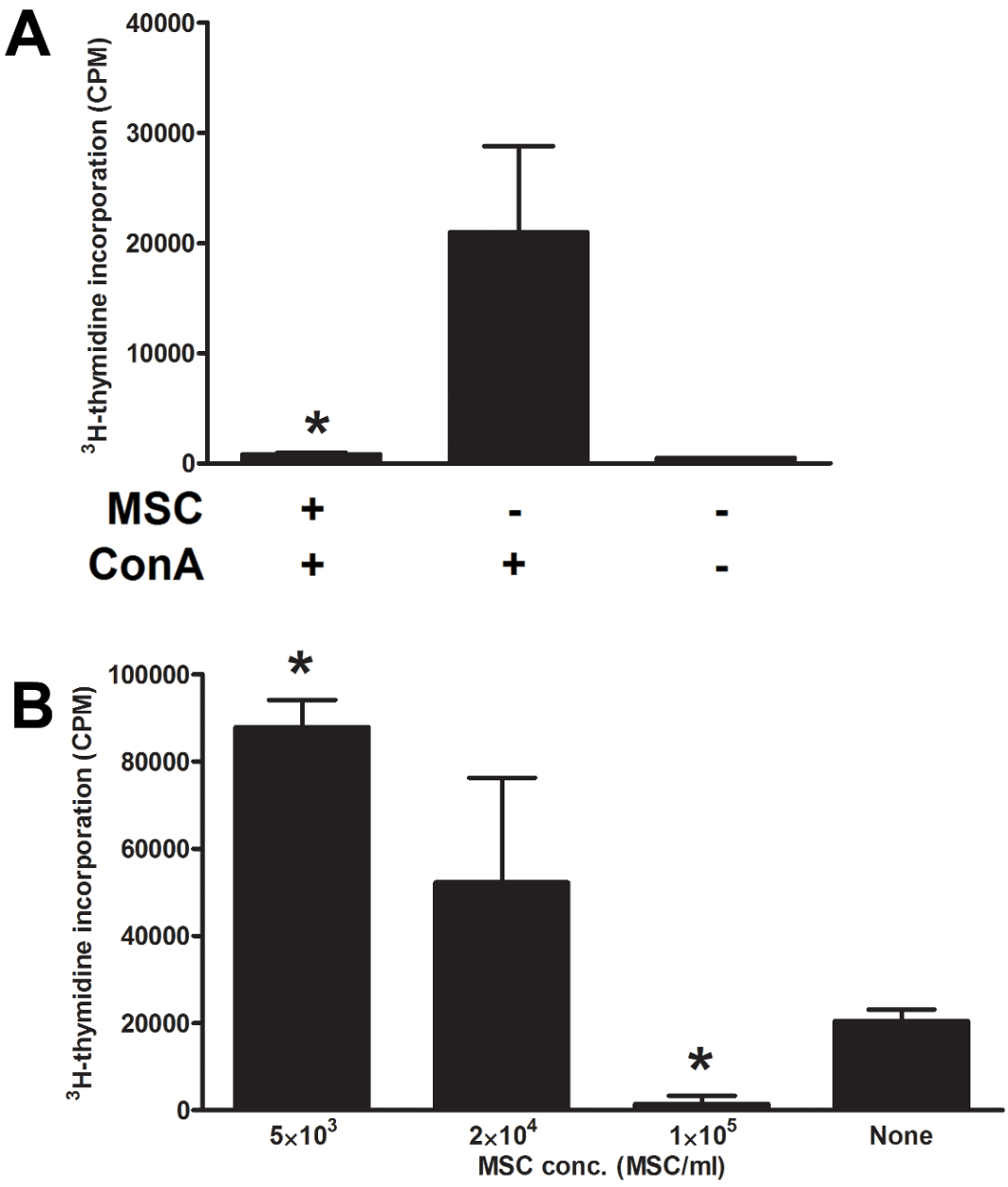

Figure 6.3 Characterisation of murine MSC immunomodulatory function. A) Murine splenocytes co-cultured with 1×10^5 MSC/ml and stimulated with conA were compared with stimulated and unstimulated splenocyte controls. B) Co-culture of conA-stimulated splenocytes with 1×10^5, 2×10^4 and 5×10^3 allogeneic MSC/ml compared with stimulated and unstimulated splenocyte controls. Proliferation by splenocytes was expressed as mean CPM of triplicate determinations. Significant suppression of proliferation is indicated (*). Error bars represent the standard deviation. Experiments were performed twice independently.

6.4 MSC Mediate Their Immunosuppressive Functions Via Changes In Progressor Fraction and Mean Division Times

To examine the immunosuppressive or immunostimulatory effects of MSC on naive allogeneic T-cells (Figure 6.3 B), a CFSE-based proliferation assay was employed. CFSE is a cell-permeable dye which is detectable via flow cytometry. When a cell stained with CFSE undergoes symmetric mitosis, the dye is divided equally between the two daughter cells. It is thus possible to determine the number of divisions that a given cell has undergone by comparing the cell's fluorescence intensity with that of undivided cells at the time of staining. $CD4^+$ $CD62L^+$ naive T-cells were isolated (Chapter 2.2.1.3) and stained with CFSE (Chapter 2.2.5.3). The isolation was validated by flow cytometry. Isolated cells were labelled with fluorescently-labelled antibodies specific for the T-cell receptor CD3 and the naive marker CD62L (Chapter 2.2.1.3, Table 2.3). Using the isolation kit following manufacturer's protocol, splenocyte isolates were enriched from 25% $CD3^+$ $CD62L^+$ (Figure 6.4 A) up to 90% $CD3^+$ $CD62L^+$ (Figure 6.4 B).

Stained naive T-cells were stimulated with αCD3, IL-2 and αCD28 and cultured alone or with MHC-mismatched MSC at 5×10^3 or 1×10^5 MSC/ml. Lymphocyte proliferation was assessed by flow cytometry at 24, 48, 72 and 96 hours (Figure 6.5). Multiple parameters contributing to gross lymphocyte proliferation were then quantified; progressor fraction, cell survival, mean time to first division and subsequent mean division time (Chapter 2.3.2).

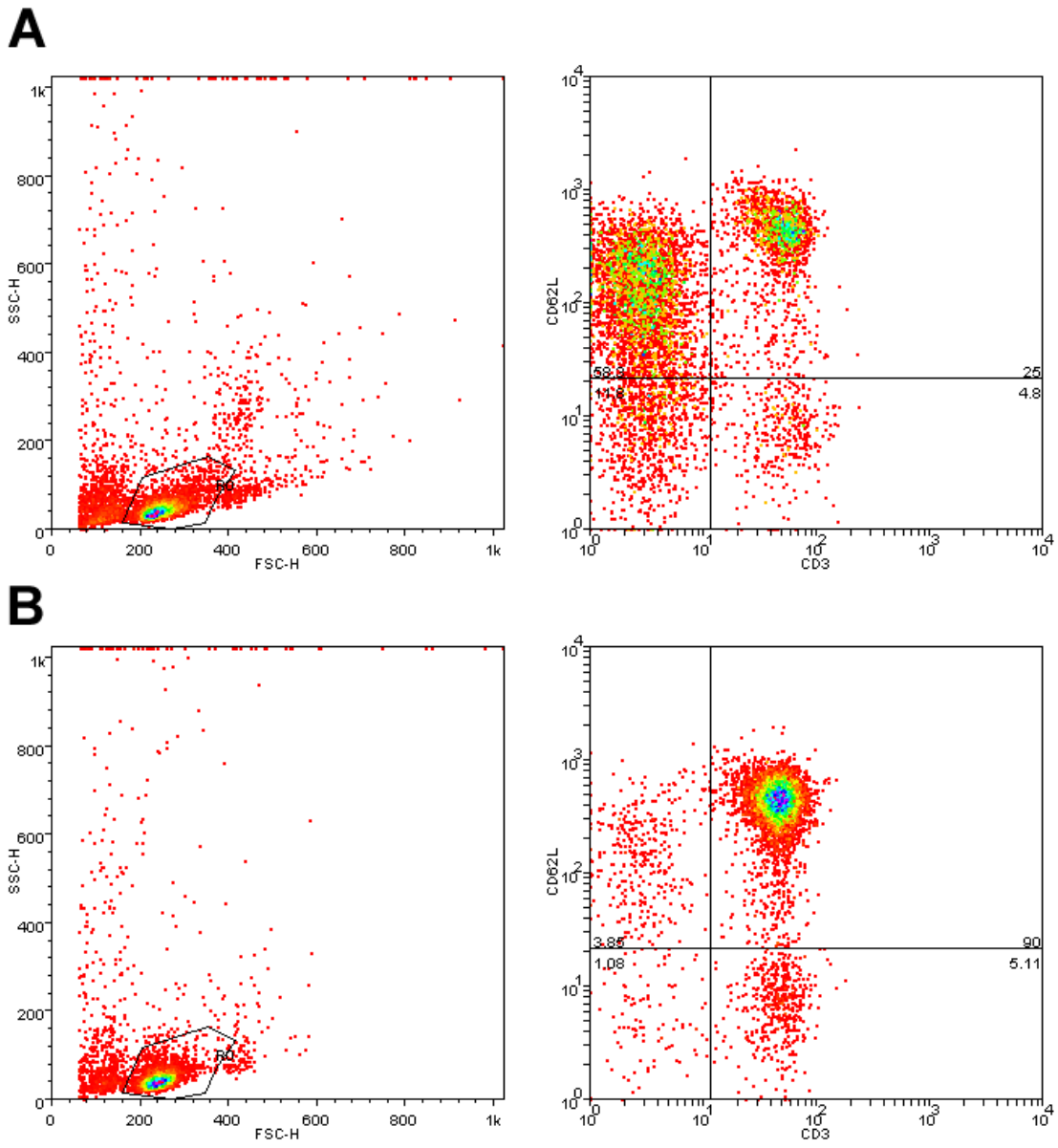

Figure 6.4 Validation of the CD3 CD62L naive T-cell isolation method. Non-separated (A) and separated (B) splenocyte suspensions were examined by flow cytometry and events were gated by side scatter (SSC-H) and forward scatter (FSC-H) for live lymphocytes (gate labelled R0 in the scatter plots). Cells were labelled with fluorescent antibodies for CD3 and CD62L. Double positive cells, considered to be naive T-cells, lie within the upper right quadrant of the CD3/62L dot plots.

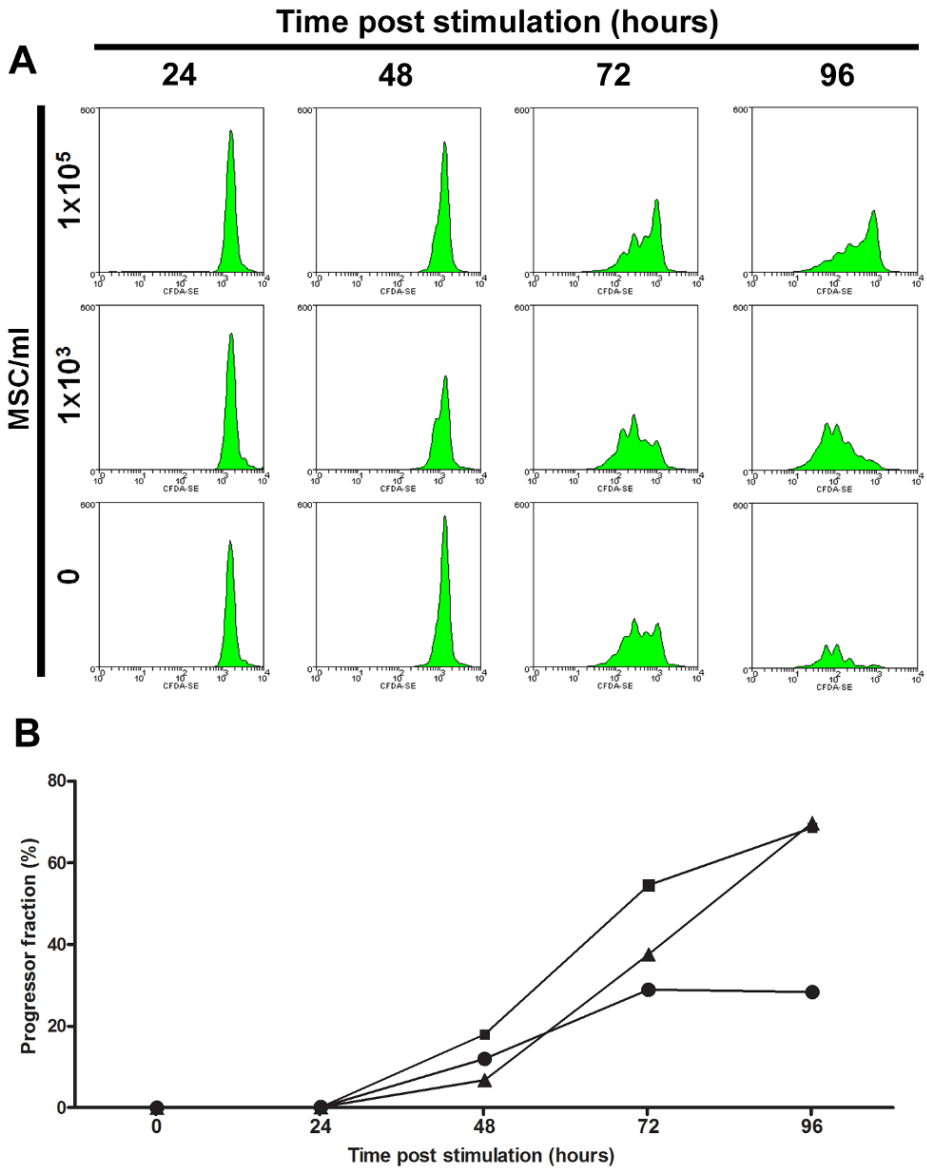

Figure 6.5 Characterisation of murine MSC immunomodulation of allogeneic splenocyte proliferation by CFSE assay. A) CFSE curves for naive T-cells stimulated with αCD3, IL-2 and αCD28 in co-culture with MSC at 1×10^5 and 1×10^3 cells/ml or without MSC. A peak representing cells in division 0 is visible at the 24 hour time point for all three treatments. Peaks appearing to the left of this peak in later time points represented cell populations in division 1 and above. B) The progressor fraction (determined as described in Chapter 2) was compared in all three cultures (1×10^5 MSC/ml co-culture, circular points; 1×10^3 MSC/ml co-culture, square points; stimulated T-cells alone, triangular points) at 24 hours, 72 hours and 96 hours.

6.4.1 MSC reduced the mitogen-stimulated naive T-cell progressor fraction

Lymphocyte proliferation can be modulated by changes to the percentage of cells which enter into a first cell division from the resting state during the course of an experiment- a feature of lymphocyte proliferation models termed the progressor fraction (Chapter 2.3.2). Progressor fractions for the naive T-cells incubated with MSC (1×10^5 MSC/ml) at 24, 48, 72 and 96 hours were compared to those of stimulated naive T-cells alone (Figure 6.5 B). When MSC were co-incubated, the naive T-cell progressor fraction (0.19% of starting cell population) was only marginally higher than stimulated controls without MSC (0.15%) at 24 hours. By 48 hours, the MSC co-incubated T-cell progressor fraction had risen to 12.16% whilst those of stimulated controls were 6.8%. However, by 72 hours the progressor fraction of the MSC co-incubated cells (28.93%) was less than that of the stimulated, MSC-negative controls (37.59%). By 96 hours the progressor fraction in the stimulated controls (69.75%) had risen to more than double that of MSC co-incubated cells (28.34%). These results indicated that modulation of progressor fraction was an important feature of the immunosuppressive capacity of MSC.

Table 6.1 Immunomodulatory effects of MSC on naive T cells

MSC conc. (MSC/ml)	Progressor faction at 96 hours (%)	Mean time to first division (hours)	Mean subsequent division time (hours)
100000	28.34	71.85	82.99
5000	68.62	63.60	41.10
0	69.75	63.75	41.40

6.4.2 MSC concentrations below a threshold enhanced the mitogen-stimulated naive T-cell progressor fraction

Naive mouse T-cells stimulated with αCD3e and IL-2 were co-incubated with allogeneic MSC at a concentration (5×10^3 MSC/ml) previously demonstrated to enhance mitogen-stimulated T-cell proliferation (Figure 6.3 B). At the 48 hour and 72 hour time points, the progressor fraction for these MSC co-incubated T-cells was higher than those of either the stimulated controls or the T-cells co-incubated with 1×10^5 MSC/ml (Figure 6.5 B). By 96 hours the stimulated control progressor fraction (69.75%) and the low concentration MSC co-incubated T-cell progressor fraction (68.62%) were comparable. Thus MSC concentrations below a threshold of 5×10^3 MSC/ml enhance the mitogen-stimulated naive T-cell progressor fraction

6.4.3 MSC delayed naive T-cell entry to first division

Lymphocyte proliferation may be modulated by changes to the mean time to first division following stimulation. A shortened mean time to first division will tend to enhance proliferation within a given time frame, whilst delay to first division will reduce gross proliferation. The mean times to first division were therefore calculated (Chapter 2.3.2) for naive T-cells stimulated with αCD3e and IL-2 alone or co-incubated with MSC at 5×10^3 cells/ml or MSC at 1×10^5 cells/ml (Table 6.1). The mean time to first division was comparable between the stimulated controls (63.8 hours) and the naive T-cells co-incubated with a low dose of MSC (63.6 hours). Thus it seems that the

stimulatory effect driven by low doses of allogeneic MSC is not related to changes in time to first division. However, naive T-cells co-incubated with the higher dose of MSC showed a delay in entering first division with a mean time of 71.8 hours. Along with progressor fraction, it seems likely that delays to mean time to first division contribute to the T-cell immunosuppressive behaviour of MSC.

6.4.4 MSC increased naive T-cell mean division time

The rate at which lymphocytes divide after first division also contributes to gross lymphocyte proliferation. A longer mean division time will reduce the number of lymphocytes generated by mitosis per unit time. Mean division times were comparable between mitogen stimulated naive T-cells in the absence (41.4 hours) or co-incubated with low dose of MSC (41.1 hours) (Table 6.1). The stimulatory effect driven by low doses of allogeneic MSC was thus not related to changes in mean division time. However, the naive T-cells co-incubated with the higher dose of MSC did show an increased mean division time (83.0 hours). Thus the immunosuppressive behaviour of MSC on naive mitogen stimulated T-cells was mediated by modulation of mean division time, progressor fraction and mean time to first division.

6.5 MSC ARE REFRACTORY TO TRANSDUCTION BY AAV-2 *GFP*

Evidence of successful transduction was also examined by flow cytometry. A human embryonic kidney cell line (HEK 293) was used as a positive transduction control. HEK 293 cells are permissive to AAV-2 transduction. Transduction of these cells (Chapter 2.2.6.1) with an AAV-2*GFP* vector at two different doses (4×10^7 drp/ml and 1.3×10^8 drp/ml) for 24 hours resulted in GFP expression detectable as an increase in mean fluorescence intensity (MFI) on FL1 compared with non-transduced HEK 293 (Figure 6.6). This approach was also adopted for murine MSC. BALB/c MSC were incubated with AAV-2*GFP* at two doses (4×10^7 drp/ml and 1.3×10^8 drp/ml) for 24 hours. Despite noticeable differences in scatter characteristics between MSC and HEK 293 cells (Figure 6.6), the auto fluorescence for non-transduced cells was comparable for both cell populations. Despite incubation with identical doses of AAV-2*GFP* for HEK 293 transduction, no increase in fluorescence could be detected for murine MSC. Although work in human and rat MSC has suggested that higher doses of AAV-2 might induce some GFP production (McMahon *et al.*, 2006; Stender *et al.*, 2007), limited stocks of the virus made testing this approach in our model impractical. Thus in order to further explore the effects of gene delivery on MSC, an alternative approach was required.

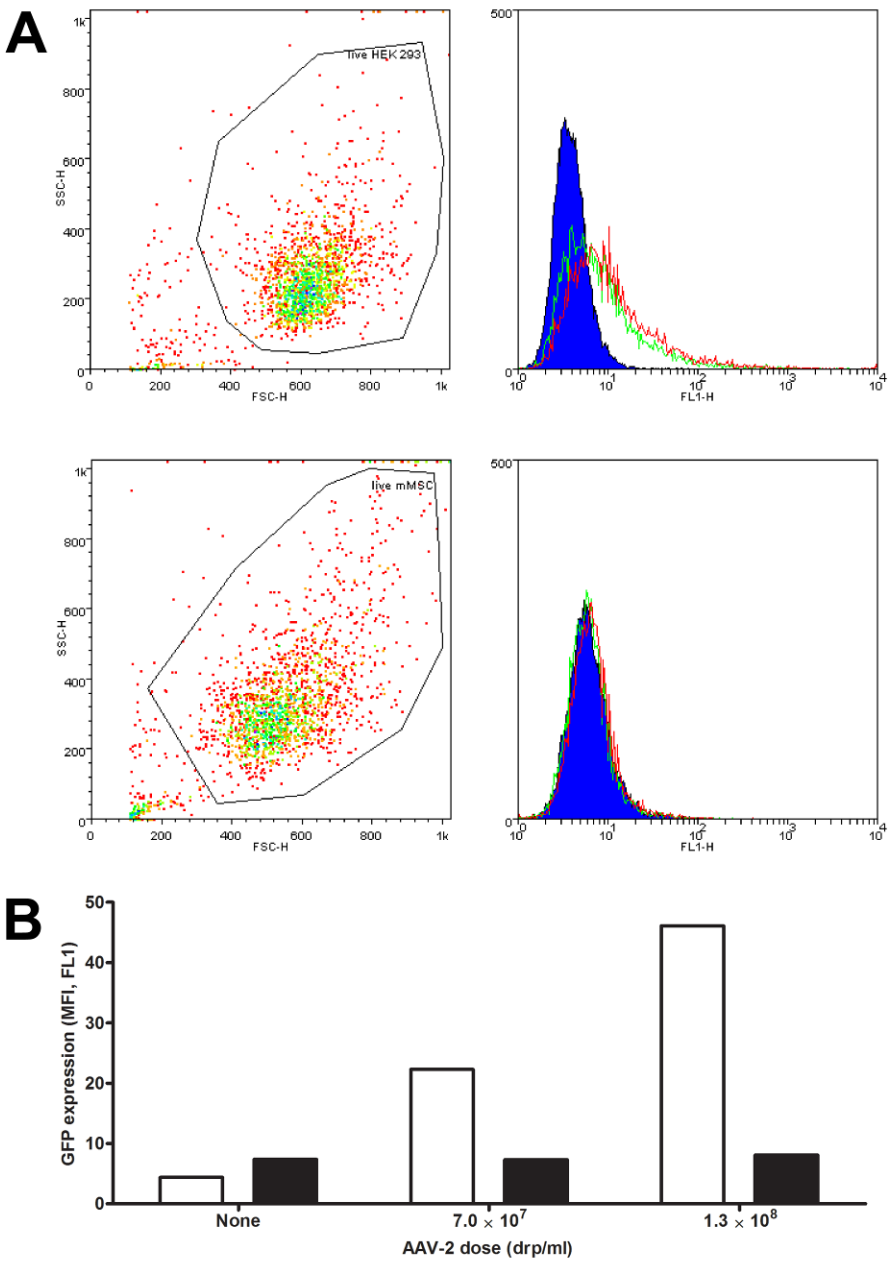

Figure 6.6 Transduction of murine MSC with an AAV-2-based vector containing a *GFP* reporter gene. A) Examination of AAV-2 permissive HEK-293 cells and murine MSC following incubation with 7×10^7 and 1.3×10^8 drp/ml of AAV-2*GFP*. Background autofluorescence (blue), 7×10^7 drp/ml dose (green) and 1.3×10^8 drp/ml dose (red). B) Fluorescence (Mean fluorescence intensity, FL1) for MSC cultures (closed bars) was compared to control HEK-293 (open bars) following incubation with 7×10^7 and 1.3×10^8 drp/ml of AAV-2*GFP*. Results are representative of two independent experiments.

6.6 MSC CAN BE TRANSFECTED WITH IDO BY LIPOFECTION

Since transduction of MSC with AAV was unsuccessful, it was decided to attempt direct transfection of the MSC using a plasmid via lipofection (Chapter 2.2.6.2). As *IDO* is a potentially useful gene for the enhancement of MSC immunomodulatory function, this gene was selected to be transfected into MSC under the control of a constitutively active promoter to assess the effects on MSC function and immunomodulatory characteristics. A pSport6CMV plasmid (Figure 2.2) encoding an IDO gene was complexed with a Lipofectamine 2000 vector and transfected into murine MSC (BALB/c). Successful transfection was assessed by RT-PCR for IDO RNA and western blot for IDO protein.

Examination of RNA isolated from transfected MSC by RT-PCR for IDO at 24 hours revealed elevated IDO transcription compared with non-transfected MSC (Figure 6.6 A). IDO expression diminished after 24 hours but remained above that of non-transfected cells until 7 days post transfection (Figure 6.7 A). Western blot analysis (Chapter 2.2.4.10) was conducted on transfected and non-transfected MSC cell lysates. IDO protein product was detected in transfected cell lysates at a greater level than non-transfected cells (Figure 6.7 B). However, similar IDO levels were found in lysates from mock transfected cells, suggesting that IDO might be induced by the lipofectamine complex. Nevertheless this work demonstrated that MSC could be transfected with immunomodulatory genes using a lipofection-based approach.

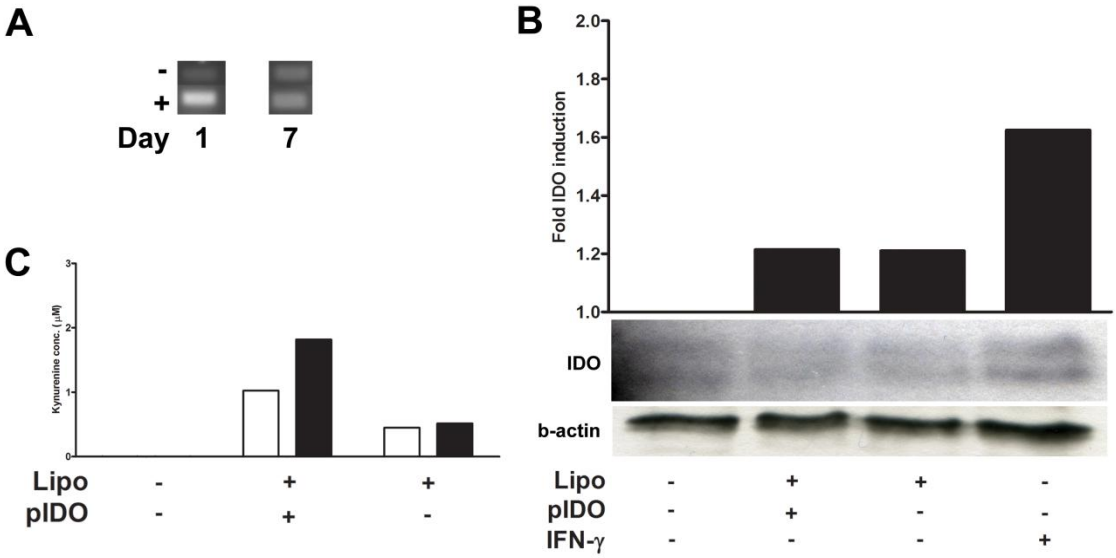

Figure 6.7 Transfection of murine MSC with an IDO plasmid by lipofection. Murine MSC were transfected as described in Chapter 2.2.6.2. A) RNA for IDO was detected by semi-quantitative RT-PCR in transfected (+) MSC at day 1 and was still detectable but reduced at day 7. B) IDO protein upregulation was detected in transfected and mock transfected MSC. C) IDO product kynurenine was detectable in supernatants from transfected and mock transfected cultures by HPLC. Supernatants were examined at 24 hours (open bars) and 48 hours (closed bars). Kynurenine levels increased in supernatants from transfected MSC cultures between 24 and 48 hours.

6.6.1 MSC transfected with the IDO transgene produced active IDO

IDO mediates its immunosuppressive effects by catalysing the metabolism of tryptophan into kynurenine. Thus kynurenine concentration may be used as a surrogate measure of IDO activity. The resulting tryptophan-depleted microenvironment inhibits microbial growth as well as suppressing T-cell proliferation (Meisel *et al.*, 2004; Mellor & Munn, 2001). It is also thought that the kynurenine by-product may itself be an active immunomodulatory soluble factor (Frumento *et al.*, 2002). To determine whether transfection of MSC with IDO produced a functional IDO product, samples of supernatant from IDO-transfected, mock transfected and non-transfected MSC cultures were examined for the presence of kynurenine by HPLC (Chapter 2.2.5.6). Despite an inability to detect differences in IDO levels between transfected and mock transfected cells, IDO activity was higher in transfected cells (Figure 6.7 C). Kynurenine levels in supernatants from IDO transfected MSC were 1.0 µM at 24 hours post transfection and 1.8 µM at 48 hours post transfection. Mock transfection, which was previously shown to induce some IDO upregulation, also resulted in some kynurenine production, but levels had not increased above 0.5µM by 48 hours post transfection. Although western blot results were ambiguous, PCR results and increased IDO activity as determined by HPLC indicated that the MSC had been successfully transfected with the IDO plasmid. A limitation of the methods employed herein to assess transfection is that the proportion of cells transfected in culture could not be determined. Thus, transfection efficiency and the impact of outgrowth from any non-transfected cells were unknown.

6.6.2 Transfection of MSC with IDO did not alter cell morphology

Based on findings in the rat (McMahon *et al.*, 2006), it was considered possible that transfection of murine MSC using a liposomal system might have profound influences on therapeutically beneficial cell behaviour including modulation of cell survival, changes to morphology and surface marker expression and potentially impacting on *in vitro* potency, immunomodulatory function and cell growth rates. Therefore, transfected MSC and non-transfected MSC were compared and examined for changes to these features. Murine MSC (BALB/c), transfected and expressing IDO as previously described (Chapter 2.2.6.2), were examined to assess whether cell morphology was altered by the transfection protocol. This was done over four culture passages. Cells were directly imaged by light microscopy. Transfected cell morphology did not change during the course of the culture period (18 days for non-transfected MSC and 22 days for transfected MSC) and was not different to morphology of non-transfected MSC cultured under the same conditions (Figure 6.8). It was noted during culture that the IDO transfected MSC grew slower than the non-transfected cells, with the non-transfected cells being split four times in 18 days whilst the transfected cells took 22 days.

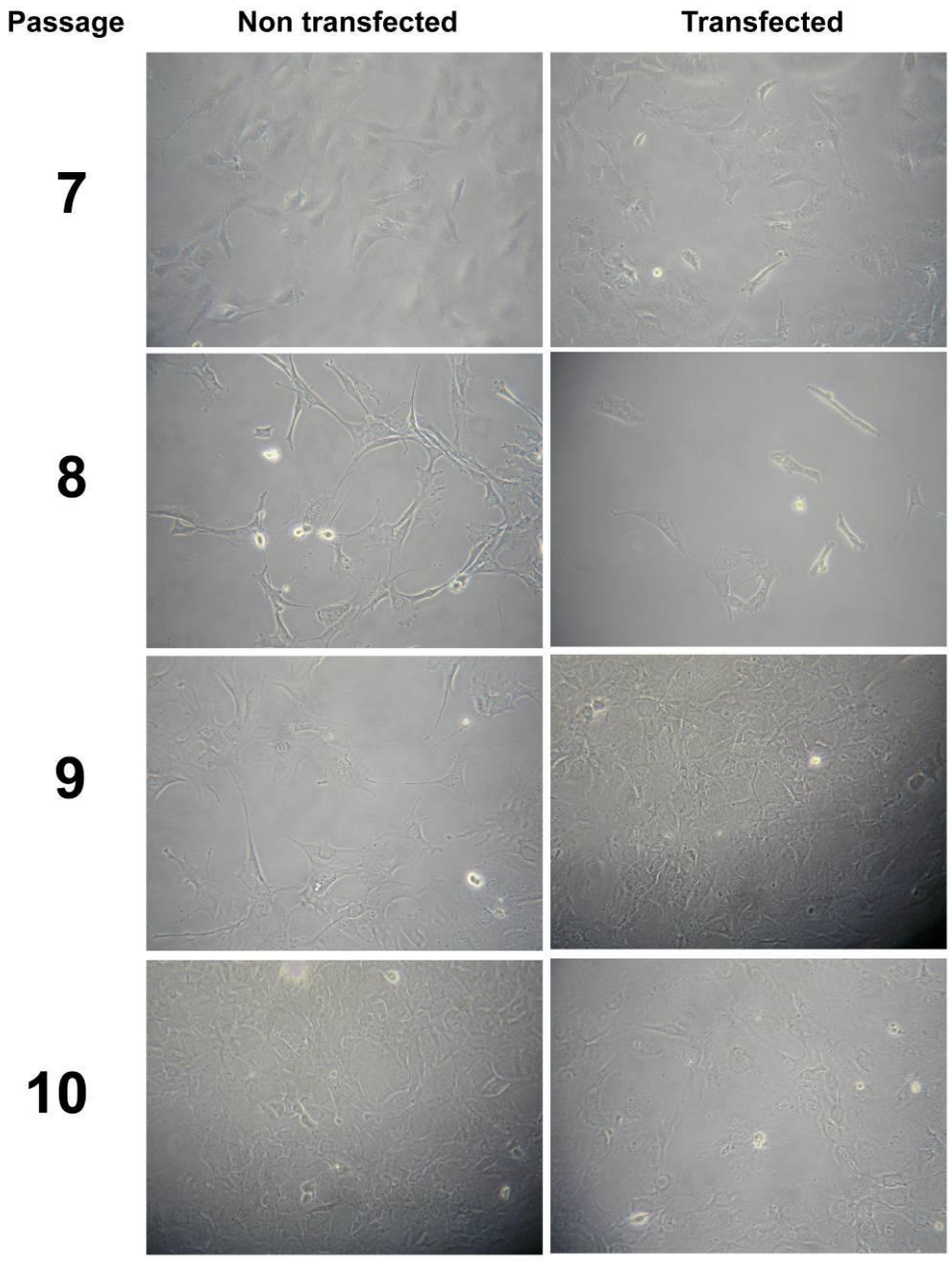

Figure 6.8 Examination of MSC morphology following transfection with an IDO plasmid by lipofection. Non-transfected and transfected cells were seeded into T-25 flasks and subcultured four times (passages 7 – 10). Cultures were examined by light microscopy at 200x magnification.

6.6.3 Transduction with IDO modulated MSC growth rates and cell survival

The extended passage time observed in IDO transfected MSC suggested that the transfection process might be impacting negatively on MSC growth rates in culture. MSC, transfected MSC, mock transfected MSC or IFN-γ stimulated MSC were cultured and MSC growth rates were measured by performing viable cell counts with ethidium bromide and acridine orange (EB/AO) at 24 hour intervals. Non-transfected MSC grew continuously in culture from 24 to 168 hours whilst IFN-γ stimulated, transfected and mock transfected MSC cell numbers declined between 24 and 72 hours (Figure 6.9). At 72 hours IFN-γ stimulated and mock transfected cell numbers were comparable, but transfected MSC numbers were significantly lower ($p \leq 0.05$) than non-transfected, mock transfected and IFN-γ stimulated MSC. Mock transfected and IFN-γ stimulated MSC cell numbers recovered from 72-96 hours and were comparable to non-transfected MSC numbers from 120 hours onwards. Although transfected MSC cell numbers began to recover after 72 hours, growth was poor and had not risen above the initial seeding density by 168 hours post transfection. Overall growth rates were determined performing a linear regression on each growth curve and finding the slope of the line. Non-transfected MSC had a growth rate of 360.9 ±45.67 cells/hour. Mock transfected and IFN-γ stimulated MSC growth rates were elevated to 449.9 ±87.10 and 494.5 ±84.03 cells/hour, respectively. The transfected MSC growth rate was a net negative rate (-8.267 ±75.79 cells/hour), despite a slow recovery after 24 hours. Therefore it can be concluded that mock lipofection negatively impacts on cell survival and growth rate, although the effect was transient. However lipofection with the IDO plasmid reduced the cell population in culture and reduced cell growth rate so significantly that it did not

recover within 7 days post transfection. These findings cast doubt over the usefulness of lipofection for the transfection of murine MSC and also highlight a possible issue with the selected IDO plasmid.

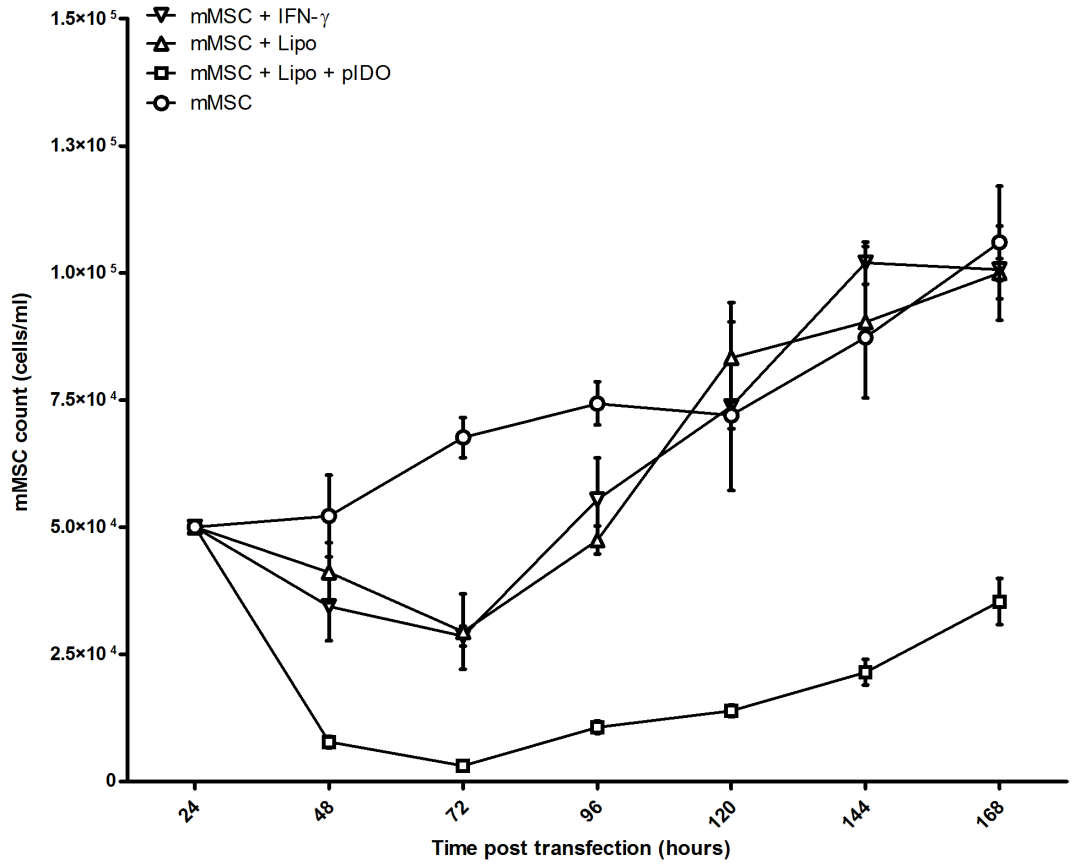

Figure 6.9 Cell survival and growth rate of lipofected murine MSC. Non-transfected, IDO transfected, mock-transfected and IFN-γ stimulated MSC (see figure key) were cultured and cell counts were performed every 24 hours for 7 days. Points (see key above) represent the mean of triplicate cell counts. Error bars represent the standard deviation. Results are representative of two independent experiments.

6.6.4 Transfection of MSC with IDO did not ablate MSC adipogenic or osteogenic differentiation capacity

MSC have the capacity to differentiate into tissue cells of the mesenchymal lineage including fat and bone, a feature which may have utility in a therapeutic setting (Pittenger *et al.*, 1999). This differentiation can be induced *in vitro* using growth medium supplemented with the appropriate growth factors. To assess whether transfection with a therapeutic transgene can abrogate MSC differentiation capacity *in vitro*, IDO transfected and non-transfected MSC were induced to differentiate along the adipogenic and osteogenic pathways, then stained and examined by light microscopy after 21 days in culture (Chapter 2.1.4.3 and 2.1.4.4).

Both transfected and non-transfected MSC were capable of adipogenesis (Figure 6.10) and osteogenesis (Figure 6.11). Although these results show that potency is not eliminated by the transfection protocol, it would nonetheless be valuable in future work to quantify any differences in plastic capacity. One drawback in the design of these experiments was the lack of a means to individually quantify potency in transfected cells. Thus in future studies it would be important to ascertain whether differentiating cells in transfected cultures represented outgrowth of a non-transfected subpopulation.

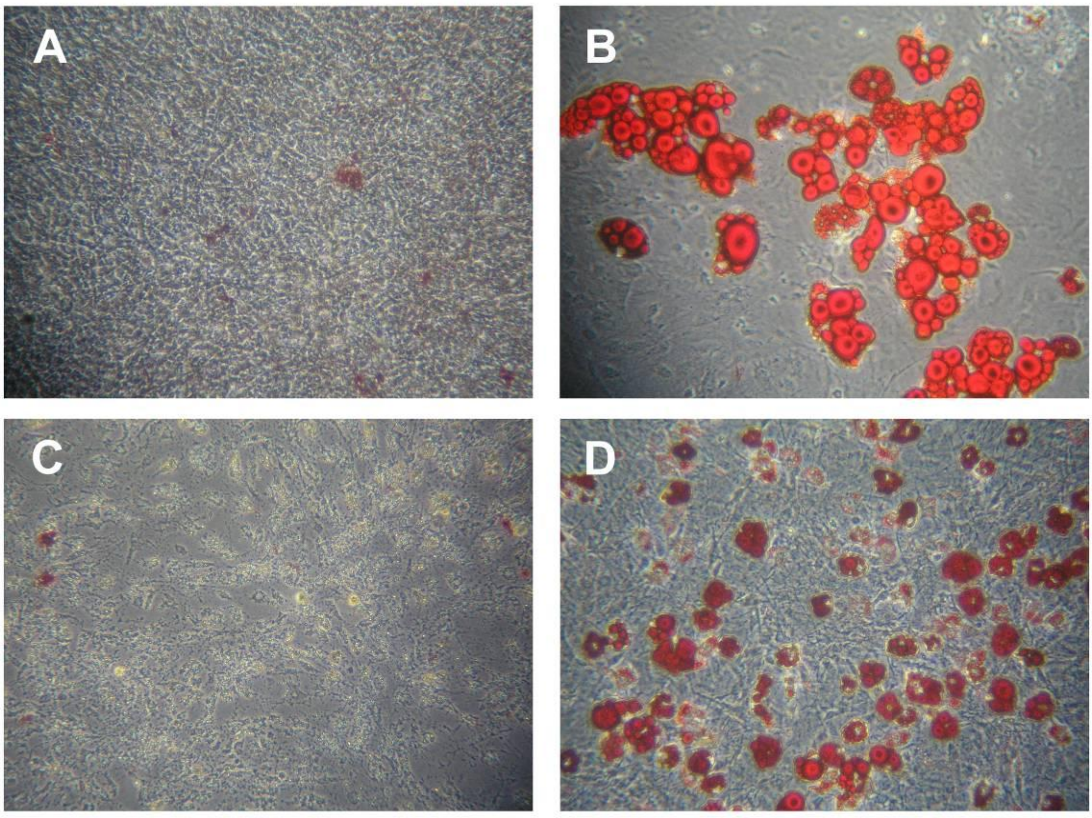

Figure 6.10 IDO transfected murine MSC cultures retain adipogenic potency *in vitro*. A) non-transfected MSC cultured in growth medium showed no evidence of adipogenesis when stained with Oil Red O, whilst B) non transfected control MSC cultured in adipogenesis medium for 21 days showed distinctive red-stained adipocytes. Similar results were observed for C) IDO transfected MSC cultured in growth medium and D) IDO transfected MSC cultured in adipogenesis medium. Cells were imaged by light microscopy at 200x magnification. Results are representative of two independent experiments.

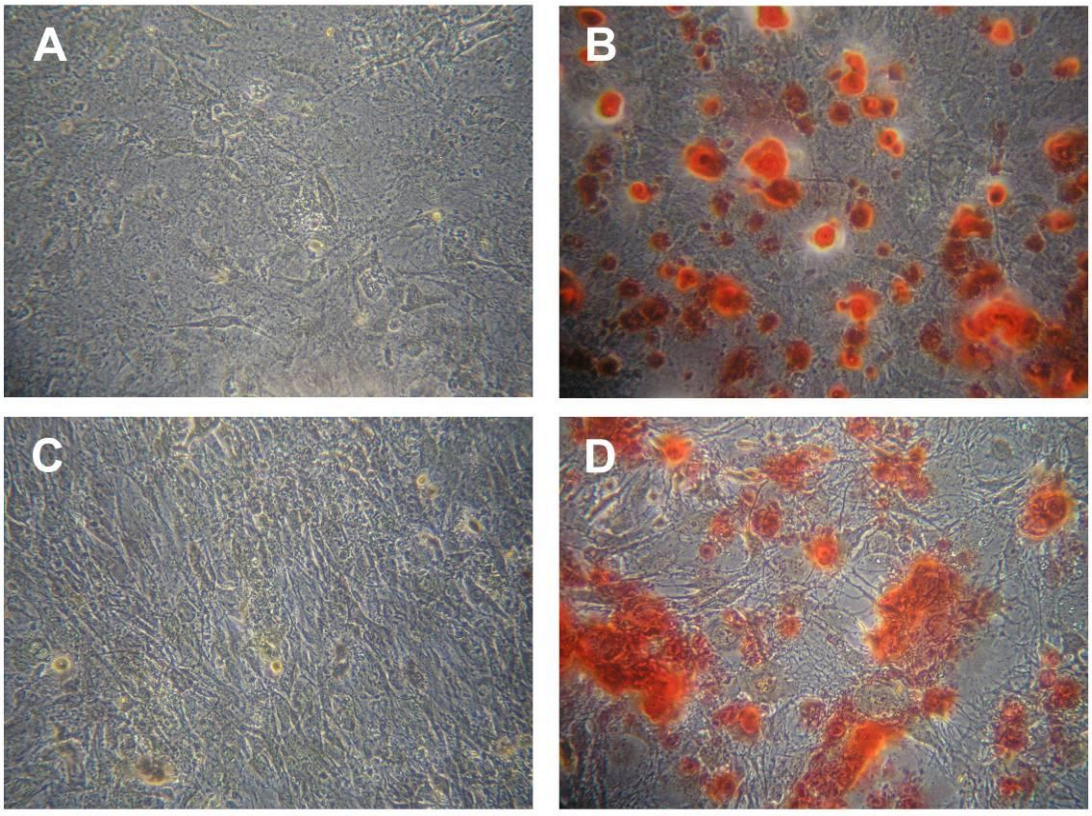

Figure 6.11 IDO transfected murine MSC cultures retain osteogenic potency *in vitro*. A) non-transfected MSC cultured in growth medium showed no evidence of osteogenesis when stained with Alizarin Red S, whilst B) non-transfected control MSC cultured in osteogenesis medium for 21 days showed distinctive red-stained osteocytes and red-stained solid deposits. Similar results were observed for C) IDO transfected MSC cultured in regular growth medium and D) IDO transfected MSC cultured in osteogenic medium. Cells were imaged by light microscopy at 200x magnification. Results are representative of two independent experiments.

6.6.5 Lipofection with IDO alters MSC cell surface marker expression

The MSC used in this study were characterised as MHC class I weak, Sca-1 positive but MHC class II and negative for the hematopoietic stem cell marker CD90 (Figure 6.1). MHC class I and II are the main mediators of antigen presentation to T-cells and the weak expression of MHC class I, coupled with the lack of class II is thought to contribute to MSC alloevasion (Barry *et al.*, 2005; Le Blanc *et al.*, 2003). Although MSC transfection by IDO plasmid did not change cell morphology or potency (Figure 6.8), cell survival and growth rate were reduced. Non-transfected, transfected, mock transfected and IFN-γ MSC were examined by flow cytometry to assess whether cell surface marker expression was also modulated. Forward and side scatter characteristics were not altered by mock-transfection or IFN-γ stimulation, nor were Sca-1 or CD90 expression (Figure 6.12). Transfection appeared to alter forward and side scatter, resulting in a more morphologically heterogeneous population. Sca-1 and CD90 expression remained unchanged for transfected cells. MHC class I was upregulated relative to isotype controls on transfected, mock-transfected and IFN-γ stimulated MSC (MFI, 24.5, 24.0 and 27.1 for non-transfected, mock-transfected and IFN-γ stimulated MSC respectively). However MHC I was more strongly increased on transfected MSC (MFI = 113.7) (Figure 6.13), indicating that transfection induced MHC I. Likewise MHC class II was at background for non-transfected, mock-transfected and IFN-γ stimulated MSC (47.5, 13.3 and 8.9 respectively) (Figure 6.13) but increased in transfected MSC (MFI = 94.7). This increased MHC class II expression is nonetheless modest when compared to that seen on professional antigen presenting cells such as DC (English *et al.*, 2008). These findings suggest that the IDO lipofection protocol, but not

mock transfection, may be inducing innate immune pathways in the murine MSC and may diminish their alloevasive capabilities.

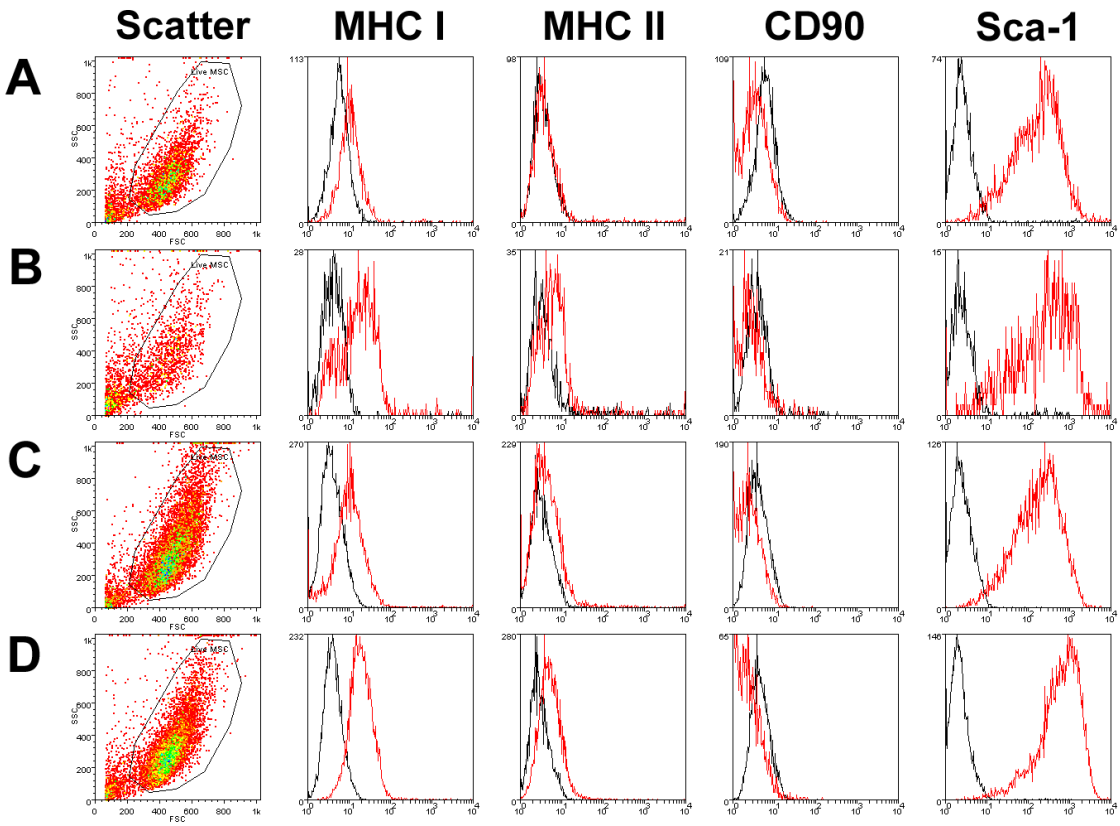

Figure 6.12 Analysis of surface marker expression on non-transfected (A), IDO transfected (B), mock-transfected (C) and IFN-γ stimulated MSC (D) by flow cytometry. MSC were labelled with monoclonal antibodies specific for MHC class I, class II, CD90 or Sca-1 (red lines). Binding of species-matched isotype controls (black lines) is indicated in each histogram. Histograms represent results for the gated populations indicated in the forward and side scatter dot plots.

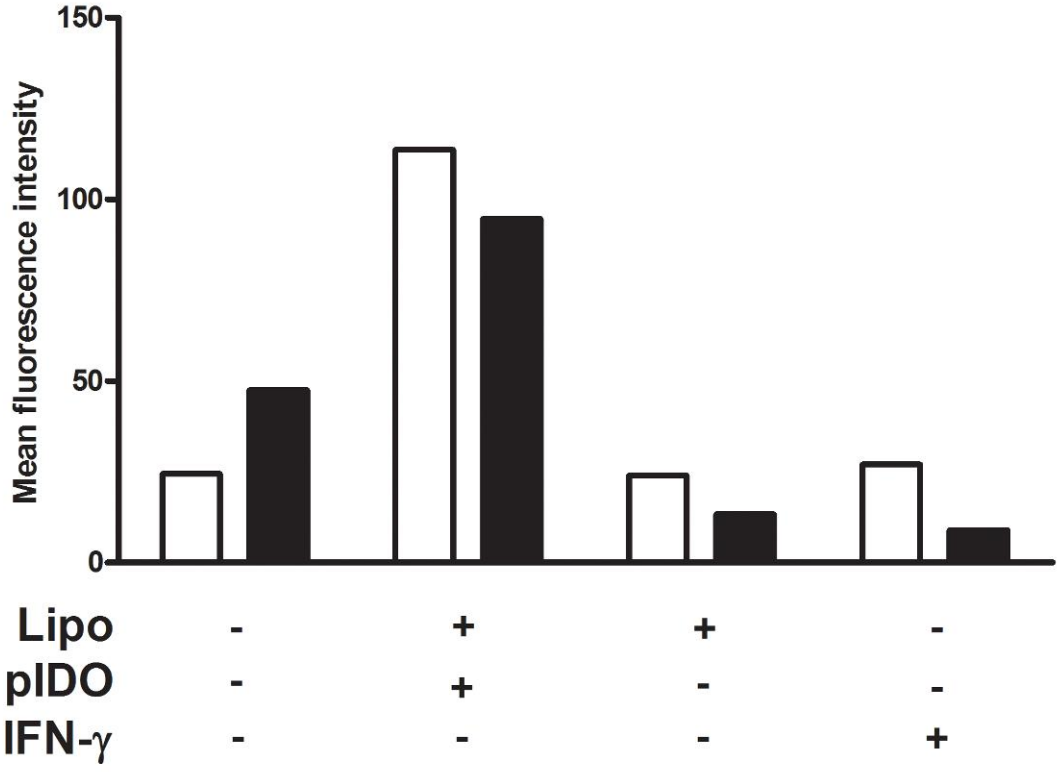

Figure 6.13 Analysis of MHC class I and class II cell surface expression on non-transfected, IDO transfected, mock-transfected or IFN-γ stimulated MSC by flow cytometry. Fluorescence of MHC class I (open bars) or MHC class II (closed bars) was compared for non-transfected, IDO transfected, mock-transfected or IFN-γ stimulated MSC. MFI values were derived from the histograms in figure 6.11 and are based on the acquisition of at least 2000 events in each case.

6.6.6 Transfection of MSC with IDO did not enhance but reduced suppression of mitogen-stimulated lymphocytes

IDO was selected as a therapeutic transgene in this study in order to enhance MSC immunosuppressive activity. Suppression of mitogen-stimulated lymphocyte proliferation by MSC was assessed by tritiated thymidine incorporation assay (Chapter 2.2.5.2). Non-transfected, IDO transfected, mock-transfected and IFN-γ stimulated MSC each at concentrations 1×10^4, 1×10^3 and 1×10^2 cells/ml were co-cultured with MHC matched splenocytes (Figure 6.14). ConA stimulated splenocytes alone produced a proliferation result of 20582 ±1123.5 CPM. 1×10^4 non-transfected MSC/ml significantly ($p \leq 0.005$) suppressed mitogen driven splenocyte proliferation (1159.6 ±557.6 CPM) to near background levels (unstimulated splenocytes alone; 371 ±47.8 CPM), and the same concentration of IFN-γ stimulated MSC produced even stronger suppression (536 ±264 CPM). The same dose of mock transfected MSC also suppressed splenocyte proliferation, but did so to a lesser degree (5547 ±4058 CPM) and with weaker statistical significance ($p \leq 0.05$). The IDO transfected cells were expected to produce enhanced suppression relative to non-transfected MSC but at the highest MSC concentration, proliferation was only slightly reduced (13,211 ±48) and the reduction was not statistically significant ($p = 0.051$). Suppression of proliferation was dose-dependent for all four MSC types, but at each concentration tested, IDO transfected MSC produced the weakest suppression, and suppression was not statistically significant at any concentration of transfected MSC. Although increased IDO activity in transfected cultures had been confirmed by HPLC, these findings suggested that this increase was not sufficient to enhance MSC immunomodulation. On the contrary, it

appeared that some side effect of the transfection protocol was reducing the immunomodulatory function.

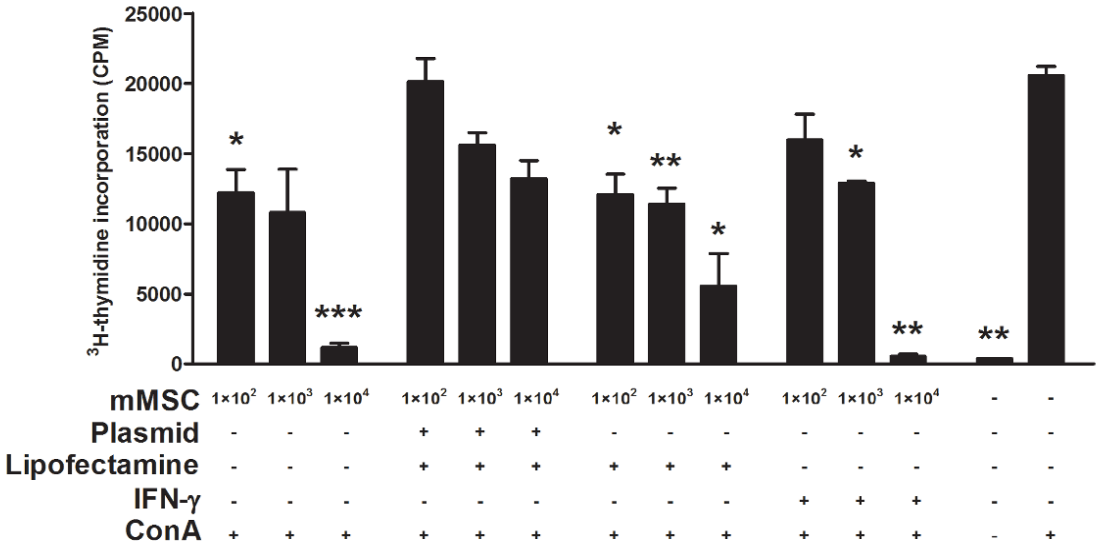

Figure 6.14 Analysis of the immunomodulatory capacity of lipofected MSC. Non-transfected, IDO transfected, mock-transfected or IFN-γ stimulated MSC were co cultured with ConA stimulated, MHC matched murine splenocytes. Statistically significant suppression of splenocyte proliferation is indicated (*, $p \leq 0.05$; **, $p \leq 0.005$; ***, $p \leq 0.0005$). Bars represent the mean of triplicate determinations expressed as CPM. Error bars represent the standard error mean. Results are representative of at least two independent experiments.

6.7 SUMMARY

The MSC used in this study were characterised and found to display spindle-like fibroblastic characteristics, were MHC class I and Sca-1 positive and MHC class II and CD90 negative (Figure 6.1). Potency was validated by differentiation assays for adipogenesis and osteogenesis (Figure 6.2). MSC immunomodulation was verified by co-incubation of MSC with mitogen-stimulated splenocytes (Figure 6.3). MHC mismatched MSC also suppressed splenocyte proliferation at high MSC concentrations, but synergised with mitogen at low doses (Figure 6.3). Suppression and stimulation of mismatched splenocyte proliferation by MSC was further examined using a CFSE-based assay, using a purified population of $CD4^+$ $CD62L^+$ naive T-cells. Suppression involved reductions in the progressor fraction as well as lengthening of both mean time to first division and subsequent mean division times (Figure 6.5; Table 6.1). The stimulatory effect previously observed may in part be explained by higher progressor fractions in the low MSC dose co-cultures at the 48 and 72 hour time points.

MSC are desirable targets for modification using gene therapy and may facilitate the delivery of transgenes for cancer therapy (Mohr *et al.*, 2008). Transduction of murine MSC using an AAV-2-based vector and lipofection was thus attempted and the MSC were examined for changes to their other therapeutic characteristics. Murine MSC were refractory to transduction using an AAV-2 vector (Figure 6.6). Lipofection successfully delivered an IDO transgene (Figure 6.7) without impacting on MSC morphology or potency (Figures 6.8, 6.10 and 6.11). However, IDO protein upregulation was modest (Figure 6.7). Interestingly MSC survival and growth rate was

reduced (Figure 6.9) suggesting that IDO activity impairs MSC function or places a metabolic burden on the cells. Transfection of MSC induced upregulation of surface-expressed MHC class I and class II. More importantly transfection of MSC with IDO (but not mock transfection) did not enhance but rather reduced suppression of mitogen-stimulated lymphocyte proliferation (Figure 6.14). Suppression of proliferation was dose-dependent for all MSC types, but IDO transfected MSC produced weaker suppression than non-transfected and mock transfected MSC at all MSC concentrations tested, and the suppression mediated was not statistically significant at any concentration of transfected MSC. These data suggest that delivery of IDO to murine MSC by lipofection must undergo substantial optimisation if it is to become effective without abrogating desirable characteristics of the target MSC.

CHAPTER 7

DISCUSSION

The paucity of data available on immune responses to AAV-2 at the study outset raised the possibility that adaptive immunological responses were not important and that pre-existing immunity would not confound clinical use of AAV-2 as a therapeutic vector (Erles *et al.*, 1999; Hernandez *et al.*, 1999). This study, and the work of others has disproved that hypothesis (Manno *et al.*, 2006; Murphy *et al.*, 2009). Specifically, the loss of AAV-2-mediated transgene expression during clinical trials has indicated that memory for AAV-2 includes a cytotoxic T lymphocyte (CTL) response against transduced cells (Manno *et al.*, 2006). In this study, AAV-2-specific IgG was detected in plasma from 41 of 45 donors sampled (>90%). IgG1 and IgG2 were the predominant IgG subclasses present. IgG3 levels were limited and IgG4 was variable and often absent entirely.

Human T-cell proliferation in response to whole AAV-2 stimulation was demonstrated in nearly half (19 of 41) of PBMC cultures isolated from a panel of Irish blood donors. The cytokine profiles associated with these responses were diverse, but IFN-γ and IL-13 production were detected indicating that an effector $CD4^+$ Th recall response is evoked in humans. 59 candidate T-cell epitopes were identified within the VP1 capsid sequence. Although a subset (n = 17) of these epitopes were recognized by PBMC from multiple donors, there was no significant correlation between stimulating epitope and respondent donor HLA haplotype, suggesting that these represent immunodominant epitopes promiscuously recognized.

Humoral memory was extensively examined in this project. A majority of Irish donors (41 of 45 donors) tested displayed significant titres of AAV-2-specific IgG in

blood plasma. This represents a high prevalence when compared to AAV-2 seroprevalence data obtained in other European studies but is similar to that seen in US populations (Chirmule *et al.*, 1999; Erles *et al.*, 1999; Halbert *et al.*, 2006). However, as no AAV-2-specific IgG standards exist and there is no standardized method for assaying AAV-2 antibody levels, it is likely that the high variability observed between studies is as much a result of differing methods as it is of geographical differences and population demographics. Despite these differences, the available evidence suggests that humoral memory for AAV-2 is prevalent.

The presence of antibodies to AAV-2 does not automatically imply neutralising activity (Erles *et al.*, 1999). To assess the prevalence of neutralising antibody in this study group, a model system was devised to measure the reduction in transformation of an AAV-2 permissive cell line. A panel of six AAV-2-specific IgG-seropositive plasma samples (from donors 17, 19, 21, 34, 42, 51) was co-incubated with an AAV-2 vector encoding a *GFP* gene under the control of a CMV promoter. Plasma from donor 51 reduced the MFI from 13.3 to 11.1 and plasma from donor 42 reduced the MFI to near background (5.8).

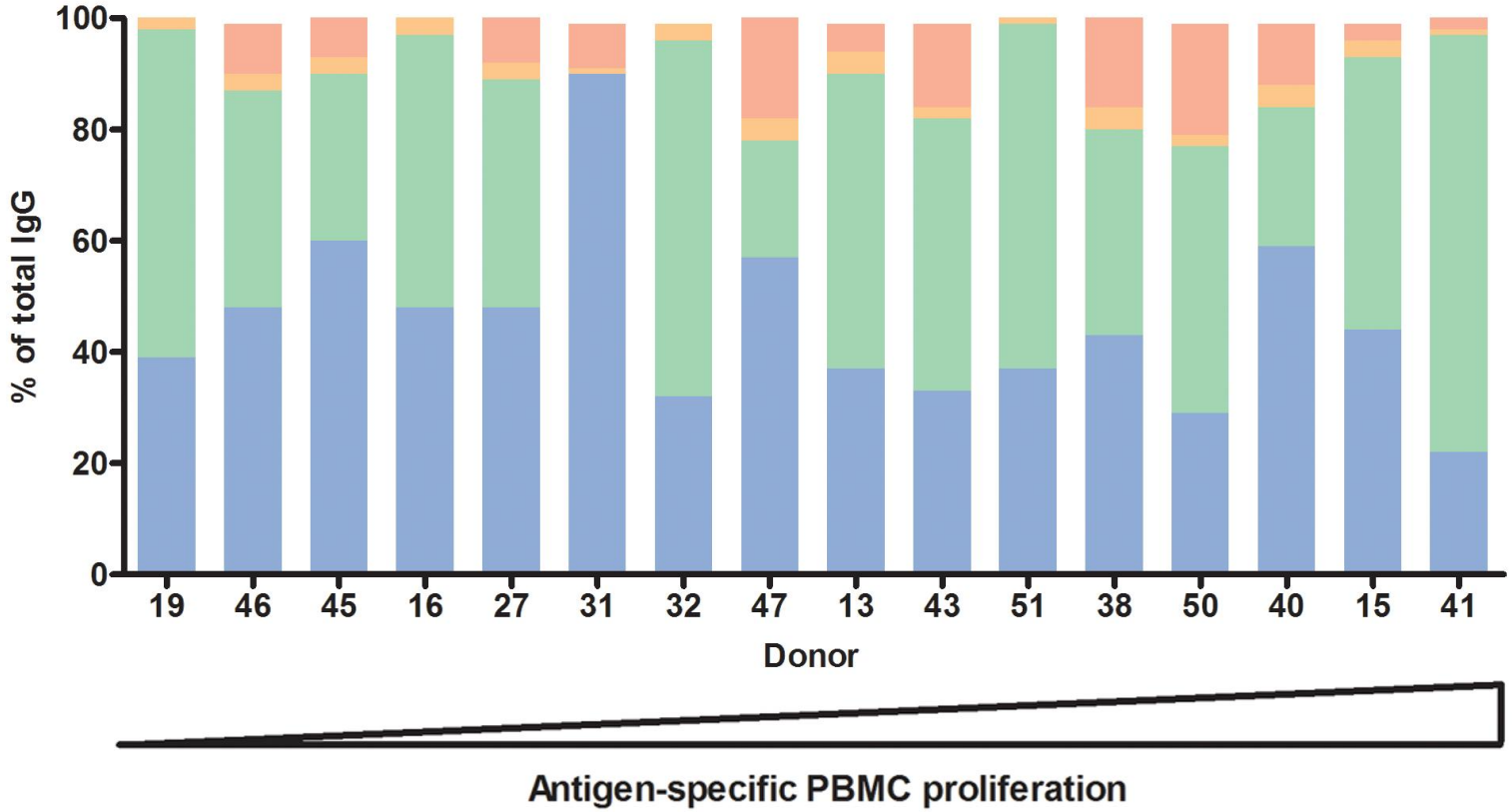

Figure 7.1 Subclass composition of AAV-2-specific IgG in plasma from donors with detectable cell-mediated memory for AAV-2. Proportions of each IgG subclass are represented as percentage of total IgG. IgG1 is indicated in blue, IgG2 is indicated in green, IgG3 is indicated in orange and IgG4 is indicated in red.

Whilst characterisation of total IgG and neutralising activity are informative, the subclass composition of an IgG response may vary greatly, impacting on factors such as APC activation, opsonisation and recruitment of complement (Jefferis & Kumararatne, 1990). AAV-2-specific IgG in this population consisted primarily of the IgG1 and IgG2 subclasses, with low levels of IgG3 present in all donors and some evidence of variable IgG4 in a smaller subset. The presence of IgG1 was anticipated as the subclass is commonly induced following viral infections such as measles, hepatitis B, HTLV-I and rubella. It is also induced by B19V which, like AAV-2 is a member of the Parvoviridae (Franssila *et al.*, 1996; Gregoreka *et al.*, 2000; Lal *et al.*, 1993; Thomas & Morgan-Capner, 1988; Toptygina *et al.*, 2005). IgG1 is typically the predominating IgG subclass for these afore-mentioned viruses, and this study shows this is the case for AAV-2, in which IgG1 is a major component of the total specific IgG (Figure 7.1).

IgG2 was also a major constituent of the AAV-2-specific antibody response, comprising an average 42% of total IgG. The proportions of AAV-2-specific IgG1 and IgG2 detected in this study broadly agree with data recently reported by Murphy *et al*. (Murphy *et al.*, 2009). Whilst IgG2 is a component of serological responses to some to measles and HTLV-I, it is notable that it is not a significant component of the response to the parvovirus B19V (Franssila *et al.*, 1996; Lal *et al.*, 1993; Toptygina *et al.*, 2005), a finding supported by the modest B19V-specific IgG2 levels detected during the optimisation of the IgG subclass ELISA. This suggests that there are differences between how the humoral response is primed by B19V and AAV-2, perhaps reflecting AAV requirement for a helper virus to disseminate.

The IgG3 subclass is usually a significant component of virus-induced IgG, typically comprising 12% to 50% of circulating virus antigen-specific IgG for measles, rubella, HTLV-1 and hepatitis B viruses in seropositive individuals (Gregoreka *et al.*, 2000; Kalvenes *et al.*, 1996; Lal *et al.*, 1993; Toptygina *et al.*, 2005). Although AAV-2-specific IgG3 was detected in all donors assayed, the subclass comprised an average of just 2.6% (0.7 ±0.2 μg/ml) of the total AAV-2-specific IgG detected in Irish donors (Figure 7.1). Given the robust humoral response induced by AAV-2, the minimal IgG3 induction is surprising but is supported by observation of similar levels in a recent US study (Murphy *et al.*, 2009). The average concentration of virus-specific IgG3 (0.6 μg/ml) observed in that study is comparable to our observations, although the IgG3 levels were considerably more variable, at times representing greater than 50% of total virus-specific IgG. IgG3 did not represent greater than 6% of total AAV-2-specific IgG in any donor examined here. The difference between the results reported by Murphy *et al.* and those reported here may reflect differences in population genetics, or in the prevalence and nature of various helper virus infections. It has been speculated that helper viruses may determine the anatomical locale in which AAV-2 is first recognized in a strong inflammatory context (Murphy *et al.*, 2009).

IgG3 is typically induced in $CD40^{+}$ naive B cells recognising antigen in the context of a similar cytokine environment to that seen in IgG1 induction (Briere *et al.*, 1994). Recognition of a soluble particulate antigen in the inductive immune sites of the upper respiratory tract typically produces a higher proportion of IgG3-producing B cells than does recognition in the circulation (Jefferis & Kumararatne, 1990). Given that the route of natural AAV-2 infection is typically cited as oral or upper respiratory tract,

AAV-2 should encounter the pharyngeal or palatine tonsils during inhalation or ingestion and thus induce IgG3 (Blacklow *et al.*, 1968a; Gould & Favorov, 2003; Rabinowitz & Samulski, 2000). Thus, the failure of AAV-2 to induce significant titres of IgG3 in any donor examined here is somewhat unexpected and remains to be explained. However it might be speculated that AAV-2 may have some capacity to evade or subvert strong IgG3 induction. Such subversion might represent a means of evading the complement cascade. This is supported by the observation that the classical complement pathway is only induced weakly by high titres of AAV-2 and the virus does not activate the alternative complement pathway (Zaiss *et al.*, 2008). It has been reported that the AAV-2 capsid binds complement protein iC3b and Factor H, both of which mediate a regulatory effect on the complement cascade by blocking the cleavage of C3 into C3a and C3b (Zaiss *et al.*, 2008). As IgG3 is the primary IgG subclass involved in C1 recruitment and thus the initiation of the classical complement pathway, the lack of IgG3 induction observed in this study may further explain the minimal involvement of the classical pathway in AAV-2 immunity observed by Zaiss *et al.* (Zaiss *et al.*, 2008). Similar to that seen in AAV-2, a minimal IgG3 response has been observed in the closely related parvovirus B19V. B19V virus-specific IgG3 levels are high in early infection but decline significantly over time (Franssila *et al.*, 1996). A similar pattern of decline over time is observed following hepatitis B vaccination (Gregoreka *et al.*, 2000). It is not possible to conclude that AAV-2 follows such a pattern without examining the sera of recently infected individuals, although given the nature of infection such a cohort will be difficult to identify.

Levels of AAV-2-specific IgG4 represented less than 10% on average of total IgG and were highly variable (2.5 ±3.8 µg/ml) with 12 of the 45 donors tested having no detectable IgG4. By comparison to the serology of other viruses, the variable IgG4 levels are perhaps unremarkable. Hepatitis B infection and vaccination typically induce little IgG4, but levels are seen to increase post infection or vaccination (Gregoreka *et al.*, 2000). Variable titres of IgG4 are also seen in B19V infection, and typically this is not observed until some 200 days post infection (Franssila *et al.*, 1996). IgG4 is also a feature of the humoral memory to some antigens of HTLV-I and measles (Lal *et al.*, 1993; Toptygina *et al.*, 2005). If the temporal characteristics of AAV-2 humoral memory mirror those of parvovirus B19V, the minimal IgG3 and elevated IgG4 levels detected here may be representative of late convalescent AAV-2 infections. As IgG3 and IgG4 levels are usable as an indicator of the stage of convalesce in B19V infection (Franssila *et al.*, 1996), further examination of the temporal characteristics of IgG3 and IgG4 induction in AAV-2 infection may be similarly useful.

It has been assumed that AAV-2 does not induce a cell-mediated immune response (Hernandez *et al.*, 1999), and few studies have examined this question in humans (Chirmule *et al.*, 1999; Manno *et al.*, 2006). This study demonstrated that AAV-2 evoked robust proliferative and cytokine recall responses detectable in PBMC cultures. Of the 41 donors assayed for PBMC proliferation, 19 demonstrated a statistically significant proliferative response to stimulation with AAV-2. Of these, 9 donors supported stimulation indices of between 1.5 and 3; 10 donors produced higher stimulation indices, with 4 of these producing SI values above 10. Chirmule *et al.* also examined human PBMC proliferation in response to AAV-2 but found that only 6%

(3/57) of their subjects produced a stimulation index greater than 2.0 (Chirmule *et al.*, 1999). This discrepancy is most likely due to the relatively low concentration of AAV-2 used for the re-stimulation, a multiplicity of infection (MOI) of 100, compared to an MOI of 10,000 for this study. These findings clearly point to the involvement of T-cells in the response to AAV-2.

The polarization of cell-mediated responses to antigens has significant impact on the nature and quality of responses generated. For example, during natural viral or intracellular bacterial infections, T helper 1 responses can recruit cytotoxic T-cells potentially mediating targeted destruction of infected cells whilst Th2 responses will skew the response towards the generation of antibody. The cytokine profiles produced by proliferating cultures can provide insight into the polarization of an *in vitro* response. Cultures stimulated with AAV-2 did not exhibit clear Th1 or Th2 polarization; although IFN-γ was the most frequently detected cytokine indicating that at least in some subjects AAV-2 can evoke a Th1 response. IL-13 was only produced by weakly proliferating cultures (SI between 1.5 and 3) whereas IL-10 production was detected across a range of donors. Chirmule *et al.* also examined AAV-2 stimulated PBMC cultures for cytokines, finding IFN-γ and IL-10 in 6% and 12% of the cultures. The group did not examine IL-13 levels, but did look for IL-4, failing to find the cytokine in any culture (Chirmule *et al.*, 1999).

Neither the extent of PBMC proliferation elicited by AAV-2 nor the resulting cytokine production correlated with the levels of AAV-2-specific IgG or IgG subclasses detected in the corresponding donor plasma samples (Table 7.1). AAV-2 serology as

currently determined is thus a poor predictor of the cell-mediated response. Despite the capacity for AAV-2 to stimulate PBMC proliferation and cytokine production in this study, it is clear that the cellular recall response to AAV-2, at least *in vitro*, is not consistently polarized. Although this response is not polarized, the induction of IFN-γ and IL-13 clearly suggests that AAV-2 can induce $CD4^+$ T-cell responses in a healthy human population, and that at least in part, AAV-2 does not behave like a classical T-independent antigen.

Table 7.1 Cytokine, serological and HLA profiles of donors proliferating in response to AAV-2

Donor #	Class I HLA alleles	Class II HLA alleles	AAV-2 specific IgG subclasses	PBMC proliferation (SI)	Cytokine increase (pg/ml)		
					IFN-g	IL-10	IL-13
13	Cw1, Cw7	DR1, DR7/DR53, DQ2, DQ5(1)	IgG1, IgG2, IgG4	2.57	85	-	-
15	A31(9), B*14, B*14, Cw*06, Cw*08	DR13(6)/DR52, DR15(2)/DR51, DQ9(3)	IgG1, IgG2, IgG4	18.65	110	-	-
16	A68, B8, Cw7, Cw8	DR3/DR52, DR17(3)/DR52, DQ2, DQ6(1)	IgG1, IgG2	2.22	-	-	-
19	A2, B7, B13, Cw5, Cw7	DR4/DR53, DR7/DR53, DQ2, DQ8(3)	IgG1, IgG2	1.75	-	-	-
27	A1, A2, B*4440, B*5615, Cw5, Cw7	DQ2, DQ7(3)	IgG1, IgG2, IgG4	2.27	5	-	1633
31	A1, B8, B51(5)	DR17(3)/DR52, DR8, DQ2, DQ4	IgG1, IgG4	2.31	7	67	1281
32	A1, A29(19), Cw7, Cw7	DR17(3)/DR52, --/DR52, DQ2, DQ6(1)	IgG1, IgG2	2.33	3	-	962
38	A2, A24(9), B7, B18, Cw5, Cw7	DR17(3)/DR52, DR15(2)/DR51, DQ2, DQ6(1)	IgG1, IgG2, IgG4	6.25	39	91	-
40	A1, B42	DR4/DR53, DR4/DR53, DQ8(3), DQ5(1)	IgG1, IgG2, IgG4	14.77	49	132	-
41	A66(10)/A26(10), B44(12), B57(17), Cw5, Cw6	DR4/DR53, DR7/DR53DQ9(3)	IgG1, IgG2	25.50	532	-	-
43	A2, B44(12), B47, Cw4	DR4/DR53, DR7/DR53, DQ2, DQ7(3)	IgG1, IgG2, IgG4	3.29	-	126	-
45	A1, Cw7, Cw7	DR17(3)/DR52, DR51, DQ2, DQ6(1)	IgG1, IgG2	2.20	-	209	-
46	B7, B8, Cw7	DR17(3)/DR52, DR15(2)/DR51, DQ2, DQ6(1)	IgG1, IgG2, IgG4	2.08	-	-	189
47	A1, B63(15), B44(12), Cw5, Cw7	DR4/DR53, DR13(6)/DR52, DQ7(3), DQ6(1)	IgG1, IgG2, IgG4	2.39	-	225	-
50	B55(2), Cw1, Cw4	DR103, DR13(6)/DR52, DQ5(1), DQ6(1)	IgG1, IgG2, IgG4	10.91	546	141	-
51	A31(19), B7, B71(70), Cw18||Cw6, Cw18	DR4/DR53, DR15(2)/DR51, DQ6(1), DQ6(1)	IgG1, IgG2	5.10	221	138	-

The proliferative response characterised here was found only in PBMC cultures from donors also displaying circulating total IgG specific for AAV-2. The low frequency of seronegative donors (4 seronegatives out of a cohort of 45) coupled with the frequency of cultures producing significant proliferation (19 positives of a cohort of 41) made this observation unsurprising as it would be unlikely that an IgG seronegative PBMC proliferation-positive donor would be identified. The presence of large numbers of seropositive donors whose PBMC did not support proliferative responses against AAV-2 indicated that the virus may not be acting as a T-cell dependent antigen during priming of the humoral response. Furthermore, when the combined AAV-2 IgG subclass levels determined in the cohort group were compared to corresponding proliferative responses, no correlation was found (Figure 4.4, $r = 0.25$, $p = 0.14$). However it should be noted that differences in the sensitivity and specificity of immunoassays versus cell-based assays may undermine this finding.

The prevalence and strength of cell-mediated responses to AAV-2 suggest that there is some risk of cytotoxicity targeted against AAV-2 transduced cells. One potential means to avoid such responses would be to identify and remove immunodominant epitopes in the virus capsid sequence. In order to identify specific stimulating epitopes in the AAV-2 capsid, PBMC from the donors characterized in Chapters 3 and 4 were stimulated with overlapping peptides from the AAV-2 capsid sequence. The AAV-2 capsid is composed of three proteins; VP1, VP2 and VP3 in a ratio of 1:1:10 (Xie *et al.*, 2002). VP2 and VP3 are products of the splicing of VP1 mRNA and both proteins represent a subsequence of the VP1 protein. Thus, the entire capsid sequence may be represented by VP1. Using a restrictive definition, 17

candidate epitope sequences were identified as recognized by at least two donors. A further 43 sequences were recognized by a single donor each. Limitations in assay sensitivity due to the modest level of PBMC proliferation induced by AAV-2 and its components mean that some of the more limited proliferative responses observed may have represented false negative results. Thus, it is likely that further single-case candidate epitopes or confirmations of existing single-case candidate epitopes were not detected here.

The panel of single-case candidate epitopes includes sequences (supplementary data) previously identified in human and mouse studies (Chen *et al.*, 2006; Manno *et al.*, 2006; Sabatino *et al.*, 2005). The RDSLVNPGPAMA sequence recognized by donor 13 was a 12-mer incorporated by the 15-mer NGRDSLVNPGPAMAS sequence identified by Sabatino *et al.* in C57BL/6 mice (Sabatino *et al.*, 2005). The sequence EIQYTSNYNKSV was also identified as a candidate epitope in donor 13 and shares a 7-mer homology with the 9-mer sequence SNYNKSVNV identified in the C57BL/6 strain (Sabatino *et al.*, 2005). The sequence GFRPKRLNFKLF identified in donor 16 shares an 11-amino acid homology with the sequence FRPKRLNFKLFNIQV identified in BALB/c mice (Sabatino *et al.*, 2005). Likewise the sequence VPQYGYLTL identified as an epitope in BALB/c mice by Sabatino's group (Sabatino *et al.*, 2005) as well as in a single human case by Manno *et al*. (Manno *et al.*, 2006) lies within the sequence VFMVPQYGYLTL identified as a candidate epitope for donor 16. Furthermore, Chen *et al*. identified an immunogenic sequence TSADNNNSEYSWTGA in mice which is contained in two sequences identified recognized by donor 50 (SKTSADNNNSEY and NSEYSWTGATKY) (Chen *et al.*, 2006).

The panel of epitopes recognized by two or more donors and identified in this study (Table 7.2) have not been previously identified in human or animal models, with two exceptions. Chen *et al.* identified the sequence QVSVEIEWELQKENS as being immunogenic in mice (Chen *et al.*, 2006), and this sequence shares 11 amino acids with the candidate epitope EIEWELQKENSK recognized by three donors (13, 50, 51) in this study (Sequence D, Table 7.2). The second sequence, FKLFNIQV (sequence L, Table 7.2), was recognized by donors 16 and 50 and shares an 8 amino acid homology with the FRPKRLNFKLFNIQV sequence identified in mice by Sabatino *et al.*, 2005.

No significant correlation could be identified between donor HLA haplotypes and the corresponding epitopes recognized. The haplotypes of AAV-2 respondent donors displayed considerable diversity. This was also the case for donors responding to the most common stimulating capsid sequences. Although it is reported here that the DQ2, DQ3 (DQ7(3), DQ8(3), DQ9(3)) and DQ6(1) serotype alleles are present at a high frequency in our study group, these results broadly agree with recent detailed examinations HLA allele frequencies and haplotypes in the Irish population in which these three serotypes represented the three most commonly identified (Dunne *et al.*, 2008). Thus, although the HLA data presented here is less exhaustive, the donors from which AAV-2-specific PBMC were isolated display HLA diversity comparable to the general Irish population. The observation that a number of sequences can be recognized by donors of different HLA haplotypes, and indeed across species in two cases, indicates that epitopes A, B, C, D and K are immunodominant human epitopes.

Table 7.2 Localisation of immunodominant VP1 epitopes

Epitope	Sequence	Responding donors	Epitope location			
			Residues	VP1	VP2	VP3
A	KEVTQNDGTTTI	4	321 - 333	+	+	+
B	ATKYHLNGRDSL	3	505 - 517	+	+	+
C	TTSTRTWALPTY	3	241 - 253	+	+	+
D	EIEWELQKENSK	3	681 - 693	+	+	+
E	DWLEDTLSEGIR	2	9 - 21	+	-	-
F	NGLDKGEPVNEA	2	57 - 69	+	-	-
G	NLGRAVFQAKKR	2	113 - 125	+	-	-
H	AKKRVLEPLGLV	2	121 - 133	+	-	-
I	LPTYNNHLYKQI	2	249 - 261	+	+	+
J	YKQISSQSGASN	2	257 - 269	+	+	+
K	GASNDNHYFGYS	2	265 - 277	+	+	+
L	FKLFNIQVKEVT	2	313 - 325	+	+	+
M	TTTIANNLTSTV	2	329 - 341	+	+	+
N	YCLEYFPSQMLR	2	393 - 405	+	+	+
O	QSRLQFSQAGAS	2	457 - 469	+	+	+
P	DIEKVMITDEEE	2	553 - 565	+	+	+
Q	TNGVYSEPRPIGTRYLT	2	716 - 728	+	+	+

Presence of immunodominant sequences in capsid sequences VP1, 2 and 3 are indicated as positive (+) or negative (-).

Since the extent of humoral immunity to AAV-2 in the human population became clear, it has been suggested that AAV-2 capsid modification may enhance the efficacy of the virus as a vector (Monahan & Samulski, 2000). It has also been suggested that if capsid antigen-specific cytotoxicity is a significant barrier to AAV-2-mediated gene therapy, the administration of immunosuppressive drugs following vector administration may prevent cell-mediated immunity (Manno *et al.*, 2006). However systemic immunosuppression may be undesirable in candidates for gene therapy and thus the immunodominant sequences identified here may thus represent appropriate targets for capsid modification in rare cases.

Modification of the AAV-2 capsid to remove immunodominant epitopes is not without potential drawbacks. The determination of the structure of the AAV-2 capsid by Xie *et al*. along with mutagenesis and neutralisation studies has shed light on the function of structural motifs on the capsid (Asokan *et al.*, 2006; DiPrimio *et al.*, 2008; Kern *et al.*, 2003; Opie *et al.*, 2003; Wu *et al.*, 2000; Xie *et al.*, 2002). For example, studies of AAV-2 binding to the virus primary receptor HSPG have shown that a group of basic amino acids (Arginines 484, 487, 585, and 588 and Lysine 532) are critical for binding (Kern *et al.*, 2003; Opie *et al.*, 2003). From the immunological perspective however, there would be little justification for the modification of this region as none of the immunodominant epitopes identified herein contains the relevant residues, although sequence B, discussed later, lies in the region between Arginine 487 and Arginine 585.

The most commonly-recognised immunodominant epitope identified in this study was sequence A (KEVTQNDGTTTI), which shared 4-mer homology with two other immunodominant epitopes, sequences L (FKLFNIQVKEVT) and M (TTTIANNLTSTV). These sequences would thus be attractive targets for modification. When sequence A was mapped onto a 3d model of the AAV-2 capsid it was found that the sequence is part of the loop formed between beta strands H and I (HI loop) of the VP subunit. This loop is located at the capsid 5-fold axis of symmetry and overlaps with the HI loops of four neighbouring subunits to form a barrel-shaped protrusion surrounding a pore in the capsid. Mutagenesis studies have demonstrated an important role for this motif in viral capsid assembly and viral DNA packaging into the capsid (DiPrimio *et al.*, 2008). There is thus some reason to be concerned that modification of sequence A, or the adjacent sequences L and M, might reduce vector production efficiency or block production entirely. DiPrimio *et al.* did however demonstrate that capsid assembly and infectivity of HI loop mutants could be rescued by substituting HI loop sequences from AAV-1 and AAV-8 (DiPrimio *et al.*, 2008).

Sequence B (ATKYHLNGRDSL) was stimulatory in three independent PBMC cultures and is located at the base of a cluster of protrusions on the AAV-2 capsid which is composed of overlapping loops from three subunits associating at the 3-fold symmetry axis at the centre of each icosahedral face. This sequence contains a motif (NGR) which is conserved in the majority of AAV serotypes and which has been shown to have an integrin-binding function (Asokan *et al.*, 2006). Mutagenesis of this region has been shown to significantly reduce binding of AAV-2 capsids to the cell surface of permissive HEK-293 cells as well as reducing virus internalisation (DiPrimio *et al.*,

2008). Thus, if modification of this sequence is to be pursued, it seems likely that the NGR motif must be left intact in order to preserve transduction efficiency and tissue tropism. Furthermore, as previously mentioned, sequence B is located in a region between the arginine residues strongly associated with HSPG binding (Opie *et al.*, 2003), so it is conceivable that modification in this region which preserves the NGR motif may negatively impact on HSPG binding activity, thus reducing transduction efficiency and modulating tissue tropism.

Sequences C and D may represent more promising targets for modification. Both sequences were recognised in 3 donors and are not directly associated with any major capsid function. Sequence C is located in the region directly adjacent to the 5 fold capsid pore structure composed of sequences A, L and M. There is some possibility that sequence C performs a scaffolding function for the 5-fold pore, though this would need to be determined by mutagenesis. Similarly, sequence N which is located close to the 5-fold axis may also serve a scaffolding function for the capsid pore. Sequence D is located along the icosahedral vertex connecting 5-fold symmetry axes, close to the 2-fold subunit border region. It may thus be involved in capsid assembly, but this again has not been established by experimentation. This may also be a consideration for sequence Q, which is also located close to the 2-fold subunit border.

Epitope sequences E-H (Table 7.2) are located within the N-terminal VP1 unique region and would thus tend to be present in transduced recipient cells in approximately 10-fold lower concentrations than those found in all three VP subunits. The location of the unique region within the capsid 3D structure is not clear, although some

conformational data has been obtained using electron cryomicroscopy (Kronenberg *et al.*, 2005). It appears that the N-terminal region of the VP1 unique region may be located within the capsid, or become exposed on the surface, protruding through the 5-fold pore structure. The conditions prompting this conformational change *in vivo* are not known. The region appears to contain a functional phospholipase A2 (PLA2) catalytic domain (Girod *et al.*, 2002). Deletion or mutation of the unique region results in significantly reduced infectivity although capsid assembly and viral DNA packaging remain intact (Tratschin *et al.*, 1984). Although viral gene expression following transduction was reduced, mutations in the active site of the PLA2 domain did not inhibit perinuclear accumulation in late endosomes or lysosomes, suggesting that PLA2 activity might be required in a later step of infection (Girod *et al.*, 2002).

An alternative to the modification of AAV-2 capsids is use of capsids from other AAV serotypes. The sequences of the VP1 capsid proteins vary across the AAV serotypes and this may mean that immunodominant epitopes present on the AAV-2 capsid may not be conserved. When the VP1 sequences for AAV serotypes 1, 2, 4, 6 and 8 are compared for the conservation of the top 4 immunodominant epitopes described here (Table 7.2) it is evident that epitopes A and D are fully or highly conserved across all 5 serotypes, raising the possibility that these serotypes may also induce cell-mediated recall responses in AAV-2 seropositive humans. Epitope C was fully conserved across all 5 serotypes and it is this likely that these serotypes will induce cellular responses in a subset of seropositive humans. Epitope B was less well conserved across the top 4 immunodominant epitopes. The epitopes were least conserved in AAV-4; although epitope C was fully conserved, only 7 of 12 amino acids

from epitope A were conserved, whilst epitopes B and D were represented by 5 of 12 and 8 of 12 amino acids respectively.

The observations herein that even a small sample of an outbred population can support diverse recall response against multiple T-cell epitopes means that genetic modification of AAV-2 to fully escape immune recognition by T-cells is not a feasible goal for general application. A more promising strategy, as suggested elsewhere (Manno *et al.*, 2006), might be that gene therapy recipients should undergo some form of immunosuppressive therapy during the relatively transient period during which AAV-2 epitope cross-presentation can occur. Vector capsid modification to remove identified epitopes might instead represent a strategy reserved for specific cases in which administration of immunosuppressive drugs is undesirable. In such cases, screening of patient serum alone as a measure of immune status, whilst informative, is likely to be insufficient. Serology has not been shown to reliably predict the presence of T-cell memory for AAV-2 (Chapter 4). Thus, detailed screening of patient humoral memory and epitope recognition would be an essential tool in ensuring the delivery of an effective treatment.

The murine mesenchymal stem cells used in this study were obtained from Dr. Karen English and Laura Tobin, working at the NUIM Cellular Immunology Lab. Although already well-characterised (English *et al.*, 2007; English *et al.*, 2008), the cells were nonetheless validated to establish that continued culture and passaging by the author did not alter cell phenotype or functions. MSC were found to display the same spindle-like fibroblastic morphology as used by English *et al*. and elsewhere for mouse

(Krampera *et al.*, 2003), rat (McMahon *et al.*, 2006) and human (Stender *et al.*, 2007). The MSC were also comparable in terms of MHC expression, and were Sca-1 positive. Self-renewal was demonstrated by passaging and differentiation along osteogenic and adipogenic pathways demonstrated potency. Finally, co-incubation of murine MSC with mitogen-stimulated splenocytes resulted in inhibition of splenocyte proliferation. These traits, morphology, surface marker expression, self-renewal, potency and immunomodulatory capacity were later used to assess the retention of the MSC phenotype.

The immunomodulatory functions of MSC co-incubated with naive T-cells were further characterised using a CFSE-based system which allowed the measurement a variety of factors determining gross T-cell proliferative response. It was determined that MSC reduced the progressor fraction of the mitogen stimulated T-cell population as well as lengthening their time to initiate their first division after the resting state. Furthermore, MSC lengthened the subsequent mean division time. Although this technique was not revisited during the course of this study, it is clear that this method could be an invaluable tool for delineating the roles of the various soluble factors and cell contact-dependent elements involved in MSC immunomodulation, particularly if used in combination with blocking studies, gene silencing and MSC sourced from knockout mice.

It was hoped that murine MSC might be amenable to transformation using the AAV-2-based vector examined in chapters 3 and 4, thereby rendering the MSC as a potential platform to deliver transgene products in a clinical setting whilst avoiding the

immune memory for AAV-2 characterised in chapters 3, 4 and 5 and elsewhere (Chirmule *et al.*, 1999; Manno *et al.*, 2006; Zaiss & Muruve, 2005). However, murine MSC appeared resistant to transduction using an AAV-2*GFP* vector. Similar results have been reported for human (Stender *et al.*, 2007) and rat MSC (McMahon *et al.*, 2006). Stender *et al*. showed some transduction of human MSC with a similar *GFP*-encoding vector but the maximum transduction efficiency was 65% and the level of transgene expression in the transduced population increased in intensity only 4-fold over a 10,000 fold AAV dose range. McMahon *et al*. conducted an examination of several transduction and transfection techniques using rat MSC as the target (McMahon *et al.*, 2006), including an AAV-2*GFP* vector but found the MSC to be resistant to transduction, despite successful transgene expression following adenoviral and lentiviral transduction.

Due to the lack of any detectable transduction and limited AAV-2 vector stocks, transduction of MSC with AAV-2 was not further examined, nor was the impact of the transduction protocol on MSC phenotype or therapeutic functions. Despite this negative outcome, it is possible that AAV-2-mediated transduction of MSC might be optimised, and so a different approach was adopted. Centrifugation of subconfluent MSC cultures in the presence of Adenoviral vectors results in efficient transduction and is well-tolerated by the MSC (Mohr *et al.*, 2008). Alternatively, the use of antibodies bispecific for the AAV vector and a cell surface receptor on the MSC may allow efficient transduction, a strategy which has been successfully employed to allow efficient AAV mediated transduction of non-permissive megakaryocyte cell lines (Bartlett *et al.*, 1999).

To assess the impact of transfection of MSC with a plasmid vector, a lipofection protocol was instead adopted. The chosen vector encoded IDO, an enzyme known to be involved in MSC immunomodulation. It was thus hoped that successful transfection might enhance MSC immunomodulatory function without impacting on MSC self-renewal and potency. Transfection was successful producing IDO RNA and protein as well as demonstrating increased IDO function in the form of tryptophan metabolism. MSC morphology was not altered and osteogenic and adipogenic functions remained. However, MSC cell numbers in culture declined sharply in the 24 hours following transfection and growth rates were poor for up to 7 days. Lipofectamine alone did not appear to be the cause, although it did appear to induce a small increase in endogenous IDO, possibly indicating some stress on the cells. Thus it seemed likely that the introduction of the CMV-regulated plasmid might be the cause of the decline in cell numbers and poor cell growth. Cell surface markers were also altered, with increased MHC class I observed in transfected cultures. Perhaps most significantly, transfected MSC displayed a reduced capacity to suppress mitogen-driven lymphocyte proliferation. The cause of this was not established; however it is probable that the observed upregulation of cell surface MHC I contributed to this effect.

Lipofection has recently been shown to result in cell death and reduced proliferation in culture in both rat and human MSC (Helledie *et al.*, 2008; McMahon *et al.*, 2006). Helledie *et al*. similarly noted that only lipofectamine-DNA complexes, and not lipofectamine alone, impacted negatively on MSC survival and proliferation. Further optimisation of the lipofection protocol might reduce MSC death and restore proliferation, but the observed changes in murine MSC immunomodulatory function as

a result of IDO transfection coupled with the cell death and loss of proliferation indicates that lipofection is a suboptimal method for the transfection of murine MSC. Viral vectors based on adenovirus and lentiviruses have proven more efficient and less cytotoxic than lipofection in other studies (McMahon *et al.*, 2006). If transduction of MSC with AAV cannot successfully be optimised, these vectors would seem to be the most promising candidates for further research.

In conclusion, this study demonstrated that both humoral and cell-mediated memory for AAV-2 is prevalent in the normal Irish population, supporting the hypothesis that immunity will complicate the use of AAV-2 in therapy. Given the known prevalence of AAV-2 infection in humans (Chirmule *et al.*, 1999; Erles *et al.*, 1999; Halbert *et al.*, 2006), it is conceivable that widespread humoral memory for the virus might negatively impact on the usefulness of the virus as a gene therapy vector. Cell-mediated responses demonstrated here, when considered in the context of emerging data on the targeting of AAV transduced by the cell-mediated response (Li *et al.*, 2009; Manno *et al.*, 2006) suggest this may also be a significant confounding influence on the use of AAV vectors in the wider population. With the identification of a panel of immunodominant epitopes and a wide range of single-case epitopes capsid modification strategies are unlikely to be a practical solution for most applications of AAV vectors due to the variety of epitopes recognized; however screening for patient cell-mediated and humoral responses may be an invaluable tool in bringing effective AAV-2 vectors to the clinic. For cases where immunosuppression to avoid CMI is undesirable, screening of specific epitope responses might be a useful tool for the identification of

targets for capsid modification, though any such modified capsids would need to be further examined for their capacity to effectively transduce donor cells *in vitro*.

Attempts to transduce murine MSC with a vector based on AAV-2 were unsuccessful, and so a lipofectamine-based protocol was adopted in conjunction with a plasmid encoding IDO. Transfection was successful producing IDO mRNA and protein as well as demonstrating increased IDO function in the form of tryptophan metabolism. MSC morphology and cell surface markers were not altered and potency was not affected. However, MSC cell numbers in culture declined sharply and growth rates were poor. Further optimisation of the lipofection protocol might be worth pursuing, but that changes in murine MSC immunomodulatory function as a result of IDO transfection were modest and taking the cell death and loss of proliferation into account, it is likely that lipofection is a suboptimal method for the transfection of murine MSC.

Transduction of MSC using AAV-2-based vectors was unsuccessful in this study. However, given the potential risks of oncogenesis (Hacein-Bey-Abina *et al.*, 2003) and inflammation (Raper *et al.*, 2003) that come with transduction using retroviruses and adenoviruses respectively, future optimisation of AAV-2-mediated transduction may yet be a worthwhile goal. Humoral memory and antibody neutralisation should be avoided and concerns raised herein and elsewhere (Manno *et al.*, 2006) regarding cell-mediated responses to AAV-2 vectors and AAV transduced cells might easily be negated by growing the transduced cells in culture until the transient presentation of exogenous AAV-2 capsid on class I MHC molecules has declined. Given that the virus does not integrate with a high frequency (Kotin *et al.*,

1990), does not cause significant MSC death (McMahon *et al.*, 2006) and does not induce strong inflammatory responses *in vivo* (Zaiss *et al.*, 2002), AAV-2 remains an attractive candidate vector for the transduction of MSC if poor transduction efficiency can be overcome.

CHAPTER 8

REFERENCES

Aggarwal, S. & Pittenger, M. F. (2005). Human mesenchymal stem cells modulate allogeneic immune cell responses. *Blood* **105**, 1815 - 1822.

Altman, D. G. & Bland, J. M. (1994). Statistics Notes: Diagnostic tests 1: sensitivity and specificity. *BMJ* **308**, 1552.

Amado, L. C., Saliaris, A. P., Schuleri, K. H., St. John, M., Xie, J.-S., Cattaneo, S., Durand, D. J., Fitton, T., Kuang, J. Q., Stewart, G., Lehrke, S., Baumgartner, W. W., Martin, B. J., Heldman, A. W. & Hare, J. M. (2005). Cardiac repair with intramyocardial injection of allogeneic mesenchymal stem cells after myocardial infarction. *Proceedings of the National Academy of Sciences of the United States of America* **102**, 11474-11479.

Arruda, V., Stedman, H., Nichols, T., Haskins, M., Nicholson, M., Herzog, R., Couto, L. & High, K. (2005). Regional intravascular delivery of AAV-2-F.IX to skeletal muscle achieves long-term correction of hemophilia B in a large animal model. *Blood* **105**, 3458-3464.

Artavanis-Tsakonas, S., Matsuno, K. & Fortini, M. E. (1995). Notch signaling. *Science* **268**, 225-232.

Asokan, A., Hamra, J. B., Govindasamy, L., Agbandje-McKenna, M. & Samulski, R. J. (2006). Adeno-Associated Virus Type 2 Contains an Integrin {alpha}5{beta}1 Binding Domain Essential for Viral Cell Entry. *J Virol* **80**, 8961-8969.

Atchison, R. W. (1970). The role of herpesviruses in adenovirusassociated virus replication in vitro. *Virology* **42**, 155-162.

Atchison, R. W., Casto, B. C. & Hammon, W. M. (1965). Adenovirus-associated defective virus particles. *Science* **149**, 754-756.

Augello, A., Tasso, R., Negrini, Simone M., Amateis, A., Indiveri, F., Cancedda, R. & Pennesi, G. (2005). Bone marrow mesenchymal progenitor cells inhibit lymphocyte proliferation by activation of the programmed death 1 pathway. *European Journal of Immunology* **35**, 1482-1490.

Baksh, D., Song, L. & Tuan, R. S. (2004). Adult mesenchymal stem cells: characterization, differentiation, and application in cell and gene therapy. *Journal of Cellular and Molecular Medicine* **8**, 301-316.

Barry, F. P. & Murphy, J. M. (2004). Mesenchymal stem cells: clinical applications and biological characterization. *Int J Biochem Cell Biol* **36**, 568 - 584.

Barry, F. P., Murphy, J. M., English, K. & Mahon, B. P. (2005). Immunogenicity of adult mesenchymal stem cells: lessons from the fetal allograft. *Stem cells and development* **in press**.

Bartholomew, A., Sturgeon, C., Siatskas, M., Ferrer, K., McIntosh, K., Patil, S., Hardy, W., Devine, S., Ucker, D., Deans, R., Moseley, A. & Hoffman, R. (2002). Mesenchymal stem cells suppress lymphocyte proliferation in vitro and prolong skin graft survival in vivo. *Exp Hematol* **30**, 42 - 48.

Bartlett, J. S., Kleinschmidt, J., Boucher, R. C. & Samulski, R. J. (1999). Targeted adeno-associated virus vector transduction of nonpermissive cells mediated by a bispecific F(ab'gamma)2 antibody. *Nat Biotechnol* **17**, 181-186.

Becerra, S. P., Koczot, F., Fabisch, P. & Rose, J. A. (1988). Synthesis of adeno-associated virus structural proteins requires both alternative mRNA splicing and alternative initiations from a single transcript. *J Virol* **62**, 2745-2754.

Becker, A. J., McCulloch, E. A. & Till, J. E. (1963). Cytological demonstration of the clonal nature of spleen colonies derived from transplanted mouse marrow cells. *Nature* **2**, 452-454.

Bhasin, M. & Raghava, G. P. S. (2004). Prediction of CTL epitopes using QM, SVM and ANN techniques. *Vaccine* **22**, 3195-3204.

Bianco, P., Robey, P. G. & Simmons, P. J. (2008). Mesenchymal Stem Cells: Revisiting History, Concepts and Assays. *Cell Stem Cell* **2**, 313-319.

Blacklow, N. R., Hoggan, M. D., Kapikian, A. Z., Austin, J. B. & Rowe, W. P. (1968a). Epidemiology of adenovirus-associated virus infection in a nursery population. *Am J Epidemiol* **88**, 368-378.

Blacklow, N. R., Hoggan, M. D. & Rowe, W. P. (1967). Isolation of adenovirus-associated viruses from man. *Proc Natl Acad Sci U S A* **58**, 1410-1415.

Blacklow, N. R., Hoggan, M. D. & Rowe, W. P. (1968b). Serologic evidence for human infection with adenovirus-associated viruses. *J Natl Cancer Inst* **40**, 319-327.

Bleker, S., Pawlita, M. & Kleinschmidt, J. A. (2006). Impact of Capsid Conformation and Rep-Capsid Interactions on Adeno-Associated Virus Type 2 Genome Packaging. *J Virol* **80**, 810-820.

Bonab, M., Alimoghaddam, K., Talebian, F., Ghaffari, S., Ghavamzadeh, A. & Nikbin, B. (2006). Aging of mesenchymal stem cell in vitro. *BMC Cell Biology* **7**, 14.

Boyle, M. P., Enke, R. A., Mogayzel, P. J., Guggino, W. B., Martin, D. B., Agarwal, S. & Zeitlin, P. L. (2003). Effect of Adeno-Associated Virus–Specific Immunoglobulin G in Human Amniotic Fluid on Gene Transfer. *Hum Gene Ther* **14**, 365-373.

Bøyum, A. (1968). Isolation of mononuclear cells and granulocytes from human blood. *Scand J Clin Invest* **21**, 77-89.

Bradford, M. M. (1976). A rapid and sensitive method for the quantitation of microgram quantities of protein utilizing the principle of protein-dye binding. *Analytical Biochemistry* **72**, 248-254.

Briere, F., Servet-Delprat, C., Bridon, J., Saint-Remy, J. & Banchereau, J. (1994). Human interleukin 10 induces naive surface immunoglobulin D+ (sIgD+) B cells to secrete IgG1 and IgG3. *J Exp Med* **179**, 757-762.

Bruder, S. P., Jaiswal, N. & Haynsesworth, S. E. (1997). Growth kinetics, self-renewal and the osteogenic potential of purified human mesenchymal stem cells during extensive subcultivation and following cryopreservation. *J Cell Biochem* **64**, 278-294.

Büning, H., Ried, M. U., Perabo, L., Gerner, F. M., Huttner, N. A., Enssle, J. & Hallek, M. (2003). Receptor targeting of adeno-associated virus vectors. *Gene Ther* **10**, 1142-1151.

Buller, R. M. & Rose, J. A. (1978). Characterization of adenovirus-associated virus-induced polypeptides in KB cells. *J Virol* **25**, 331-338.

Buller, R. M. L., Janik, J. E., Sebring, E. D. & Rose, J. A. (1981). Herpes Simplex Virus Types 1 and 2 Completely Help Adenovirus-Associated Virus Replication. *J Virol* **40**, 241-247.

Cassinotti, P., Weitz, M. & Tratschin, J. D. (1988). Organization of the adeno-associated virus (AAV) capsid gene: mapping of a minor spliced mRNA coding for virus capsid protein 1. *Virology* **167**, 176-184.

Cavazzana-Calvo, M., Hacein-Bey, S., Basile, G., egrave, ve de, S., Gross, F., Yvon, E., Nusbaum, P., Selz, F., ccedil, oise, Hue, C., Certain, S., eacute, phanie, Casanova, J.-L., Bousso, P., Deist, F., oise, L. & Fischer, A. (2000). Gene Therapy of Human Severe Combined Immunodeficiency (SCID)-X1 Disease. *Science* **288**, 669-672.

Cerottini, J. C. & Brunner, K. T. (1974). Cell-mediated cytotoxicity, allograft rejection, and tumor immunity. *Adv Immunol* **18**, 67-132.

Chang, J., Sonoyama, W., Wang, Z., Jin, Q., Zhang, C., Krebsbach, P. H., Giannobile, W., Shi, S. & Wang, C.-Y. (2007). Noncanonical Wnt-4 Signaling Enhances Bone Regeneration of Mesenchymal Stem Cells in Craniofacial Defects through Activation of p38 MAPK. *Journal of Biological Chemistry* **282**, 30938-30948.

Chang, S. C. N., Chuang, H. L., Chen, Y. R., Chen, J. K., Chung, H. Y., Lu, Y. L., Lin, H. Y., Tai, C. L. & Lou, J. (2003). Ex vivo gene therapy in autologous

bone marrow stromal stem cells for tissue-engineered maxillofacial bone regeneration. *Gene Ther* **10**, 2013-2019.

Chao, H., Liu, Y., Rabinowitz, J., Li, C., Samulski, R. J. & Walsh, C. E. (2000). Several log increase in therapeutic transgene delivery by distinct adeno-associated viral serotype vectors. *Mol Ther* **2**, 619-623.

Chen, J., Wu, Q., Yang, P., Hsu, H. C. & Mountz, J. D. (2006). Determination of specific CD4 and CD8 T-cell epitopes after AAV2- and AAV8-hF.IX gene therapy. *Mol Ther* **13**, 260-269.

Chen, S.-l., Fang, W.-w., Ye, F., Liu, Y.-H., Qian, J., Shan, S.-j., Zhang, J.-j., Chunhua, R. Z., Liao, L.-m., Lin, S. & Sun, J.-p. (2004). Effect on left ventricular function of intracoronary transplantation of autologous bone marrow mesenchymal stem cell in patients with acute myocardial infarction. *The American Journal of Cardiology* **94**, 92-95.

Cheung, A. K., Hoggan, M. D., Hauswirth, W. W. & Berns, K. I. (1980). Integration of the adeno-associated virus genome into cellular DNA in latently infected human Detroit 6 cells. *J Virol* **33**, 739-748.

Chiorini, J. A., Kim, F., Yang, L. & Kotin, R. M. (1999). Cloning and characterization of adeno-associated virus type 5. *J Virol* **73**, 1309-1319.

Chirmule, N., Propert, K. J., Magosin, S. A., Qian, Y., Qian, R. & Wilson, J. M. (1999). Immune responses to adenovirus and adeno-associated virus in humans. *Gene Ther* **6**, 1574-1583.

Chirmule, N., Xiao, W., Truneh, A., Schnell, M. A., Hughes, J. V., Zoltick, P. & Wilson, J. M. (2000). Humoral Immunity to Adeno-Associated Virus Type 2

Vectors following Administration to Murine and Nonhuman Primate Muscle. *J Virol* **74**, 2420-2425.

Corcoran, A., Doyle, S., Waldron, D., Nicholson, A. & Mahon, B. P. (2000). Impaired Gamma Interferon Responses against Parvovirus B19 by Recently Infected Children. *J Virol* **74**, 9903-9910.

Corcoran, A., Mahon, BernardÂ P. & Doyle, S. (2004). B Cell Memory Is Directed toward Conformational Epitopes of Parvovirus B19 Capsid Proteins and the Unique Region of VP1. *The Journal of Infectious Diseases* **189**, 1873-1880.

Coura, R. d. S. & Nardi, N. B. (2007). The state of the art of adeno-associated virus-based vectors in gene therapy. *Virol J* **4**.

Crigler, L., Robey, R. C., Asawachaicharn, A., Gaupp, D. & Phinney, D. G. (2006). Human mesenchymal stem cell subpopulations express a variety of neuro-regulatory molecules and promote neuronal cell survival and neuritogenesis. *Experimental Neurology* **198**, 54-64.

D'Ippolito, G., Diabira, S., Howard, G. A., Menei, P., Roos, B. A. & Schiller, P. C. (2004). Marrow-isolated adult multilineage inducible (MIAMI) cells, a unique population of postnatal young and old human cells with extensive expansion and differentiation potential *J Cell Sci* **117**, 2971-2981.

da Silva Meirelles, L., Caplan, A. I. & Nardi, N. B. (2008). In Search of the In Vivo Identity of Mesenchymal Stem Cells. *Stem Cells* **26**, 2287-2299.

De Ugarte, D. A., Morizono, K., Elbarbary, A., Alfonso, Z., Zuk, P. A., Zhu, M., Dragoo, J. L., Ashjian, P., Thomas, B., Benhaim, P., Chen, I., Fraser, J. &

Hedrick, M. H. (2003). Comparison of Multi-Lineage Cells from Human Adipose Tissue and Bone Marrow. *Cells Tissues Organs* **174**, 101-109.

Deng, W., Han, Q., Liao, L., Li, C., Ge, W., Zhao, Z., You, S., Deng, H. & Zhao, R. C. (2004). Allogeneic bone marrow-derived flk-1+Sca-1- mesenchymal stem cells leads to stable mixed chimerism and donor-specific tolerance. *Exp Hematol* **32**, 861 - 867.

Di Nicola, M., Carlo-Stella, C., Magni, M., Milanesi, M., Longoni, P. D., Matteucci, P., Grisanti, S. & Gianni, A. M. (2002). Human bone marrow stromal cells suppress T-lymphocyte proliferation induced by cellular or nonspecific mitogenic stimuli. *Blood* **99**, 3838 - 3843.

DiGirolamo, C. M., Stokes, D., Colter, D., Phinney, D. G., Class, R. & Prockop, D. J. (1999). Propagation and senescence of human marrow stromal cells in culture: a simple colony-forming assay identifies samples with the greatest potential to propagate and differentiate. *British Journal of Haematology* **107**, 275-281.

DiPrimio, N., Asokan, A., Govindasamy, L., Agbandje-McKenna, M. & Samulski, R. J. (2008). Surface Loop Dynamics in AAV Capsid Assembly. *J Virol* **82**, 5178-5179.

Djeha, A. H., Thomson, T. A., Leung, H., Searle, P. F., Young, L. S., Kerr, D. J., Harris, P. A., Mountain, A. & Wrighton, C. J. (2001). Combined Adenovirus-Mediated Nitroreductase Gene Delivery and CB1954 Treatment: A Well-Tolerated Therapy for Established Solid Tumors. *Molecular Therapy* **3**, 233-240.

Djouad, F., Bouffi, C., Ghannam, S., Noel, D. & Jorgensen, C. (2009). Mesenchymal stem cells: innovative therapeutic tools for rheumatic diseases. *Nat Rev Rheumatol* **5**, 392-399.

Dong, J.-Y., Fan, P.-D. & Frizzell, R. A. (1996). Quantitative Analysis of the Packaging Capacity of Recombinant Adeno-Associated Virus. *Human Gene Therapy* **7**, 2101-2112.

Douar, A. M., Poulard, K., Stockholm, D. & Danos, O. (2001). Intracellular trafficking of adeno-associated virus vectors: routing to the late endosomal compartment and proteasome degradation. *J Virol* **75**, 1824-1833.

Duan, D., Yue, Y., Yan, Z., McCray, P. B., Jr. & Engelhardt, J. F. (1998). Polarity influences the efficiency of recombinant adenoassociated virus infection in differentiated airway epithelia. *Hum Gene Ther* **9**, 2761-2776.

Dunne, C., Crowley, J., Hagan, R., Rooney, G. & Lawlor, E. (2008). HLA-A, B, Cw, DRB1, DQB1 and DPB1 alleles and haplotypes in the genetically homogenous Irish population. *Int J Immunogenet* **35**, 295-302.

Edelstein, M. L., Abedi, M. R. & Wixon, J. (2007). Gene therapy clinical trials worldwide to 2007 - an update. *The Journal of Gene Medicine* **9**, 833-842.

Edelstein, M. L., Abedi, M. R., Wixon, J. & Edelstein, R. M. (2004). Gene therapy clinical trials worldwide 1989-2004 - an overview. *The Journal of Gene Medicine* **6**, 597-602.

English, K., Barry, F. P., Field-Corbett, C. P. & Mahon, B. P. (2007). IFN-[gamma] and TNF-[alpha] differentially regulate immunomodulation by murine mesenchymal stem cells. *Immunology Letters* **110**, 91-100.

English, K., Barry, F. P. & Mahon, B. P. (2008). Murine mesenchymal stem cells suppress dendritic cell migration, maturation and antigen presentation. *Immunology Letters* **115**, 50-58.

Engvall, E. & Perlmann, P. (1971). Enzyme-linked immunosorbent assay (ELISA). Quantitative assay of immunoglobulin G. *Immunochemistry* **8**, 871-874.

Erles, K., Sebökovà, P. & Schlehofer, J. R. (1999). Update on the prevalence of serum antibodies (IgG and IgM) to adeno-associated virus (AAV). *J Med Virol* **59**, 406-411.

Felgner, P. L., Gadek, T. R., Holm, M., Roman, R., Chan, H. W., Wenz, M., Northrop, J. P., Ringold, G. M. & Danielsen, M. (1987). Lipofection: a highly efficient, lipid-mediated DNA-transfection procedure. *Proceedings of the National Academy of Sciences of the United States of America* **84**, 7413-7417.

Franssila, R., Söderlund, M., Brown, C. S., Spaan, W. J. M., Seppälä, I. & Hedman, K. (1996). IgG subclass response to human parvovirus B19 infection. *Clin Diagn Virol* **6**, 41-49.

Friedenstein, A. J. P., Deriglasova, U. F., Kulagina, N. N., Panasuk, A. F., Rudakowa, S. F., Luria, E. A. & Ruadkow, I. A. (1974). Precursors for fibroblasts in different populations of hematopoietic cells as detected by the in vitro colony assay method. *Exp Hematol* **2**, 83-92.

Friedenstein, A. J. P. & Petrokova, K. V. (1966). Osteogenesis in transplant of bone marrow cells. *Journal of Embryological Experimental Morphology* **16**, 381-390.

Frumento, G., Rotondo, R., Tonetti, M., Damonte, G., Benatti, U. & Ferrara, G. B. (2002). Tryptophan-derived catabolites are responsible for inhibition of T and

natural killer cell proliferation induced by indoleamine 2,3-dioxygenase. *J Exp Med* **196**, 459 - 468.

Gadi, T., Debbie, D. P., Ralph, M., Basan Gowda, K., Shuanhu, Z., Gadi, P., Amos, P., Yoram, Z., Ioannis, K. M. & Dan, G. (2001). Engineered human mesenchymal stem cells: a novel platform for skeletal cell-mediated gene therapy. *The Journal of Gene Medicine* **3**, 240-251.

Gao, G., Vandenberghe, L. H., Alvira, M. R., Lu, Y., Calcedo, R., Zhou, X. & Wilson, J. M. (2004). Clades of Adeno-Associated Viruses Are Widely Disseminated in Human Tissues. *J Virol* **78**, 6381-6388.

Gao, G. P., Alvira, M. R., Wang, L., Calcedo, R., Johnston, J. & Wilson, J. M. (2002). Novel adeno-associated viruses from rhesus monkeys as vectors for human gene therapy. *Proc Natl Acad Sci U S A* **99**, 11854-11859.

Girod, A., Wobus, C. E., Zadori, Z., Ried, M., Leike, K., Tijssen, P., Kleinschmidt, J. A. & Hallek, M. (2002). The VP1 capsid protein of adeno-associated virus type 2 is carrying a phospholipase A2 domain required for virus infectivity. *J Gen Virol* **83**, 973-978.

Glennie, S., Soeiro, I., Dyson, P. J., Lam, E. W. & Dazzi, F. (2005). Bone marrow mesenchymal stem cells induce division arrest anergy of activated T-cells. *Blood* **105**, 2821 - 2827.

Goncalves, M. (2005). Adeno-associated virus: from defective virus to effective vector. *Virology Journal* **2**, 43.

Gould, D. J. & Favorov, P. (2003). Vectors for the treatment of autoimmune disease. *Gene Ther* **10**, 912-927.

Greenwood, M. J. & Lansdorp, P. M. Telomeres, telomerase, and hematopoietic stem cell biology. *Archives of Medical Research* **34**, 489-495.

Gregoreka, H., Madalinski, K., Woynarowskib, M., Mikolajewiczc, J., Syczewskad, M. & Sochab, J. (2000). The IgG subclass profile of anti-HBs response in vaccinated children and children seroconverted after natural infection. *Vaccine* **18**, 1210-1217.

Grimm, D., Zhou, S., Nakai, H., Thomas, C. E., Storm, T. A., Fuess, S., Matsushita, T., Allen, J., Surosky, R., Lochrie, M., Meuse, L., McClelland, A., Colosi, P. & Kay, M. A. (2003). Preclinical in vivo evaluation of pseudotyped adeno-associated virus vectors for liver gene therapy. *Blood* **102**, 2412-2419.

Gronthos, S., Franklin, D. M., Leddy, H. A., Robey, P. G., Storms, R., W. & Gimble, J., M. (2001). Surface protein characterization of human adipose tissue-derived stromal cells. *Journal of Cellular Physiology* **189**, 54-63.

Hacein-Bey-Abina, S., Garrigue, A., Wang, G. P., Soulier, J., Lim, A., Morillon, E., Clappier, E., Caccavelli, L., Delabesse, E., Beldjord, K., Asnafi, V., Macintyre, E., Dal Cortivo, L., Radford, I., Brousse, N., Sigaux, F., Moshous, D., Hauer, J., Borkhardt, A., Belohradsky, B. H., Wintergerst, U., Velez, M. C., Leiva, L. E., Sorensen, R., Wulffraat, N., Blanche, S., Bushman, F. D., Fischer, A. & Cavazzana-Calvo, M. (2008). Insertional oncogenesis in 4 patients after retrovirus-mediated gene therapy of SCID-X1. *J Clin Invest* **118**, 3132-3142.

Hacein-Bey-Abina, S., Von Kalle, C., Schmidt, M., McCormack, M. P., Wulffraat, N., Leboulch, P., Lim, A., Osborne, C. S., Pawliuk, R., Morillon, E.,

Sorensen, R., Forster, A., Fraser, P., Cohen, J. I., de Saint Basile, G., Alexander, I., Wintergerst, U., Frebourg, T., Aurias, A., Stoppa-Lyonnet, D., Romana, S., Radford-Weiss, I., Gross, F., Valensi, F., Delabesse, E., Macintyre, E., Sigaux, F., Soulier, J., Leiva, L. E., Wissler, M., Prinz, C., Rabbitts, T. H., Le Deist, F., Fischer, A. & Cavazzana-Calvo, M. (2003). LMO2-Associated Clonal T-cell Proliferation in Two Patients after Gene Therapy for SCID-X1. *Science* **302**, 415-419.

Halbert, C. L., Allen, J. M. & Miller, A. D. (2001). Adeno-Associated Virus Type 6 (AAV6) Vectors Mediate Efficient Transduction of Airway Epithelial Cells in Mouse Lungs Compared to That of AAV2 Vectors. *J Virol* **75**, 6615-6624.

Halbert, C. L., Miller, A. D., McNamara, S., Emerson, J., Gibson, R. L., Ramsey, B. & Aitken, M. L. (2006). Prevalence of Neutralizing Antibodies Against Adeno-Associated Virus (AAV) Types 2, 5, and 6 in Cystic Fibrosis and Normal Populations: Implications for Gene Therapy Using AAV Vectors. *Human Gene Therapy* **17**, 440-447.

Halbert, C. L., Standaert, T. A., Aitken, M. L., Alexander, I. E., Russell, D. W. & Miller, A. D. (1997). Transduction by adeno-associated virus vectors in the rabbit airway: efficiency, persistence, and readministration. *J Virol* **71**, 5932-5941.

Halbert, C. L., Standaert, T. A., Wilson, C. B. & Miller, A. D. (1998). Successful readministration of adeno-associated virus vectors to the mouse lung requires transient immunosuppression during the initial exposure. *J Virol* **72**, 9795-9805.

Hauswirth, W. W. & Berns, K. I. (1979). Adeno-associated virus DNA replication: Nonunit-length molecules. *Virology* **93**, 57-68.

Hawkins, E. D., Hommel, M., Turner, M. L., Battye, F. L., Markham, J. F. & Hodgkin, P. D. (2007). Measuring lymphocyte proliferation, survival and differentiation using CFSE time-series data. *Nat Protoc* **2**, 2057-2067.

Helledie, T., Nurcombe, V. & Cool, S. M. (2008). A Simple and Reliable Electroporation Method for Human Bone Marrow Mesenchymal Stem Cells. *Stem cells and development* **17**, 837-848.

Hellman, S., Grate, H. E., Chaffey, J. T. & Carmel, R. (1970). Hematopoietic stem cell compartment: patterns of differentiation following radiation or cyclophosphamide. *Hemopoietic Cellular Proliferation*, 36-48.

Hernandez, Y. J., Wang, J., Kearns, W. G., Loiler, S., Poirier, A. & Flotte, T. R. (1999). Latent Adeno-Associated Virus Infection Elicits Humoral but Not Cell-Mediated Immune Responses in a Nonhuman Primate Model. *J Virol* **73**, 8549-8558.

High, K. A., Manno, C. S., Sabatino, D., Hutchison, S., Dake, M., Razavi, M., Kaye, R., Aruda, V., Herzog, R., Rustagi, P., Rasko, J., Hoots, K., Blatt, P., Sommer, J., Ragni, M., Ozelo, M., Konkle, B., Lessard, R., Luk, A., Glader, B., Pierce, G., Couto, L. & Kay, M. (2004). Immune Responses to AAV and to Factor IX in a Phase I Study of AAV-Mediated, Liver-Directed Gene Transfer for Hemophilia B. *Mol Ther* **9**, S383-384.

Iso, Y., Spees, J. L., Serrano, C., Bakondi, B., Pochampally, R., Song, Y.-H., Sobel, B. E., Delafontaine, P. & Prockop, D. J. (2007). Multipotent human stromal

cells improve cardiac function after myocardial infarction in mice without long-term engraftment. *Biochemical and Biophysical Research Communications* **354**, 700-706.

Jackson, K. A., Mi, T. & Goodell, M. A. (1999). Hematopoietic potential of stem cells isolated from murine skeletal muscle. *Proceedings of the National Academy of Sciences of the United States of America* **96**, 14482-14486.

Janik, J. E., Huston, M. M. & Rose, J. A. (1984). Adeno-associated virus proteins: origin of the capsid components. *J Virol* **52**, 591-597.

Jankowski, R. J., Deasy, B. M. & Huard, J. (2002). Muscle-derived stem cells. *Gene Ther* **9**, 642-647.

Jefferis, R. & Kumararatne, D. S. (1990). Selective IgG subclass deficiency: quantification and clinical relevance. *Clin exp Immunol* **81**, 357-367.

Jefferis, R. & Lund, J. (2002). Interaction sites on human IgG-Fc for Fc[gamma]R: current models. *Immunology Letters* **82**, 57-65.

Jiang, Y., Jahagirdar, B. N., Reinhardt, R. L., Schwartz, R. E., Keene, C. D., Ortiz-Gonzalez, X. R., Reyes, M., Lenvik, T., Lund, T., Blackstad, M., Du, J., Aldrich, S., Lisberg, A., Low, W. C., Largaespada, D. A. & Verfaillie, C. M. (2002a). Pluripotency of mesenchymal stem cells derived from adult marrow. *Nature* **418**, 41 - 49.

Jiang, Y., Vaessen, B., Lenvik, T., Blackstad, M., Reyes, M. & Verfaillie, C. M. (2002b). Multipotent progenitor cells can be isolated from postnatal murine bone marrow, muscle, and brain. *Experimental Hematology* **30**, 896-904.

Johansson, B. M. & Wiles, M. V. (1995). Evidence for involvement of activin A and bone morphogenetic protein 4 in mammalian mesoderm and hematopoietic development. *Mol Cell Biol* **15**, 141-151.

Jones, E. & McGonagle, D. (2007). Human bone marrow mesenchymal stem cells in vivo. *Rheumatology*, kem206.

Kalvenes, M. B., Kalland, K. H. & Haukenes, G. (1996). Immunoglobulin G subclass antibodies to rubella virus in chronic liver disease, acute rubella and healthy controls. *FEMS Immunol Med Microbiol* **13**, 43-50.

Kaplitt, M. G., Feigin, A., Tang, C., Fitzsimons, H. L., Mattis, P., Lawlor, P. A., Bland, R. J., Young, D., Strybing, K., Eidelberg, D. & During, M. J. (2007). Safety and tolerability of gene therapy with an adeno-associated virus (AAV) borne GAD gene for Parkinson's disease: an open label, phase I trial. *The Lancet* **369**, 2097-2105.

Kern, A., Schmidt, K., Leder, C., Muller, O. J., Wobus, C. E., Bettinger, K., Von der Lieth, C. W., King, J. A. & Kleinschmidt, J. A. (2003). Identification of a Heparin-Binding Motif on Adeno-Associated Virus Type 2 Capsids. *J Virol* **77**, 11072-11081.

Koc, O. N., Day, J., Nieder, M., Gerson, S. L., Lazarus, H. M. & Krivit, W. (2002). Allogeneic mesenchymal stem cell infusion for treatment of metachromatic leukodystrophy (MLD) and Hurler syndrome (MPS-IH). *Bone Marrow Transplant* **30**, 215 - 222.

Kofron, M. D. & Laurencin, C. T. (2006). Bone tissue engineering by gene delivery. *Advanced Drug Delivery Reviews* **58**, 555-576.

Kogler, G., Sensken, S., Airey, J. A., Trapp, T., Muschen, M., Feldhahn, N., Liedtke, S., Sorg, R. V., Fischer, J., Rosenbaum, C., Greschat, S., Knipper, A., Bender, J., Degistirici, O., Gao, J., Caplan, A. I., Colletti, E. J., Almeida-Porada, G., Muller, H. W., Zanjani, E. & Wernet, P. (2004). A New Human Somatic Stem Cell from Placental Cord Blood with Intrinsic Pluripotent Differentiation Potential. *J Exp Med* **200**, 123-135.

Kotin, R. M., Siniscalco, M., Samulski, R. J., Zhu, X. D., Hunter, L., Laughlin, C. A., McLaughlin, S., Muzyczka, N., Rocchi, M. & Berns, K. I. (1990). Site-specific integration by adeno-associated virus. *Proc Natl Acad Sci USA* **87**, 2211-2215.

Krampera, M., Glennie, S., Dyson, J., Scott, D., Laylor, R., Simpson, E. & Dazzi, F. (2003). Bone marrow mesenchymal stem cells inhibit the response of naive and memory antigen-specific T-cells to their cognate peptide. *Blood* **101**, 3722 - 3729.

Krause, D. S., Theise, N. D., Collector, M. I., Henegariu, O., Hwang, S., Gardner, R., Neutzel, S. & Sharkis, S. J. (2001). Multi-Organ, Multi-Lineage Engraftment by a Single Bone Marrow-Derived Stem Cell. *Cell* **105**, 369-377.

Kremer, E. J. & Perricaudet, M. (1995). Adenovirus and adeno-associated virus mediated gene transfer. *Br Med Bull* **51**, 31-44.

Kronenberg, S., Bottcher, B., von der Lieth, C. W., Bleker, S. & Kleinschmidt, J. A. (2005). A Conformational Change in the Adeno-Associated Virus Type 2 Capsid Leads to the Exposure of Hidden VP1 N Termini. *J Virol* **79**, 5296-5303.

Kucia, M., Reca, R., Campbell, F. R., Zuba-Surma, E., Majka, M., Ratajczak, J. & Ratajczak, M. Z. (2006). A population of very small embryonic-like (VSEL) CXCR4+SSEA-1+Oct-4+ stem cells identified in adult bone marrow. *Leukemia* **20**, 857-869.

Lagasse, E., Connors, H., Al-Dhalimy, M., Reitsma, M., Dohse, M., Osborne, L., Wang, X., Finegold, M., Weissman, I. L. & Grompe, M. (2000). Purified hematopoietic stem cells can differentiate into hepatocytes in vivo. *Nat Med* **6**, 1229-1234.

Lal, R. B., Buckner, C., Khabbaz, R. F., Kaplan, J. E., Reyes, G., Hadlock, K., Lipka, J., Foung, S. K. H., Chan, L. & Coligan, J. E. (1993). Isotypic and IgG Subclass Restriction of the Humoral Immune Responses to Human T-Lymphotropic Virus Type-I. *Clin Immunol Immunopathol* **67**, 40-49.

Le Blanc, K., Rasmusson, I., Sundberg, B., Götherström, C., Hassan, M., Uzunel, M. & Ringdén, O. (2004). Treatment of severe acute graft-versus-host disease with third party haploidentical mesenchymal stem cells. *The Lancet* **363**, 1439-1441.

Le Blanc, K., Tammik, C., Rosendahl, K., Zetterberg, E. & Ringden, O. (2003). HLA expression and immunologic properties of differentiated and undifferentiated mesenchymal stem cells. *Exp Hematol* **31**, 890 - 896.

Levine, B. L., Humeau, L. M., Boyer, J., MacGregor, R.-R., Rebello, T., Lu, X., Binder, G. K., Slepushkin, V., Lemiale, F., Mascola, J. R., Bushman, F. D., Dropulic, B. & June, C. H. (2006). Gene transfer in humans using a

conditionally replicating lentiviral vector. *Proceedings of the National Academy of Sciences* **103**, 17372-17377.

Li, C., Hirsch, M., DiPrimio, N., Asokan, A., Goudy, K., Tisch, R. & Samulski, R. J. (2009). Cytotoxic-T-Lymphocyte-Mediated Elimination of Target Cells Transduced with Engineered Adeno-Associated Virus Type 2 Vector In Vivo. *J Virol* **83**, 6817-6824.

Li, H., Murphy, S. L., Giles-Davis, W., Edmonson, S., Xiang, Z., Li, Y., Lasaro, M., High, K. A. & Ertl, H. C. (2007). Pre-existing AAV capsid-specific CD8+ T-cells are unable to eliminate AAV-transduced hepatocytes. *Mol Ther* **15**, 792-800.

Lieberman, J. R., Le, L. Q., Wu, L., Finerman, G. A. M., Berk, A., Witte, O. N. & Stevenson, S. (1998). Regional gene therapy with a BMP-2-producing murine stromal cell line induces heterotopic and orthotopic bone formation in rodents. *Journal of Orthopaedic Research* **16**, 330-339.

Liu, D. W., Tsao, Y. P., Kung, J. T., Ding, Y. A., Sytwu, H. K., Xiao, X. & Chen, S. L. (2000). Recombinant adeno-associated virus expressing human papillomavirus type 16 E7 peptide DNA fused with heat shock protein DNA as a potential vaccine for cervical cancer. *J Virol* **74**, 2888-2894.

Mackay, A. M., Beck, S. C., Murphy, J. M., Barry, F. P., Chichester, C. O. & Pittenger, M. F. (1998). Chondrogenic differentiation of cultured human mesenchymal stem cells from marrow. *Tissue Eng* **4**, 415 - 428.

Manning, W. C., Zhou, S., Bland, M. P., Escobedo, J. A. & Dwarki, V. (1998). Transient immunosuppression allows transgene expression following readministration of adeno-associated viral vectors. *Hum Gene Ther* **9**, 477-485.

Manno, C. S., Pierce, G., Arruda, V. R., Glader, B., Ragni, M., Rasko, J. J., Ozelo, M. C., Hoots, K., Blatt, P., Konkle, B., Dake, M., Kaye, R., Razavi, M., Zajko, A., Zehnder, J., Rustagi, P. K., Nakai, H., Chew, A., Leonard, D., Wright, J., Lessard, R. R., Sommer, J. M., Tigges, M., Sabatino, D., Luk, A., Jiang, H., Mingozzi, F., Couto, L., Ertl, H. C., High, K. A. & Kay, M. A. (2006). Successful transduction of liver in hemophilia by AAV-Factor IX and limitations imposed by the host immune response. *Nat Med* **12**, 342-347.

Markert, C. D., Atala, A., Cann, J. K., Christ, G., Furth, M., Ambrosio, F. & Childers, M. K. (2009). Mesenchymal Stem Cells: Emerging Therapy for Duchenne Muscular Dystrophy. *PM&R* **1**, 547-559.

Martin, G. R. (1981). Isolation of a pluripotent cell line from early mouse embryos cultured in medium conditioned by teratocarcinoma stem cells. *Proc Natl Acad Sci U S A* **78**, 7634-7638.

Martinez-Agosto, J. A., Mikkola, H. K. A., Hartenstein, V. & Banerjee, U. (2007). The hematopoietic stem cell and its niche: a comparative view. *Genes & Development* **21**, 3044-3060.

Matsuoka, S., Ebihara, Y., Xu, M.-j., Ishii, T., Sugiyama, D., Yoshino, H., Ueda, T., Manabe, A., Tanaka, R., Ikeda, Y., Nakahata, T. & Tsuji, K. (2001). CD34 expression on long-term repopulating hematopoietic stem cells changes during developmental stages. *Blood* **97**, 419-425.

Maximow, A. A. (1906). Über experimentelle erzeugung von knochenmarks-gewebe. *Anatomischer Anzeiger* **28**, 24-38.

McMahon, J. M., Conroy, S., Lyons, M., Greiser, U., O'Shea, C., Strappe, P., Howard, L., Murphy, M., Barry, F. & O'Brien, T. (2006). Gene Transfer into Rat Mesenchymal Stem Cells: A Comparative Study of Viral and Nonviral Vectors. *Stem cells and development* **15**, 87-96.

McTaggart, S. & Al-Rubeai, M. (2002). Retroviral vectors for human gene delivery. *Biotechnology Advances* **20**, 1-31.

Meisel, R., Zibert, A., Laryea, M., Gobel, U., Daubener, W. & Dilloo, D. (2004). Human bone marrow stromal cells inhibit allogeneic T-cell responses by indoleamine 2,3-dioxygenase-mediated tryptophan degradation. *Blood* **103**, 4619 - 4621.

Mellor, A. L. & Munn, D. H. (2001). Tryptophan catabolism prevents maternal T-cells from activating lethal anti-fetal immune responses. *J Reprod Immunol* **52**, 5 - 13.

Mendelson, E., Trempe, J. P. & Carter, B. J. (1986). Identification of the trans-acting Rep proteins of adeno-associated virus by antibodies to a synthetic oligopeptide. *J Virol* **60**, 823-832.

Miller, C. L., Llenos, I. C., Dulay, J. R. & Weis, S. (2006). Upregulation of the initiating step of the kynurenine pathway in postmortem anterior cingulate cortex from individuals with schizophrenia and bipolar disorder. *Brain Research* **1073-1074**, 25-37.

Miura, M., Gronthos, S., Zhao, M., Lu, B., Fisher, L. W., Robey, P. G. & Shi, S. (2003). SHED: Stem cells from human exfoliated deciduous teeth. *Proceedings*

of the National Academy of Sciences of the United States of America **100**, 5807-5812.

Miura, M., Miura, Y., Padilla-Nash, H. M., Molinolo, A., A. , Fu, B., Patel, V., Seo, B.-M., Sonoyama, W., Zheng, J. J., Baker, C. C., Chen, W., Ried, T. & Shi, S. (2006). Accumulated Chromosomal Instability in Murine Bone Marrow Mesenchymal Stem Cells Leads to Malignant Transformation. *Stem Cells* **24**, 1095-1103.

Mohr, A., Lyons, M., Deedigan, L., Harte, T., Shaw, G., Howard, L., Barry, F., O'Brien, T. & Zwacka, R. (2008). Mesenchymal stem cells expressing TRAIL lead to tumour growth inhibition in an experimental lung cancer model. *Journal of Cellular and Molecular Medicine* **12**, 2628-2643.

Monahan, P. E. & Samulski, R. J. (2000). AAV vectors: is clinical success on the horizon? *Gene Ther* **7**, 24-30.

Monahan, P. E., Samulski, R. J., Tazelaar, J., Xiao, X., Nichols, T. C., Bellinger, D. A., Read, M. S. & Walsh, C. E. (1998). Direct intramuscular injection with recombinant AAV vectors results in sustained expression in a dog model of hemophilia. *Gene Ther* **5**, 40-49.

Moore, K. A. & Lemischka, I. R. (2006). Stem Cells and Their Niches. *Science* **311**, 1880-1885.

Mori, S., Wang, L., Takeuchi, T. & Kanda, T. (2004). Two novel adeno-associated viruses from cynomolgus monkey: pseudotyping characterization of capsid protein. *Virology* **330**, 375-383.

Moskalenko, M., Chen, L., van Roey, M., Donahue, B. A., Snyder, R. O., McArthur, J. G. & Patel, S. D. (2000). Epitope Mapping of Human Anti-Adeno-Associated Virus Type 2 Neutralizing Antibodies: Implications for Gene Therapy and Virus Structure. *J Virol* **74**, 1761-1766.

Moss, R. B., Milla, C., Colombo, J., Accurso, F., Zeitlin, P. L., Clancy, J. P., Spencer, L. T., Pilewski, J., Waltz, D. A., Dorkin, H. L., Ferkol, T., Pian, M., Ramsey, B., Carter, B. J., Martin, D. B. & Heald, A. E. (2007). Repeated aerosolized AAV-CFTR for treatment of cystic fibrosis: a randomized placebo-controlled phase 2B trial. *Hum Gene Ther* **18**, 726-732.

Moss, R. B., Rodman, D., Spencer, L. T., Aitken, M. L., Zeitlin, P. L., Waltz, D. A., Milla, C., Brody, A. S., Clancy, J. P., Ramsey, B., Hamblett, N. & Heald, A. E. (2004). Repeated adeno-associated virus serotype 2 aerosol-mediated cystic fibrosis transmembrane regulator gene transfer to the lungs of patients with cystic fibrosis: a multicenter, double-blind, placebo-controlled trial. *Chest* **125**, 509-521.

Mountford, J. C. (2008). Human embryonic stem cells: origins, characteristics and potential for regenerative therapy. *Transfusion Medicine* **18**, 1-12.

Mueller, C. & Flotte, T. R. (2008). Clinical gene therapy using recombinant adeno-associated virus vectors. *Gene Ther* **15**, 858-863.

Muraglia, A., Cancedda, R. & Quarto, R. (2000). Clonal mesenchymal progenitors from human bone marrow differentiate in vitro according to a hierarchical model. *J Cell Sci* **113**, 1161-1166.

Muramatsu, S.-I., Mizukami, H., Young, N. S. & Brown, K. E. (1996). Nucleotide Sequencing and Generation of an Infectious Clone of Adeno-Associated Virus 3. *Virology* **221**, 208-217.

Murphy, S. L., Li, H., Mingozzi, F., Sabatino, D. E., Hui, D. J., Edmonson, S. A. & High, K. A. (2009). Diverse IgG subclass responses to adeno-associated virus infection and vector administration. *J Med Virol* **81**, 65-74.

Nishikage, S., Koyama, H., Miyata, T., Ishii, S., Hamada, H. & Shigematsu, H. (2004). In vivo electroporation enhances plasmid-based gene transfer of basic fibroblast growth factor for the treatment of ischemic limb. *Journal of Surgical Research* **120**, 37-46.

Nishizaki, K., Mazda, O., Dohi, Y., Kawata, T., Mizuguchi, K., Kitamura, S. & Taniguchi, S. (2000). In vivo gene gun-mediated transduction into rat heart with Epstein-Barr virus-based episomal vectors. *The Annals of Thoracic Surgery* **70**, 1332-1337.

Ogura, N., Kawada, M., Chang, W.-J., Zhang, Q., Lee, S.-Y., Kondoh, T. & Abiko, Y. (2004). Differentiation of the human mesenchymal stem cells derived from bone marrow and enhancement of cell attachment by fibronectin. *Journal of Oral Science* **46**, 207-213.

Ohshima, S., Shin, J.-H., Yuasa, K., Nishiyama, A., Kira, J., Okada, T. & Takeda, S. i. (2008). Transduction Efficiency and Immune Response Associated With the Administration of AAV8 Vector Into Dog Skeletal Muscle. *Mol Ther* **17**, 73-80.

Okada, T. (1980). Cellular metaplasia or transdifferentiation as a model for retinal cell differentiation. *Curr Top Dev Biol* **16**, 349-380.

Opie, S. R., Warrington, K. H., Jr., Agbandje-McKenna, M., Zolotukhin, S. & Muzyczka, N. (2003). Identification of Amino Acid Residues in the Capsid Proteins of Adeno-Associated Virus Type 2 That Contribute to Heparan Sulfate Proteoglycan Binding. *J Virol* **77**, 6995-7006.

Opitz, C. A., Litzenburger, U. M., Lutz, C., Lanz, T. V., Tritschler, I., Köppel, A., Tolosa, E., Hoberg, M., Anderl, J., Aicher, W. K., Weller, M., Wick, W. & Platten, M. (2009). Toll-Like Receptor Engagement Enhances the Immunosuppressive Properties of Human Bone Marrow-Derived Mesenchymal Stem Cells by Inducing Indoleamine-2,3-dioxygenase-1 via Interferon-beta and Protein Kinase R. *Stem Cells* **27**, 909-919.

Ortiz, L. A., DuTreil, M., Fattman, C., Pandey, A. C., Torres, G., Go, K. & Phinney, D. G. (2007). Interleukin 1 receptor antagonist mediates the antiinflammatory and antifibrotic effect of mesenchymal stem cells during lung injury. *Proceedings of the National Academy of Sciences* **104**, 11002-11007.

Oswald, J., Boxberger, S., Jørgensen, B., Feldmann, S., Ehninger, G., Bornhäuser, M. & Werner, C. (2004). Mesenchymal Stem Cells Can Be Differentiated Into Endothelial Cells In Vitro. *Stem Cells* **22**, 377-384.

Parsch, D., Fellenberg, J., Brümmendorf, T., Eschlbeck, A.-M. & Richter, W. (2004). Telomere length and telomerase activity during expansion and differentiation of human mesenchymal stem cells and chondrocytes. *Journal of Molecular Medicine* **82**, 49-55.

Partridge, K. A. & Oreffo, R. O. C. (2004). Gene Delivery in Bone Tissue Engineering: Progress and Prospects Using Viral and Nonviral Strategies. *Tissue Engineering* **10**, 295-307.

Peden, C. S., Burger, C., Muzyczka, N. & Mandel, R. J. (2004). Circulating Anti-Wild-Type Adeno-Associated Virus Type 2 (AAV2) Antibodies Inhibit Recombinant AAV2 (rAAV2)-Mediated, but Not rAAV5-Mediated, Gene Transfer in the Brain. *J Virol* **78**, 6344-6359.

Peter, C., Anne, L. A., Alessandra, G., David, R. P. & Pamela, A. W. (2005). Mechanisms of MHC class I-restricted antigen processing and cross-presentation. *Immunological Reviews* **207**, 145-157.

Pevsner-Fischer, M., Morad, V., Cohen-Sfady, M., Rousso-Noori, L., Zanin-Zhorov, A., Cohen, S., Cohen, I. R. & Zipori, D. (2007). Toll-like receptors and their ligands control mesenchymal stem cell functions. *Blood* **109**, 1422-1432.

Pittenger, M. F., Mackay, A. M., Beck, S. C., Jaiswal, R. K., Douglas, R., Mosca, J. D., Moorman, M. A., Simonetti, D. W., Craig, S. & Marshak, D. R. (1999). Multilineage potential of adult human mesenchymal stem cells. *Science* **284**, 143 - 147.

Prindull, G., Prindull, B. & Meulen, N. v. d. (1978). Haematopoietic stem cells (CFUc) in human cord blood. *Acta Paediatrica* **67**, 413-416.

Qing, K., Mah, C., Hansen, J., Zhou, S., Dwarki, V. & Srivastava, A. (1999). Human fibroblast growth factor receptor 1 is a co-receptor for infection by adeno-associated virus 2. *Nat Med* **5**, 71-77.

Rabinowitz, J. E., Bowles, D. E., Faust, S. M., Ledford, J. G., Cunningham, S. E. & Samulski, R. J. (2004). Cross-dressing the virion: the transcapsidation of adeno-associated virus serotypes functionally defines subgroups. *J Virol* **78**, 4421-4432.

Rabinowitz, J. E. & Samulski, R. J. (2000). Building a Better Vector: The Manipulation of AAV Virions. *Virology* **278**, 301-308.

Rammensee, H. G., Bachmann, J., Emmerich, N. P. N., Bachor, O. A. & Stevanović, S. (1999). SYFPEITHI: database for MHC ligands and peptide motifs. *Immunogenetics* **50**, 213-219.

Raper, S. E., Chirmule, N., Lee, F. S., Wivel, N. A., Bagg, A., Gao, G.-p., Wilson, J. M. & Batshaw, M. L. (2003). Fatal systemic inflammatory response syndrome in a ornithine transcarbamylase deficient patient following adenoviral gene transfer. *Molecular Genetics and Metabolism* **80**, 148-158.

Reya, T., Duncan, A. W., Ailles, L., Domen, J., Scherer, D. C., Willert, K., Hintz, L., Nusse, R. & Weissman, I. L. (2003). A role for Wnt signalling in self-renewal of haematopoietic stem cells. *Nature* **423**, 409-414.

Reyes, M. & Verfaillie, C. M. (2001). Characterization of multipotent adult progenitor cells, a subpopulation of mesenchymal stem cells. *Ann N Y Acad Sci* **938**, 231 - 233.

Robbins, P. D. & Ghivizzani, S. C. (1998). Viral Vectors for Gene Therapy. *Pharmacology & Therapeutics* **80**, 35-47.

Roos, A.-K., Eriksson, F., Timmons, J. A., Gerhardt, J., Nyman, U., Gudmundsdotter, L., Bråve, A., Wahren, B. & Pavel, P. (2009). Skin

Electroporation: Effects on Transgene Expression, DNA Persistence and Local Tissue Environment. *PLoS One* **4**, e7226.

Rossant, J. (2006). Stem cells and lineage development in the mammalian blastocyst. *Reprod Fertil Dev* **19**, 111-118.

Rubio, D., Garcia-Castro, J., Martin, M. C., de la Fuente, R., Cigudosa, J. C., Lloyd, A. C. & Bernad, A. (2005). Spontaneous Human Adult Stem Cell Transformation. *Cancer Res* **65**, 3035-3039.

Russell, D. W. & Kay, M. A. (1999). Adeno-Associated Virus Vectors and Hematology. *Blood* **94**, 864-874.

Rutledge, E. A., Halbert, C. L. & Russell, D. W. (1998). Infectious Clones and Vectors Derived from Adeno-Associated Virus (AAV) Serotypes Other Than AAV Type 2. *J Virol* **72**, 309-319.

Ryan, J., Barry, F., Murphy, J. M. & Mahon, B. (2005). Mesenchymal stem cells avoid allogeneic rejection. *Journal of Inflammation* **2**, 8.

Ryan, J. M., Barry, F., Murphy, M. & Mahon, B. P. (2007). Interferon-gamma does not break, but promotes the immunosuppressive capacity of adult human mesenchymal stem cells. *Clinical and experimental immunology* **149**, 10.

Sabatino, D. E., Mingozzi, F., Hui, D. J., Chen, H., Colosi, P., Ertl, H. C. J. & High, K. A. (2005). Identification of Mouse AAV Capsid-specific CD8+ T-cell Epitopes. *Mol Ther* **12**, 1023-1033.

Sakaguchi, Y., Sekiya, I., Yagishita, K., Ichinose, S., Shinomiya, K. & Muneta, T. (2004). Suspended cells from trabecular bone by collagenase digestion become

virtually identical to mesenchymal stem cells obtained from marrow aspirates. *Blood* **104**, 2728-2735.

Samulski, R. J. & Giles, J. (2005). Adeno-Associated Viral Vectors for Clinical Gene Therapy in the Brain. *Prog Neurol Surg* **18**, 154-168.

Schlehofer, J. R., Ehrbar, M. & zur Hausen, H. (1986). Vaccinia virus, herpes simplex virus, and carcinogens induce DNA amplification in a human cell line and support replication of a helpervirus dependent parvovirus. *Virology* **1**, 110-117.

Shizuru, J. A., Negrin, R. S. & Weissman, I. L. (2005). Hematopoietic Stem and Progenitor Cells: Clinical and Preclinical Regeneration of the Hematolymphoid System. *Annual Review of Medicine* **56**, 509-538.

Silva, W. A. J., Covas, D. T., Panepucci, R. A., Proto-Siqueira, R., Siufi, J. L., Zanette, D. L., Santos, A. R. & Zago, M. A. (2003). The Profile of Gene Expression of Human Marrow Mesenchymal Stem Cells. *Stem Cells* **21**, 661-669.

Siminovitch, L., McCulloch, E. A. & Till, J. E. (1963). The distribution of colony-forming cells among spleen colonies. *J Cell Physiol* **62**, 327-336.

Song, L., Webb, N. E., Song, Y. & Tuan, R. S. (2006). Identification and Functional Analysis of Candidate Genes Regulating Mesenchymal Stem Cell Self-Renewal and Multipotency. *Stem Cells* **24**, 1707-1718.

Spaggiari, G. M., Capobianco, A., Becchetti, S., Mingari, M. C. & Moretta, L. (2006). Mesenchymal stem cell-natural killer cell interactions: evidence that

activated NK cells are capable of killing MSCs, whereas MSCs can inhibit IL-2-induced NK-cell proliferation. *Blood* **107**, 1484-1490.

Srivastava, A., Lusby, E. W. & Berns, K. I. (1983). Nucleotide sequence and organization of the adeno-associated virus 2 genome. *J Virol* **45**, 555-564.

Stender, S., Murphy, M., O'Brien, T., Stengaard, C., Ulrich-Vinther, M., Søballe, K. & Barry, F. (2007). Adeno-associated viral vector transduction of human mesenchymal stem cells. *Eur Cell Mater* **13**, 93-99.

Stenderup, K., Justesen, J., Clausen, C. & Kassem, M. (2003). Aging is associated with decreased maximal life span and accelerated senescence of bone marrow stromal cells. *Bone* **33**, 919-926.

Stilwell, J. L. & Samulski, R. J. (2004). Role of viral vectors and virion shells in cellular gene expression. *Mol Ther* **9**, 337-346.

Straus, S. E., Sebring, E. D. & Rose, J. A. (1976). Concatemers of alternating plus and minus strands are intermediates in adenovirus-associated virus DNA synthesis. *Proc Natl Acad Sci U S A* **73**, 742-746.

Studeny, M., Marini, F. C., Champlin, R. E., Zompetta, C., Fidler, I. J. & Andreeff, M. (2002). Bone Marrow-derived Mesenchymal Stem Cells as Vehicles for Interferon-{beta} Delivery into Tumors. *Cancer Res* **62**, 3603-3608.

Summerford, C., Bartlett, J. S. & Samulski, R. J. (1999). AlphaVbeta5 integrin: a co-receptor for adeno-associated virus type 2 infection. *Nat Med* **5**, 78-82.

Summerford, C. & Samulski, R. J. (1998). Membrane-associated heparan sulfate proteoglycan is a receptor for adeno-associated virus type 2 virions. *J Virol* **72**, 1438-1445.

Suzawa, M., Takada, I., Yanagisawa, J., Ohtake, F., Ogawa, S., Yamauchi, T., Kadowaki, T., Takeuchi, Y., Shibuya, H., Gotoh, Y., Matsumoto, K. & Kato, S. (2003). Cytokines suppress adipogenesis and PPAR-[gamma] function through the TAK1/TAB1/NIK cascade. *Nat Cell Biol* **5**, 224-230.

Temple, S. (2001). Stem cell plasticity: building the brain of our dreams. *Nat Rev Neurosci* **2**, 513-520.

Thomas, H. I. J. & Morgan-Capner, P. (1988). Rubella-Specific IgG Subclass Concentrations in Sera Using an Enzyme-Linked Immunosorbent Assay (ELISA): The Effect of Different Sources of Rubella Antigen. *Epidemiol Infect* **101**, 599-604.

Thomson, J. A., Itskovitz-Eldor, J., Shapiro, S. S., Waknitz, M. A., Swiergiel, J. J., Marshall, V. S. & Jones, J. M. (1998). Embryonic Stem Cell Lines Derived from Human Blastocysts. *Science* **282**, 1145-1147.

Tobiasch, E., Rabreau, M., Geletneky, K., Laruë-Charlus, S., Severin, F., Becker, N. & Schlehofer, J. (1994). Detection of adeno-associated virus DNA in human genital tissue and in material from spontaneous abortion. *J Med Virol* **44**, 215-222.

Toptygina, A. P., Pukhalsky, A. L. & Alioshkin, V. A. (2005). Immunoglobulin G Subclass Profile of Antimeasles Response in Vaccinated Children and in Adults with Measles History. *Clin Diagn Lab Immunol* **12**, 845-847.

Tran, S. D., Pillemer, S. R., Dutra, A., Barrett, A. J., Brownstein, M. J., Key, S., Pak, E., Leakan, R. A., Kingman, A., Yamada, K. M., Baum, B. J. & Mezey,

E. (2003). Differentiation of human bone marrow-derived cells into buccal epithelial cells in vivo: a molecular analytical study. *The Lancet* **361**, 1084-1088.

Tratschin, J. D., Miller, I. L. & Carter, B. J. (1984). Genetic analysis of adeno-associated virus: properties of deletion mutants constructed in vitro and evidence for an adeno-associated virus replication function. *J Virol* **51**, 611-619.

Tse, W. T., Pendleton, J. D., Beyer, W. M., Egalka, M. C. & Guinan, E. C. (2003). Suppression of allogeneic T-cell proliferation by human marrow stromal cells: implications in transplantation. *Transplantation* **75**, 389 - 397.

Uprichard, S. L. (2005). The therapeutic potential of RNA interference. *FEBS Letters* **579**, 5996-6007.

Van Weemen, B. K. & Schuurs, A. H. (1971). Immunoassay using antigen-enzyme conjugates. *FEBS Lett* **15**, 232-236.

Verfaillie, C. M. (2002). Adult stem cells: assessing the case for pluripotency. *Trends in Cell Biology* **12**, 502-508.

Vignau, J., Jacquemont, M. C., Lefort, A., Imbenotte, M. & Lhermitte, M. (2004). Simultaneous determination of tryptophan and kynurenine in serum by HPLC with UV and fluorescence detection. *Biomedical Chromatography* **18**, 872-874.

Vincent-Lacaze, N., Snyder, R. O., Gluzman, R., Bohl, D., Lagarde, C. & Danos, O. (1999). Structure of adeno-associated virus vector DNA following transduction of the skeletal muscle. *J Virol* **73**, 1949-1955.

Von Lüttichau, I., Notohamiprodjo, M., Wechselberger, A., Peters, C., Henger, A., Seliger, C., Djafarzadeh, R., Huss, R. & Nelson, P. J. (2005). Human Adult CD34- Progenitor Cells Functionally Express the Chemokine Receptors CCR1,

CCR4, CCR7, CXCR5, and CCR10 but Not CXCR4. *Stem cells and development* **14**, 329-336.

Wagers, A. J. & Weissman, I. L. (2004). Plasticity of Adult Stem Cells. *Cell* **116**, 639-648.

Wagner, J. A., Messner, A. H., Moran, M. L., Daifuku, R., Kouyama, K., Desch, J. K., Manley, S., Norbash, A. M., Conrad, S. K., Friborg, S., Reynolds, T., Guggino, W. B., Moss, R. B., Carter, B. J., Wine, J. J., Flotte, T. R. & Gardner, P. (1999). Safety and biological efficacy of an adeno-associated virus vector-cystic fibrosis transmembrane regulator (AAV-CFTR) in the cystic fibrosis maxillary sinus. *Laryngoscope* **109**, 266-274.

Wagner, J. A., Nepomuceno, I. B., Messner, A. H., Moran, M. L., Batson, E. P., Dimiceli, S., Brown, B. W., Desch, J. K., Norbash, A. M., Conrad, C. K., Guggino, W. B., Flotte, T. R., Wine, J. J., Carter, B. J., Reynolds, T. C., Moss, R. B. & Gardner, P. (2002). A Phase II, Double-Blind, Randomized, Placebo-Controlled Clinical Trial of tgAAVCF Using Maxillary Sinus Delivery in Patients with Cystic Fibrosis with Antrostomies. *Human Gene Therapy* **13**, 1349-1359.

Wakitani, S., Goto, T., Pineda, S. J., Young, R. G., Mansour, J. M., Caplan, A. I. & Goldberg, V. M. (1994). Mesenchymal cell-based repair of large, full-thickness defects of articular cartilage. *J Bone Joint Surg Am* **76**, 579-592.

Walsh, J. & Andrews, P. W. (2003). Expression of Wnt and Notch pathway genes in a pluripotent human embryonal carcinoma cell line and embryonic stem cells. *Apmis* **111**, 197-211.

Walters, R. W., Pilewski, J. M., Chiorini, J. A. & Zabner, J. (2002). Secreted and transmembrane mucins inhibit gene transfer with AAV4 more efficiently than AAV5. *J Biol Chem* **277**, 23709-23713.

Walters, R. W., Yi, S. M. P., Keshavjee , S., Brown, K. E., Welsh, M. J., Chiorini, J. A. & Zabner, J. (2001). Binding of Adeno-associated Virus Type 5 to 2,3-Linked Sialic Acid Is Required for Gene Transfer. *J Biol Chem* **276**, 20610-20616.

Wang, L., Figueredo, J., Calcedo, R., Lin, J. & Wilson, J. M. (2007). Cross-Presentation of Adeno-Associated Virus Serotype 2 Capsids Activates Cytotoxic T-cells But Does Not Render Hepatocytes Effective Cytolytic Targets. *Hum Gene Ther* **18**, 185-194.

Wang, X., Willenbring, H., Akkari, Y., Torimaru, Y., Foster, M., Al-Dhalimy, M., Lagasse, E., Finegold, M., Olson, S. & Grompe, M. (2003). Cell fusion is the principal source of bone-marrow-derived hepatocytes. *Nature* **422**, 897-901.

Weitzman, M. D., Kyöstiö, S. R., Kotin, R. M. & Owens, R. A. (1994). Adeno-associated virus (AAV) Rep proteins mediate complex formation between AAV DNA and its integration site in human DNA. *Proceedings of the National Academy of Sciences of the United States of America* **91**, 5808-5812.

Wert, G. d. & Mummery, C. (2003). Human embryonic stem cells: research, ethics and policy. *Hum Reprod* **18**, 672-682.

Wexler, S. A., Donaldson, C., Denning-Kendall, P., Rice, C., Bradley, B. & Hows, J. M. (2003). Adult bone marrow is a rich source of human mesenchymal 'stem'

cells but umbilical cord and mobilized adult blood are not. *British Journal of Haematology* **121**, 368-374.

Wiles, M. V. & Johansson, B. M. (1999). Embryonic Stem Cell Development in a Chemically Defined Medium. *Experimental Cell Research* **247**, 241-248.

Wu, P., Xiao, W., Conlon, T., Hughes, J., Agbandje-McKenna, M., Ferkol, T., Flotte, T. & Muzyczka, N. (2000). Mutational analysis of the adeno-associated virus type 2 (AAV2) capsid gene and construction of AAV2 vectors with altered tropism. *J Virol* **74**, 8635-8647.

Wu, Z., Asokan, A. & Samulski, R. J. (2006). Adeno-associated Virus Serotypes: Vector Toolkit for Human Gene Therapy. *Mol Ther* **14**, 316-327.

Xiao, W., Chirmule, N., Berta, S. C., McCullough, B., Gao, G. & Wilson, J. M. (1999). Gene Therapy Vectors Based on Adeno-Associated Virus Type 1. *J Virol* **73**, 3994-4003.

Xiao, W., Chirmule, N., Schnell, M. A., Tazelaar, J., Hughes, J. V. & Wilson, J. M. (2000). Route of administration determines induction of T-cell-independent humoral responses to adeno-associated virus vectors. *Mol Ther* **1**, 323-329.

Xiao, W., Warrington, K. H., Jr., Hearing, P., Hughes, J. & Muzyczka, N. (2002). Adenovirus-Facilitated Nuclear Translocation of Adeno-Associated Virus Type 2. *J Virol* **76**, 11505-11517.

Xie, Q., Bu, W., Bhatia, S., Hare, J., Somasundaram, T., Azzi, A. & Chapman, M. S. (2002). The atomic structure of adeno-associated virus (AAV-2), a vector for human gene therapy. *Proc Natl Acad Sci USA* **99**, 10405-10410.

Yang, S.-H., Park, M.-J., Yoon, I.-H., Kim, S.-Y., Hong, S.-H., Shin, J.-Y., Nam, H.-Y., Kim, Y.-H., Kim, B. & Park, C.-G. (2009). Soluble mediators from mesenchymal stem cells suppress T-cell proliferation by inducing IL-10. *Exp Mol Med* **41**, 315-324.

Zaiss, A. K., Cotter, M. J., White, L. R., Clark, S. A., Wong, N. C. W., Holers, V. M., Bartlett, J. S. & Muruve, D. A. (2008). Complement Is an Essential Component of the Immune Response to Adeno-Associated Virus Vectors. *J Virol* **82**, 2727-2740.

Zaiss, A. K., Liu, Q., Bowen, G. P., Wong, N. C. W., Bartlett, J. S. & Muruve, D. A. (2002). Differential Activation of Innate Immune Responses by Adenovirus and Adeno-Associated Virus Vectors. *J Virol* **76**, 4580-4590.

Zaiss, A. K. & Muruve, D. A. (2005). Immune responses to adeno-associated virus vectors. *Current Gene Therapy* **5**, 323-331.

Zhang, J., Wu, X., Qin, C., Qi, J., Ma, S., Zhang, H., Kong, Q., Chen, D., Ba, D. & He, W. (2003). A novel recombinant adeno-associated virus vaccine reduces behavioral impairment and [beta]-amyloid plaques in a mouse model of Alzheimer's disease. *Neurobiol Dis* **14**, 365-379.

Zwezdaryk, K. J., Coffelt, S. B., Figueroa, Y. G., Liu, J., Phinney, D. G., LaMarca, H. L., Florez, L., Morris, C. B., Hoyle, G. W. & Scandurro, A. B. (2007). Erythropoietin, a hypoxia-regulated factor, elicits a pro-angiogenic program in human mesenchymal stem cells. *Experimental Hematology* **35**, 640-652.